



**D**octorate program  
**M**ilan  
**EXPERIMENTAL**  
**MEDICINE**



**Università degli Studi di Milano**

**PhD Course in  
Experimental Medicine**

**CYCLE XXXIV**

**PhD thesis**

---

**Extracellular vesicles-mediated communication in remodeling  
multiple myeloma microenvironment: a new role for the Notch  
pathway**

---

**Candidate: Dr. Domenica Giannandrea**

**Tutor: Prof. Raffaella Chiamonte**

**Director: Prof. Nicoletta Landsberger**

**Academic Year 2020-2021**

## INDEX

|  |           |
|--|-----------|
| <b>ABSTRACT .....</b>  | <b>1</b>  |
| <b>DISCLOSURE FOR RESEARCH INTEGRITY .....</b>   | <b>2</b>  |
| <b>ABBREVIATIONS .....</b>   | <b>2</b>  |
| <b>INTRODUCTION .....</b>  | <b>5</b>  |
| 1. <i>MULTIPLE MYELOMA .....</i>   | <i>5</i>  |
| 1.1 <i>Pathogenesis of multiple myeloma .....</i>  | <i>5</i>  |
| 1.2 <i>Therapy .....</i>   | <i>8</i>  |
| 1.3 <i>The complexity of bone marrow microenvironment in Multiple Myeloma .....</i>      | <i>8</i>  |
| 2. <i>NOTCH PATHWAY .....</i>  | <i>10</i> |
| 2.1 <i>Notch family .....</i>  | <i>10</i> |
| 2.2 <i>Notch pathway activation .....</i>  | <i>12</i> |
| 2.3 <i>Notch in multiple myeloma .....</i>   | <i>13</i> |
| 3. <i>EXTRACELLULAR VESICLES .....</i>   | <i>15</i> |
| 3.1 <i>General features .....</i>  | <i>15</i> |
| 3.2 <i>Role of extracellular vesicles in cancer .....</i>                                | <i>17</i> |
| 3.3 <i>Role of extracellular vesicles in multiple myeloma .....</i>                      | <i>18</i> |
| 4. <i>OSTEOCLASTOGENESIS IN MULTIPLE MYELOMA .....</i>                                   | <i>20</i> |
| 4.1 <i>The role of Notch pathway in the osteoclastogenesis in multiple myeloma .....</i> | <i>21</i> |
| 4.2 <i>The role of extracellular vesicles in the myeloma osteoclastogenesis .....</i>    | <i>22</i> |
| 5. <i>ANGIOGENESIS IN MULTIPLE MYELOMA .....</i>   | <i>23</i> |
| 5.1 <i>The role of Notch pathway in angiogenesis .....</i>                               | <i>24</i> |
| 5.2 <i>The role of extracellular vesicles in the myeloma angiogenesis .....</i>          | <i>26</i> |
| <b>AIM OF THE THESIS .....</b>   | <b>28</b> |
| <b>MATERIALS AND METHODS .....</b>   | <b>30</b> |
| 1. <i>CELL LINES AND TREATMENT .....</i>   | <i>30</i> |
| 1.1 <i>HMCLs transfection and co-culture experiments .....</i>                           | <i>31</i> |
| 2. <i>TUBE FORMATION ASSAY .....</i>   | <i>33</i> |
| 3. <i>RNA EXTRACTION AND qRT-PCR FOR GENE EXPRESSION ANALYSIS .....</i>                  | <i>34</i> |
| 3.1 <i>RNA extraction .....</i>  | <i>34</i> |
| 3.2 <i>Reverse transcription .....</i>   | <i>34</i> |
| 3.3 <i>Quantitative Real-Time PCR .....</i>  | <i>35</i> |
| 4. <i>ELISA FOR VEGF-A .....</i>   | <i>36</i> |
| 5. <i>ISOLATION AND PURIFICATION OF EXTRACELLULAR VEICLES FROM MM CELL LINES .....</i>   | <i>36</i> |
| 6. <i>ANALYSIS OF EVs BY NANOPARTICLE TRACKING ANALYSIS .....</i>                        | <i>37</i> |

|  |           |
|--|-----------|
| 7. TRANSMISSION ELECTRON MICROSCOPY .....  | 37        |
| 8. IN VITRO INTERNALIZATION ASSAYS OF EVs .....  | 38        |
| 8.1 Flow cytometry analysis.....   | 38        |
| 8.2 Fluorescence microscopy analysis .....   | 38        |
| 9. WESTERN BLOT ANALYSIS .....   | 39        |
| 10. DETENTION SYSTEM TO TRACK NOTCH2 EV-MEDIATED TRANSFER FROM<br>DONOR TO RECEIVING CELLS .....                             | 41        |
| 11. LUCIFERASE NOTCH REPORTER ASSAY .....  | 42        |
| 12. IN VIVO EXPERIMENTS .....  | 43        |
| 13. FUNCTIONAL ASSAY WITH EVs.....   | 44        |
| 13.1 Osteoclastogenic assay.....   | 44        |
| 13.2 Tube formation assay with EVs .....   | 44        |
| 14. CELL VIABILITY ASSAY .....   | 44        |
| 15. EX VIVO EXPERIMENTS.....   | 45        |
| 16. STATISTICAL ANALYSIS.....  | 46        |
| <b>RESULTS.....</b>  | <b>47</b> |
| 1. MYELOMA CELL-DERIVED JAGGED LIGANDS PROMOTE TUMOR<br>ANGIOGENESIS.....  | 47        |
| 1.1 Direct effect of Jagged ligands in the stimulation of the angiogenic potential of<br>endothelial cells .....             | 47        |
| 1.2 Effect of MM-derived soluble factors on angiogenic potential of EC.....  | 50        |
| 2. MYELOMA CELL DERIVED JAGGED1 AND 2 INCREASE BONE MARROW<br>STROMAL CELL ANGIOGENIC POTENTIAL.....                         | 52        |
| 3. MYELOMA CELL RELEASE EXTRACELLULAR VESICLES THAT CARRY<br>NOTCH2 AS CARGO.....  | 55        |
| 3.1 Characterization of EVs isolated from MM cells.....  | 55        |
| 3.2 Uptake of MM-EVs on target cells .....   | 57        |
| 3.3 Analysis of the presence of Notch2 in MM-EVs.....  | 59        |
| 3.4 Analysis of the ability of MM-EVs to transfer Notch2 to distant cells.....   | 62        |
| 4. MM-EVS INCREASE THE PRO-TUMORIGENIC ACTIVITY OF BONE MARROW<br>HEALTHY CELLS IN A NOTCH DEPENDENT WAY.....                | 64        |
| 4.1 Analysis of the effect of Notch2 silencing on MM cell-derived EVs.....   | 64        |
| 4.2 Analysis of MM-EVs ability to activate Notch pathway in recipient cells .....  | 68        |
| 4.3 Evaluation of Notch2 role in MM-EVs-mediated osteoclastogenesis and<br>angiogenesis .....                                | 70        |
| 4.4 Effect of Notch pathway pharmacological blockade on pro-tumorigenic potential of<br>MM-EVs.....                          | 73        |
| 4.5 Effect of Notch pathway pharmacological blockade on pro-tumorigenic potential of<br>EVs from the BM of MM patients ..... | 75        |
| <b>DISCUSSION AND CONCLUSIONS .....</b>  | <b>77</b> |

|   |            |
|---|------------|
| 1. <i>MM CELLS INDUCE ANGIOGENESIS IN A JAGGED 1/2 MEDIATED WAY</i> ..... | 78         |
| 2. <i>NOTCH PATHWAY IN THE EV-MEDIATED COMMUNICATION</i> .....            | 80         |
| <b>ACKNOWLEDGMENTS</b> .....  | <b>86</b>  |
| <b>REFERENCES</b> .....   | <b>87</b>  |
| <b>LIST OF FIGURES AND TABLES</b> .....                                   | <b>97</b>  |
| <b>DISSEMINATION OF RESULTS</b> .....                                     | <b>99</b>  |
| <b>APPENDIX</b> .....   | <b>102</b> |

## ABSTRACT

Multiple myeloma (MM) is a still incurable hematological neoplasm mainly due to the localization of malignant plasma cells (PC) in the bone marrow (BM) where they can create pathological interaction with the surrounding resident cell populations. Indeed, upon localization within the BM, myeloma cells “educate” the resident cells to support the progression from monoclonal gammopathy of undetermined significance (MGUS) to active MM. The pathological crosstalk is also mediated by aberrant Notch signaling pathway due to the overexpression of Notch pathway members, such as Notch2 and the ligands Jagged1 and Jagged2. MM cells can enhance Notch signaling activation in the BM cells, leading to pro-tumorigenic processes such as drug resistance, osteoclastogenesis and angiogenesis.

In this complex microenvironment, extracellular vesicles (EVs) shed from MM cells (MM-EVs) are reported to be involved the BM reprogramming thanks to their ability to carry molecular messengers both at long and short distance.

Starting from this evidence, the aims of this thesis are: 1) to investigate the role of Notch pathway in MM microenvironment, focusing on the incompletely explored role of Jagged ligands in MM angiogenesis; 2) to evaluate the role of Notch in the ability of MM-EVs to induce osteoclastogenesis and angiogenesis, focusing on Notch2 receptor.

To assess the first point, I used an inhibitory approach to study the role of Jagged ligands on MM cells and their outcome on MM-induced angiogenesis was assessed *in vitro*. To investigate the second aim, I used *in vitro*, *in vivo* and *ex vivo* models to assess the ability of EVs to carry and transfer the Notch2 to recipient cells, activating the Notch signaling and leading to their pro-tumorigenic effect. The role of Notch2 was assessed by RNA interference using lentiviral inducible vectors.

The results obtained in the first part of this thesis indicate that Jagged ligands on MM cells can induce the angiogenic activity of endothelial cells promoting MM cell release of vascular endothelial growth factor (VEGF) and by directly activating the endothelial Notch pathway. Moreover, Jagged-mediated Notch pathway activation in BMSCs boosts their support to the angiogenic process.

The second part of my PhD work focused on MM-EVs mediated communication showing that Notch2 is transferred to distant cells *via* MM-EVs and is able to increase Notch signaling in recipient cells also at distant sites. MM-EVs may increase the osteoclastogenic potential and the angiogenic ability in the tumor microenvironment in a Notch2 dependent way.

Indeed, interfering with Notch2 expression decreases the amount of Notch2 in MM-EVs and their pro-tumorigenic effect, suggesting that MM-EVs may be the target of a Notch-directed therapeutic approach. I investigated the possibility to translate these results in the clinical practice using currently available Notch inhibitors, such as a  $\gamma$ -secretase inhibitor, i.e. DAPT. I found out that DAPT may hamper the effect of MM-EVs on both angiogenesis and osteoclastogenesis. The effectiveness of this pharmacological approach was confirmed *ex vivo* demonstrating DAPT ability to reduce the angiogenic effect of EVs from the BM aspirate of MM patients which better recapitulate the complexity of MM microenvironment.

Overall, these results contribute to increase the knowledge on the role of Notch pathway in two pro-tumorigenic processes involving the MM microenvironment, such as tumor angiogenesis and osteoclastogenesis, indicating that the pathological Notch pathway activation may be triggered also at long distance *via* MM-EVs. Thereby, we provide the proof of concept that to hamper the pro-tumorigenic role of EVs could be a promising therapeutic strategy in MM as well as other tumors.

#### **DISCLOSURE FOR RESEARCH INTEGRITY**

I state that this scientific research was conducted following the principles of good research practice of the European Code of Conduct for Research Integrity, based on the principles of reliability, rigor, honesty, respect, and accountability.

#### **ABBREVIATIONS**

ASCT autologous stem cell transplantation

BM bone marrow

BMSC bone marrow stromal cell

CAF cancer-associated fibroblast

CHT caudal hematopoietic tissue

DLL Delta-like family

EC endothelial cell

ECM extracellular matrix

EGF endothelial growth factor

ESCRT endosomal sorting complex required for transport

EV extracellular vesicle

FGF fibroblast growth factor

HES Hairy and enhancer of split

HEY Hairy related transcription factor

HIF-1  $\alpha$  Hypoxia-inducible

IgH immunoglobulin heavy chain

ILVs intraluminal vesicles

KD knock down

MAPK mitogen-activated protein kinase

M-CSF macrophage colony-stimulating factor

MDSC myeloid immunosuppressive cell subset

MGUS monoclonal gammopathy of undetermined significance

MHC Major histocompatibility complex

MM multiple myeloma

MMBD MM bone disease

MMP matrix metalloproteinase

MSC mesenchymal stem cells

MVBs multivesicular bodies

NECD Notch extracellular domain

NEXT Notch Extracellular Truncation

NICD Notch C-terminal intracellular domain

NK Natural killer

OBL osteoblast

OCL osteoclast

OPG osteoprotegerin

PC plasma cell

PCL plasma cell leukemia

PDGFR $\beta$  platelet-derived growth factor receptor beta

PM plasma membrane

PMN pre-metastatic niche

RANKL receptor activator of nuclear factor  $\kappa$ B (NF- $\kappa$ B) ligand

ROS reactive oxygen species

SDF-1 Stromal Cell-Derived Factor-1

SMM smoldering multiple myeloma

TGF $\beta$  transforming growth factor beta

TRAP tartrate resistant acid phosphatase

VEGF vascular endothelial growth factor



## INTRODUCTION

### 1. MULTIPLE MYELOMA

Multiple Myeloma (MM) is a fatal cancer of plasma cells (PCs) that represents approximately 10% of hematologic malignancies and 1% of cancers (1).

This hematological disease has an incidence of 4,5-6,0 per 100.000 people per year in Europe and affects patients with a median age of 72 years. The mortality is 4.1/100.000 people per year (2). Although the improvements in the therapy, MM is still an incurable disease with a survival rate at 5 years of 52% (3).

Bone disease is the main cause of morbidity. Other clinical manifestations include anemia, hypercalcemia, renal failure, and an increased risk of infections (4).

MM is characterized by clonal expansion of terminally differentiated long-lived PCs within the bone marrow (BM) producing antigen-specific immunoglobulin detected in the blood. It is always the evolution of the asymptomatic pre-malignant stage of monoclonal gammopathy of undetermined significance (MGUS), which is defined by the presence of less than 10% of monoclonal PCs in the BM and by the detection of monoclonal protein in serum and urine. The progress to MM occurs at an average rate of 1% per year for MGUS (5) (**fig.1**).

In some MM patients can be recognized an intermediate clinical stage named smoldering (SMM) characterized by the presence of more than 10% of monoclonal PCs in the BM (10-60%) along with monoclonal protein in serum and/or urine, in the absence of myeloma-defining events (6-8). SMM is a heterogenic phase that can include low-risk patients with a slow progression to active MM and a high-risk SMM (9) (**fig.1**).

MM cells can lose the dependence from the BM microenvironment evolving into the more aggressive phase of plasma cell leukemia (PCL) and migrate toward extra-medullary sites (plasmacytoma) or circulate in the peripheral blood (plasma cell leukemia-PCL)(10) (**fig.1**).

#### *1.1 Pathogenesis of multiple myeloma*

All the stages of MM progression are characterized by genetic mutations in malignant PCs (**fig.1**). The first oncogenic event occurs in the germinal center during the genomic rearrangement of immunoglobulin heavy chain (IgH) and takes place in the IgH locus on

chromosome 14q32.3 (11) and less frequently the IgL locus (2p12,  $\kappa$  or 22q11,  $\lambda$ )(12). In particular, the translocation t(11,14) (q13;q32) occurring in 15-20% of patients (13) and t(6;14)(p21;q32), present in 5% of myeloma cases, leads to the increased expression of cyclin D1 and D3, respectively, thus leading to anomalies in the control of the cell cycle machinery (14). Another frequent translocation is t(4,14)(p16;q32) which takes place in the 13-15% of patients and dysregulates the expression of the Wolf-Hirschhorn syndrome candidate 1 gene (WHSC1), encoding for the receptor tyrosine kinase fibroblast growth factor receptor 3 (FGFR3) gene thus providing a continuous oncogenic signal to tumor cells (15). Finally, the t(14;16)(q32;q23) occurring in the 5-10% of patients dysregulates the oncogene MAF and t(14;20)(q32;q11) MAFB, with a frequency lower than 5%(16)

In addition to reciprocal chromosomal translocation, another crucial early event in malignant transformation is the hyperdiploidy which occurs in the transition from MGUS to MM and it is observed 55%-60% of MM patients with trisomies of chromosomes including 3, 5, 7, 9, 11, 15, 19 and 21(17). The role of hyperdiploidy in PC transformation is not completely understood. Nevertheless, it is known that patients with hyperdiploidy have a poor prognosis in comparison with the no-hyperdiploidy conditions. For instance, trisomy of chromosome 11 presents in the 30% of patients, may lead to cyclin D1 overexpression (18).

Recently, it has been proposed that the transition from MGUS to MM is also characterized by the hypomethylation of the genome, whereas the re-methylation occurs in the transition to the aggressive form of PCL (19). For instance, the histone methyltransferase MMSET is overexpressed in patients carrying t(4;14) leading to the activation of the oncogenic mitogen-activated protein kinase (MAPK) pathway (20, 21). Moreover, the histone deacetylases (HDAC) are hyperactive in MM, and HDAC inhibitors are the most investigated epigenetic drugs (21). Among the HDAC, the HDAC3 is important for MM survival since its inhibition is more toxic for MM cells(22).

Moreover the observation that MGUS and/or SMM patients also carry these initial mutations suggests that other oncogenic events occur in MM pathogenesis (23). Indeed, many focal genetic lesions related to MM progression have been recently identified such as mutation in tumor-suppressor genes including TP53, PTEN and the cyclin-dependent kinase inhibitors CDKN2A and CDKN2C (24). In addition, in approximately 10% of MM patients with t(4;14) are present oncogenic activating mutations of FGFR3 (25). Importantly, two members of the Ras family (NRAS and KRAS) are mutated at codons 12, 13 and 61 in 40–

55% of MM patients compared to the only 5% of MGUS (26), suggesting that the activation of the MAPK pathway is involved in the progression from MGUS to the active myeloma.

Besides the genomic rearrangements involved in the myeloma pathogenesis, the BM microenvironment actively contributes to its transformation and progression. The BM supports MM growth and infiltration at a structural and nutritional level(6). Indeed, it has been reported that the reactive oxygen species (ROS) and reactive nitrogen intermediates (RNI)(27) derived from the hypoxic state of BM contribute to the homing of malignant PCs and their proliferation (28, 29). In addition the BM can also provide activated inflammatory agents including cytokines, chemokines, adipokines, and growth factors secreted by the BM cells supporting MM growth (30). The mutual interaction between tumor cells and BM cells also leads to pro-tumorigenic processes favoring the aggressiveness of MM, such as the angiogenic switch that characterized the transition from MGUS to the malignant MM (31).

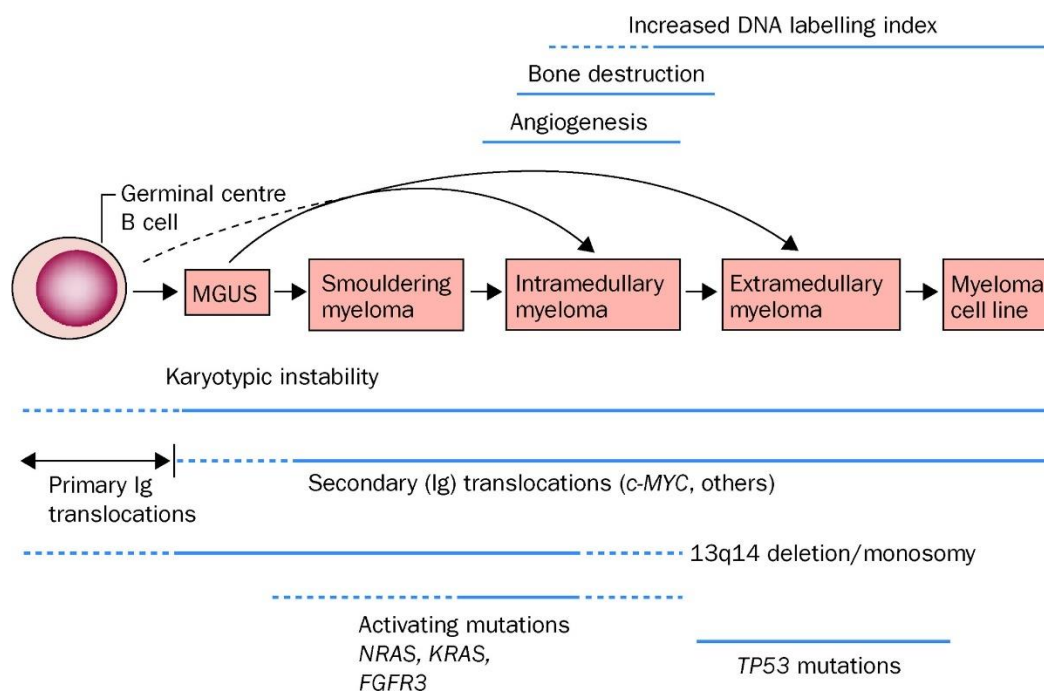


**Figure 1: Pathogenesis of MM. MM starts from the asymptomatic MGUS to the active MM within BM.** During the last phase of PCL, malignant cells escape from BM and start circulating in blood. The initial mutation starts in the germinal center and accumulate in the progress of the disease. Image taken from Sirohi *et al* (32).

## *1.2 Therapy*

The typical therapeutic protocol for MM patients younger than 65 years and in good clinical conditions, includes 3–4 cycles of induction therapy with the proteasome inhibitor bortezomib, the immune modulator lenalidomide and the corticosteroid dexamethasone (VRd), followed by the autologous stem cell transplantation (ASCT). Other bortezomib-containing regimens include bortezomib, thalidomide and dexamethasone (VTD), bortezomib, cyclophosphamide and dexamethasone (VCD), and bortezomib, doxorubicin and dexamethasone (PAD) (33). Patients with newly diagnosed MM not eligible for ASCT are treated with VRd, administered for 8–12 cycles and maintained therapy with lenalidomide (33).

For MM treatment, different classes of chemotherapeutic drugs have recently been released such as melphalan (a DNA alkylating agent), thalidomide (a pleiotropic therapeutic drug), carfilzomib (a proteasome inhibitor) and lenalidomide and pomalidomide (released as immunomodulatory agents) (34).

Despite novel drugs and novel protocols, MM patients often relapse developing drug resistance to treatment due to intrinsic and extrinsic mechanisms (35), associated to genetic alteration as well as the supportive role of BM microenvironment.

Considering the supportive role of the BM in the MM progression, targeting the molecular pathways involved in the pathological interaction in the BM microenvironment could be a valid strategy to overcome the failure of pharmacologic therapy in MM.

## *1.3 The complexity of bone marrow microenvironment in Multiple Myeloma*

The BM microenvironment plays a leading role in MM progression. Indeed, the aggressiveness of MM relies on the pathological crosstalk established between malignant PCs and the BM cell populations leading to tumor growth and the consequent clinical manifestations, like bone disease and anemia, which affect the poor prognosis of MM patients.

The BM is a dynamic and heterogenic environment that includes a cellular and a non-cellular component. The cellular compartment comprises both non-hematopoietic and hematopoietic cells. The former consists of mesenchymal stem cells (MSC) and their derived stromal cells, such as endothelial cells (ECs), adipocytes, osteoblasts (OBLs) and osteoclasts (OCLs). The hematopoietic niche includes myeloid cells, macrophages, T

lymphocytes, B lymphocytes, and natural killer cells (NK). The cellular actors interact with the non-cellular component composed by the extracellular matrix (ECM) proteins, such as laminin, fibronectin and collagen, and soluble factors such as cytokines, growth factors, and chemokines (36).

BM is a supportive microenvironment for MM cells. Their localization in the BM requires the interaction with the ECs and the extravasation through the binding of adhesion molecules on BMSCs and members of the integrin family on MM cells (37). These interactions induce the activation of survival pathway in MM cells, such as NF- $\kappa$ B and p38 MAPK (38, 39) and the release of supportive soluble factor from BMSC. Indeed, the homing of MM cells from the blood to the BM is guided by chemokine stimuli, such as the Stromal Cell-Derived Factor-1 (SDF-1), released by both MM cells (40) and the BM cell population (41). MM cells express the receptor CXCR4 able to bind the chemokine SDF-1 (42, 43) leading to the migration of MM cells in the BM. Upon localization, MM cells create their own space in the bone matrix by inducing the OCL mediated bone resorption leading to the generation of osteolytic lesions (44). After homing in the bone, MM cells may recirculate in the blood and localize in different bone distant sites thus leading to a process similar to the metastatic event in solid tumor, leading to the spreads of several bone lesions which are the main cause of poor prognosis in MM patients (44).

The recirculation of MM cells to form further lesions in distant bone sites makes BM microenvironment the favored metastatic niche for MM. Indeed, MM cells establish anomalous signaling loops with the neighboring resident BM cells by reprogramming them in order to support the different steps of MM progression (45). The binding between MM and BM cells has been demonstrated to enhance both the autocrine and paracrine production of several molecules involved in tumor progression (45). The biological outcome of this activation is the promotion of cell growth, survival, drug resistance and migration of MM cells but also leading to pro-tumorigenic processes such as osteoclastogenesis, angiogenesis, immunosuppression, and the instauration of drug resistance, affecting the poor prognosis of MM patients (45).

The mechanisms of interaction involved in these aberrant interplays are intricate and still unexplored completely. In particular, they rely both on the direct cellular contact as well as the release of soluble factor. Among these, an emerging role is played by the extracellular vesicles (EVs), which represent a new and still unknown form of cellular communication.

In the next paragraphs, I will cover in depth the role of Notch pathway and the EVs as key mechanisms of communication in the complex interactions of BM microenvironment.

## 2. NOTCH PATHWAY

Notch is a highly conserved signaling pathway implicated in different biological processes. Indeed, it mediates the communication between neighboring cells through physical interactions involving the direct contact between the Notch receptors and ligands expressed in opposite cells, thus regulating crucial cellular processes such as differentiation, proliferation, and apoptosis (46).

The first evidence of Notch gene was observed during the genetic studies in *Drosophila melanogaster* conducted by J. Dexter (1914) and T.H. Morgan (1917) and the mutant flies with notched wings provided the name of this signaling pathway. Nowadays, it is well established that Notch pathway plays a crucial role in the development regulating key processes such as cells differentiation, tissue homeostasis and stem cell maintenance. So, it is not surprising that its deregulation plays a key role in different pathologies and in particular in cancer (47).

In mammals, Notch family includes four transmembrane receptors (Notch1-4), which are activated by two class of ligands, Jagged (Jagged1 and 2) and Delta-like (DLL1,3, 4). The interaction with the ligands expressed on neighboring cells leads to proteolytic cleavages on receptor and the release of the intracellular portion of Notch (NICD), which is the Notch active intracellular Notch2 (Notch-IC) able to translocate into the nucleus and modulating the transcription of target genes expression(48).

### 2.1 Notch family

Notch genes (9q34.3, 1p12, 19p13.12, 6p21.32) encode for four receptors, Notch1, Notch2, Notch3 and Notch4. In their mature form, they are single-pass transmembrane proteins composed of an extracellular and intracellular portion (49) .

As schematized in **fig. 2**, Notch extracellular domain (NECD) contains epidermal growth factor (EGF)-like repeats involved in the binding with the ligands. In particular, repeats 11-12 are involved in *trans*-interaction, thus in signaling activation, while repeats 24-29 lead to signaling inhibition through *cis*-interaction (50). EGF-like repeats are followed by a negative

regulatory region (NRR) composed by three LIN12/Notch-related (LNR) residues and a heterodimerization domain (HD). NRR region avoids abnormal Notch activation in absence of ligand by maintaining a specific conformation that changes after the binding of the ligands (51). The extracellular portion is linked by the transmembrane domain (TM) to the C-terminal intracellular domain (NICD) which consists of RBPj (Recombination Signal Binding Protein 2 for Immunoglobulin Kappa J Region) association module (RAM) domain linked to seven ankyrin repeats (ANK domain) through a linker containing one nuclear localizing sequence (NLS). ANK is followed by are an additional bipartite NLS and a transactivation domain (TAD). The very C-terminus contains conserved proline/glutamic acid/serine/threonine-rich motifs (PEST), containing regions involved in that regulate of NICD (51). The RAM domain in cooperation with ANK repeats are required for the interaction with DNA-binding complex CBF1-Suppressor of Hairless-LAG1 (CSL) and the transactivation of RBPJ/CBF1-dependent genes (51).

Regarding the ligands (**fig.2**), there are five Notch ligands belonged to the Delta-like family (DLL1, DLL3 and DLL4) and to the Jagged family of Serrate homologs (Jagged1 and Jagged2). They are single-pass transmembrane proteins with an extracellular domain with varied EGF-like repeats and a cysteine-rich N-terminal Delta, Serrate and Lag2 (DSL) domain, required for the binding to Notch receptors. The number of EGF repeats are higher in Jagged ligands compared to DLL ligands. The intracellular regions contain multiple lysine residues and a C-terminal PDZ (PSD-95/Dlg/ZO-1)-ligand motif (absent in DLL3 only), needed for ligand signaling activity and interactions with the cytoskeleton, respectively (51).

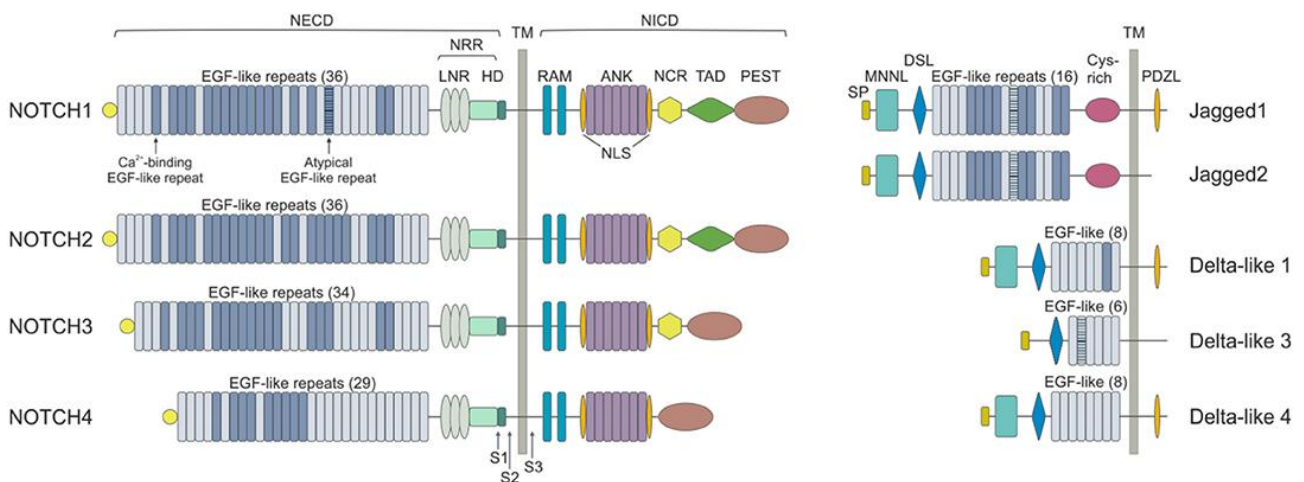


**Figure 2: Notch pathway family.** The figure shows the structure of Notch receptors (1,2,3,4), the two classes of family Delta-like (DLL1,2,3,4) and Jagged family of Serrate homologs (Jagged1 and Jagged2). Image taken from Arruga *et al.* (52).

## 2.2 Notch pathway activation

Notch receptors are synthesized in the endoplasmic reticulum as single polypeptides made of an intracellular and an extracellular portion and modified into Golgi apparatus by Fringe glycosyl-transferases, which adds N-acetylglucosamine (GlcNAc) to the primary O-fucose conferring the specificity for the ligand. After that, the acquisition of the final conformation required the cuts by the furin-like convertase at the level of S1 domain generating a heterodimer composed by an extracellular and a transmembrane domain, linked by non-covalent Ca<sup>2+</sup> interactions and the subsequent O-Glycosylation changing the protein folding and enhancing their stability in the cell surface (51) (**fig. 3**).

The Notch signaling starts with the binding with the ligand and the consequent two sequential proteolytic cleavages. The first one occurs when the ADAM10/17 metalloprotease cleaves Notch receptor at site 2 (S2), releasing its extracellular domain. The remaining NEXT (Notch Extracellular Truncation) is cleaved at S3 by a  $\gamma$ -secretase, a protein complex belonged to a family of Intramembrane cleaving proteases (53). The NEXT cleavage releases NICD which can translocate into the nucleus, acting as a transcriptional factor through the binding with an inactive CSL, via the RAM domain that increasing the local concentration of ANK and the consequent bind to RBPjk promoting the dissociation of transcriptional repressors and the starting of gene target transcription (54, 55) (**fig. 3**).

The main Notch target genes include the Hairy and enhancer of split (HES) and Hairy-related transcription factor (HEY) families, which are made of basic DNA-binding specificity domain and a helix-loop-helix domain(56). In particular, HES and HEY proteins regulate the transcription of cell fate genes involved in apoptosis, cell cycle, proliferation, differentiation and metabolism (56). Other notable Notch target genes are the transcription factors c-Myc (57); cell cycle regulators such as the positive regulator cyclin D1/3 (58, 59), and suppressor p21(60); nuclear factor kappa-light-chain-enhancer of activated B cells (NF- $\kappa$ B2)(61) and the receptor tyrosine kinase platelet-derived growth factor receptor beta (PDGFR $\beta$ )(62). Finally, Notch pathway is involved in different pathway such as Wnt, transforming growth



factor beta (TGF $\beta$ ), Hypoxia-inducible factor (HIF-1 $\alpha$ ), YAP/TAZ, epidermal growth factor receptor (EGFR) and AKT signaling pathways, thus playing a key role in development, inflammation, and cell function (63).

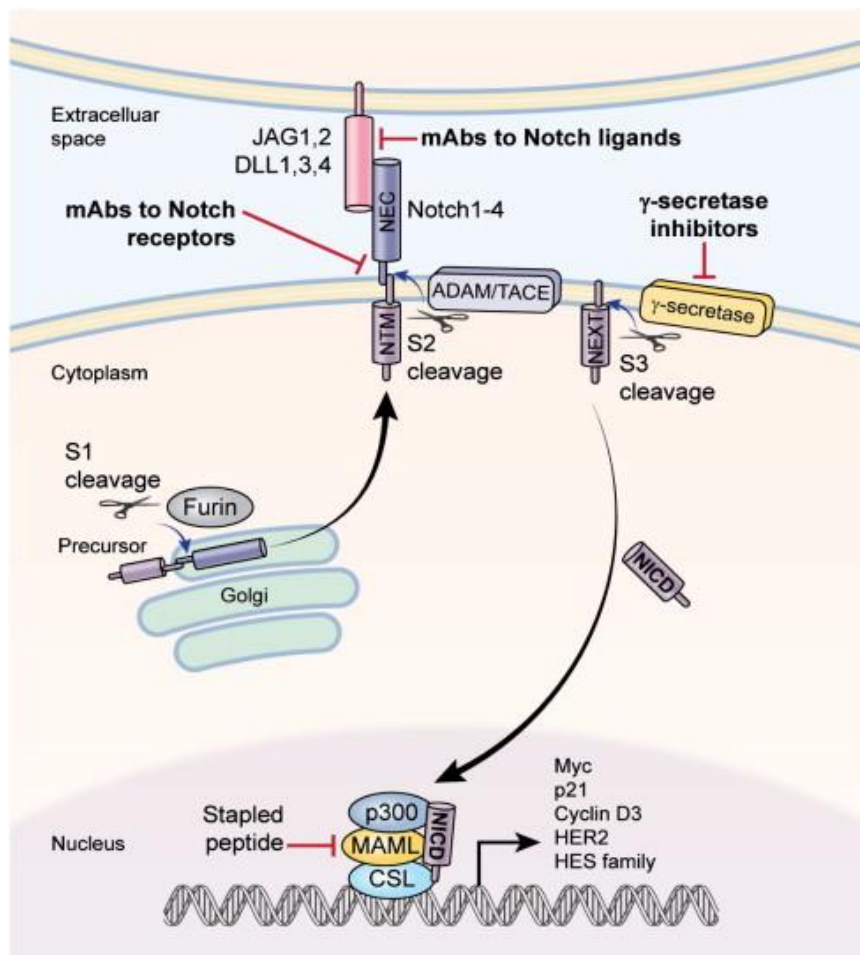


**Figure 3: Notch signaling pathway activation.** The figure shows that the binding of ligands to receptors induces proteolytic cleavages of Notch receptor at site S2 by ADAM and at site S3 by  $\gamma$ -secretase, leading to NICD released and translocation into the nucleus starting the transcription of Notch target genes. Image taken from Takebe *et al.* (64).

### 2.3 Notch in multiple myeloma

Myeloma cells overexpress receptor Notch2 and ligands Jagged1 and 2. The receptor Notch1 is overexpressed in the transition from MGUS to MM stage along with Jagged1 (65). Notch2 levels are increased in 6% of MM patients with the translocation t(14;16)(q32;q23) and t(14;20)(q32;q11) and the consequent hyper-expression of two transcription factors C-MAF and MAFB, responsible of Notch2 transcription (66, 67). Jagged2 seems to play a more

important role in the pathogenesis of MM since its deregulation occurs in the early MGUS phase (68)

The Notch pathway activation plays a crucial role in MM progression. Indeed, the inhibition of Notch signaling in MM cells hampers proliferation and increases apoptotic cells and sensitivity to drugs (69). Moreover, the homotypic Notch pathway activation between the same MM cells positively regulates the SDF-1/CXCR4 axis. Indeed, the inhibition of Notch significantly reduces the infiltration of MM cells in the BM of mouse xenograft model (70, 71).

The outcome of Notch pathway activation in the surrounding BM population is the reprogramming of healthy cells to a more supportive behavior. Indeed, tumor cell-derived Jagged ligands may trigger Notch signaling in the same neighboring MM cells (72) leading to the release of key cytokines such as the vascular endothelial growth factor (VEGF), insuline-like growth factor (IGF-1), and interleukine-6 (IL-6) (68). Indeed, VEGF induces the proliferation of MM cell and increase the angiogenic activity in EC (73), while IGF-1 supports the instauration of the drug resistance (74). More importantly IL-6 plays a survival role and correlates with the progression of MM (71, 75). In particular, myeloma derived Jagged ligands trigger the release of IL-6 by MM cells and in surrounding BM cells, inducing an autocrine and paracrine loop in the production of IL-6 (71).

Importantly, one of the major outcomes of this Notch-mediated pathological interplay is the instauration of tumor drug resistance. Indeed, Jagged1 and 2 overexpression in MM cells is able to educate the BM niche to promote the release of the pro-survival factors BCL2, Survivin, and ABCC1, and the chemokine receptor CXCR4 (76). Meanwhile, MM-derived Jagged1-2 may also activate Notch in the surrounding BMSCs boosting their ability to produce SDF1 $\alpha$  which, in turn, promotes the expression of the mentioned anti-apoptotic factors. At the end, this pathological communication enhances MM cell pharmacological resistance to standard-of-care drugs, such as bortezomib, lenalidomide and melphalan(76). Moreover, Notch pathway boosts the release of pro-osteoclastogenic and angiogenic cytokines (77, 78), playing a key role also in these processes as reported in the next paragraphs.

### 3. EXTRACELLULAR VESICLES

#### 3.1 General features

EVs are lipidic membrane-delimited nanoparticles, not able to replicate and released from all kinds of cells both in physiological and pathological condition (79). EV mediated-cellular communication represents a new emerging mechanism of cellular interaction at short and long distance, due to their ability to carry molecular messengers, such as nucleic acids (DNA, mRNA, microRNA, and other non-coding RNAs), proteins, metabolites, and lipids affecting the biological function of receiving cells (80).

According to the international society of extracellular vesicles (ISEV) guidelines, EVs could be defined for size, shape, density, internal cargo, surface molecules, membrane components, cellular origin, and function. EVs are classified especially based on size in small and medium/large vesicles, respectively, of < 100nm or < 200nm [small], or > 200nm [medium/large] (79). According to the way they are released from the cells, EVs are classified into exosomes (30-150 nm) and microvesicles (100-1000 nm)(79).

Exosomes derive from the endosomal system. Their biogenesis involves the invagination of plasma membrane (PM) and the consequential formation of early and late endosome. Late endosome with intraluminal vesicles (ILVs) are defined as multivesicular bodies (MVBs). MVBs can fuse either with lysosomes or autophagosomes, or with the PM, with the consequent release of the contained ILV as exosomes (81). ILVs formation requires mainly the reorganization of the tetraspanins on the endosomal membrane and the recruitment of the endosomal sorting complex required for transport (ESCRT) machinery (81), which consist of ESCRT-0, -I, -II, and -III complexes and related AAA ATPase Vps4 proteins (82). Nevertheless, an ESCRT-independent way process has been also described (83). The exosome secretion requires the active release of ILVs from the PM mediated by membrane fusion factors including soluble *N*-ethylmaleimide-sensitive factor attachment protein receptors (SNAREs), tethering factors, and other Ras GTPases (84) (**fig.4**).

The biogenesis of microvesicles is less defined compared to exosome. The shedding of microvesicles derives from changes and rearrangements in the composition of PM and it is followed by the outward budding of PM, the fission and release into the extracellular space (85) (**fig.4**).

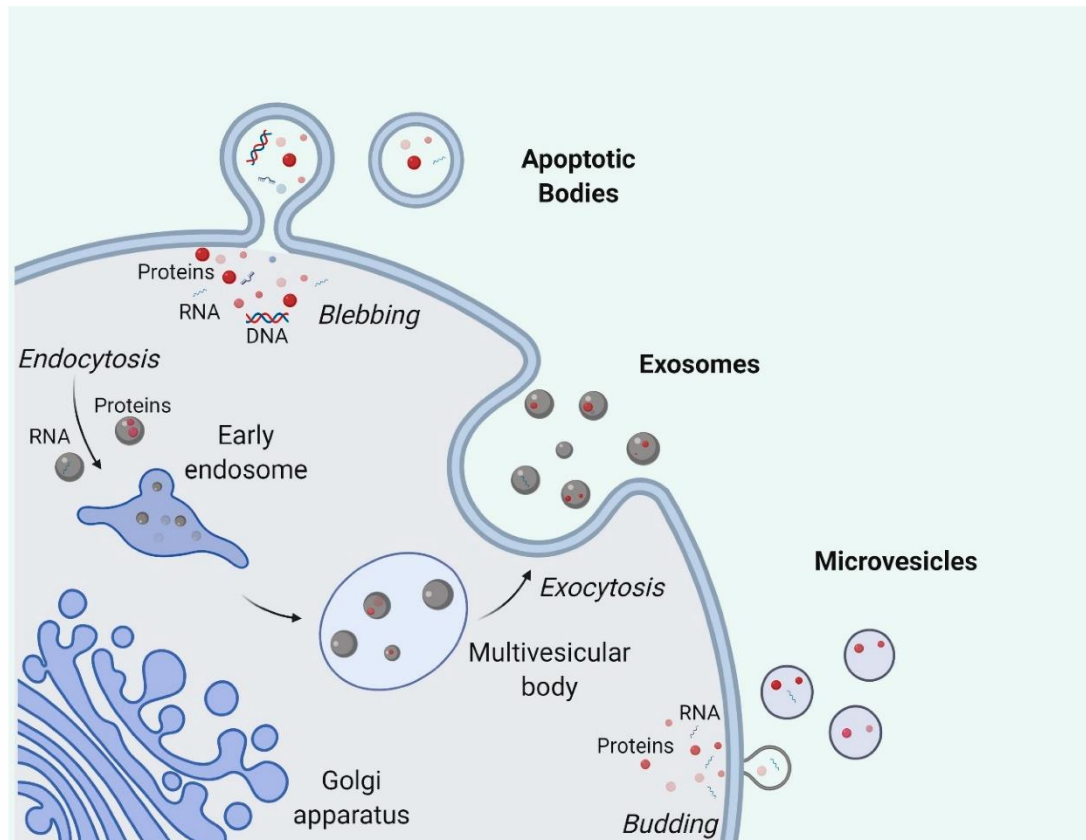


**Figure 4: Biogenesis of EVs.** Vesicles population includes microvesicles, exosome and apoptotic bodies with different mechanism of biogenesis. Image taken from Dang *et al* (86).

The different role of EVs relies on their ability to interact and be internalized in recipient cells, depending on the type of acceptor cell and its physiologic state (87). EVs can trigger the cellular pathway by the surface interaction, such as the interaction between ligands and receptors. On the other hand, in the case of membrane fusion, the cargo is transferred directly in the cytoplasm or into the nucleus. If the uptake is mediated by endocytosis (clathrin-mediated endocytosis, caveolin-mediated endocytosis, lipid raft-mediated endocytosis, macropinocytosis, and phagocytosis) (87), the EVs cargo must exit from the degradative pathway of the endosomal compartment, but the mechanism involved is still unclear(87).

Although EVs are reported to be involved both in physiological and pathological processes, their role in cancer is becoming an interesting new field of research.

### 3.2 Role of extracellular vesicles in cancer

EVs are reported to play a key role in the different steps of tumor formation from the instauration of the primary mass to the spread in distant organs (88).

The early formation of the tumor mass relies also on the ability of tumor cells to release EVs with oncogenic molecule promoting their growth and survival (89), and reprogramming the surrounding non-tumor cells promoting their supportive behavior. For instance, glioma cells can transfer EGFRvIII to malignant cells activating pro-survival pathway such as mitogen-activated protein kinase (MAPK) and AKT signaling(89).

Multiple evidence reported that tumor derived EVs may contribute to the aggressiveness and invasion of cancer cells by inducing pro-metastatic processes (90), such as the epithelial-to-mesenchymal transition and the modulation of immune system by inhibiting Fas ligand (Fas-L) (91) or downregulating natural killer (NK) cells cytotoxicity through the binding of the vesicle Major histocompatibility complex (MHC) class 1 to NK cells receptor NKG2D (92). Moreover, tumor EVs may impair monocyte differentiation into myeloid immunosuppressive cell subset (MDSC), which inhibits T lymphocyte proliferation (93).

EVs may contribute to the tumor diffusion in the circulation and the homing in distant sites by promoting the vascular leakiness and permeability (94, 95). Indeed, metastatic breast cancer cells secrete exosomes enriched of miR-105 causing the destruction of tight junction protein ZO1 in recipient ECs thus increasing their metastatic invasion (96).

Moreover, EVs may contribute to the formation of the pre-metastatic niche (PMN) favoring specific changes supporting the settlement of circulating tumor cells. For instance, tumor exosomal miR-494 and miR-542p transferred to lymph node stromal cells and lung fibroblasts can down-regulate cadherin-17 and up-regulate matrix metalloproteinase (MMP2, MMP3, and MMP14) thus favoring the homing of tumor cells (97). Moreover, breast cancer-derived microvesicles change the metabolic behavior of stromal cells reducing their glucose uptake *via* miR-122-mediated inhibition of pyruvate kinase, thereby increasing the glucose availability for tumor cells (98). Interestingly, melanoma-secreted exosomes foster PMN formation in lung via reprogramming the BM progenitors through the transfer of MET receptor (94).

Since cancer cells can release a higher amount of EVs compared to non-malignant cells, which can contain different tumor markers, circulating EVs are becoming a novel diagnostic marker for the non-invasive diagnosis (99). For instance, exosomes carrying the epithelial cell adhesion molecule (EpCAM) are increased during ovarian cancer progression and are

higher compared to benign patients and healthy subjects (100). Moreover, specific exosomal integrins seem to be associated with organ-specific metastasis such as  $\alpha 6\beta 4$  and  $\alpha 6\beta 1$  (for lung metastasis),  $\alpha v\beta 5$  (for liver metastasis), and  $\alpha v\beta 3$  (for brain metastasis) models (101). Also, miRNAs within circulating EVs have diagnostic and/or prognostic potential for many cancer types. For example, exosomal miR-17-92a correlates with increased colon cancer relapse while exosomal miR-19a is associated with its poor prognosis(102); exosomal miR-141(103) and miR-375 (104) have been associated with metastatic prostate cancer; lower levels of miR-125b in serum circulating exosomes were observed in advanced melanoma(105) and miR-21 in circulating exosomes has been correlated with esophageal cancer relapse and metastasis (106).

### 3.3 Role of extracellular vesicles in multiple myeloma

In recent years, several evidence reported that MM patients are characterized by increased levels of circulating EVs expressing the myeloma cell markers CD38 and/or CD138 compared to the healthy subjects or MGUS patients (107, 108). Moreover, EVs from MM patients' serum and BM are enriched in MHC class I and in CD44. Of note, CD44 expression increased with the reduction of the overall survival of MM patients, suggesting a prognostic value for the EVs in MM (109). Indeed, CD44 is involved in the adhesion of MM cells to BMSC and the release of IL-6, involved in MM cell survival (110).

The miRNA in circulating myeloma EVs represent a novel attractive biomarker. The study of Manier *et al.* identified 22 circulating exosomal miRNAs lower in MM patients compared to healthy donors, but only let-7b and miR-18a were associated with poor prognosis (111). Interestingly, circulating exosomal miRNA could be also used to predict the outcome of drug treatment. Six miRNAs (miR-26a-5p, miR-29c-3p, miR-30b-5p, miR-30c-5p, miR-193a-5p, and miR-331-3p) were reduced in poor responders to lenalidomide (112) and the down regulation of miR-16-5p, miR-15a-5p, miR-20a-5p, and miR-17-5p was observed in bortezomib resistant patients (113).

Regarding the role of MM-EVs in BM microenvironment, they are reported to be involved in myeloma survival and growth in an autocrine manner (114). Indeed, Arendt *et al.* reported that microvesicles from MM cells or patients carry the active transmembrane glycoprotein CD147 (115), overexpressed in MM cell and associated to their growth (116). Indeed, CD147 enhances MM proliferation *in vitro* by the upregulation of growth molecular pathway such as MAPK and mTOR (115). Moreover, the presence of acid sphingomyelinase (ASM) in MM-derived exosomes correlated with the drug resistance to melphalan or bortezomib

treatment suggesting the role of the ceramide pathway in conferring drug resistance *via* exosome transfer (117). Nevertheless, the role of ceramide pathway is controversial. Indeed, according to another study the ceramide pathway hampers MM proliferation and upregulates the release of MM-exosome able to induce the apoptosis *in vitro* in recipient tumor cells (118).

MM-EVs also induce the supportive behavior of the surrounding BM cells. Indeed, MM exosomes increase the release of pro-tumoral IL-6 from mesenchymal cells *via* APE1/NF- $\kappa$ B pathway (119). Moreover, MSC could be converted into cancer-associated fibroblast (CAF) through the transfer of the exosomal miR-21, increasing the expression of SDF-1, FAP and  $\alpha$ -SMA that, in turn, support tumor survival in BM (120). Another miRNA involved in the education of MSC is the exosomal miR-146a, that induces the release of pro-tumorigenic factors such as CXCL-1, IL-10, CCL2 and CCL5 (120).

Several studies have described the role of MM-EVs in the immune regulation, as a key step in the progress of MM. Indeed, in a recent study, it was demonstrated that malignant plasma cells with the aberrant chromosome 13 (Del13) release EVs deficient in the tumor suppressor miR-16 inducing the differentiation of monocytes to M2 tumor-supportive macrophages. At a molecular level, miR-16 targets the IKK $\alpha$ /b complex of the NF- $\kappa$ B canonical pathway, leading to lowered expression of key growth factors and cytokines implicated in macrophage M2 differentiation (121).

The ability of MM-EVs to modulate MDSCs is another key step in MM progression. Interestingly, Wang *et al.* demonstrated that exosome from murine MM cell line can be internalized in MDSCs, improving their viability and the expression of CD11b<sup>+</sup> on the plasma membrane. Moreover, MM-exosome exploit the STAT3 pathway inducing the production of iNOS and arginase 1, involved in the immunosuppressive activity on T cells *in vivo* (122).

MM-EVs also regulate the activity of NK. Indeed, they can reduce the expression of activating receptors on NK, such as NKp46, NKp30 and NKG2D involved in their cytotoxic activity of NK cells (123).

#### 4. OSTEOCLASTOGENESIS IN MULTIPLE MYELOMA

The bone remodeling is a highly regulated process based on the balance between the OCL-mediated bone resorption and the production of new bone matrix by OBL, which is important in myeloma pathogenesis.

OCL are multinucleated cells originating from hematopoietic stem cells committed to monocyte-macrophage lineage. Their activity relies on the release of acid and proteolytic enzymes, such as cathepsin K (CTSK), that dissolve collagen and other matrix proteins during bone resorption and it is regulated by the balance between the pro-osteoclastogenic receptor activator of nuclear factor  $\kappa$ B (NF- $\kappa$ B) ligand (RANKL), macrophage colony-stimulating factor (M-CSF), and the inhibitor osteoprotegerin (OPG). On the other hand, the mononucleated OBL derives from MSCs, and their main function is bone formation(124).

In the MM microenvironment, OBL/OCL homeostasis is altered leading to osteolytic lesions and the consequent MM bone disease (MMBD), including bone loss and pain, and skeletal fractures which affect dramatically the quality of life of MM patients (44).

MM cells can directly release osteogenic factors such as RANKL, inflammatory protein-1 alpha (MIP-1 $\alpha$ ), SDF-1 $\alpha$ , IL-3, IL-6 and Tumor Necrosis Factor (TNF $\alpha$ ). Moreover, they can also induce the osteoclast differentiation by promoting the supportive behavior of BMSC in the producing of RANKL, IL-6, IL-3 and GM-CSF, MIP-1 $\alpha$  and VEGF (44). MM cells contribute to alter the bone homeostasis by also inhibiting the transcription factor Runx2/Cbfa1 in mesenchymal and osteoprogenitor cells through the direct contact mediated by the very late antigen (VLA)-4 on MM cells and VCAM-1 on OBL(125). Other key factors involved in the inhibition of OBL differentiation and the consequent bone loss are IL-7, TNF- $\alpha$ , and the inhibitors of Wnt pathway Dkkopf-1 (DKK1) and sclerostin (44).

On the other hand, OCLs sustain MM progression by supporting MM cell growth and survival, drug resistance, and angiogenesis. Moreover, the osteoclastic resorption releases immobilized IGF-1, TGF- $\beta$  and endothelial growth factor (EGF) involved in tumor progression (126). These, in turn, increase the osteoclastogenic stimuli provided by MM cells creating a vicious circle that leads to the progression of MM and bone lesions formation (44).

Currently MMBD is still incurable. The standard treatments rely on the use of bisphosphonates that are able to inhibit the osteoclast activity reducing new osteolytic lesions and hypercalcemia (127). The monoclonal antibody Denosumab has been approved for the treatment of bone lesions in solid tumor since it is able to antagonize the binding of



RANKL to its receptor on OCL, and it is used in clinical trial for the treatment of MMBD (128). Finally, the proteasome inhibitors seem to be promising therapeutic approach since they can inhibit MM cell growth as well as the osteolytic lesions and increase the new bone formation (129, 130).

#### *4.1 The role of Notch pathway in the osteoclastogenesis in multiple myeloma*

Among the pathway involved in the osteoclastogenesis, Notch pathway plays a key role (131). Indeed, the inhibition of Notch signaling in OCL precursors affects the bone resorption activity both *in vivo* and *ex vivo* (132). The Notch receptors and ligands play different role in osteoclast differentiation. Indeed, Notch2 receptor is up-regulated during RANKL-induced osteoclastogenesis thus playing a critical role in the OCL differentiation (133), while Notch3 induces the expression of RANKL in OBL and osteocyte thus promoting their supportive role in the osteoclast differentiation (134). On the contrary, Notch4 is poorly expressed in OCL (131) and Notch1 displays an inhibitory role in osteoclastogenesis (135). Indeed, the Jagged1 binding to the receptor Notch1 suppress the osteoclast activity, while the Notch2/DLL1 axis promotes osteoclastogenesis(136).

In MM, the aberrant Notch signaling in MM cells leads to the release of RANKL which bounds the RANK receptor in OCL progenitors activating the NF- $\kappa$ B pathway resulting in the upregulation of RANK receptor and Notch2 and the autocrine release of RANKL by pre-OCLs. The Jagged ligands in MM cells can also activate Notch signaling in pre-OCLs or increase the Notch-mediated release of RANKL from BMSC (77) (**fig. 5**).

Moreover, Notch pathway may also enhance the spread of osteolytic lesions by inhibiting the activity of OBL thus contributing to the imbalance ratio OCL/OBL. Although the mechanisms are still unclear, MM cells may directly inhibit the OBL activity through Notch pathway activation. Indeed, the inhibition of Notch signaling in OBL can restore Runx2 expression and the osteogenic capacity in OBL precursors from MM patients *in vitro* (137, 138)(**fig. 5**).

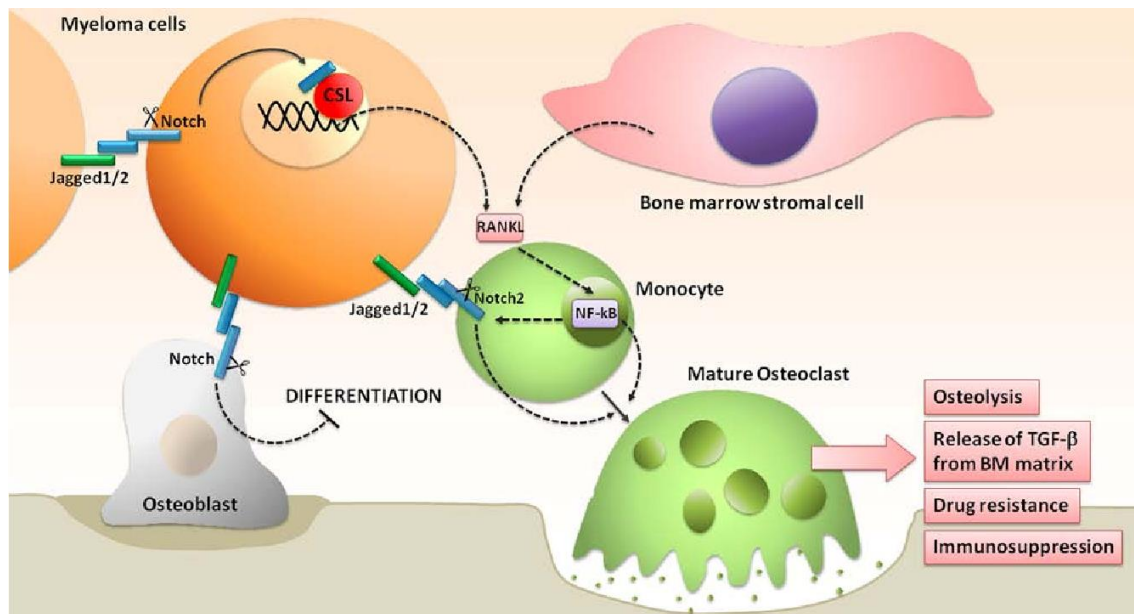


**Figure 5: Notch pathway in the osteoclastogenic process in MM.** Image taken from Colombo *et al.* (139).

#### 4.2 The role of extracellular vesicles in the myeloma osteoclastogenesis

Several evidence reports the role of EVs in the bone lesions occurring in myeloma BM. MM cell-derived exosomes play a direct role on the osteoclast activity. Indeed, Raimondi *et al* reported that MM-exosomes can enhance the expression of CXCR4 and anti-apoptotic genes in OCL, thus increasing their migration and survival (140). Moreover, they can trigger the expression of marker of bone resorption such as cathepsin K, MMP9, and tartrate resistant acid phosphatase (TRAP) expression in OCL, promoting their osteoclast formation and resorption activity both *in vitro* and *ex vivo* (140). Faict *et al.* demonstrated that exosome from the MM murine model 5TGM1 cells not only trigger the osteolysis and osteoclast differentiation both *in vivo* and *in vitro*, but they can mediate the OBL differentiation through the induction of apoptosis and the inhibition of Wnt pathway through the exosomal transfer of DKK-1, responsible for the phosphorylation of b-catenin, involved in the transcriptional activation of Wnt pathway. Indeed, MM-exosome reduced the expression of osteoblast activity markers such as RUNX2, osterix, Collagen 1 A1 and ALP (141).

Interestingly, the endoplasmic reticulum-associated unfolded protein response (UPR) signaling molecules are reported to be a novel osteoclastogenic component of EVs cargo consistently with their abundance in MM cells due to the Endoplasmic reticulum (ER) stress induced by their high production of immunoglobulin. Indeed, the analysis of the activation of the IRE1 $\alpha$ /XBP1 axis in recipient RAW264.7 demonstrated that MM-EVs induce the

activation of ER transmembrane glycoprotein (IRE1 $\alpha$ ) that results in the transcription of NFATc1, a transcription factor involved in OCs differentiation (142).

Among the soluble factors carried by MM-EVs, the amphiregulin AREG is involved not only in the activation of the osteoclastogenic EGFR in pre-OCL *in vitro*, but also in modulating the behavior of MSC. Indeed, upon uptake, the vesicle AREG can inhibit the osteoblast differentiation of MSCs, increasing the release of the pro-osteoclastogenic IL-8. Accordingly, anti-AREG mAb inhibited the release of IL-8 by MSCs confirming the direct and indirect role of AREG-enriched exosomes involvement on MM-induced osteoclastogenesis (143). Also, another group has demonstrated that MM-EVs could indirectly induce bone lesions by inhibiting the osteogenesis potential of MSC. Indeed, Zhang *et al* showed that MM-EVs from MM cell line and from the BM plasma of MM patients are enriched in molecules and miRNA involved in negatively controlling the osteoclastogenesis such as miR-103a-3p, miR-181a-3p and miR-21-3p and the proteins DKK1, IL-7 and sFRP2 (144). Moreover, MM-EV transfer the bioactive lncRNA RUNX2-AS1 to MSC, thus repressing their osteogenic ability. Indeed, RUNX2-AS1 arises from the antisense strand of RUNX2 and forming an RNA duplex with RUNX2 pre-mRNA can transcriptionally repressed RUNX2 expression, resulting in decreased osteogenic potential of MSCs (145).

## 5. ANGIOGENESIS IN MULTIPLE MYELOMA

Angiogenesis is characterized by a sequence of complex and well-modulated steps required for the formation of new capillary blood vessels starting from a pre-existing vasculature. The angiogenic process sustains the tissue by providing oxygen and nutrients thus representing a key pro-tumorigenic process for tumor progression.

The physiologic angiogenesis is efficiently coordinated by several pro-angiogenic factors, such as VEGF, bFGF, TGF- $\beta$ , HGF, and angiopoietin1-2. Among this, VEGF is the major angiogenic factor which modulates the EC activation into “tip” and “stalk” phenotype(146). These two types of EC differ in their molecular profiling and function. The “tip” cells are characterized by multiple filopodia and a dynamic phenotype that allows the starting of new vessel toward the attractive angiogenic stimuli. Indeed, they express VEGF receptor 2 (VEGFR2) and follow the VEGFA gradient creating the sprouting defining route necessary for the formation of new vessels. On the contrary, “stalk cells” have a higher proliferative rate and provide the stability maintenance of the new vessels by creating adherent and tight junctions among themselves and the ECM (147).

In MM, the angiogenic switch characterizes the transition from the avascular phase of MGUS to the vascular stage of MM, defined by a progressive increase in the BM microvascular density, that positive correlates with the progression of the disease (4). This event corresponds to a transition of ECs from a quiescent to an active state in response to the unbalance between anti- and pro-angiogenic factors regulated by the pathological interaction between tumor cells, ECs and the other BM cells in an autocrine and paracrine loop.

BMSCs, OCLs, OBLs and ECs secrete angiogenic factors such as VEGF, FGF-2, TNF- $\alpha$ , Hepatocyte growth factor (HGF), IL-6 and IL-8, OPN, Ang-1, SDF1- $\alpha$ , which are further up-regulated by tumor cells (148). Moreover, activated ECs modulate the expression of cell surface receptors, such as VEGF receptor-2 (VEGFR-2), HGF receptor (HGFR), FGFR, integrins, and other adhesion molecules that are necessary for adhesion to the ECM elements and cell motility(149).

MM cells can directly stimulate ECs through the release of soluble factors or reprogramming the BM microenvironment. Indeed, the interaction between tumor cells and BMSC upregulates also IL-6 secretion, involved in the angiogenesis stimulation. In particular, IL-6 binds its receptor expressed on MM cells inducing the secretion of VEGF which in turn enhances BMSC production of IL-6 via VEGFR-2, thus establishing a paracrine loop for tumor growth (150).

Interestingly, ECs from MM patients produce higher amount of soluble factors including chemokines such as CXCL8, SDF1 $\alpha$  and CCL2 which binding their receptors expressed on MM cells, stimulate proliferation and chemotaxis thus favoring tumor progression (151).

### *5.1 The role of Notch pathway in angiogenesis*

Notch pathway plays a key role also in the angiogenic process. Upon the regulation of the VEGF-VEGFR axis, Notch ligands play a different role in the EC phenotype and differentiation. Indeed, VEGF-A upregulates DLL4 expression on tip cells (152, 153), that in turn activates Notch pathway in stalk cells through Notch1 receptor. Stalk cells in an autocrine manner negatively regulate VEGFR-2 decreasing their capability to respond to VEGF-A stimulation(154). While DLL4 reduces the sprouting on adjacent EC, Jagged1 is a positive regulator of angiogenesis and downregulates the DLL4 reducing tip cells formation and increased number of branches (155) (**fig. 6**).

The regulation of the expression of DLL4 and Jagged 1 is crucial in the angiogenic processes. The glycosyltransferase Fringe, involved in post-translational modification of EGF-like repeats within Notch receptors extracellular portion, play a crucial role in the balance between DLL4 and Jagged1. Indeed, the Fringe mediated modification of Notch positively regulated Tip cells by increasing DLL-mediated activation and reducing it upon Jagged binding (155, 156) (**fig. 6**).

The loss of this well-controlled process leads to the generation of a disorganized network of vessels. Different works show that DLL4 inhibition leads to the formation of vessels with low perfusion unable to support tumor growth (157). On the contrary, DLL4 overexpression in ECs reduces tumor angiogenesis but develops vessels with higher diameter and higher perfusion that well sustain tumor growth(158). Since Jagged1 antagonizes DLL4 action, the overexpression of Jagged1 induces the stabilization of vessel wall enhancing tumor growth showing a proangiogenic function within tumoral microenvironment(155).

Although Notch signaling is crucial in the regulation of the angiogenic process, its role in the myeloma angiogenesis is still unclear. Nevertheless, the Notch/ $\gamma$ -secretase inhibitor RO4929097 decreases the angiogenic process resulting in a significant inhibition of the vascular structure formation in a pre-clinical model (159). The Notch expression increases in EC from MM patients correlating positively with the progress of the disease(160). Indeed, as demonstrated from our collaboration with the group of Vacca MM cells induce the angiogenic potential of ECs by activating Notch signaling *via* Notch1/2 receptors both *in vitro* and *in vivo* (160).

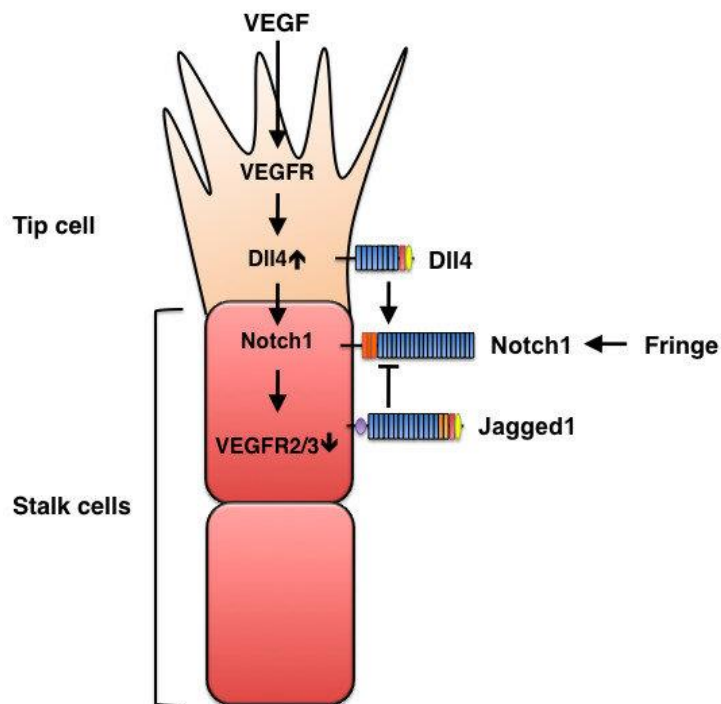


**Figure 6: Notch pathway in the angiogenic process.** VEGF and Notch signaling pathway regulate the tip and stalk cells behavior. Fringe regulates the opposite role of the ligands. Image taken from Kume *et al.* (161).

### 5.2 The role of extracellular vesicles in the myeloma angiogenesis

Several studies have reported that MM-EVs enhance the pro-tumorigenic activity of ECs through the transfer of various angiogenic factors and non-coding RNAs. Liu *et al.* reported that microvesicles from myeloma cell line RPMI8226 transfer sydecan-1 into receiving ECs that, in turn, produce an increased levels of VEGF and IL-6, that positively regulate the angiogenic process (162). In addition, MM-exosomes also induce angiogenesis *in vitro* and *in vivo*. Indeed, Wang *et al.* reported that exosome from MM murine cells carry angiogenic factors that can modulate different angiogenic pathways in ECs and BMSCs such as STAT3, c-Jun N-terminal kinase, and p53 (122).

The MM-EVs involvement in the angiogenic process could be modulated by external stimuli. Indeed, in hypoxic conditions MM cells increase the release of exosome enriched in miR-135b that suppressing its target factor—inhibiting hypoxia-inducible factor 1 (FIH-1) in ECs thus promoting their angiogenic behavior (163). Consistently, Zhang *et al.* demonstrated the correlation between miR-135b and HIF-1 $\alpha$  expression in case of hypoxic condition (164).

Regarding the presence of non-coding RNAs as a cargo of EVs, MM-EVs from cell line and peripheral blood of MM patients are reported to be enriched in piRNA-823(165). The transfer of piRNA-823 induces proliferation, angiogenesis, and invasion of EC stimulating the secretion of IL-6 and VEGF, and the expression of ICAM-1 and CXCR4. Moreover, piRNA-823 is also able to enhance the proliferation and reduce the apoptosis of ECs, adopting a supportive behavior for tumor growth. Indeed, ECs pre-treated with piRNA-823 enriched EVs have a pro-tumorigenic and angiogenic activity in a murine model, suggesting the survival advantage for tumor cells (165).

Interestingly, two different groups reported that the bortezomib and lenalidomide treatments can reduce the angiogenic potential of MM-EVs *in vitro*, reducing the amount of pro-angiogenic factors such as VEGF-A, bFGF, IL-6, PDGF and affecting their angiogenic outcome on ECs compared to MM-EV not derived from the bortezomib treatment (166, 167). Accordingly, exosomes released from MM cells treated with the Ceramide pathway activator, C6-ceramide, display a decreased angiogenic effect on EC associated to the increased level of the tumor-suppressive miR-29b and the decrease expression of AKT3, PI3K and VEGFA (168).

## AIM OF THE THESIS

Multiple Myeloma (MM) is a still incurable hematological disease characterized by clonal expansion of malignant plasma cells (PCs) in the bone marrow (BM), where they establish pathological interactions with the BM cell populations educating them to support MM progression.

MM cells overexpress the Notch pathway members, Notch2 receptor and Jagged1 and 2 ligands, whose direct contact triggers Notch signaling in MM cells, resulting in the promotion of MM proliferation and survival, and in surrounding BM cells, leading to key processes of MM progression such as osteoclastogenesis and angiogenesis.

MM cells can also release extracellular vesicles (EVs) to shape the BM microenvironment, thanks to their ability to carry the molecular messengers. Moreover, they can carry Notch pathway members.

Starting from this evidence, the aim of this thesis work is to investigate the role of Notch signaling members in osteoclastogenesis and angiogenesis, focusing on different mechanisms of communication that could occur in the pathological interplay between MM cells and the BM cell populations.

The first part of the work aimed to elucidate the role of ligands Jagged1 and Jagged2 in MM angiogenesis by directly affecting the endothelial angiogenic behavior or inducing the supportive role of BMSCs. To assess the role of Jagged1 and 2 an RNA interference approach was used on MM cell line and the angiogenic processes was elucidated by performing tube formation assay in the presence of different stimuli to discriminate the mechanisms involved in myeloma induced angiogenesis.

The second part of this thesis is focused on the role of Notch2 in EV-mediated osteoclastogenesis and angiogenesis.

To address these issues, EVs from MM cell lines (MM-EVs) were characterized for size, concentration, and morphology, as well as their ability of being internalized within target cells. The ability of MM-EVs to carry Notch2 and to transfer it into recipient cells were investigated by using an *in vitro* model of EV-mediated cellular communication. A functional analysis of MM-EVs was carried out by using an inhibitory approach through RNA interference on MM cell lines to assess the effects of Notch2 inhibition on the size and concentration of shed MM-EVs, their content, and their ability to modulate Notch pathway activation in recipient cells, by using *in vitro* and *in vivo* models. Finally, the role of Notch2



on the osteoclastogenic and angiogenic potential of MM-EVs was assessed by performing functional *in vitro* assays and further confirmed by using a pharmacological blockade of Notch signaling, DAPT. The effectiveness of a pharmacological approach was also confirmed *ex vivo* by performing a tube formation assay with the EVs from the BM aspirates of monoclonal gammopathy of undetermined significance (MGUS) and MM patients.

## **MATERIALS AND METHODS**

### **1. CELL LINES AND TREATMENT**

The human multiple myeloma cells (HMCLs) used are RPMI8226 (ATCC® CCL-155™) and H929 (ATCC® CRL-906); OPM2 (ACC-50), AMO1 (ACC-538), JJN3 (ACC-541), KMS12 (ACC-551), LP1 (ACC- 41). All HMCLs were grown in RPMI1640 medium (Euroclone, Italy) supplemented with 10% Fetal Bovine Serum (FBS, Euroclone, Italy), 2 mM L-glutamine (Microgem, Italy), 100 U/ml penicillin/streptomycin (Microgem, Italy) at the optimal concentration of  $3 \times 10^5$  cell/ml.

The human pulmonary arterial endothelial cells (HPAECs) (ATCC® PCS-100-022™) purchased from the American Type Culture Collection were cultured in Vascular Basal medium (ATCC® PCS-100-030™) supplemented with Endothelial cells Growth Kit-VEGF (ATCC® PCS-100-041™) following manufacturer instruction, at final concentration of  $5 \times 10^3$  cells/cm<sup>2</sup>.

Human embryonic kidney 293 cells, HEK293T (ATCC® CRL-157), HeLa cells (ATCC® CCL-2™), human bone marrow stromal cell line (HBMSCs) HS5 (ATCC® CRL-11882™) and the murine pre-osteoclasts Raw264.7 (ATCC® TIB-71) were cultured in Dulbecco's modified Eagle's medium (DMEM; Euroclone, Italy) with 10% FBS, 100 U/ml penicillin/streptomycin and 2 mM L-glutamine.

All cell lines were cultured in a humidified incubator in 5% CO<sub>2</sub> at 37°C and maintained at the optimal concentration and were subcultured every 48 hours completely changing the medium.

For the cell treatment, Human recombinant Jagged1 (#188-204, AnaSpec) or Jagged2 (R&D Systems Inc., Minneapolis, MN, USA) were used for the tube formation assay at the concentration of 20 µg/mL according to manufacturer's instruction. RANKL (immunotools, Germany) was used for the osteoclastogenesis assay at the concentration of 50 ng/ml or 30 ng/ml and resuspended in PBS with BSA 0,1%. DAPT (N-[N-(3,5-difluorophenacetyl-L-alanyl)]-S-phenylglycine t-Butyl ester; Merck, Germany) were resuspended in DMSO and used for the osteoclastogenesis and tube formation assay at the concentration 50 µM.

### 1.1 HMCLs transfection and co-culture experiments

HMCLs were transiently transfected using two siRNAs (short interfering RNAs) for Jagged1 and Jagged2 (J1/2KD) at final concentration of 50 nM (25 nM for each shRNA). Cells were seeded  $1,5 \times 10^5$  cells/well in 24-well plate and transfected with RNAi Lipofectamine (Thermo Fisher Scientific) following manufacturer instruction. Transfection were repeated twice, at day1 and day3. At day5 cells were collected for RNA extraction and qRT-PCR analysis, and their conditioned medium (CM) was recovered for the analysis of VEGF by ELISA.

For co-culture experiments with HBMSCs, 8h after the second transfection (day 3), transfected HMCLs were cultured for 40h with HBMSCs. More specifically, HS5 cells were seeded in 24-well plates at a density of  $7,5 \times 10^4$  cells/well, and transfected HMCLs were added at the concentration  $3 \times 10^5$  cells/mL (ratio 1:4). After 16 hours, the CM was replaced and analyzed 24 hours later by ELISA or used for tube formation assay with HPAECs (as reported in the Matrigel assay section). HS5 cells were collected and analyzed by qRT-PCR. (Schematic protocol was shown in **table1**)

|                             | Day 1                 | Day 2                       | Day 3  | Day 4                               | Day 5   |
|-----------------------------|-----------------------|-----------------------------|--|-------------------------------------|---|
| <b>Morning</b>              | Transfection of HMCLs |                             | Transfection of HMCLs  | CM changed in single HMCLs culture  | Collect HMCLs used for qRT-PCR analysis<br>CM used for ELISA analysis                       |
| <b>8h post transfection</b> |                       | HS5 seeded in 24-well plate | Set-up of co-culture between HS5 and HMCLs transfected cells | CM changed in the co-culture system | ELISA analysis<br>Collect HS5 cells used for qrt-PCR analysis<br>CM used for ELISA analysis |

**Table 1: schematic protocol used for the transfection of HMCLs.**

### 1.2 Lentivirus production and transduction of stable HMCLs with shRNAs.

Lentiviral vectors pTRIPZ expressing scrambled (SCR) or Notch2 shRNAs were transfected with Trans-Lentiviral shRNA Packaging mix (Horizon Discovery, United Kingdom) into Phoenix™-Ampho using calcium phosphate reagent according to the manufacturer's instructions. As showed in **table 2**, for the transfection of Phoenix™-Ampho, 5,5x10<sup>6</sup> cells seeded in 10 cm<sup>2</sup> petri dish 24 hours prior was transfected with pTRIPZ shRNA vector and Trans-Lentiviral packaging mix as followed reported:

- pTRIPZ shRNA vector 42 µg
- Sterile H<sub>2</sub>O 945 µl
- Trans-Lentiviral Packaging mix 30 µl
- CaCl<sub>2</sub> 250 mM
- HBS (Hank's Balanced Salt Solution) 2X

After 16h, the medium was replaced with DMEM supplemented with 5% FBS. The viral supernatants were collected after 24 hours and 48 hours, filtered, and ultracentrifugated with a 20% sucrose cushion for 4 hours at 40,000 g at 4°C. The obtained pellet containing the viral particles was resuspended in serum free DMEM.

For the infection of RPMI8226 and OPM2 cell lines, the lentiviral particles were added to the medium in the presence of IL-6 20 ng/ml (Peprotech, USA) and IGF1 20 ng/ml (Peprotech, USA) for 48 hours by exposing the cells twice to fresh viral supernatant. After 48 hours, the infected RPMI8226 and OPM2 cells were selected for stable expression with puromycin at a minimum concentration of 1 µg/mL and 0,5 ug/ml, respectively. After 7-10 days under puromycin selection the pools were selected, and the KD efficiency was monitored in transduced cells using 1 µg/mL doxycycline to induce RFP and shRNA expression. RFP expression was detected in PE channel by flow cytometry using FACS Verse (BD Biosciences, Italy) whereas the efficiency of Notch2 KD (N2KD) was evaluated by western blot analysis. Single cell colonies were obtained from a stable SCR and Notch2 shRNAs cell

pools by limiting dilution. Colonies with maximum Notch2 KD efficiency were chosen for the further experiments.

| Production of viral particles                    |   |                                       |   | Infection of MM cells  |                                  |                          |
|--|---|---------------------------------------|---|--|----------------------------------|--------------------------|
| Time 0   | 16h   | 24h                                   | 48h   | Time 0   | 24h                              | 48h                      |
| Transfection of Phoenix with pTRIPZ shRNA vector | the medium was replaced with DMEM supplemented 5% FBS | The viral supernatants were collected | The viral supernatants were collected and concentrated by ultracentrifugation | Infection of RPMI8226 and OPM2 with the lentiviral particles | Addition of lentiviral particles | Selection with puromycin |

**Table 2: schematic protocol for HMCLs infection.**

To distinguish, RPMI8226 and OPM2 KD cells transfected with siRNA are named as HMCL<sup>SCR</sup> and HMCL<sup>J1/2KD</sup>, while RPMI8226 and OPM2 KD infected with pTripz shRNA virus are named as MM<sup>SCR</sup> and MM<sup>N2KD</sup>.

## 2. TUBE FORMATION ASSAY

Growth factor reduced Matrigel (Corning, NY, USA) was dispensed 50  $\mu$ L/well in a 96-well plate and incubated 1 hours at 37 °C. The HPAECs were seeded on Matrigel-coated wells at  $2 \times 10^4$  cells/well and treated with:

- HMCLs<sup>SCR</sup> or HMCLs<sup>J1/2KD</sup> in co-culture with HPAECs at a ratio 1:2 (HPAECs:HMCLs)
- 100  $\mu$ l of CM from HMCLs<sup>SCR</sup> and HMCLs<sup>J1/2KD</sup> or from co-cultures systems of HS5 cells and HMCLs<sup>SCR</sup> or HMCLs<sup>KD</sup>
- Human recombinant Jagged1 or Jagged2 at the concentration of 20  $\mu$ l/mL according to manufacturer's instruction

After 16 hours of incubation at 37 °C, photos of the tube-like structures were acquired after overnight incubation with at Zeiss PrimoVert at 4X magnification. Numbers of area and branch points were analyzed using the ImageJ program.

### 3. RNA EXTRACTION AND qRT-PCR FOR GENE EXPRESSION ANALYSIS

#### 3.1 RNA extraction

HMCLs ( $5 \times 10^5$  cells) were lysed with 200  $\mu$ l of TRI Reagent (Sigma-Aldrich) 5 minutes at room temperature (RT). To isolate RNA, 1/5 of initial Tri reagent volume of chloroform was added and incubated 15 minutes RT. The mixture was centrifuged 12000g for 15 minutes at 4°C, obtaining the separation of a lower red phenol-chloroform, an interphase and the upper aqueous phase. The aqueous phase containing the RNAs was collected in a new centrifuge tube e 100% isopropanol was added to precipitate RNA. of. After incubation 10 minutes RT, the suspension was centrifuged 12000g for 10 minutes at 4°C. The obtained pellet was washed twice with 75% ethanol at 7500g for 5 minutes at 4°C. The purified RNA was dried 5 minutes RT and quantified by Nanodrop (ThermoFisher). RNA was considered usable for gene expression analysis only with 260/280 and 260/230 ratios higher then 1,8 and 1,9.

#### 3.2 Reverse transcription

cDNA was obtained by reverse transcription with RevertAid M-MuLV Reverse Transcriptase (ThermoFisher).

RNA sample was incubated with random primers 65°C for 5' as followed:

- 1 $\mu$ g RNA
- 1 $\mu$ l of Random primers (300 ng/ $\mu$ l)
- H<sub>2</sub>O up to 14 $\mu$ l

At the RNA and random primers were added the following mix (6 ml/ tube):

- 4  $\mu$ l of 5x Buffer
- 1 $\mu$ l dNTPs 10mM
- 1 $\mu$ l of RevertAid M-MLV Reverse Transcriptase (200 U/ $\mu$ l)

The mix were incubated as followed:

- 10 minutes 25 °C

- 50 minutes 37°C
- 10 minutes 70 °C

### 3.3 Quantitative Real-Time PCR

Quantitative PCR (qRT-PCR) was performed with a Step-One Plus PCR system (Applied Biosystems, Life Technologies Italia, Italy) using GoTaq® qPCR (Promega, Italy).

The reaction mix for a 96-well plate is the following (final volume of 10 µl):

- 5µl GoTaq® Green Master Mix (2X)
- 0,1µl CXR dye
- 0,5µl 10 mM Primer Mix (final concentration 0,5 µM) (The primer sequences are reported in **Table 3**)
- 1µl cDNA (10ng total)
- 3,4µl H<sub>2</sub>O RNase-free

Gene target expression was obtained using the  $\Delta$ Ct method, using GAPDH as housekeeping gene. Differences in gene expression were determined using the  $\Delta\Delta$ Ct method applying the following formula  $2^{(-\Delta\Delta Ct)}$ .

|                 |                              |                               |
|-----------------|------------------------------|-------------------------------|
| <b>hGAPDH</b>   | 5'-ACAGTCAGCCG ATC TTC TT-3' | 5'-AATGGAGGGGTCATTGATGG-3'    |
| <b>h18S</b>     | 5'-GTAACCCGTTGAACCCATT-3'    | 5'-CCATCCAATCGGTAGTAGCG-3'    |
| <b>hJagged1</b> | 5'-GCAACACCTTCAACCTCAAG-3'   | 5'-GTTGAACGGTGTCTACTGG-3'     |
| <b>hJagged2</b> | 5'-TCATCCCCTTCCAGTTCG-3'     | 5'-TGGTATCGTTGTCCCAGTC-3'     |
| <b>hHES1</b>    | 5'-AGGCGGACATTCTGGAAATG-3'   | 5'-CGGTACTIONCCCCAGCACACTT-3' |
| <b>hHES6</b>    | 5'-CGTGAGGATGAGGACGG-3'      | 5'-AGGCTCTCGTTGATCCG-3'       |
| <b>hVEGF-A</b>  | 5'-GGGCAGAATCATCACGAAGT-3'   | 5'-TGGTGATGTTGGACTCCTCA-3'    |
| <b>hHPRT</b>    | 5'-TTTATGTCCCCTGTTGACTGGT-3' | 5'-GTAGCCCTCTGTGTGCTCAA-3'    |

**Table 3: sequence of the primers used for qRT-PCR.**

#### 4. ELISA for VEGF-A

The collected supernatants of single cultures or co-cultures system were centrifuged twice at 101 g for 5 minutes to remove the cells and put in ice or frozen at -80 °C for the analysis of VEGF content by an ELISA kit (Thermo Scientific) following manufacturer instructions. The sample was diluted 10 times and analyzed in duplicate. Secreted VEGF protein concentration was normalized to the numbers of cells. For co-cultures, the total VEGF protein content was subtracted from the VEGF protein content of the HMCLs and normalized to the number of HS5 cells.

#### 5. ISOLATION AND PURIFICATION OF EXTRACELLULAR VESICLES FROM MM CELL LINES

For extracellular vesicle (EVs) isolation, MM cell lines were seeded at a density of  $3 \times 10^5$  cells/ml in RPMI1640 medium with 10% FBS depleted of bovine EV previously obtained with 16 hours ultracentrifugation at 110,000 g at 4°C. After 48 hours, CM was collected and centrifuged 101 g for 5 minutes at room temperature (RT) to completely remove all the cells in suspension. For the experiment with the EVs, MM<sup>SCR</sup> and MM<sup>N2KD</sup> were treated for 7 days with Doxycycline 1 µg/ml and maintained in medium with FBS depleted of bovine EVs for the last 48 hours.

The CM obtained was purified by performing 3 sequentially centrifugation at increasing speed (1000 g, 2000 g, 3000 g) for 15 minutes at 4°C. After every centrifugation the pellet was discarded, and the supernatant transferred into a new tube. After the last centrifugation, the supernatant was ultracentrifuged for 75 minutes at 110.000 g at 4°C using a Himac CP100NX ultracentrifuge (Himac Japan), as previously reported from the group of prof. Bollati (169).

The obtained pellet was resuspended as followed:

- 0,1 µm filtered PBS for characterization of size and concentration by Nanoparticles Tracking Analysis (NTA) or for the analysis by transition electronic microscopy (TEM).
- For the western blot analyses, EVs were resuspended in Radioimmunoprecipitation assay (RIPA) buffer and quantified using a Bradford assay (Himedia, Italy).
- For functional assays, EVs were resuspended in serum-free medium RPMI1640. For osteoclastogenesis and angiogenesis we used an amount of EVs isolated from the



equivalent volume of medium used in each experiment, while for Notch reporter assay *in vitro* EVs were concentrated 40 times respect of initial volume.

For the *in vitro* and *in vivo* experiments with EVs, the ultracentrifuged fresh medium previously depleted of bovine EVs was used as negative control.

To isolate different EV subpopulations, CM was firstly ultracentrifuged 30 minutes at 10,000 g at 4°C to remove cell debris and apoptotic bodies, and then the supernatant was subsequently ultracentrifuged 75 minutes at 20,000 g to obtain large EVs and after at 110,000 g for 75 minutes at 4 °C to collect small vesicles respectively. The obtained pellets were resuspended in RIPA buffer for western blot analysis.

## 6. ANALYSIS OF EVs BY NANOPARTICLE TRACKING ANALYSIS

EVs were characterized by Nanoparticle Tracking Analysis (NTA) using the NanoSight NS300 (Malvern Panalytical Ltd, Malvern, UK) in collaboration with the group of prof. Valentina Bollati, Università degli Studi di Milano. The advantages of this technique rely on the properties of both light scattering and Brownian motion to obtain the nanoparticle size distribution of samples in liquid suspension.

Particles in liquid suspension are loaded into a sample chamber, which is illuminated by a specially shaped laser beam. Particles in the path of the beam scatter the laser light which is easily collected by a microscope objective and is viewed with a digital camera. A camera level of 12 and five recordings of 30 seconds were used for acquisition of each sample. The NTA software (Malvern Panalytical Ltd, Malvern, UK) analyses many particles individually and simultaneously, and by using the Stokes Einstein equation, calculates their hydrodynamic diameters.

## 7. TRANSMISSION ELECTRON MICROSCOPY

Transmission electron microscopy (TEM) allowed us to investigate the morphology of the isolated EVs and was performed in collaboration with the group of Vincenza Dolo, Università degli Studi dell'Aquila. EVs resuspended in 0,1 µm-filtered cold PBS 1X were adsorbed into 300-mesh carbon-coated copper grids for 5 minutes at RT. Then, EVs were fixed in 2% glutaraldehyde, previously diluted in PBS, for 10 minutes and briefly rinsed in Milli-Q water. The negative staining was performed with 2% phosphotungstic acid brought to pH 7,0 with NaOH. Finally, the grids were examined with a Microscope Zeiss STEM GEMINI 500. All materials are from Electron Microscopy Sciences (Hatfield, PA, USA).

## 8. IN VITRO INTERNALIZATION ASSAYS OF EVs

For the *in vitro* analysis of EVs uptake, the 48 hours-CM of RPMI8226 were ultracentrifuged and the obtained pellet was resuspended in cold 0.1 µm-filtered PBS and stained with cell-tracker CM-DIL (Invitrogen, USA) at the final concentration of 1 µg/ml by incubating it at 37°C for 5 minutes and then at 4°C for 15 minutes, according to the manufacturer's instructions. To remove the non-binding dye, the labelled EVs were washed with 0,1 µm-filtered PBS by ultracentrifugation for 75 minutes at 110.000 g at 4°C. An ultracentrifugation tube containing the dye resuspended in PBS without EVs was used as a negative control. The pellet with labelled EVs was resuspended in phenol red-free RPMI1640 without FBS and quantify using the reported below Bradford assay.

The uptake efficiency was assessed by flow cytometry and fluorescence microscopy.

### 8.1 Flow cytometry analysis

Quantitative analysis of EV uptake was performed seeding Raw264.7 and HPAEC cells at the density of  $1.5 \times 10^5$  cells/ml in 48-well plate with 250 µl of the appropriate medium of culture as reported above. After 24 hours, cells were treated with 15 µg of CM-DIL dye labelled-EVs or with CM-DIL alone as a control for 4 hours at 37°C and 4°C. After 4 hours of treatment, the medium was removed, and the cells were detached and washed with PBS. For flow cytometric analysis, cells resuspended in PBS were analyzed in PE channel to assess the CM-DIL positive cells by using the FACS Verse flow cytometry (BD Biosciences, Italy).

### 8.2 Fluorescence microscopy analysis

For microscopy analysis, Raw264.7 and HPAEC cells were stained with 5 µM CFSE (Biolegend, Italy) following manufacturer's instructions and seeded  $3.5 \times 10^4$  cells/ml in 24 chamber slides in 500µl of appropriated completed medium. After 24 hours, cells were treated with 15 µg of CM-DIL positive-EVs or with the negative control, for 4 hours at 37°C or 4°C. After 4 hours of treatment, the slides were washed with PBS and fixed with PFA 2% for 15 minutes. Fixed cells were washed with PBS and stained with 4',6-diamidino-2-phenylindole (DAPI; 1:10.000). The analysis was performed with a DM-IRE 2 Leica microscope equipped with a Retiga Electro CCD camera and Micro-Manager software and the images were acquired in z-stack scan mode with a HCX PL APO 63x objective, by applying the same acquisition setting, excitation intensity, acquisition time, step size.

## 9. WESTERN BLOT ANALYSIS

Total protein concentration of cells and EV lysates was quantified using the Bradford protein assay. Samples were prepared adding 5X loading dye and RIPA buffer to the needed quantity of proteins (5-40 µg), to the final volume of 20 µl/ well. Then, samples were loaded into a 4-12% polyacrylamide precast gel in presence of SDS (SDS-PAGE; Genscript, USA) As reference for protein molecular weight, 5µl of Colour Prestained Protein Standard marker (New England Biolabs, Ipswich, MA) were loaded as well. Electrophoresis run was performed using Mini-PROTEAN Tetra (Bio-Rad Laboratories, Inc., Hercules, CA). Separated proteins were transferred onto a nitrocellulose membrane (Hybond-ECL, Amersham Bioscience, Italy), and blocked with 5% nonfat milk in TBS-T (20 mM Tris-Cl, pH 7.5, 150 mM NaCl, 0.05% Tween 20). Membranes were incubated overnight at 4°C with primary antibody (**table 4**) followed by incubation with the appropriated HRP-conjugated species-specific secondary antibody (Promega, Italy). Chemiluminescence was detected by the Western Bright ECL HRP substrate (Advansta Inc., USA) or by Super Signal™ West Femto Maximum Sensitivity Substrate (Thermo Fisher Scientific, Italy) and using the Alliance HD 6 western blot imaging system (Uvitec, UK).

|                              | <b>Company</b>                 | <b>Molecular weight</b> | <b>type</b> | <b>dilution</b> |
|------------------------------|--------------------------------|-------------------------|-------------|-----------------|
| anti-Jagged1 (D4Y1R)         | Cell Signaling Technology, USA | 180 kDa                 | Rabbit      | 1:500           |
| anti-Jagged2 (H-143)         | Santa Cruz Biotechnology, USA  | 150 kDa                 | Rabbit      | 1:500           |
| anti-Notch2 (D76A6)          | Cell Signaling Technology, USA | 250 and 110 kDa         | Rabbit      | 1:1000          |
| Anti-Notch2-ICN (SAB4502022) | Sigma-aldrich                  | 83 kDa                  | Rabbit      | 1:1000          |
| Anti-Notch1 (D1E11)          | Cell Signaling Technology, USA | 300 and 110 kDa         | Rabbit      | 1:1000          |
| Anti-Notch3 (D11B8)          | Cell Signaling Technology, USA | 270 and 90 kDa          | Rabbit      | 1:1000          |
| Anti-Notch4 (STJ90070)       | St John's Laboratoty, London   | 210 and 65 kDa          | Rabbit      | 1:1000          |
| anti-HA (C29F4)              | Cell Signaling Technology, USA | –                       | Rabbit      | 1:1000          |
| anti-TSG101 (ab125011)       | AbCam, UK                      | 44 kDa                  | Rabbit      | 1:500           |
| $\beta$ -actin               | Sigma Aldrich, Italy           |                         |             | 1:1000          |
| $\alpha$ -tubulin (sc-12462) | Santa Cruz Biotechnology, USA  | 55 kDa                  | Rabbit      | 1:1000          |

**Table 4: list of the monoclonal antibody used for western blot analysis.** In the table were included their target molecular weight, type and the dilution applied.

## 10. DETENTION SYSTEM TO TRACK NOTCH2 EV-MEDIATED TRANSFER FROM DONOR TO RECEIVING CELLS

For the *in vitro* model of EV-mediated cellular communication, HEK293 cells were seeded  $2.5 \times 10^6$  in 100 mm plate and transfected with pcDNA3.1 expressing Notch2 protein conjugated with a hemagglutinin amino acid tag (HA; pcDNA-3.1-N2HA) or mock pcDNA3.1 plasmid using TurboFect transfection reagent (ThermoScientific) according to the manufacturer's protocol. After 16 hours, the medium was replaced with DMEM 10% FBS.

For EVs isolation, after 24 hours, the medium was replaced with DMEM with 10% EV-depleted FBS previously obtained by a 16-hour ultracentrifugation at 110.000 g at 4°C. After 48 hours of transfection, cells were lysate for western blot analysis and the derived EVs were isolated by ultracentrifugation following the above-mentioned protocol. Half of the isolated EVs (from both pcDNA3.1-empty and pcDNA3.1-N2-HA) was resuspended serum-free DMEM and used to treat receiving HEK293 cells. The other half was resuspended in 40  $\mu$ l RIPA buffer with the proteases and phosphatases inhibitors cocktail for western blot analysis.

Receiving HEK293 cells were seeded  $1 \times 10^5$  cells/ml in 2 wells of a 6-multiwell plate and treated with 60  $\mu$ l of previously isolated EVs six times within 48 hours (once the same day, three times the day after, twice the third day). A protein lysate of these cells was obtained in 50  $\mu$ l of RIPA buffer + proteases and phosphatases inhibitors cocktail.

Protein extracts obtained from donor and receiving HEK293 cells and from EVs derived by donor cells were analyzed by western blot using an anti-HA primary antibody.

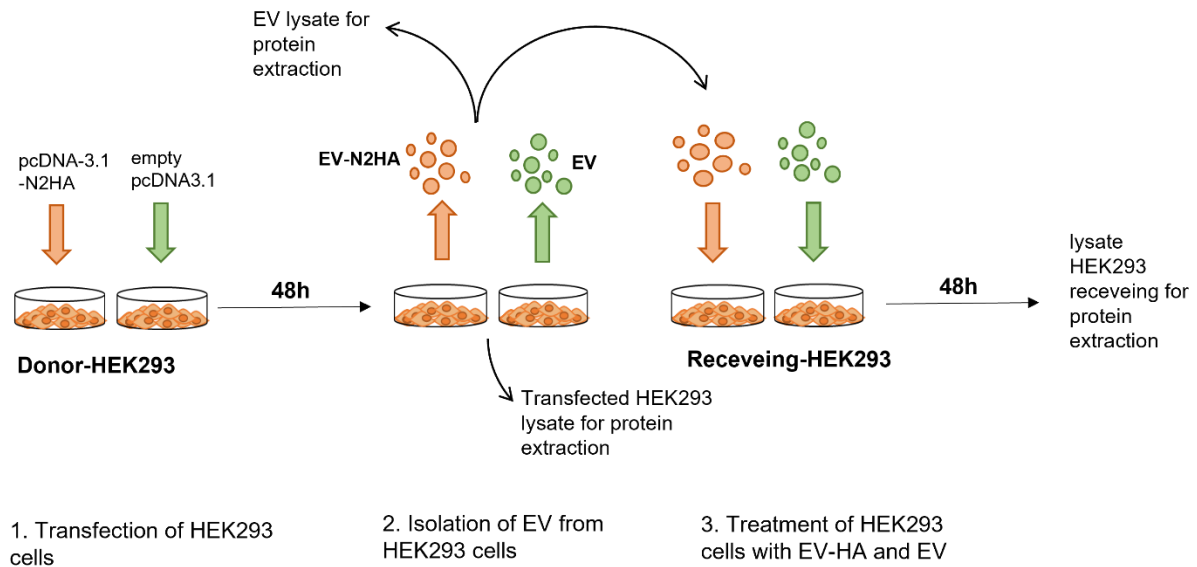


**Figure 7: schematic protocol of the *in vitro* system of cellular communication mediated by EVs.**

## 11. LUCIFERASE NOTCH REPORTER ASSAY

To perform the dual luciferase Notch reporter assay, HeLa cells were transfected with pNL2.1[Nluc/Hygro], a plasmid containing both a Notch responsive element (6XCSL) and NanoLuc® luciferase expressing system. The transfection efficiency was normalized co-transfecting HeLa cells with a thymidine kinase promoter-driven Firefly luciferase expressing vector, pGL4.54 [luc2 / TK].

For transient transfection, HeLa were seeded  $2.5 \times 10^5$  cells/well in a 6-multiwell plate and transfected with the TurboFect system (Thermofisher, Italy) using the following mix (previously incubated 20 minutes at RT).

- vector pNL2.1 [Nluc/Hygro]                      240 ng
- vector pGL4.54 [luc2/TK]                        240 ng
- empty pcDNA as a carrier                        up to 2µl
- serum-free DMEM                                 400µl

After 16 hours, transfected HeLa cells were seeded  $12.5 \times 10^3$  cell/well in a 96-well and treated with MM-EVs or the appropriate negative control as reported before. After 24 hours,

luciferase activity was measured using Nano-Glo® Dual-Luciferase® Reporter substrate kit (NanoDLR™, N1620, Promega, Italy) and the Glowmax instrument (Promega, Italy) following manufacturer instruction.

## 12. IN VIVO EXPERIMENTS

The *in vivo* experiments were conducted in collaboration with the group of Prof. Anna Pistocchi, Università degli Studi di Milano. EVs were injected in the Transgenic zebrafish (*Danio rerio*) embryos obtained by crossing *Tg(T2KTp1bglob:hmgb1-mCherry)* with *Tg(fli1a:EGFP)* from the Wilson lab (University College London, United Kingdom). Zebrafish embryos were raised and maintained under standard conditions and national guidelines (Italian decree 4th March 2014, n.26).

For the EV microinjections, zebrafish embryos were washed, dechorionated for 5 to 10 min with 1 mg/ml pronase 48 hpf and anaesthetized with 0.016% tricaine (Ethyl 3-aminobenzoate methanesulfonate salt; Sigma-Aldrich). For the experiment, 10nl of RPMI8226-EV resuspended in PBS were injected into the duct of Cuvier with a manual microinjector (Eppendorf, Hamburg, Germany) using glass microinjection needles. After the injections, embryos were kept at 28 °C for 30 min and at 32 °C for the duration of the experiments.

To evaluate MM-EVs mediated Notch activation in zebrafish embryos, the efficiency of MM-EV uptake was evaluated 4 hours post injection (hpi) by fluorescence microscopy using the Leica DM 5500B microscope equipped with the DC480 camera. The fluorescence intensity was evaluated in the trunk region, specifically in the caudal hematopoietic tissue (CHT) area on photomicrographs with ImageJ software. Images were processed using the Adobe Photoshop program.

Representative images were acquired in confocal microscopy using Leica TCS SP2 AOBS equipped with 405 diodes, 488 Ar/ArKr and 543 HeNe lasers and analyzed by Leica Confocal Software (Leica Microsystems, Wetzlar, Germany). 20x images were acquired in xyz scan mode with a 20x objective, by applying comparable arrangement parameters: PMT gain/offset voltages, step size, scan speed, frame, and line average. Sequential scan mode between frames was applied to reduce the fluorophore cross talking between 543 and 488 emission and obtain all scans at the same current z position. 60x images were acquired with the same parameters using a 20x objective with additional 3x electronic zoom.

### 13. FUNCTIONAL ASSAY WITH EVs

#### 13.1 *Osteoclastogenic assay*

Raw264.7 cells were seeded in a 48-well plate in 250µl of RPMI1640 supplemented with 10% FBS at a density of  $1.25 \times 10^4$  cells/ well with or without 30 ng/ml RANKL and treated every 48 hours with RPMI8226 derived-EV or control. For experiment with DAPT, cells were treated with EVs or the control medium with or without the drug or the vehicle in the presence of RANKL.

After 7 days, Raw264.7 cells were fixed on the culture plates with citrate-acetone solution and stained for tartrate resistant acid phosphatase (TRAP kit, Sigma-Aldrich) following manufacturer instruction. Briefly, Raw264.7 were washed three times with PBS and fixed with citrate-acetone solution. The cells were washed three times with PBS and stained for 16 hours with the TRAP staining solution. After washing with PBS, the nuclei were stained with hematoxyline solution. Osteoclasts were identified under light microscopy enumerating TRAP positive cells with  $\geq 3$  nuclei. Representative images of TRAP positive osteoclasts were acquired with Olympus U-CMAD3 phase-contrast microscope equipped with a Zeiss Axiocam ICc1 camera at 4x magnification.

#### 13.2 *Tube formation assay with EVs*

HPAEC were seeded in each well 8000 cells in 100 µl of serum free-RPMI1640 onto Matrigel and treated for 13 hours with EVs or control medium. For experiment with the DAPT, cells were treated with MM-EVs or the control medium with the drug or the vehicle. After 13 hours the images were acquired with EVOS-inverted microscope (Euroclone S.p.A., Italy) at 4X magnification and the number of areas and branch points were analyzed through ImageJ program.

### 14. CELL VIABILITY ASSAY

The cell viability after treatment with DAPT was assessed by using the ability of the MTT assay to identify any cells with recognizable levels of mitochondrial activity.

To perform the assay, Raw264.7 and HPAEC cells were seeded at concentration used for the functional assays with EVs and treated with 50 µM of DAPT for 13 hours or 7 days, respectively. After the appropriate experimental time, 3-(4,5-dimethylthiazole-2-yl)-2,5-diphenyl tetrazolium bromide (MTT) (0,6 mg/ml) (Sigma) was added to each well for 3 hours at 37°C, only live cells can release the formazan crystals as reaction products of the



mitochondrial activity. To solubilize formazan crystals, the medium was gently removed, and acid isopropanol supplemented with HCl 0.025N was added. After 1 hour, the absorbance of the formazan solution was read with spectrophotometer at 550-570 nm, which is the only light absorbed by formazan, and 620-650 nm, absorbed by cell debris and well imperfections that was subtracted. Percentage cell survival is expressed as: (absorbance treated wells / absorbance of control wells) x 100%.

## 15. EX VIVO EXPERIMENTS

For the *ex vivo* experiment, EVs were isolated from the BM aspirates of Monoclonal gammopathy of undetermined significance (MGUS) and MM patients. The Institutional Review Board of Insubria Italy approved the design of this study (approval n. 1/2018). Written informed consent was obtained in accordance with the Declaration of Helsinki. Clinical information of patients is reported in **table 5**.

The blood samples were collected at the diagnosis in tubes containing disodium EDTA and processed to obtain plasma through centrifugation at 250 × g for 20 minutes at RT not later than 4 hours after withdrawal. To isolate EVs, the obtained plasma sample was diluted 1:3 with cold PBS and centrifuged three times at increasing speed as previously reported. The plasma was ultracentrifuged as reported above. For tube formation assay, EVs were resuspended in serum-free RPMI1226 in the same original volume and used at a 0.5x final concentration.

|   | All patients   | MGUS          | MM             |
|---|----------------|---------------|----------------|
| <b>Patients, no. (M/F)</b>                  | 18 (10/8)      | 6 (3/3)       | 12 (7/5)       |
| <b>Median age, y (IQR)</b>                  | 74 (16)        | 74 (16)       | 77 (15)        |
| <b>Median BM PC, % (IQR)</b>                | 37.5 (57.0)    | 8.0 (3.0)     | 57.5 (30)      |
| <b>Median M-protein, g/dl (IQR)</b>         | 2.33 (2.99)    | 0.90 (0.78)   | 3.57 (2.07)    |
| <b>Median U-protein, g/24h (IQR)</b>        | 0.35 (0.43)    | 0.17 (0.25)   | 0.50 (0.98)    |
| <b>Median sFLC, mg/L (IQR)</b>              | 397.5 (1083.1) | 132.2 (318.2) | 605.0 (1244.1) |
| <b>Median B2-MG, mg/L (IQR)</b>             | 3.77 (3.80)    | 2.30 (1.40)   | 4.30 (3.56)    |
| <b>Median calcemia, mg/dl (IQR)</b>         | 9.5 (0.8)      | 9.6 (0.3)     | 9.0 (1.0)      |
| <b>Median WBC, x 10<sup>9</sup>/L (IQR)</b> | 5.00 (2.78)    | 4.75 (2.78)   | 5.21 (2.42)    |
| <b>Median Hb, g/dl (IQR)</b>                | 12.2 (4.2)     | 13.1 (1.3)    | 10.3 (3.8)     |
| <b>Median PLT, x 10<sup>9</sup>/L (IQR)</b> | 195 (75)       | 188 (46)      | 207 (123)      |

**Table 5: clinical characteristics at presentation of patients. B2-MG:** B2-microglobulin; **BM PC:** bone marrow plasmacells; **Hb:** hemoglobin; **IQR:** interquartile range; **M-protein:** seric monoclonal protein; **MGUS:** monoclonal gammopathy of undetermined significance; **MM:** multiple myeloma;

PLT: platelets; sFLC: involved seric free light chains; U-protein: urinary monoclonal protein; WBC: white blood cells.

## 16. STATISTICAL ANALYSIS

Statistical analyses were performed using one-tailed or two-tailed Student t-test to compare the mean values and analysis of variance was performed by one-way ANOVA with Tukey post-test.

The sample minimum size for each *in vivo* experiment was determined based on a priori power analysis for a one-way ANOVA with an alpha level of 0.05 aimed to have power of 0.95, performed on data from a pilot study with 5 embryos for each condition (G-power 3.2 software)(170). Each *in vivo* experiment involved at least 16 embryos divided in 4 groups. The final analysis was performed by one-way ANOVA with Tukey post-test on data from 4 independent experiments, excluding outliers identified through the ROUT method (Q=1%) (171).

## RESULTS

### 1. MYELOMA CELL-DERIVED JAGGED LIGANDS PROMOTE TUMOR ANGIOGENESIS

Multiple-myeloma (MM) cells are characterized by an aberrant Notch signaling due to the overexpression of Notch2 receptor and ligands Jagged1 and 2. The Jagged-mediated homotypic interaction activates Notch pathway in MM cells leading to their proliferation and survival (71). The heterotypic interaction between MM cell derived-ligands and the receptor on the surface of surrounding bone marrow (BM) cells triggers Notch pathway leading to pro-tumorigenic effects, such as osteoclastogenesis and drug resistance (76, 77).

The first aim of my thesis work is to contribute to further clarify the outcome of Notch mediated communication between MM cells and non-tumor cell population in the surrounding BM. Considering the key role of the angiogenic switch in MM progression and of Notch signaling in angiogenesis, in this thesis work I investigated the outcome of Notch signaling triggered by Jagged 1 and 2 ligands expressed on MM cell surface on the angiogenic differentiation of endothelial cells (EC).

#### *1.1 Direct effect of Jagged ligands in the stimulation of the angiogenic potential of endothelial cells*

An inhibitory approach was used to evaluate the role of MM cell-derived Jagged ligands in angiogenesis. The ligands were knock down (KD) in two human myeloma cell lines (HMCLs), RPMI8226 and OPM2, by using siRNAs specific for Jagged1 and Jagged2 (HMCLs<sup>J1/2KD</sup>) or the scrambled (SCR) siRNA as control (HMCLs<sup>SCR</sup>). The KD efficacy was assessed by analyzing changes in the expression of Jagged1 and 2 mRNA and of the Notch transcriptional target genes by quantitative qRT-PCR, and of Jagged1 and 2 protein levels by Western blot. As shown in **fig. 8**, Jagged 1 and 2 are efficiently inhibited at gene (**fig. 8A**) and at protein level (**fig. 8B**), and inhibition of the Notch pathway activation was confirmed by the downregulation of the Notch target gene HES6 (**fig. 8B**).

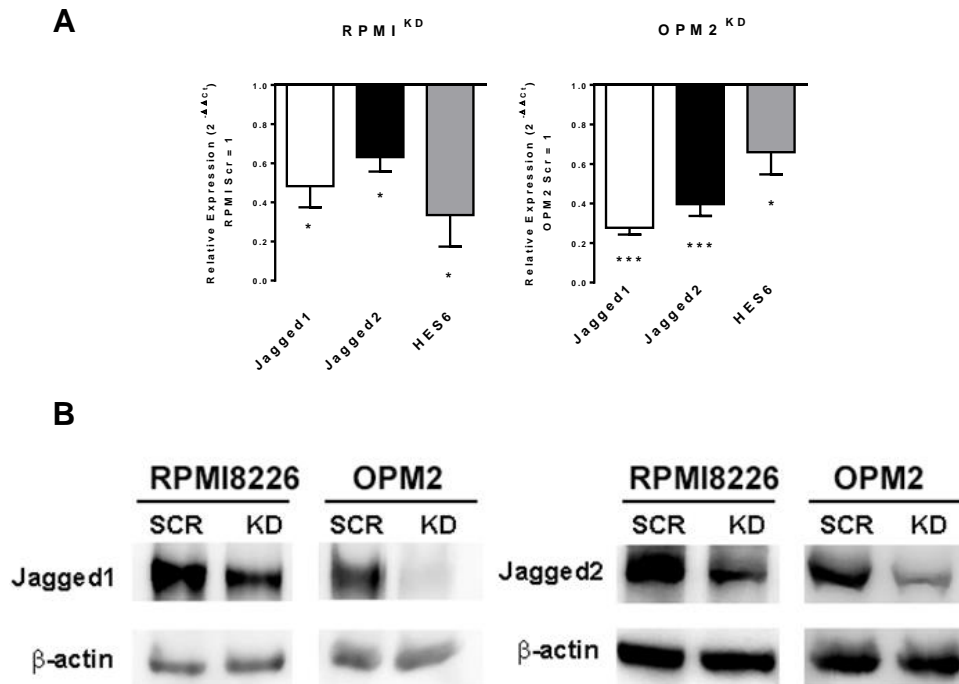


**Figure 8: analysis of Jagged1 and 2 KD efficiency both at a gene and protein level. (A)** qRT-PCR analysis to evaluate the KD efficiency at gene expression level. The variation of gene expression of Jagged1 and Jagged2 and the Notch target gene HES6 was normalized to GAPDH and calculated by the  $2^{-\Delta\Delta C_t}$  formula. Data are expressed as the mean value  $\pm$  SEM. Statistical analyses were carried out by one-tailed t-test; \* is for  $p \leq 0.05$ ; \*\*\* is for  $p \leq 0.001$ . **(B)** Western blot analysis of Jagged1 and Jagged2 in  $HMCLs^{SCR}$  or  $HMCLs^{J1/2KD}$ . Protein loading was normalized to  $\beta$ -actin.

Considering that MM cell derived Jagged1/2 boost Notch activation in the ECs (160), changes in EC angiogenic ability promoted by the Notch heterotypic activation triggered by MM cell-derived Jagged ligands were measured by using a tube formation assay. This assay reflects in the bidimensional system of Matrigel the endothelial ability to organize in a network of tubes.

At this purpose, primary human pulmonary artery endothelial cells (HPAECs) were seeded on Matrigel-coated wells and co-cultures in the presence of  $HMCLs^{SCR}$  or  $HMCLs^{J1/2KD}$  for 24 hours. Areas and branch points were analyzed by optical microscope (Zeiss PrimoVert). In **fig. 9**, representative images show that HPAECs cultured with  $HMCLs^{SCR}$  displayed a significantly increased ability to create a grid of tubes compared to HPAECs in direct contact with  $HMCLs^{J1/2KD}$ . Indeed, the count of the number of areas and branch points indicates that

a significant reduction in the angiogenic potential of ECs is present (approximately 50% for areas and 60% for branch points) suggesting the involvement of MM cell-derived Jagged ligands.

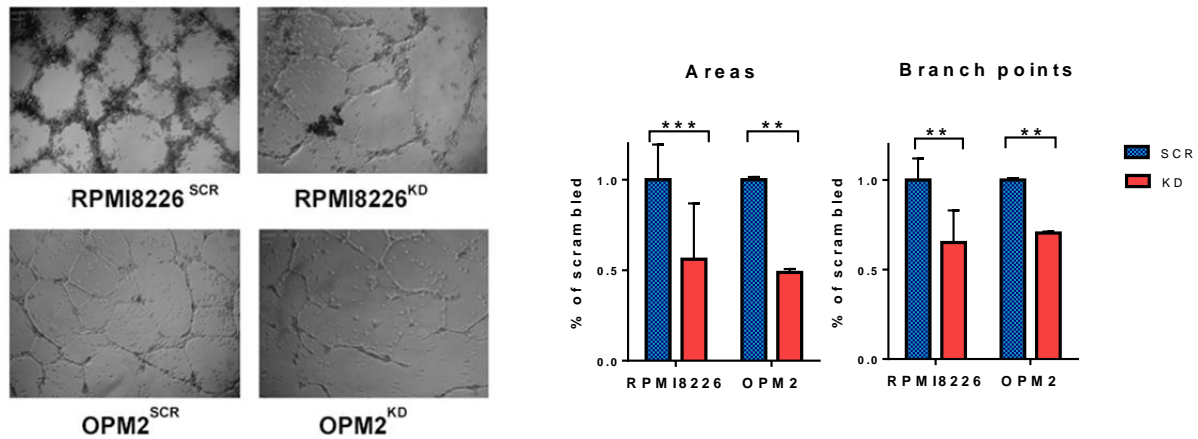


**Figure 9: tube formation assay on Matrigel with co-culture systems of HMCLs<sup>SCR</sup> or HCMLsJ<sup>1/2KD</sup> and HPAECs.** The panel on the left shows 4X magnification images representative of each condition (Zeiss PrimoVert). The graph on the right shows the analysis of the number of areas and branch points. Data are expressed as mean values +/- SEM. Statistical analysis was carried out by one-tailed t-test; \* =  $p \leq 0.05$ ; \*\* =  $p \leq 0.01$ ; \*\*\* =  $p \leq 0.001$ .

To elucidate if the mechanism involved in MM cell-derived induced angiogenesis relies on a direct contact and/or on the release of soluble angiogenic factors, this assay was repeated using different stimuli.

To assess if MM cell-derived Jagged ligands may induce angiogenesis, I performed the tube formation assay by stimulating HPAECs with soluble Jagged1 and Jagged2 peptides. These results indicated that the Jagged ligands might increase the organizing ability of HPAECs (**fig. 10**), indicating that MM cell-derived Jagged ligands could directly trigger the endothelial Notch activation and the angiogenic response. Interestingly, Jagged2 showed a greater effect than Jagged1. Indeed, considering the analysis of branch points, Jagged2 induces a stronger angiogenic effect (350%) in comparison to the effect of Jagged1 peptide (192%).

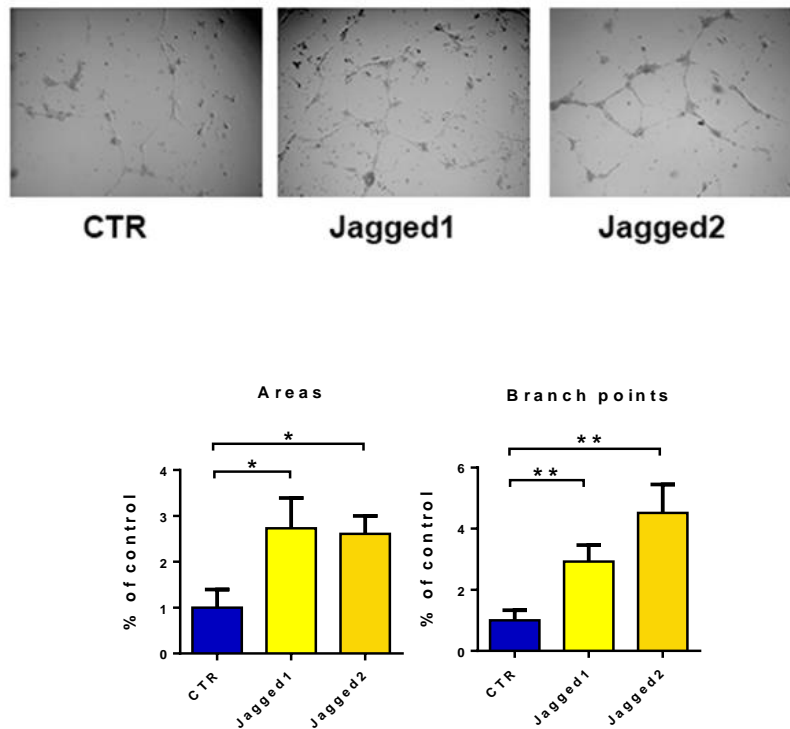


**Figure 10: tube formation stimulated by Jagged1 and Jagged2 peptides 20  $\mu\text{g/ml}$ .** The upper panel reported representative images of each condition (4X magnification). Areas and branch points were enumerated by optical microscope (EVOS-inverted microscope). Results are expressed as the mean value  $\pm$  SEM. Statistical analysis was performed by a one-tailed t test; \* =  $p \leq 0.05$ ; \*\* is for  $p \leq 0.01$ ; \*\*\* =  $p \leq 0.001$ .

### 1.2 Effect of MM-derived soluble factors on angiogenic potential of EC

Considering the role of Notch pathway in MM ability to release cytokines, I investigated the contribution of Jagged ligands in the release of MM-derived angiogenic factors. To address this point, the tube formation assay was assessed by treating ECs with the conditioned medium (CM) of HMCLs<sup>SCR</sup> or HMCLs<sup>J1/2KD</sup>. As shown in **fig. 11**, CM produced by HMCLs<sup>J1/2KD</sup> showed a significantly reduced ability to induce HPAECs to organize a grid-like structure if compared to HMCLs<sup>SCR</sup> derived CM, displaying a decreased number of areas (23% and 35%, for RPMI8226 and OPM2, respectively) and branch points (20% and 27%).

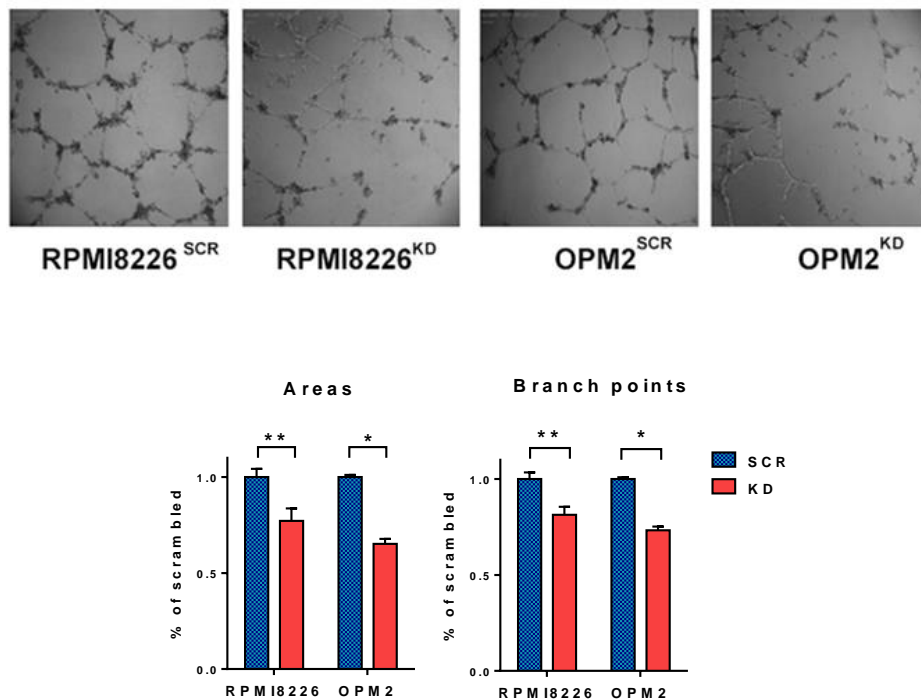


**Figure 11: tube formation assay on HPAECs with conditioned media (CM) of HMCLs<sup>SCR</sup> or HCMLs<sup>J1/2KD</sup>.** The upper panel shows 4X magnification images (Zeiss PrimoVert). The bottom graphs show the percentage of variation of areas and branch points of HCMLs<sup>J1/2KD</sup> in comparison to HMCLs<sup>SCR</sup>. Data are expressed as the mean value +/- SEM. Statistical analysis was carried out by a one-tailed t test; \* is for  $p \leq 0.05$ ; \*\* is for  $p \leq 0.01$ ; \*\*\* is for  $p \leq 0.001$ .

These results indicate that HMCLs<sup>SCR</sup> or HCMLs<sup>J1/2KD</sup> produce different levels of angiogenic factors responsible of the different angiogenic effects of the produced CM. Since vascular endothelial growth factor (VEGF-A) is an angiogenic factor whose expression has been reported to be promoted in MM cells by stimulation of BMSC-derived Jagged (68), we investigated its possible modulation. **Fig. 12** shows qRT-PCR analysis (**12A**) and an ELISA (**12B**) demonstrating that Jagged ligands KD in HMCLs decreases VEGF-A gene expression and its protein secretion, respectively.

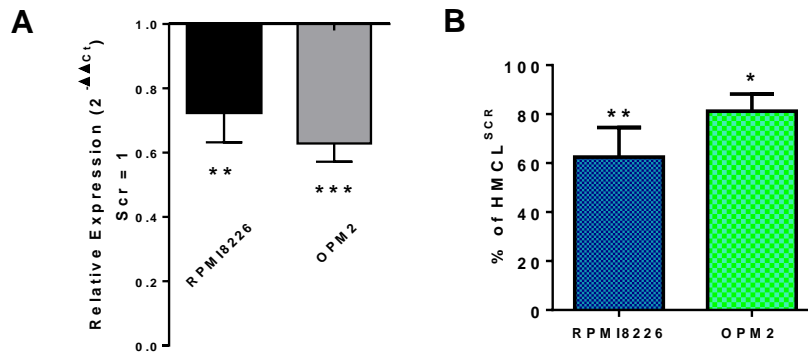


**Figure 12: VEGF variation in HMCLs<sup>SCR</sup> and HMCLs<sup>J1/2KD</sup>.** (A) the mRNA level was assessed by qRT-PCR analysis, shown as relative gene expression variation normalized to GAPDH calculated by the 2<sup>-ΔΔCt</sup> formula. (B) The protein level was analyzed by ELISA, as amount of VEGF-A released by HMCLs<sup>J1/2KD</sup> normalized on VEGF-A expressed by HMCLs<sup>SCR</sup>. For each sample, the amount of VEGF-A (pg/mL) was normalized to the concentration of producing cells and expressed as the mean value +/- SEM. Statistical analyses were carried out by one-tailed t-test; \* = p ≤ 0.05; \*\* = p ≤ 0.01; \*\*\* = p ≤ 0.001.

These obtained results suggested that HMCLs may induce angiogenesis by triggering Notch signaling activation in ECs *via* heterotypic Jagged-mediated Notch activation and, additionally, by the secretion of pro-angiogenic VEGF-A promoted by Jagged-mediated homotypic activation.

## 2. MYELOMA CELL DERIVED JAGGED1 AND 2 INCREASE BONE MARROW STROMAL CELL ANGIOGENIC POTENTIAL

Starting from the well documented role of MM-associated bone marrow stromal cells (BMSCs) in tumor angiogenesis (151, 172) and from the observed effect of Notch pathway activation in inducing BMSC release of protumor factors, among which those involved in angiogenesis such as VEGF and the stromal cells derived factor 1 (SDF-1)(68, 76) we investigated if the myeloma Jagged ligands could trigger Notch signaling in BMSCs boosting their pro-angiogenic potential.

To address this issue, I evaluated changes in the angiogenic potential of BMSC pre-treated for 24 hours with HMCLs<sup>SCR</sup> or HMCLs<sup>J1/2KD</sup>.

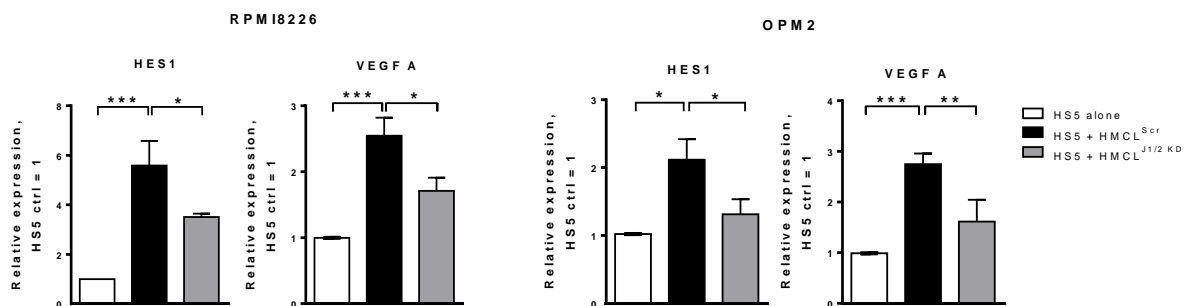
First, I assessed the ability of MM-derived Jagged ligands mediated activation of Notch in the BMSCs by co-cultivating HMCLs<sup>SCR</sup> and HMCLs<sup>J1/2KD</sup> with the human BMSC line HS5



and measuring the variation in the transcription of the Notch target gene HES1. The quantitative qRT-PCR analysis in **fig. 13A** indicates that HMCLs<sup>SCR</sup> upregulate HES1 gene expression if compared to the expression level analyzed in HS5 cultured alone; on the other hand, HES1 genes expression is significantly reduced with HMCLs<sup>J1/2KD</sup>, indicating that MM cell-derived Jagged ligands activate Notch signaling in stromal cells.

In the same cells, the possible variation of VEGF-A gene expression was also assessed. Results indicate that HMCLs<sup>SCR</sup> increased VEGF-A gene expression in HS5 cells, while the effect was significantly lower in the presence of HMCLs<sup>J1/2KD</sup> (**fig. 13A**). Consistently, ELISA of CM of HS5 cells cultured for further 24 hours after the pretreatment with HMCLs<sup>SCR</sup> and HMCLs<sup>J1/2KD</sup> confirmed that VEGF-A protein expression in HS5 cells was strongly upregulated by HMCLs<sup>SCR</sup> compared to HS5 alone, of approximately 193% for RPMI8226 and 76% for OPM2 (**fig. 13B**). On the contrary, VEGF secretion was significantly lower when HS5 cells were stimulated by HMCLs<sup>J1/2KD</sup>, indicating that the MM cell ability to induce VEGF-A secretion relies on Notch signaling activation in the BMSCs mediated by Jagged ligands.

**A**



**B**

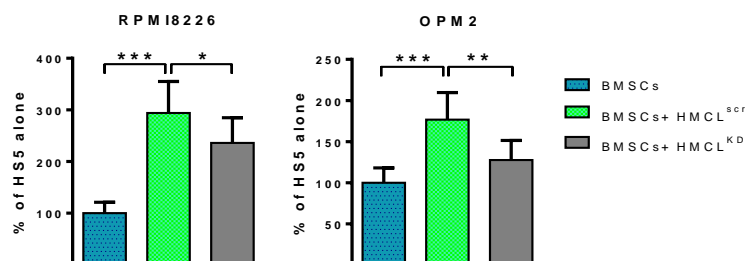


**Figure 13: activation of Notch signaling and VEGF-A expression in HS5 cells or in co-cultured with HMCLs<sup>SCR</sup> or HMCLs<sup>J1/2KD</sup>. A) qRT-PCR of the relative gene expression variation**

for the Notch target gene HES1 and VEGF (normalized to HRPT) calculated by the  $2^{-\Delta\Delta Ct}$  formula; **(B)** ELISA for VEGF-A secreted by HS5 alone in the medium. Data represent the amount of VEGF released by each culture normalized on VEGF expressed by HMCL cultured alone. In each sample, the amount of VEGF (pg/mL) was normalized to the cell concentration. Data are expressed as the mean value  $\pm$  SEM. For the two assays the statistical analyses were carried out by one-way ANOVA and Tukey post-hoc test. \* =  $p \leq 0.05$ ; \*\* =  $p \leq 0.01$ ; \*\*\* =  $p \leq 0.001$

To assess the biological outcome of the Notch-mediated VEGF release by BMSCs, I performed a tube formation assay by treating HPAEC with the CM derived from the co-culture between HS5 and HMCLs<sup>SCR</sup> or HMCLs<sup>J1/2KD</sup>. Results in **fig. 14** show that the CM from HS5 cells cultured alone can intrinsically stimulate EC organization, which is boosted in the presence of HMCLs<sup>SCR</sup>. Indeed, the CM from the co-culture system of HS5 cells and HMCLs<sup>SCR</sup> increased the grid structure of HPAEC, confirmed by the count of areas (94% and 60%, for RPMI8226 and OPM2, respectively) and branch points (approximately 60% for both HMCLs). On the contrary, CM from HS5 cells cultured with HMCLs<sup>J1/2KD</sup> did not increase the tube organization ability of HPAECs compared to the CM from unstimulated HS5.

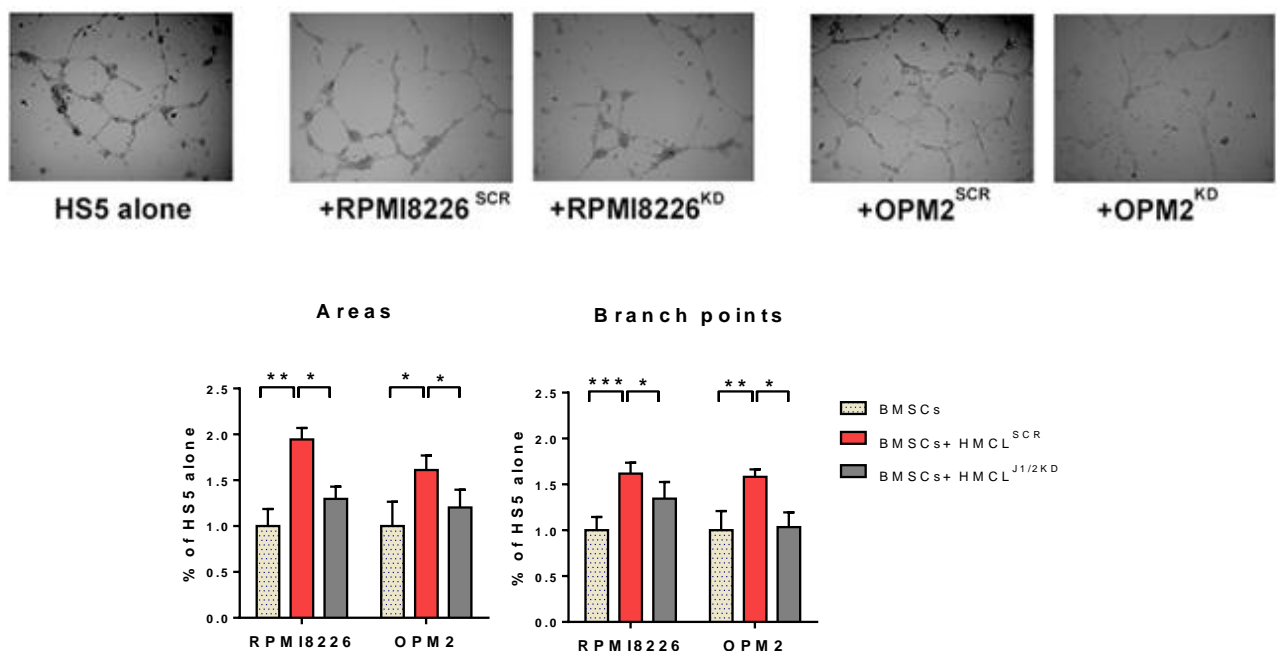


**Figure 14: tube formation assay of the HPAECs stimulated with CM secreted by co-culture systems of the HS5 cells and HMCLs<sup>SCR</sup> or HMCLs<sup>J1/2KD</sup>. The upper panel shows 4X**

magnification images representative of each condition. The bottom graphs show the quantification of the number of areas and branch points. Data are expressed as the mean value +/- SEM. Statistical analyses were carried out by ANOVA and Tukey's post-tests; \* $p \leq 0.05$ ; \*\* $p \leq 0.01$ ; \*\*\* $p \leq 0.001$

These obtained results suggested that Notch signaling activation in the BMSCs induced by myeloma Jagged ligands improved the BMSC angiogenic potential by promoting the release of soluble factors, such as VEGF-A.

### 3. MYELOMA CELL RELEASE EXTRACELLULAR VESICLES THAT CARRY NOTCH2 AS CARGO

Previous works of this and other research group together with the first part of my thesis indicate a key role of Notch signaling in the pathological communication between MM cells and the cell population present in the BM.

The evidence that extracellular vesicles (EVs) play a key role in MM progression and may transfer important molecular messages from MM cells to nearby cells (173), prompted us to further study their possible involvement in Notch mediated pathological communication as possible vehicles at long distance of Notch signaling members from MM cells to BM cell populations. In particular, this work focuses osteoclast (OCL) progenitors and EC with the purpose to investigate the outcome on the osteoclastogenesis and the angiogenic switch, two key features of MM progression also involved in metastatic dissemination of MM cells.

#### *3.1 Characterization of EVs isolated from MM cells*

I firstly investigated the ability of the two MM cell models in exam, RPMI8226 and OPM2, to release EVs. As reported in the methods section, after 48 hours of culture, the CM was purified from cell debris by performing three centrifugations at increasing speed and EVs were isolated by high-speed ultracentrifugation (110 g for 75 minutes) (169). According to Society of Extracellular Vesicles (ISEV) guidelines (79), RPMI8226 and OPM2-derived EVs (MM-EVs) were characterized for size and concentration by nanoparticle tracking analysis (NTA) and morphology through transmission electronic microscopy (TEM).

The NTA, using the properties of laser light scattering microscopy and Brownian motion, permits to obtain information on the size distributions of particles in liquid suspension, in

particular the nanosight instrument detect particles in the range of 10–1000 nm (174). The representative graphs of NTA reported in **fig. 15** show a vesicle size distribution ranging from 50 and 800 nm, peaking around 200 nm with a mean size of 230.6 nm and 222.4 nm, and an average D50 (size point below which 50% of EVs is contained) of 205.1 nm and 196.4 nm, for RPMI8226 and OPM2 respectively. The asymmetrical distribution of the graphs reveals the presence of a heterogeneous size population characterized by both small (30-200 nm) and large vesicles (200-1000 nm), according to the ISEV classification of EVs (79).

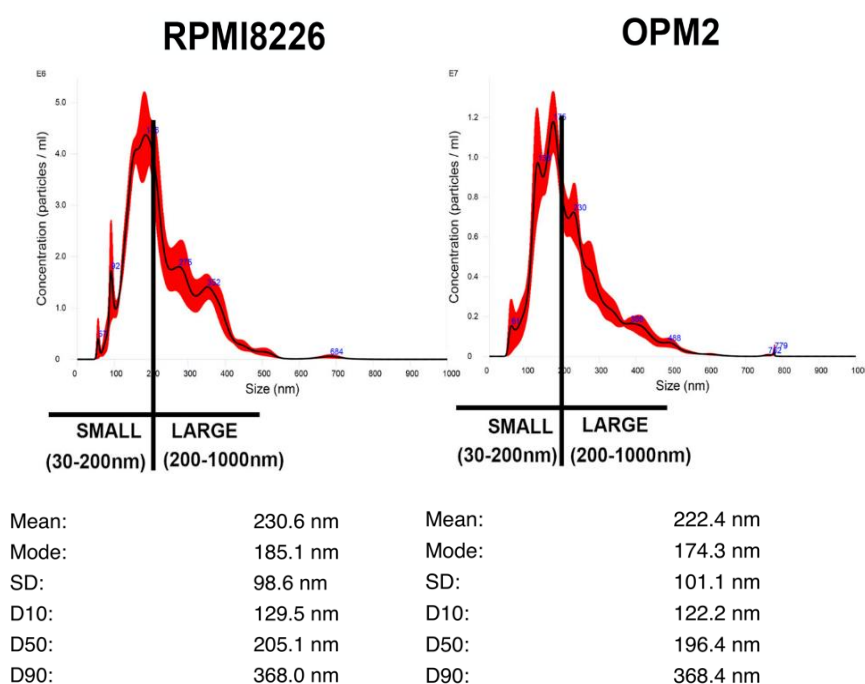


**Figure 15: representative NTA analysis on MM-EVs from RPMI8226 and OPM2 cell lines.** The concentration/size graphs reveal the presence of both small and large EVs.

To characterize the morphology of MM-EVs, a TEM analysis was also performed. This technique permits to distinguish EVs from non-EV particles thanks to its nanometer resolution and to assess EV integrity. According to the representative images reported in **fig. 16**, results from TEM analysis suggest the presence of intact small and large EVs, heterogeneous in shape.

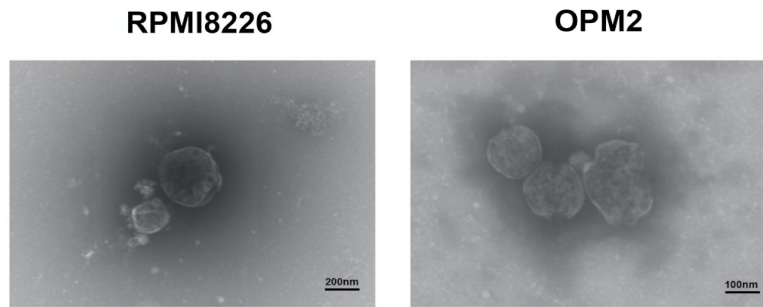


**Figure 16: representative TEM images of MM-EVs from RPMI8226 and OPM2.** Images were acquired by using 100X magnification (Microscope Zeiss 112 STEM GEMINI 500).

### *3.2 Uptake of MM-EVs on target cells*

The key role of EVs in cellular communication is based on their ability to interact with the recipient cells, through a superficial contact or after the uptake(87). So, to assess the possible effect of MM-EVs on target cells, I investigated their ability to be internalized in the monocyte and endothelial cell models, Raw264.7 and HPAECs, respectively.

To track EV uptake, RPMI8226 derived EVs (RPMI8226-EVs) were purified and fluorescently labeled with the red lipophilic dye CM-DIL, which upon internalization through the membrane is transformed into cell membrane-impermeant reaction products. The uptake was visualized by fluorescent microscopy and measured by flow cytometry after 4 hours of MM-EVs addition to Raw264.7 and HPAECs cell media. To exclude false-positive signals associated to micelles or aggregates from the analysis of EV internalization analysis, CM-DIL without EVs was added to media as negative control.

RPMI8226-EVs uptake was assessed by confocal analysis (Leica TCS SP2 AOBS) of receiving Raw264.7 and HPAECs cells and quantified by flow cytometry analysis of CM-DIL+ receiving cells. According to results reported in **fig. 17A**, CM-DIL positive RPMI-EVs can be internalized in both Raw264.7 cells and HPAECs. The two receiving cell types were previously stained with CSFE (green) to color the cytoplasm, and the presence of the yellow fluorescent dots within the cytoplasm represents internalized CM-DIL-positive RPMI8226-EVs. Notably, the yellow color is due to the contemporary presence of green CSFE in the cytoplasm and red CM-DIL in the RPMI8226-EVs. As expected, the internalization is

strongly reduced at 4 °C, indicating that an active, energy-dependent endocytic processes is involved.

These results were confirmed through a quantitative analysis in flow cytometry, performed by measuring CM-DIL positive cells in the PE channel. In this case, the recipient cells were not labeled with the CFSE, thus the flow-cytometry analysis was used to discriminate the yellow uptaken cells, positive for CM-DIL, from the non-uptaken cells. After 4 hours of treatment with RPMI8226-EVs, 75,77% of Raw264.7 cells uptook EV at 37°C, but only 4,28% Raw264.7 cells uptook EVs at 4°C. Similarly, 64,31% of HPAEC internalized RPMI8226-EVs at 37° C, with an almost completely inhibition at 4°C (**fig. 17B**).

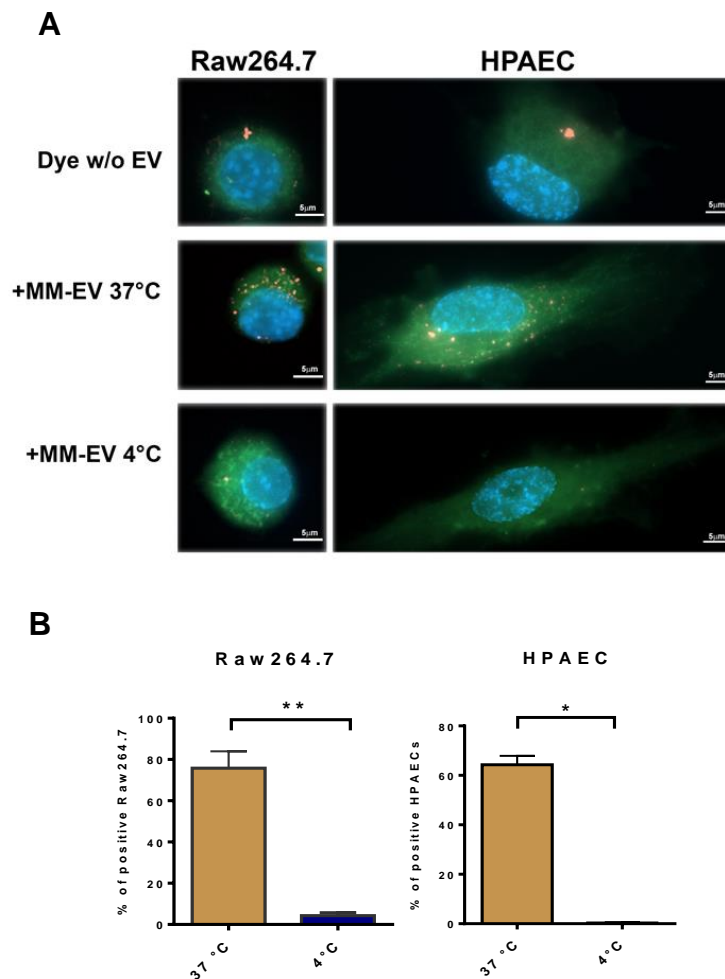


**Figure 17: uptake experiments with MM-EVs from RPMI8226. A)** Fluorescent microscopy analysis on Raw264.7 and HPAECs have been treated with CM-DIL stained MM-EVs for 4 hours at 37°C or 4°C. Treatment with CM-DIL alone was used as negative control. The images were obtained by Leica TCS SP2 AOBS and represent the maximum intensity projection of MM-EVs in target cells. Red fluorescence: MM-EVs labeled with CM-DIL dye; green fluorescence: CFSE+ cell cytoplasm; Yellow dots: overlapping of green and red signals corresponding to internalized MM-EVs; blue fluorescence: nuclei with DAPI (63x magnification). **B)** Flow cytometry analysis confirms the uptake of MM-EVs labelled with CM-DIL on Raw264.7 and HPAEC. The analysis was performed by measuring CM-DIL positive cells in the PE channel. Data are expressed as the mean value +/- SEM. Statistics was carried out by two-tailed t-test: \*= $p < 0.05$ ; \*\*= $p < 0.001$ .

### 3.3 Analysis of the presence of Notch2 in MM-EVs

Due to the importance of Notch signaling to the pathological communication between MM cells (48) and the healthy population of the BM(48, 139) and to the recently discovered role

of EVs in cancer cell communication, I wondered if Notch signaling members overexpressed in MM could be play their role at distance thank to EV-mediated transfer.

In this second part of thesis work, the research was focused on the Notch receptor. Below, the analysis of the expression of the four Notch receptor isoforms in a panel of seven HMCLs and the corresponding shed EVs, indicates a higher diffusion of Notch2 (**fig.18** and **19**).

**Fig. 18** reports a western blot analysis performed on cell protein extracts of AMO1, JJN3, H929, RPMI8226, LP1, KMS12, OPM2 cells and the corresponding EVs isolated from their CM by ultracentrifugation after 48 hours of culture. To identify the different form of the receptor including the immature full-length form (Notch-FL), the mature transmembrane portion (Notch2-TM) and the active cleaved intracellular portion (Notch2-IC) on cells and vesicular protein samples, primary antibodies specific for Notch2 (recognizing the first two forms) and for Notch2-IC were used. To control protein loading and purification efficacy was used  $\beta$ -Actin as a housekeeping protein for cell extracts and TSG101, a cytosolic component of the ESCRT-I complex, associated with membranes of vesicles as a housekeeping protein for the vesicular extracts.

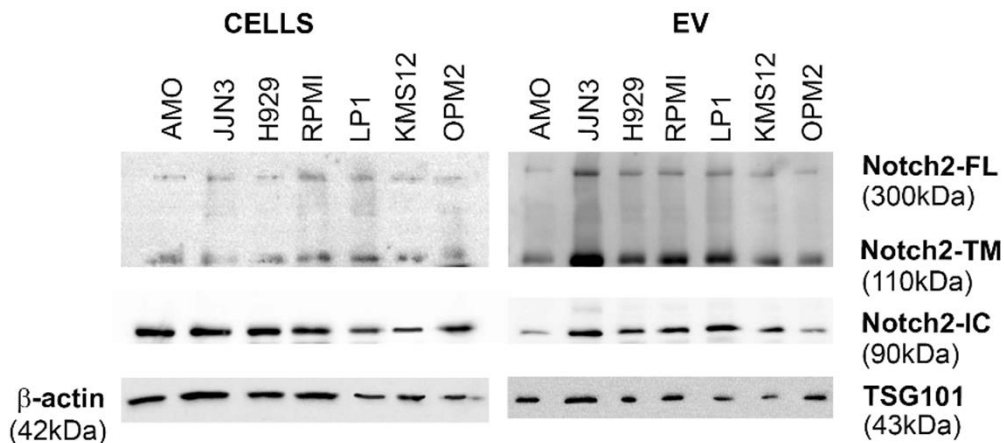


**Figure 18: Western blot analysis for Notch2 expression in MM-EVs from 7 HMCLs.** Notch2-FL (full length), Notch2-TM (transmembrane form), and Notch2-IC (active intracellular Notch2) are expressed in 7 different HMCL and their shed EVs.  $\beta$ -Actin and TSG101 have been used as loading controls for cells and vesicle protein extracts, respectively.

The obtained results indicated that the three forms of Notch2 were expressed in MM-EVs.



The expression levels of the other Notch are reported in **fig. 19**. We found out that Notch1 is widely expressed, while the expression levels of Notch3 and Notch4 is barely visible.

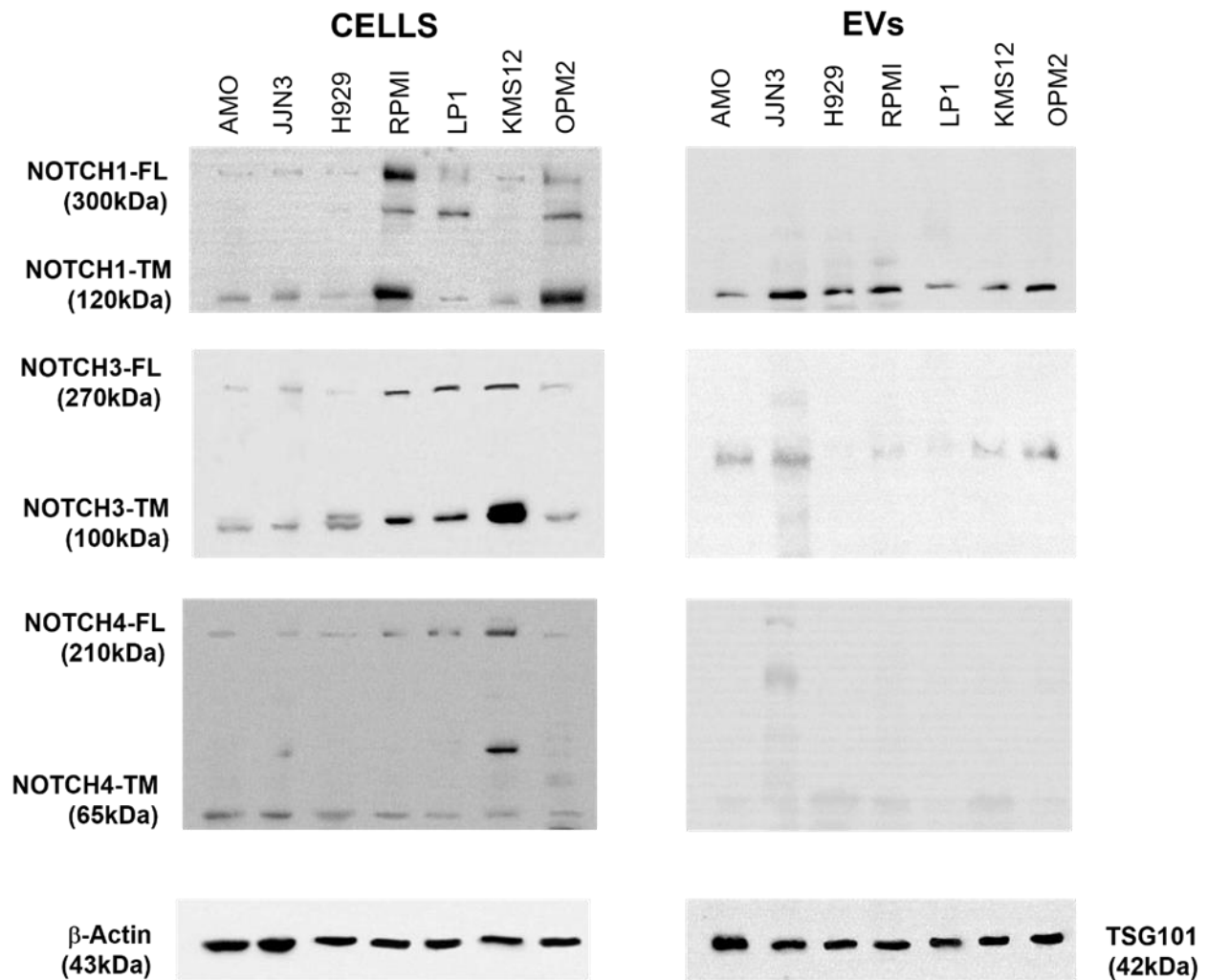


**Figure 19: Western blot analysis for Notch1, Notch3 and Notch4 expressed in 7 different HMCLs and their EVs.** Notch1 is widely expressed in HMCLs and their EVs, while Notch3 and Notch4 presence is less detectable.  $\beta$ -Actin and TSG101 have been used as loading controls for cells and vesicle protein extracts, respectively.

The observed high expression levels of Notch2 in MM cell lines and to its overexpression in patients presenting, at onset, plasma cell leukemia, the most aggressive form of myeloma (66), prompted me to initially focused my attention on Notch2.

Due to the heterogenic particle population present in EVs with ultracentrifugation at 110.000 g, composed by large and small vesicles, I wondered which type of vesicles carried Notch2. To address this issue, the CM of RPMI8226 and OPM2 were sequentially ultracentrifugated at 20.000 g and at 110.000 g to enrich the pellet with large and small vesicles, respectively. The western blot analysis reported in **fig. 20** suggests that the mature transmembrane Notch2 (Notch2-TM) and the cleaved intracellular portion of Notch2 (Notch2-IC) are present in both large and small vesicles of RPMI8226-EV and OPM2-derived EVs (OPM-EVs), although Notch2-IC is enriched in the small EVs consistently with its localization in the endocytic pathway which is the source of exosomes, mostly distributed among the small EVs.

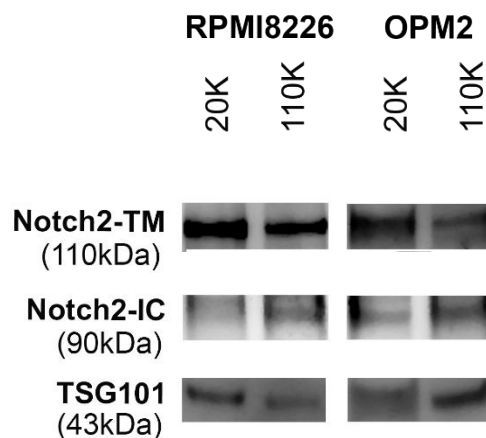


**Figure 20: Western blot analysis for the expression of Notch2 in small and large vesicles.** MM-EVs from RPMI8226 and OPM2 cells were separated by sequential centrifugation at 20.000g and 110.000g. The expression of the two Notch2 forms was separately assessed using specific primary antibodies for Notch2 and Notch2-IC; TSG101 was used as controls for vesicle protein extracts TGS101 was used as housekeeping protein.

#### 3.4 Analysis of the ability of MM-EVs to transfer Notch2 to distant cells

The evidence that Notch2 is present in MM-EVs cargo prompted me to investigate if it can be transferred to distant cells *via* EVs.

To address this issue, we used an EV-mediated cellular communication system *in vitro* composed by EV-donor and EV-receiving cells. The EV-donor cells are represented by the HEK293 cell line transfected with the plasmid vector pCDNA3.1 carrying Notch2 tagged with an amino acid sequence of hemagglutinin (N2-HA; HEK293-N2-HA) at the C-terminus. This

tag allowed us to discriminate N2-HA from the endogenous Notch2 and to follow its transfer from donor cells, to shed EVs and receiving cells treated with the purified EVs. HEK293 cells carrying the empty pcDNA-3.1 were used as mock control. After 48 hours, EVs were isolated from the transfected donor cells and used to treat receiving HEK293 cells (non-transfected) for 24 hours.

The protein extracts from donor and receiving cells, and the produced EVs were analyzed by western blot using an anti-HA primary antibody. **Fig. 21** showed that the HA signal is detectable in donor cells transfected with pCDNA3.1 carrying Notch2, the corresponding produced EVs and receiving cells. While the signal is absent in negative controls. These results suggest that Notch2 can be transferred from donor to receiving cells via EVs.

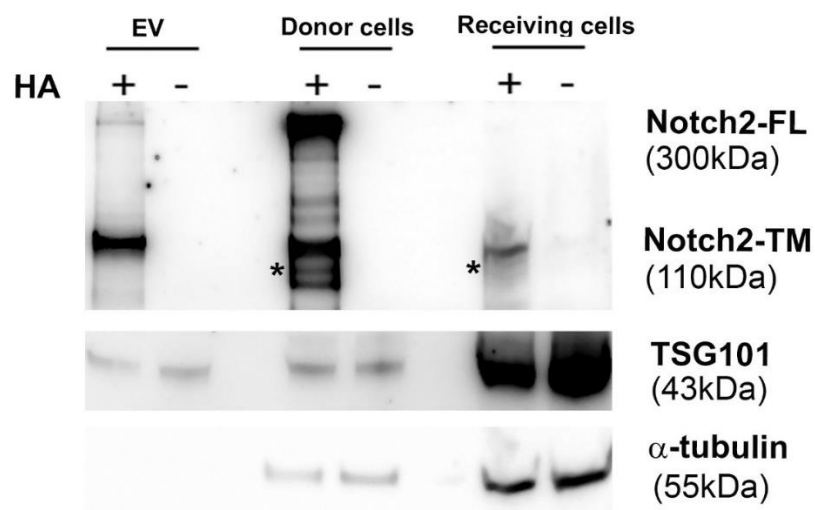


**Figure 21: western blot analysis of Notch2-HA transfer via EVs.** The western blot analysis shows the presence of N2-HA in donor cells N2-HA, in EV-N2-HA, and in receiving cells treated with EV-N2-HA. Cell and EV protein extracts were analyzed by Western blot using a primary antibody anti-HA and normalized on  $\alpha$ -tubulin and TSG101, respectively. Notch2-IC tagged with HA is indicated by an asterisk and was identified thank to the hybridization of the same filter with a primary antibody anti-Notch2-IC (not shown).

#### 4. MM-EVs INCREASE THE PRO-TUMORIGENIC ACTIVITY OF BONE MARROW HEALTHY CELLS IN A NOTCH DEPENDENT WAY

The ability of MM-EVs to carry and transfer Notch2 to recipient distant cells, prompted me to investigate the role of Notch2 in the vesicle-mediated pro-tumorigenic effect.

To understand the role of Notch pathway in MM-EV-mediated communication, Notch2 expression was inhibited in RPMI8226 and OPM2 cells by stable transduction with the pTRIPZ lentiviral vector that inducible express shRNAs specific for Notch2 gene (MM<sup>N2KD</sup>) or a scrambled sequence (MM<sup>SCR</sup>) as negative control. The MM clones were isolated by serial dilution and variation in Notch2 expression was assessed by RT-PCR and western blot analysis specific for Notch receptors following induction with doxycycline (1 µg/ml) (data not shown). Once identified the most promising clones, HMCLs were treated for 7 days with doxycycline (1 µg/ml), and in the last 48 hours EVs were isolated by high-speed ultracentrifugation from both the MM<sup>SCR</sup> (MM-EVs<sup>SCR</sup>) and MM<sup>N2KD</sup> (MM-EVs<sup>N2KD</sup>).

After a western blot for Notch receptors confirming Notch2 KD, but the lack of effect on the other Notch receptors, I assessed the effect of Notch2 inhibition in the content of EVs, their size and concentration. Then, I investigated the role of Notch2 in the pro-tumorigenic role of MM-EVs, focusing on tumor-osteoclastogenesis and angiogenesis, and assessed if MM-EVs may induce the activation of Notch signaling in recipient cells.

##### *4.1 Analysis of the effect of Notch2 silencing on MM cell-derived EVs*

To confirm the silencing at protein level, a western blot was performed on MM<sup>SCR</sup> and MM<sup>N2KD</sup> cell lysates and their derived EVs, MM-EVs<sup>SCR</sup> and MM-EVs<sup>N2KD</sup> respectively. The western blot in **fig. 22A** shows the effective Notch2 silencing in both RPMI8226 and OPM2, confirmed by the reduction in the expression of both Notch2-FL and Notch2-TM. Notably, this effect is visible also in their EVs, suggesting that the vesicles Notch2 protein levels depend on its amount in the producing cells. We also assessed Notch2-IC expression in cells and their EVs upon Notch2 inhibition. Ours results suggest that its expression decreased in OPM2 cells and their shed EVs, while Notch2-IC decrease in EV released RPMI8226 was not evident (**fig. 22B**).

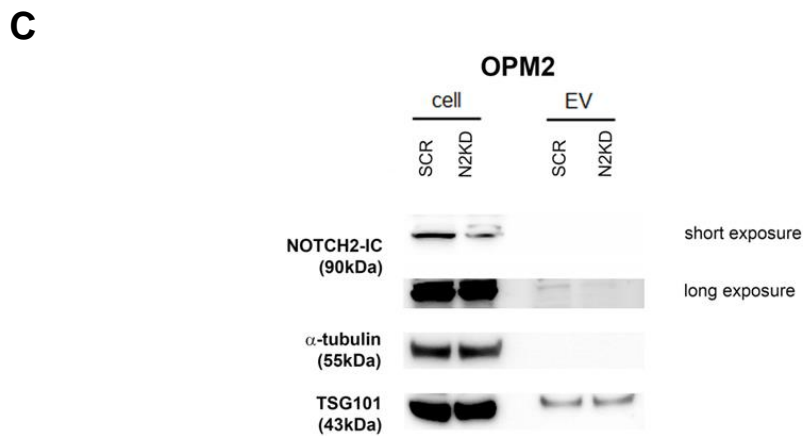
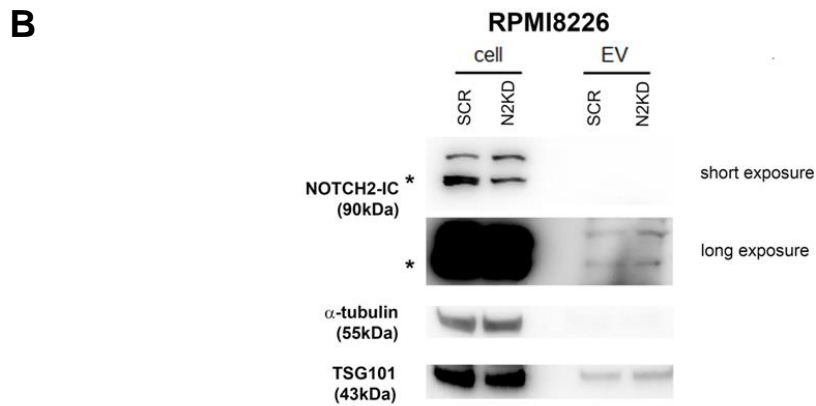
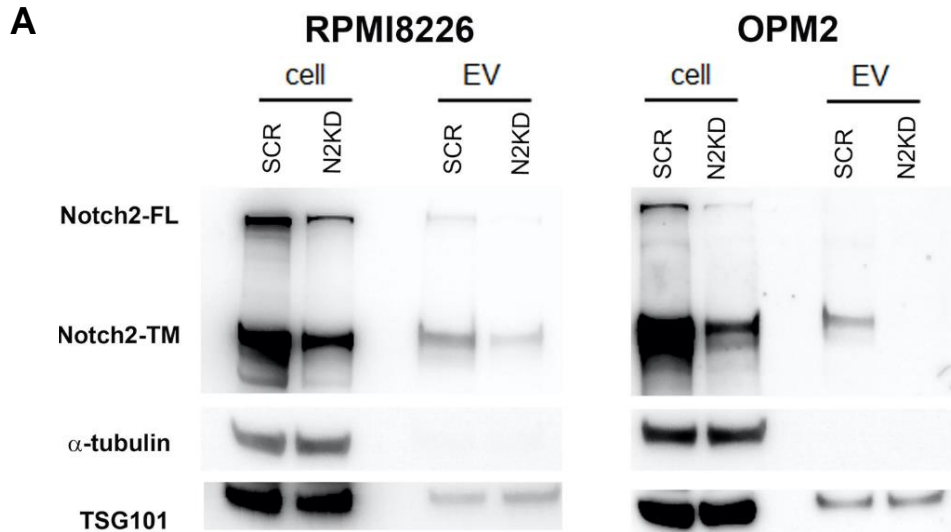


**Figure 22: western blot on Notch2 expression on MM<sup>SCR</sup> and MM<sup>N2KD</sup> cell lysates and their derived EVs.  $\alpha$ -tubulin and TSG101 were used as controls of loading and purity of cell and vesicles lysates, respectively. **A)** Western blot analysis reveals the efficiency of inhibition on Notch2-TM both**

in RPMI and OPM2 cells and their shed EVs. **B-C)** Western blot revealed a decrease in Notch2-IC in both cell type upon Notch2 lentiviral silencing, moreover it shows a clear reduction in RPMI8226-derived EVs (**B**), while no significant differences are detectable in OPM2-derived EVs (**C**). EV protein extract loading was half as cell extracts, therefore, to detect Notch2-IC in cell lysates a short exposure is shown, while to detect it in EV extracts a long exposure is shown.

Considering the presence of four Notch receptors on MM cells, I performed a western blot analysis to assess the effect of Notch2 inhibition on Notch1, Notch3 and Notch4 cellular protein level and the outcome on MM-EVs. As shown in **fig. 23**, the inhibition of Notch2 did not affect the expression of the other Notch receptors, suggesting that shRNAs specifically inhibit the expression of Notch2 both in cells and the derived EVs.

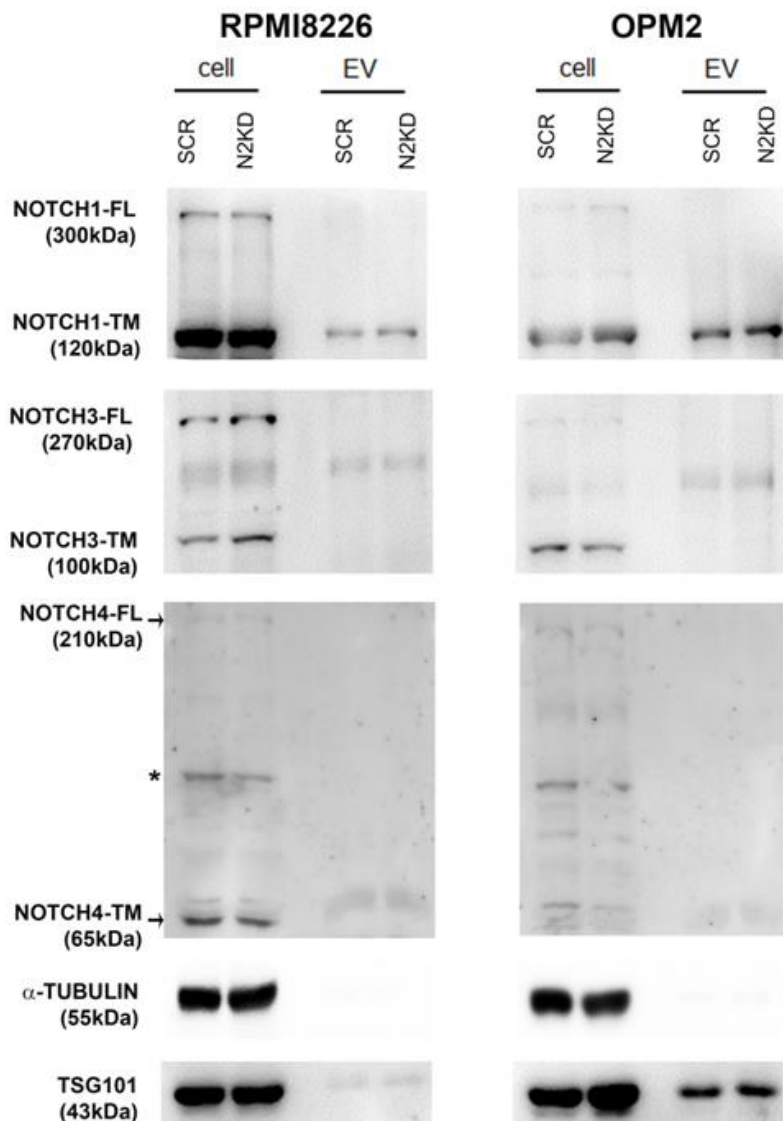


**Figure 23: Western blot for the expression of Notch receptor 1, 3 and 4 in MM<sup>SCR</sup> and MM<sup>N2KD</sup> cell and their EVs.** The cell lysates and their derived EVs were analyzed for the expression of Notch-FL and TM of Notch 1, 3, 4.  $\alpha$ -tubulin and TSG101 were used as controls of loading and purity of cell and vesicles lysates, respectively.

Then, I verified if Notch2 KD may affect the size and concentration of the released EVs. The NTA analysis (**fig. 24**) on MM-EVs<sup>SCR</sup> and MM-EVs<sup>N2KD</sup> showed that Notch2 inhibition did not significantly affect neither the concentration nor the size of MM-EVs.

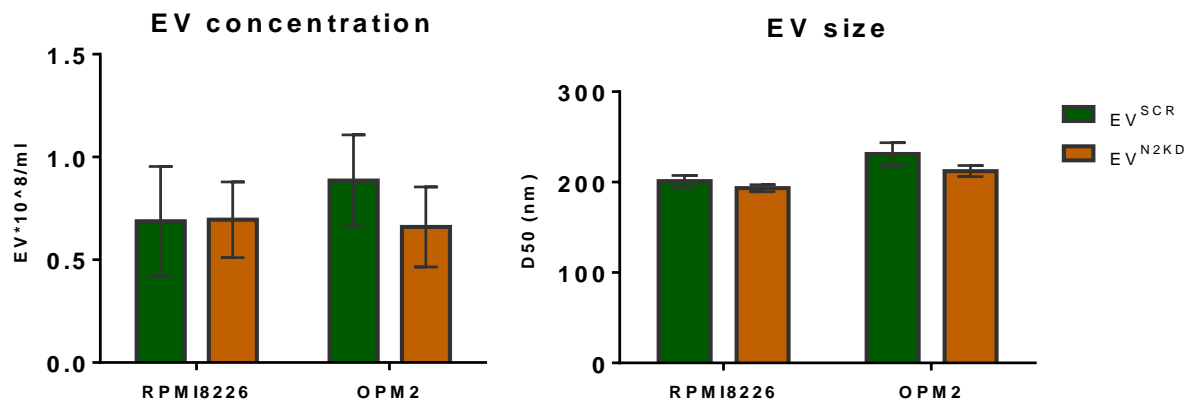


**Figure 24: NTA on MM-EVs<sup>SCR</sup> and MM-EVs<sup>N2KD</sup>.** The NTA analysis does not detect significant changes in concentration and size. D50 is the size point below which 50% of the EVs are contained. EV concentration was normalized on the starting volume used for the isolation of EVs in each experiment. Data are expressed as the mean value +/- SEM.

#### 4.2 Analysis of MM-EVs ability to activate Notch pathway in recipient cells

To assess if Notch2 protein carried by MM-EVs may trigger Notch signaling pathway in receiving cells, we performed a luciferase Notch reporter assay *in vitro*. In particular, I assessed the ability of MM-EV<sup>SCR</sup> isolated from OPM2 to activate a Notch reporter in HeLa cells and whether this effect was reduced using MM-EVs<sup>N2KD</sup>.

In this system, HeLa cells were transiently transfected with pNL2.1[Nluc/Hygro] plasmid, with a Notch responsive element (6XCLS) controlling the expression of the NanoLuc luciferase. To normalize the transfection efficiency, I co-transfected with the plasmid pGL4.54 [Luc2/TK], expressing the Firefly Luciferase under the control of a thymidine kinase promoter. Transfected HeLa cells were treated with MM-EVs<sup>SCR</sup> and MM-EVs<sup>N2KD</sup> and after 24 hours the luciferase assay was carried out.

As reported in the graph of **fig. 25**, MM-EVs<sup>SCR</sup> increase Notch pathway activation in HeLa cells of 53% compared the unstimulated HeLa cells, and this EV-mediated effect is reduced to 25,8% when HeLa cells were treated with MM-EVs<sup>N2KD</sup>.



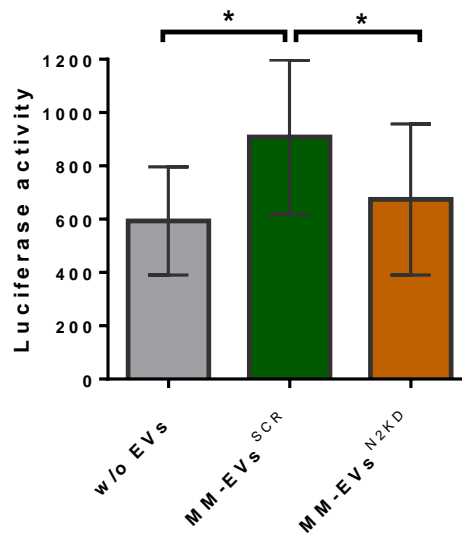


**Figure 25: luciferase Notch reporter assay on HeLa cells treated with MM-EVs<sup>SCR</sup> and MM-EVs<sup>N2KD</sup>.** The graph represents Nanoluc/luciferase activity levels that reflect Notch activation. Untreated HeLa cells (w/o EVs) were used as negative control. Data are expressed as the mean value +/- SEM. Statistical analysis was carried out by ANOVA and Tukey's post-test: \*=p<0.05.

To validate this result, EVs ability to activate Notch signaling at distant sites was evaluated *in vivo*, by injecting MM-EVs<sup>SCR</sup> and MM-EVs<sup>N2KD</sup> in transgenic zebrafish embryos obtained by crossing Tg(T2KTP1bglob:hmgb1-mCherry) with Tg(fli1a:EGFP) (**fig. 26**). This model displays GFP+ endothelial cells (green) and express the mCherry protein (red) under the control of a Notch responsive element. MM-EVs<sup>SCR</sup> were injected in the duct of Cuvier of 2dpf (days post fertilization) transgenic zebrafish embryos. The representative images in **fig. 25** on the left acquired 4 hours post-injection show that MM-EVs trigger Notch signaling in the intersegmental vessels, caudal artery and, importantly, in the caudal hematopoietic tissue (CHT), that represents the main fish hematopoietic organ analogous to human BM (175). The graph shows the corrected total fluorescence (CTF) measured in the CHT region of each embryo and demonstrates that MM-EVs<sup>SCR</sup> induce Notch activation, while MM-EVs<sup>N2KD</sup> effect is far less effective.

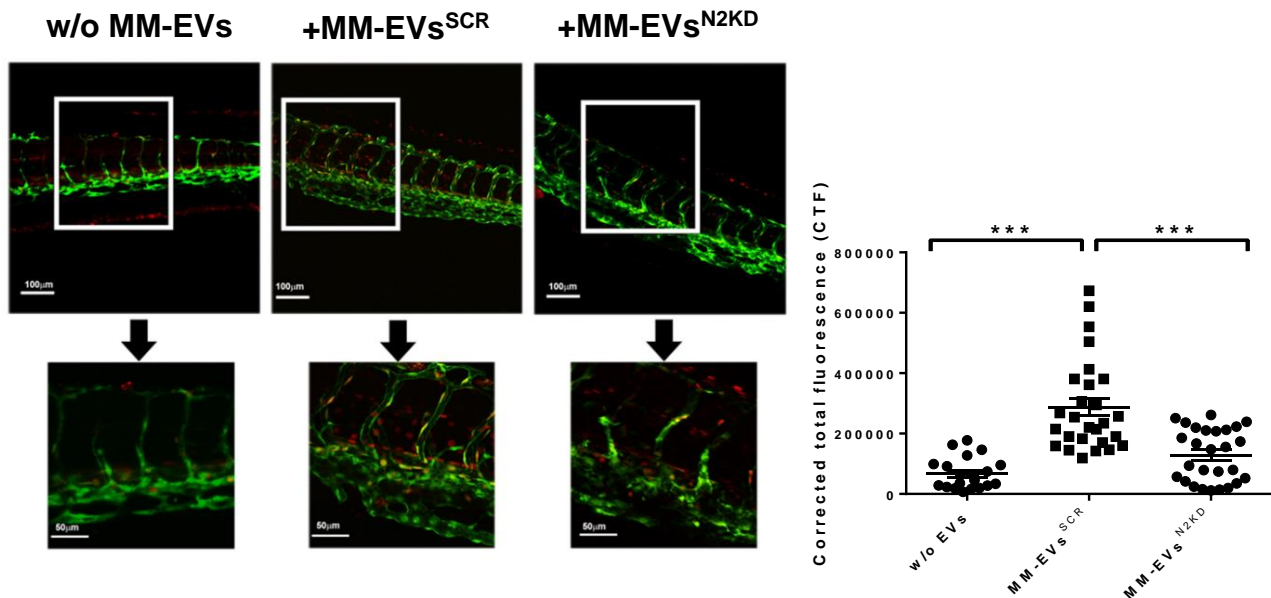


**Figure 26. *In vivo* Notch reporter assay.** The figure shows activation of Notch signaling in caudal hematopoietic tissue (CHT) of zebrafish embryos 4 hours after the injection of MM-EVs<sup>SCR</sup> and MM-EVs<sup>N2KD</sup> from RPMI8226 cells. Representative pictures of each condition are reported on the upper panel with 20x and 60x magnification imaged (upper and lower pictures respectively). The graph on the bottom represents the values of the fluorescence intensity (CTF) measured in the CHT region of each fish. Data are expressed as the mean values +/- SEM. Statistics by ANOVA and Tukey's post-test: \*\*\*=p<0.0001

#### 4.3 Evaluation of Notch2 role in MM-EVs-mediated osteoclastogenesis and angiogenesis

Considering the crucial role of osteoclastogenesis and angiogenesis for MM progression and diffusion, I assessed if these processes could be mediated also by MM-EVs. To address this issue, Raw264.7 cells and HPAECs were treated with MM-EVs<sup>SCR</sup> and MM-EVs<sup>N2KD</sup>. I performed the experiments of osteoclast differentiation and tube formation assay by treating target cells with the same amount of EVs isolated from the equivalent volume of CM used in each experiment as explained in the methods section. The rationale stems out from the consideration that Notch2 inhibition did not significantly affect the amount of EVs.

To investigate the osteoclastogenic potential of MM-EVs and the involvement of Notch2 in this process, the monocyte cell line Raw264.7 was treated with suboptimal amount of the osteoclastogenic chemokine RANKL (30 ng/ml) and MM-EVs<sup>SCR</sup> or MM-EVs<sup>N2KD</sup> from the RPMI8226 cell line. This cell line was chosen since it has osteoclastogenic potential differently from OPM2 cells. After 7 days of treatment with MM-EVs, OCLs were enumerated with light microscopy as cells with more than 3 nuclei and positive for the osteolytic enzyme

tartrate-resistant acid phosphatase (TRAP). The graph reported in **fig. 27** shows that MM-EVs<sup>SCR</sup> increase Raw264.7 cell differentiation of approximately 275%, while MM-EVs<sup>N2KD</sup> lost this ability. The representative picture of TRAP positive OCLs suggests that MM-EVs<sup>SCR</sup> not only increased the number of mature OCLs but also their size, and both these features are reduced with the treatment with MM-EVs<sup>N2KD</sup>.

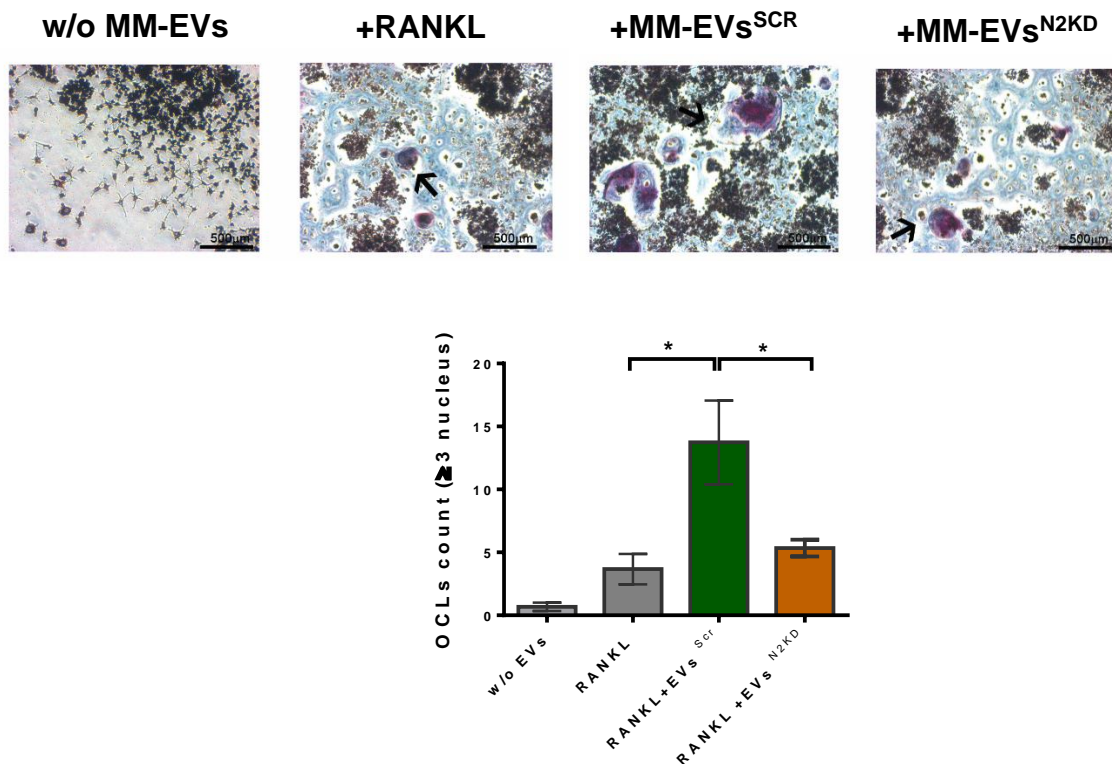


**Figure 27: OCLs differentiation assay on the monocyte cell line Raw264.7 treated with MM-EVs<sup>SCR</sup> and MM-EVs<sup>N2KD</sup>.** The cells were treated in the presence or absence of 30 ng/ml RANKL and treated or not with MM-EVs<sup>SCR</sup> and MM-EVs<sup>N2KD</sup> isolated from RPMI8226 cell line. After 7 days TRAP+ multinucleated cells were enumerated ( $\geq 3$  nuclei) indicated with an arrow in the representative images. The upper panel shows representative images for each condition (4x magnification); on the bottom, a graph shows the mean values of the absolute number of TRAP+ multinucleated cells, (+/- SEM). Statistical analysis was performed by a one-way ANOVA with Tukey's post-test; \* =  $p < 0.05$

To assess the angiogenic potential of MM-EVs and the role of Notch2, I performed a tube formation assay on HPAEC seeded on a Matrigel layer and treated for 13 hours with MM-EVs<sup>SCR</sup> and MM-EVs<sup>N2KD</sup>. Results indicated that MM-EVs<sup>SCR</sup> boosted HPAEC ability to

create a network of tubes, as shown by the increased number of areas (+120% and +286% respectively for EVs produced by RPMI8226 and OPM2 cells), and branch points (+200% and +150%). On the contrary, MM-EVs<sup>N2KD</sup> angiogenic activity was comparable to that of untreated cells (**fig. 28**).

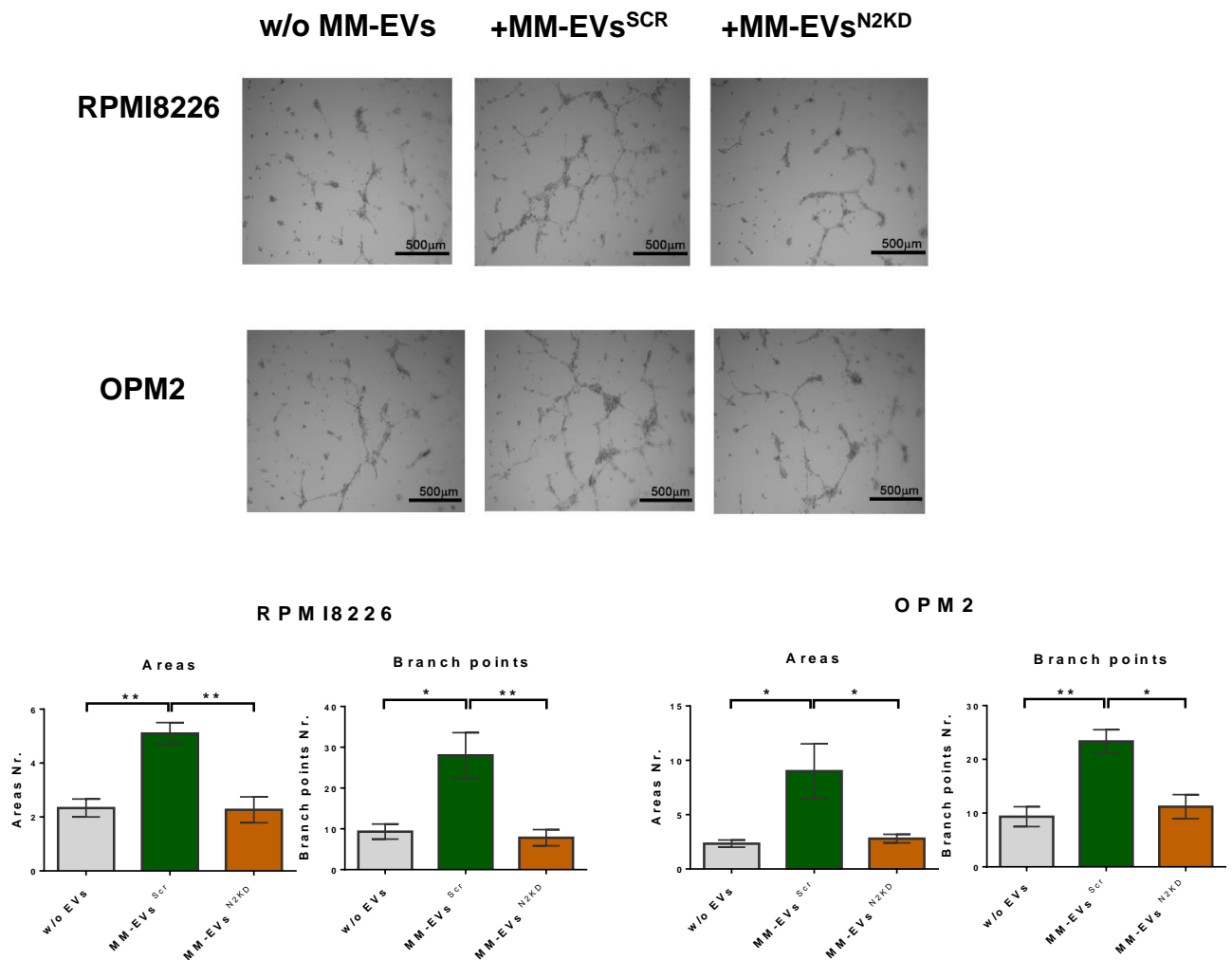


**Figure 28: tube formation assay on endothelial cells HPAECs treated with MM-EVs<sup>SCR</sup> and MM-EVs<sup>N2KD</sup>.** For each condition, representative images in the upper panel are shown at 4x magnification. The bottom graphs show the mean values of areas and branch points +/- SEM. Statistical analysis by ANOVA and Tukey's post-test; \* = p < 0.05; \*\* = p < 0.01.

#### 4.4 Effect of Notch pathway pharmacological blockade on pro-tumorigenic potential of MM-EVs

To confirm that the pro-tumorigenic effect of MM-EVs depends on Notch signaling activation boosted by MM-EVs, a pharmacological approach was used. More specifically, the osteoclastogenesis and angiogenesis assays were performed by treating Raw264.7 cells and HPAECs with MM-EVs in the presence of 50  $\mu$ M DAPT, an inhibitor of Notch pathway activation. DAPT is an inhibitor of  $\gamma$ -secretase, a protease complex involved in the proteolytic cleavage of Notch receptor resulting in its activation.

The graph in **fig. 29** clearly shows that the osteoclastogenic effect of MM-EVs from RPMI8226 cells is almost completely reduced in the presence of DAPT. Although DAPT could inhibit the endogenous Notch signaling in Raw264.7 cells, its ability to inhibit the osteoclastogenic effect of MM-EVs was definitively ( $\Delta$  OCL formation in the presence or absence of DAPT= 60%;  $\Delta$  OCL formation in the presence of EVs with or without DAPT = 95,5%). This result indicates that the osteoclastogenic effect of MM-EVs correlated positively with Notch signaling activation in recipient cells.

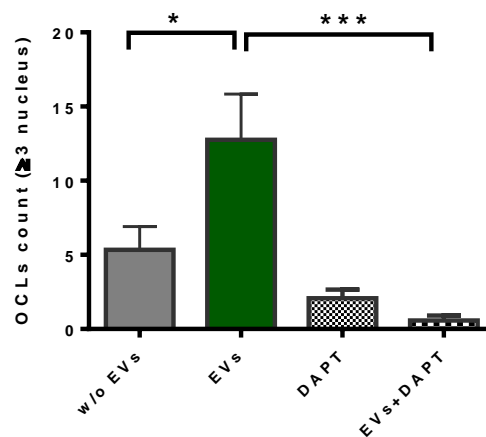


**Figure 29: osteoclast differentiation of Raw267.4 cells treated with MM-EVs in the presence of DAPT (50  $\mu$ M).** After 7 days TRAP+ multinucleated cells ( $\geq 3$  nuclei) were enumerated. The graph shows the mean values of TRAP+ multinucleated cells obtained in the different conditions for RANKL treated subtracted from mean value of the respective Raw264.7 control without RANKL. Data are expressed as the mean value  $\pm$  SEM. Statistical analysis was performed by one-way ANOVA with Tukey's post-test; \* =  $p < 0.05$ ; \*\*\* =  $p < 0.001$

An analogous experiment with similar results was performed to assess the effect of DAPT on MM-EVs induced angiogenesis. The graph in **fig. 30** shows that Notch activation blockade significantly affects MM-EVs induced tube organization of HPAECs on a Matrigel layer. Indeed, the experiments performed for 13 hours with both MM-EVs from OPM2-EVs and RPMI8226-EVs showed a strongly reduction of the number of areas and branch points upon treatment with DAPT. Also in this case, the effect of DAPT on MM-EVs-induced angiogenesis is higher than that on spontaneous angiogenesis. Therefore, these results confirm that MM-EVs mediated angiogenesis is due to Notch signaling activation in ECs.

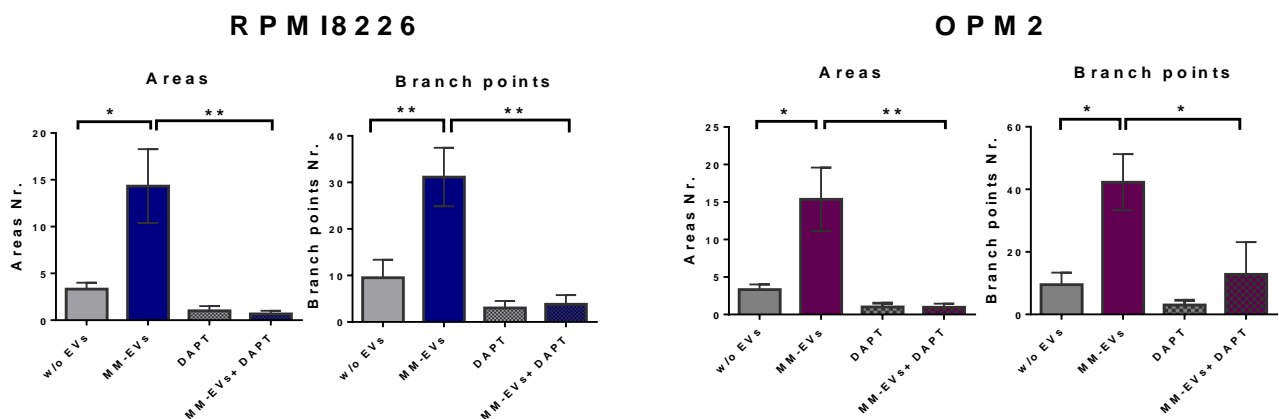


**Figure 30: tube formation assay on HPAECs treated with MM-EVs in the presence or absence of DAPT (50  $\mu$ M).** The graphs show the mean values of areas and branch points +/- SEM. Statistical analysis was performed by ANOVA and Tukey's post-test; \* =  $p < 0.05$ , \*\* =  $p < 0.01$ .

Finally, since the inhibition of Notch pathway could affect cell viability (176), to discern if the observed effect of DAPT on MM-EV induced angiogenesis and osteoclastogenesis could be due to a general toxicity of DAPT on ECs and monocytes respectively, and not to a specific effect on their differentiation, we assessed the possible toxic effect of DAPT on Raw264.7 cells and HPAECs. To this, I performed a MTT assay in the same experimental conditions of the biological assays shown in figures 21 and 22, by treating Raw264.7 cells and HPAECs with 50  $\mu$ M of DAPT for 7 days and 13 hours, respectively. According to the results in **fig. 31**, DAPT induced a slight reduction of cell viability (-16% in HPAECs and -26% in Raw264.7 cells) that does not explain the higher effects on MM-EVs-induced angiogenesis and osteoclastogenesis.

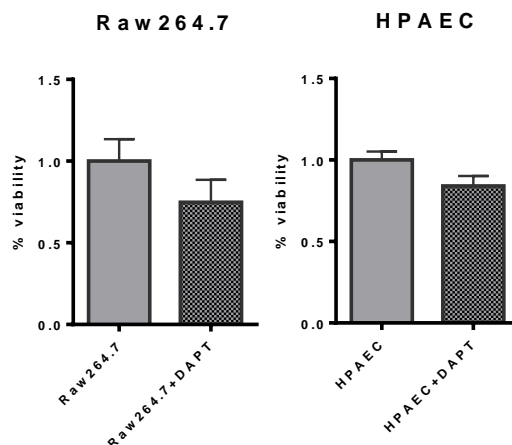


**Figure 31: MTT assay on Raw264.7 cells and HPAECs treated with DAPT 50  $\mu$ M.** The data were expressed as percentage of mean values  $\pm$  SEM of treated respect non treated cells. Data are expressed as the. The statistical analysis carried out with one-tailed t-test did not detect any statistically significant difference.

#### 4.5 Effect of Notch pathway pharmacological blockade on pro-tumorigenic potential of EVs from the BM of MM patients

To strength the obtained *in vitro* results concerning the role of Notch in the pathogenic effect of MM-EVs on osteoclastogenesis and angiogenesis, and to verify if a Notch directed treatment can be effective also in a more complex and realistic context, the functional assays were repeated in the presence or the absence of EVs purified from the BM of MM patients with MM (MM-BM-EVs) or the benign form of monoclonal gammopathy of uncertain significance (MGUS-BM-EVs), with or without DAPT.

To assess the angiogenic potential of BM-derived EVs, I performed a 13 hours-tube formation assay by treating HPAEC seeded on a Matrigel layers in the presence of MGUS-BM-EVs (n=6) or MM-BM-EV (n=12), with or without DAPT 50  $\mu$ M. According to the results in **fig. 32**, MM-BM-EVs significantly increased the angiogenic potential of HPAECs, confirmed by the increased number of areas (590%) and branch points (810%) compared to the negative control, and this effect is reduced in the presence of DAPT. On the contrary, MGUS-BM-EVs from patients with the benignant early stage of MM, did not have a significant effect on the angiogenic potential of ECs and, interestingly, DAPT did not affects the angiogenic effect of MGUS-BM-EV on ECs. These results suggest that the angiogenic potential of MM-BM-EVs is Notch mediated and correlate with the MM progression since DAPT did not affect the effect mediated by MGUS-BM-EVs. These results are coherent with

the angiogenic switch occurring in the BM during the progression from MGUS to MM stage and the increase expression of Notch increased expression.

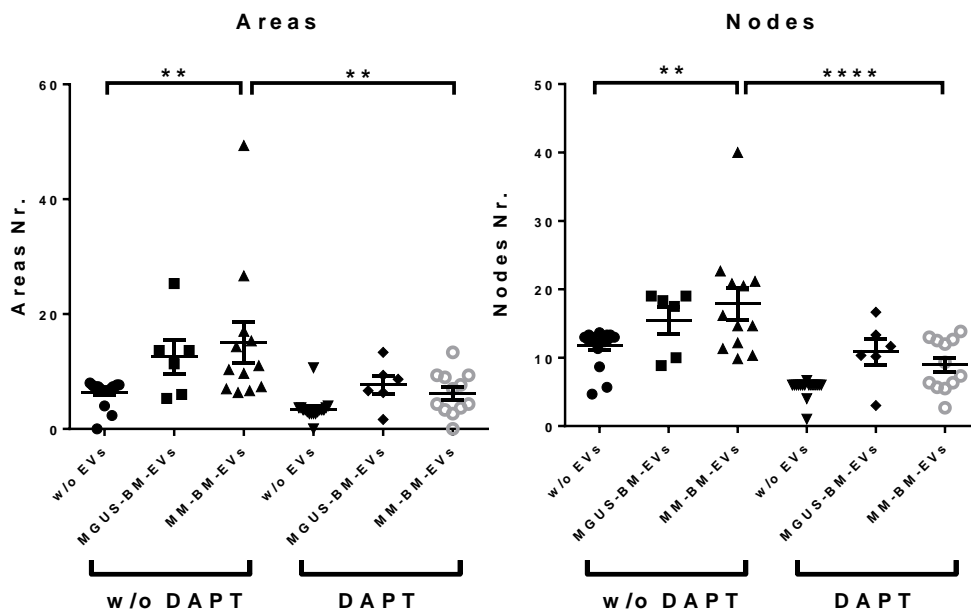


**Figure 32: Tube formation assay on HPAEC treated with BM-derived EVs of MM patients at different stage of disease.** HPAEC were treated with EVs isolated from the BM of MGUS (MGUS-BM-EVs) (n=6) and MM patients (MM-BM-EVs) (n=12) in the presence or absence of DAPT (50  $\mu$ M). The graphs show the mean values of areas and branch points +/- SEM. Statistical analysis was performed by ANOVA and Tukey's post-test; \*\*=  $p < 0.01$ ; \*\*\*\*=  $p < 0.0001$

Overall, these results suggest that the angiogenic and osteoclastogenic effect of MM-BM-EVs may be mediated by Notch pathway and the that a Notch-directed pharmacological approach may be effective to inhibit the pathological role of EV-mediated communication in MM.



## DISCUSSION AND CONCLUSIONS

Multiple Myeloma (MM) is a still incurable disease, mainly due to the localization of malignant plasma cells in bone marrow (BM) where they establish pathological communication with the resident healthy cell population. This aberrant interplay promotes neoplastic cell growth and survival and induces the supportive behavior of BM cells in the tumor progression (177). Indeed, the transition from the benign Monoclonal Gammopathy of Undetermined Significance (MGUS) to overt MM relies also on the increasing dependence from the BM microenvironment (177); this therefore becomes an important target for anti-tumor therapeutic approaches.

Current evidence indicates that the pathological crosstalk between MM cells and the nearby BM cells may be mediated by direct cell-cell contact or the release of pro-tumoral soluble factors (114, 178).

Among the pathway involved in cellular communication, Notch signaling pathway plays a crucial role in physiological and pathological processes mediating direct cell-cell communication (114).

In MM, Notch pathway mediated direct interaction plays a key role in the pathogenesis of the disease due to the overexpression of ligands Jagged1 and 2, and the receptor Notch2 (114). In particular, Jagged1 expression increases during the transition from MGUS to MM (65), while Jagged2 deregulation occurs in the early benign MGUS phase thus playing a key role in MM pathogenesis (68). Notch2 gene is overexpressed in MM cells derived from high-risk patients. Indeed, it is reported to be a MAF target gene, associated to the antiapoptotic effect (66).

The homotypic Notch pathway activation in MM cells leads to the inhibition of apoptotic pathway, proliferation, and drug resistance of tumor cells (71). Moreover, malignant plasma cells trigger Notch signaling activation in the BM niche leading to tumor growth, osteoclastogenesis, drug resistance and angiogenesis (76-78).

Among the mechanism of cellular interaction, the release of extracellular vesicles (EVs) in the extracellular space has been described as a new crucial mechanism in tumor progression and metastasis thanks to their ability to transfer molecular messengers between distant cells. In MM, specific miRNAs and proteins carried by circulating EVs have been

proposed as biomarker of disease progression (111, 179, 180). Moreover, EVs promote different events associated with MM progression, increasing its aggressiveness by sustaining key processes such as angiogenesis, osteoclastogenesis, immune escape and the drug resistance(173), thus increasing the aggressiveness of the disease and representing a new promising therapeutic target in MM (180).

To dissect the complexity of the cellular communication in the myeloma BM microenvironment, in this thesis I focused on the role of Notch pathway in crucial pro-tumorigenic processes in active MM progression considering different mechanism of interaction, i.e. communication mediated by direct cell-cell interaction, release of soluble factors and EV-mediated transfer of tumorigenic factors. In particular, I explored the contribution of the direct cell-cell interaction mediated by ligands Jagged 1 and 2 in MM-associated angiogenesis and the role of Notch pathway in MM-EVs induced angiogenesis and osteoclastogenesis at long-distance.

#### 1. MM CELLS INDUCE ANGIOGENESIS IN A JAGGED 1/2 MEDIATED WAY

The angiogenic switch is a key event of MM progression occurring in the myeloma-BM, and it is associated to MM patient's poor prognosis and MM progression (181). Indeed, the increased BM total microvessel density supports tumor cells growth by providing nutrients and oxygen, and favoring tumor spread and dissemination. Accordingly, endothelial cells (ECs) from MM patients display an angiogenic phenotype compared to MGUS patients (181).

The role of Notch signaling in physiologic and tumor angiogenesis displays a specific pattern among tip and stalk cells. Upon the vascular endothelial growth factor (VEGF) stimulation, DLL4 regulates the differentiation of tip cells and Notch2 activation in stalk cells, that in turn express Jagged1 which positively regulate the angiogenesis by leading to the formation of the vascular lumen and inhibiting the DLL4-Notch axis (155). Indeed, the downregulation of Notch with a specific decoy peptide causes the reduction of EC angiogenic activity (182) suggesting that MM-derived Jagged might play a key role in promoting MM-associated angiogenesis.

In MM microenvironment, Notch activation in the endothelium may be triggered by homotypic activation between ECs as well as the heterotypic interaction mediated by the hyperexpression of Jagged1 and 2 ligands (160). Indeed, previous results of my research group in collaboration with Prof. Vacca's teams demonstrated that the *ex vivo* Notch

signaling activation in ECs induces their angiogenic potential (160) and that Jagged-derived MM cells may induce heterotypic activation of Notch in ECs.

This evidence prompted me to better elucidate the mechanism underlying the angiogenesis mediated by cell-derived Jagged ligands. We reasoned that could be involved two mechanisms: 1) the direct stimulation of ECs and 2) their role in the angiogenic potential of the BM stromal cells (BMSCs).

To study the direct stimulation of ECs, we considered that MM-derived Jagged may induce EC differentiation by directly triggering the angiogenic Notch signaling or boosting the secretion of MM-derived angiogenic factors.

The silencing of Jagged1 and 2 expressions in MM cell lines RPMI8226 and OPM2 demonstrated that the angiogenic potential of MM cells was Notch mediated and relied on the direct cell-to-cell contact as well as the release of soluble tumor-derived factors.

The administration of Jagged1 and 2 peptides allowed us to discriminate the two mechanisms involved. Indeed, their angiogenic effect demonstrated that soluble ligands could trigger the activation of Notch signaling in ECs stimulating angiogenesis. On the other side, the ability of the conditioned medium (CM) from HMCLs<sup>SCR</sup> to induce the tube formation of HPAECs clearly demonstrated that MM cells induce the angiogenesis by releasing soluble factors. This process was mediated by Jagged1/2 since their inhibition negatively affected the angiogenic potential of ECs. MM-derived VEGF-A was identified as a Notch-dependent angiogenic soluble factor released upon Jagged-mediated Notch signaling activation. As a matter of fact, its mRNA and protein level were inhibited by Jagged1 and 2 knock down (KD).

Since MM cells have been reported to induce a different supportive pro-tumoral behavior of BMSCs in a Notch mediated way (71, 76, 77), we also explored the effect of MM-derived Jagged on the angiogenic potential of BMSCs.

To this purpose, HPAECs were treated with the CM of HS5 alone or pre-conditioned with HMCLs<sup>SCR</sup> or HMCLs<sup>J1/2KD</sup> after 48h-co-culture. As expected, the CM from HS5 showed an angiogenic effect on ECs consistently with the supportive role of BMSC in the angiogenic process in myeloma microenvironment (183), but, in addition, we observed that their potential was boosted when they were in co-culture with HMCLs<sup>SCR</sup>. This effect was dependent on the MM-cell-derived Jagged ligands ability to activate Notch signaling in the

BMSCs. As a matter of fact, Jagged1 and 2 inhibition in HMCLs reduced the ability to trigger Notch signaling in the BMSCs and the stimulation of their angiogenic activity. Additionally, since VEGF-A is mainly released from BMSCs in the BM (184), we investigated if Notch signaling, activated by the MM cell-derived Jagged ligands, was associated with an increase in VEGF-A secretion by the BMSCs. Our results confirmed this hypothesis since HMCLs<sup>SCR</sup> induce the secretion of VEGF-A by the BMSCs, but HMCLs<sup>J1/2KD</sup> lost this ability.

In conclusion, the first part of thesis work provides a new tassel to the picture of the complex interaction between MM cells and the BM cell populations, showing that the aberrant Jagged expression in MM cells contribute to stimulate the angiogenic process by promoting the release of VEGF-A by MM cells and BMSCs or by directly triggering the Notch pathway in ECs. This evidence strengthens the crucial role of Notch pathway in the “education” of the BM niche to assume a supportive behavior promoting tumor growth; thus, hampering this Notch mediated pathological interaction could be a valid therapeutic strategy.

This work contributed to better characterize the role of Notch signaling activated by Jagged ligands in the education of BM microenvironment specifically focusing on the mechanisms involved in MM-associated angiogenesis and resulted in the publication of a paper on Cancers in which I am co-first author (*Palano et al., Cancers 2020*).

## 2. NOTCH PATHWAY IN THE EV-MEDIATED COMMUNICATION

The results obtained during this thesis work on the role of Notch signaling in myeloma-associated angiogenesis (78), previous results of my research group demonstrating the ability of MM cells to induce both angiogenesis (160) and osteoclastogenesis in a Notch dependent way (77), together with the evidence that myeloma EVs also promote osteoclastogenesis (142-145, 185) and angiogenesis (163, 168) prompted me to wonder if Notch effects on these two features of MM progression may be mediated by EVs shed by MM cells (MM-EVs).

My first question concerned if Notch signaling could be delivered by MM-EVs. I reasoned that, in this case, Notch signaling receptors or ligands should have been carried in MM-EV cargo. An increasing number of scientific data reported the presence of Notch pathway members in the cargo of EVs shed from different cell types. Two different groups demonstrated that DLL4 ligand can be carried by endothelial exosomes as new mechanism for the regulation of the tip cells (186, 187). Jagged1 has been reported to be present in EVs from different cancer cell lines such as melanoma cell lines (188). Finally, Wang *et al.*

demonstrated that Notch2 receptor are enclosed within ARMMs (arrestin domain-containing protein 1 (ARRDC1)-mediated microvesicles), which are able to bud directly by the plasma membrane (189).

My results demonstrated for the first time the presence of the Notch receptors in MM-EVs. In particular, the western blot analysis on EVs shed from seven MM cell lines revealed the presence of the four isoforms of Notch receptors, suggesting that Notch1 and Notch2 are the most expressed in MM-EVs, while Notch3 and Notch4 are barely present. This research focused on Notch2, since it is the most expressed in MM cell lines, and it is associated with high-risk MM patients (66, 71). MM-EVs showed to express the Notch2-TM and the immature, uncleaved Notch2-FL present in the Golgi apparatus and, importantly, they carry also Notch2-IC, giving the first evidence that MM-EVs may deliver the activated form of Notch2 which might directly activate the transcription of the Notch target genes into the nucleus.

This suggests that MM-EVs may deliver both the mature form of Notch2 that still requires the activation mediated by Notch ligands and the active form of Notch2 which does not requires the interaction with Notch ligands and cleavage by ADAM protease and  $\gamma$ -Secretase.

Since the EVs population is composed by exosomes and microvesicles and both of them have been reported to carry Notch1 (190, 191), we investigated which type of vesicles carries Notch2.

We found out that Notch2 was carried both by large particles and small particles (isolated at 20.000xg or 110.000xg, respectively). Although the limit of our examination that did not allow to discriminate the origin of the different EV population on the basis of their dimension, these results suggest that Notch2 could be carried by microvesicles (usually composed by larger particles), as reported also by Wang *et al.* (189), but also in exosomes, presumably enriched in small vesicles.

In the light of this evidence, we aimed to understand the possible molecular and functional outcomes of the presence of Notch2 in MM-EVs. In particular, I investigated if Notch2 could induce the osteoclastogenesis and angiogenesis mediated by the long-distance communication of EVs, by activating the Notch signaling in the recipient cells.

To address this issue, firstly, we assessed if MM-EVs could be internalized in Raw264.7 cells and Human Pulmonary Artery Endothelial Cells (HPAEC), used as OCL and EC models respectively. To visualize the uptake, MM-EVs were labeled with the fluorescent CM-Dil, which allowed us to follow the vesicles internalization in two different ways. Indeed, flow cytometry and Z-stack confocal analysis showed that CM-Dil positive EVs can be internalized in the two cell models after 4 hours. The almost absence of internalization at 4 °C demonstrated that an active process is involved. This data obtained on OCL progenitors and ECs is coherent with the literature. Indeed, the internalization of MM-EVs requires the endocytic mechanism of uptake especially through a caveolin-dependent endocytosis and partially through macropinocytosis and membrane fusion (192).

More importantly, I demonstrated that not only MM-EVs carry Notch2 as a cargo, but they can transfer it to recipient cells. To assess this point, we set up an experimental system of cellular communication mediated by EVs composed by donor and receiving cells that do not share any contact. This model is composed of HEK293 cells forced to express Notch2 tagged with HA, allowing to follow of N2-HA transfer from donor cells, to EVs and receiving cells. In this system, we confirmed that high level of Notch2-TM is present in EVs, while Notch2-FL is visible at lower level. On the contrary, Notch2-IC form was not detectable in HEK293-derived EVs, maybe because of the lower level of Notch activation in HEK293 cells in comparison to HMCLs. The transmembrane form of N2-HA is clearly visible in recipient HEK293 cells, that also showed a faint band corresponding to ICN2, consistently with a slight Notch2-HA activation in recipient cells after the EVs uptake.

To characterize the role of Notch pathway in EV-mediated communication with the BM cell populations, Notch2 expression was KD in RPMI8226 and OPM2 cell lines by using an inducible lentiviral vector carrying a specific shRNA against Notch2. Upon Notch2 KD, we confirmed that its protein expression decreased in MM cells and, interestingly, also in MM-EVs. Therefore, I demonstrated that it was possible to reduce the amount of Notch2 in MM-EV by RNA interfering in producing HMCLs.

To investigate if MM-EVs might activate Notch pathway in recipient cells, two different Notch reporter systems were used. The first *in vitro* reporter assay relied on HeLa cells transfected with a Nanoluc-expressing Notch reporter vector. These cells were treated with MM-EVs<sup>SCR</sup> or MM-EVs<sup>N2KD</sup>. The analysis of the luminescent signal of Nanoluc suggested that MM-EVs<sup>SCR</sup> might activate Notch signaling. On the contrary, MM-EVs<sup>N2KD</sup> induced a significantly

lower activation, demonstrating that the MM-EV-mediated activation of Notch signaling relied on vesicular Notch2 expression.

This *in vitro* result was strengthened by the evidence that the injection of MM-EV<sup>SCR</sup> in a transgenic zebrafish embryo reporter for Notch pathway activation increases considerably the Notch signaling in recipient cells, mainly in the caudal hematopoietic tissue (CHT), which represents the main Zebrafish hematopoietic organ, analogously to the human BM (175). The evidence that Notch activation in recipient zebrafish cells was almost lost when MM-EV<sup>N2KD</sup> were injected, indicated that this effect depended on Notch2 carried by EVs.

These results show that MM-EVs injected in the duct of Cuvier may exploit the fish circulation to induce Notch signaling activation at distant sites (interestingly analogous to human BM), confirming their ability to deliver tumor-deriving message at distant sites and suggesting the possible role of MM-EVs in the metastatic process.

Accordingly, the role of EVs in the reprogramming of cells at distant sites has been largely described. In particular, Peinado *et al.* (94) showed that exosomes from metastatic melanoma cells can increase the metastatic behavior of primary tumors by reprogramming the BM niche *via* transferring MET receptor favoring a pro-vasculogenic phenotype of BMSCs. Much more interesting, Notch signaling activation in pancreatic cancer cells enhances the release of a premetastatic secretome trafficking via exosomes (193). In the same way, MM-EVs could favor the dissemination of MM cells by reprogramming the Notch signaling in distant BM sites. We will explore this hypothesis in a future work.

The evidence that MM-EVs may carry Notch2 originated by MM cells, and the role of this oncogene in angiogenesis and osteoclastogenesis prompted me to investigate if MM-EVs might direct these two processes in ECs and OCLs in a Notch dependent way. I found out that EVs shed from MM cells RPMI8226 and OPM2 can increase the number and the size of multinucleated OCLs and the ability of ECs to create a network of vessels on a Matrigel layer *in vitro*.

These results were coherent with literature data. Indeed, MM-EVs are reported to carry different molecules such as UPR signaling molecules (142), AREG (143), IL32 (185) able to directly regulate the osteoclast differentiation leading to the sprouting of osteolytic lesions. Moreover, the angiogenic effect of MM-EVs has been reported to be mediated also by the transfer of angiogenic factors such as VEGF, angiogenin, fibroblast growth factor (FGF),

Serpin E1, TIMP-1 and Platelet-Derived Growth Factor (PDGF) (122, 166) or molecular messengers like miR-135b (163).

The results of our inhibitory approach suggest that among the osteoclastogenic and angiogenic factors carried by MM-EVs, vesicular Notch also plays a significant role. As a matter of fact, MM-EVs<sup>N2KD</sup> display a significantly lower impact *in vitro* on both angiogenesis and osteoclastogenesis. Interestingly, we verified that Notch2 KD in HMCLs did not interfere with EVs size and concentration, allowing us to exclude their possible involvement in the biological outcomes.

To demonstrate that the pathological effect mediated by MM-EVs on the BM cell populations may be inhibited by an already available anti-Notch drugs, I used a pan-Notch inhibitory small molecule which blocks the  $\gamma$ -Secretase mediated cleavage of Notch receptor, thus inhibiting the formation of the active oncogenic form.

The results obtained with DAPT demonstrated that the inhibition of the MM-EVs mediated Notch activation significantly hampers osteoclastogenesis and angiogenesis widely overcoming the effect of endogenous Notch signaling. I could also exclude that the effect of DAPT could be due to inhibition of cell viability, which, although present, is very low in comparison to the outcomes on osteoclastogenesis and angiogenesis.

Finally, the translational relevance of these results has been further strengthened by the ability of DAPT to reduce the pro-tumorigenic effect of EVs derived from the BM aspirates of MM patients (MM-BM-EVs). As a matter of fact, although BM-EVs increase significantly the angiogenic potential of HPAECs, these biological effects are reduced in the presence of DAPT.

Interestingly, we also measured the pro-angiogenic effect of EVs from the BM aspirates of benignant MGUS patients (MGUS-BM-EVs) and verified that it is not affected by presence of DAPT which displayed only a basal effect on the endogenous Notch signaling. These results are consistent with the increased expression of Notch pathway members in the transition from the MGUS to MM and its association with the angiogenic switch.

It should be noted that this result confirms the efficacy of a pharmacological approach directed to the vesicular Notch2 also on the complex EV mixture present in the BM microenvironment of MM patients, which is composed by MM-EVs but also by EVs released



from the surrounding BM populations that provide an important contribution to MM progression (194-196).

Although this approach requires further investigations, these results suggest that it is possible to target the pathological communication between MM cells and the surrounding microenvironment mediated by EVs using a Notch inhibitory approach.

In conclusion, this work of thesis furthered the central role of Notch pathway in shaping the MM microenvironment also through a cellular communication mediated by tumor-derived EVs. In addition, we provided evidence of an alternative long-distance communication of MM cells mediated by shed EVs.

The pro-tumorigenic activity of MM-EVs along with their ability to activate Notch signaling at distant sites suggests that the MM-EVs could have a role in “educating” distant BM sites to support the spread of the osteolytic lesions which represents a key feature in the poor prognosis of MM patients. Indeed, we can hypothesize that the dissemination of MM cells could be favored by the modulation of the vessel permeability and their new aberrant angiogenesis, leading to the extravasation of tumor cells and their localization at distant BM sites by making space through the induction of osteolysis and destruction of the bone matrix.

The study on MM-EVs, together with previously evidence concerning the pathological role of Notch mediated communication *via* direct cell contact or soluble factors, that I contributed to obtain in collaboration with the group where I have conducted my PhD studies, indicate that targeting the interaction between the ligands and Notch receptors pathway could be a valid therapeutic strategy to hamper MM progression and aggressiveness.

I showed that a pharmacological approach with  $\gamma$ -Secretase inhibitors (GSIs) is effective in downregulating Notch activation mediated by MM-EVs. The experiments conducted in the presence of DAPT represent a first proof-of-concept of the efficacy of a Notch inhibitory approach that should lead to future investigation on a more specific inhibition of Notch2.

Indeed, although the GSIs drugs efficiently inhibited the Notch pathway activation, their effect is not specific since the  $\gamma$ -secretase is involved in the regulation of other substrates such as E-cadherin, N-cadherin and syndecan-3, ErbB4 and CD44 (197, 198) and even more importantly, GSIs inhibit the activation of all the four Notch isoforms, thereby affecting all the physiologic functions mediated by the Notch pathway resulting in the adverse effects as weakness, skin disorders, headache, hypophosphatemia and severe gastrointestinal

toxicity(199). A more specific effect could be obtained with the use of selectively inhibitors of the receptor activity with monoclonal antibody such as OMP-59R5 (Tarextumab, OncoMed Pharmaceuticals-GlaxoSmithKline), which targets selectively Notch2 and 3 receptors (200). Additionally, in the laboratory where I attended my PhD program recently identified a first set of small molecules disrupting the interaction between Jagged ligands and Notch receptors (201), an approach that according to Kagsmaskin *et al.* (202, 203) should be far less toxic than pan Notch inhibition. Finally, the approach shown in this work, based on the use of anti-Notch2 shRNA, provides an indication that the new emerging therapeutic approach based on the use of RNA-based drugs(204) may represent a new possible future approach to selectively target the Notch2 expression in MM cells.

## **ACKNOWLEDGMENTS**

I would like to express my deep gratitude to my supervisor, prof. Raffaella Chiaramonte, who guided me throughout this project. I wish to acknowledge the technical and moral support provided from the research group where I conducted my PhD work, in particular dr. Natalia Platonova, dr. Valentina Citro and dr. Lavinia Casati. I would like to thank the University of Milan and the PhD in Experimental Medicine for giving me the opportunity to complete my research training and engage in this exciting research project.

## REFERENCES

1. Multiple myeloma: 2018 update on diagnosis, risk-stratification, and management. *American journal of hematology*. 2018;93(8):981-1114.
2. Moreau P, San Miguel J, Sonneveld P, Mateos MV, Zamagni E, Avet-Loiseau H, et al. Multiple myeloma: ESMO Clinical Practice Guidelines for diagnosis, treatment and follow-up. *Annals of oncology : official journal of the European Society for Medical Oncology*. 2017;28(suppl\_4):iv52-iv61.
3. Guzdar A, Costello C. Supportive Care in Multiple Myeloma. *Current hematologic malignancy reports*. 2020;15(2):56-61.
4. Rajkumar SV, Mesa RA, Fonseca R, Schroeder G, Plevak MF, Dispenzieri A, et al. Bone marrow angiogenesis in 400 patients with monoclonal gammopathy of undetermined significance, multiple myeloma, and primary amyloidosis. *Clinical cancer research : an official journal of the American Association for Cancer Research*. 2002;8(7):2210-6.
5. Kyle RA, Therneau TM, Rajkumar SV, Offord JR, Larson DR, Plevak MF, et al. A long-term study of prognosis in monoclonal gammopathy of undetermined significance. *The New England journal of medicine*. 2002;346(8):564-9.
6. Fairfield H, Falank C, Avery L, Reagan MR. Multiple myeloma in the marrow: pathogenesis and treatments. *Annals of the New York Academy of Sciences*. 2016;1364:32-51.
7. Kyle RA, Remstein ED, Therneau TM, Dispenzieri A, Kurtin PJ, Hodnefield JM, et al. Clinical course and prognosis of smoldering (asymptomatic) multiple myeloma. *The New England journal of medicine*. 2007;356(25):2582-90.
8. Rajkumar SV, Dimopoulos MA, Palumbo A, Blade J, Merlini G, Mateos MV, et al. International Myeloma Working Group updated criteria for the diagnosis of multiple myeloma. *The Lancet Oncology*. 2014;15(12):e538-48.
9. Jamet B, Bailly C, Carlier T, Touzeau C, Michaud AV, Bourgeois M, et al. Imaging of Monoclonal Gammopathy of Undetermined Significance and Smoldering Multiple Myeloma. *Cancers*. 2020;12(2).
10. Jelinek T, Kryukov F, Rihova L, Hajek R. Plasma cell leukemia: from biology to treatment. *European journal of haematology*. 2015;95(1):16-26.
11. Bergsagel PL, Chesi M, Nardini E, Brents LA, Kirby SL, Kuehl WM. Promiscuous translocations into immunoglobulin heavy chain switch regions in multiple myeloma. *Proceedings of the National Academy of Sciences of the United States of America*. 1996;93(24):13931-6.
12. Fonseca R, Debes-Marun CS, Picken EB, Dewald GW, Bryant SC, Winkler JM, et al. The recurrent IgH translocations are highly associated with nonhyperdiploid variant multiple myeloma. *Blood*. 2003;102(7):2562-7.
13. Gabrea A, Bergsagel PL, Chesi M, Shou Y, Kuehl WM. Insertion of excised IgH switch sequences causes overexpression of cyclin D1 in a myeloma tumor cell. *Molecular cell*. 1999;3(1):119-23.
14. Shaughnessy J, Jr., Gabrea A, Qi Y, Brents L, Zhan F, Tian E, et al. Cyclin D3 at 6p21 is dysregulated by recurrent chromosomal translocations to immunoglobulin loci in multiple myeloma. *Blood*. 2001;98(1):217-23.
15. Chesi M, Nardini E, Brents LA, Schrock E, Ried T, Kuehl WM, et al. Frequent translocation t(4;14)(p16.3;q32.3) in multiple myeloma is associated with increased expression and activating mutations of fibroblast growth factor receptor 3. *Nature genetics*. 1997;16(3):260-4.
16. Chesi M, Bergsagel PL, Shonukan OO, Martelli ML, Brents LA, Chen T, et al. Frequent dysregulation of the c-maf proto-oncogene at 16q23 by translocation to an Ig locus in multiple myeloma. *Blood*. 1998;91(12):4457-63.
17. Smadja NV, Fruchart C, Isnard F, Louvet C, Dutel JL, Cheron N, et al. Chromosomal analysis in multiple myeloma: cytogenetic evidence of two different diseases. *Leukemia*. 1998;12(6):960-9.
18. Furukawa Y, Kikuchi J. Molecular pathogenesis of multiple myeloma. *International journal of clinical oncology*. 2015;20(3):413-22.

19. Amodio N, D'Aquila P, Passarino G, Tassone P, Bellizzi D. Epigenetic modifications in multiple myeloma: recent advances on the role of DNA and histone methylation. *Expert opinion on therapeutic targets*. 2017;21(1):91-101.
20. Mirabella F, Wu P, Wardell CP, Kaiser MF, Walker BA, Johnson DC, et al. MMSET is the key molecular target in t(4;14) myeloma. *Blood cancer journal*. 2013;3:e114.
21. Ohguchi H, Hideshima T, Anderson KC. The biological significance of histone modifiers in multiple myeloma: clinical applications. *Blood cancer journal*. 2018;8(9):83.
22. Minami J, Suzuki R, Mazitschek R, Gorgun G, Ghosh B, Cirstea D, et al. Histone deacetylase 3 as a novel therapeutic target in multiple myeloma. *Leukemia*. 2014;28(3):680-9.
23. Bianchi G, Munshi NC. Pathogenesis beyond the cancer clone(s) in multiple myeloma. *Blood*. 2015;125(20):3049-58.
24. Kuehl WM, Bergsagel PL. Multiple myeloma: evolving genetic events and host interactions. *Nature reviews Cancer*. 2002;2(3):175-87.
25. Intini D, Baldini L, Fabris S, Lombardi L, Ciceri G, Maiolo AT, et al. Analysis of FGFR3 gene mutations in multiple myeloma patients with t(4;14). *British journal of haematology*. 2001;114(2):362-4.
26. Corradini P, Ladetto M, Voena C, Palumbo A, Inghirami G, Knowles DM, et al. Mutational activation of N- and K-ras oncogenes in plasma cell dyscrasias. *Blood*. 1993;81(10):2708-13.
27. Hole PS, Darley RL, Tonks A. Do reactive oxygen species play a role in myeloid leukemias? *Blood*. 2011;117(22):5816-26.
28. Asosingh K, De Raeve H, de Ridder M, Storme GA, Willems A, Van Riet I, et al. Role of the hypoxic bone marrow microenvironment in 5T2MM murine myeloma tumor progression. *Haematologica*. 2005;90(6):810-7.
29. Martin SK, Diamond P, Williams SA, To LB, Peet DJ, Fujii N, et al. Hypoxia-inducible factor-2 is a novel regulator of aberrant CXCL12 expression in multiple myeloma plasma cells. *Haematologica*. 2010;95(5):776-84.
30. Grivennikov SI, Greten FR, Karin M. Immunity, inflammation, and cancer. *Cell*. 2010;140(6):883-99.
31. Giuliani N, Colla S, Rizzoli V. Angiogenic switch in multiple myeloma. *Hematology*. 2004;9(5-6):377-81.
32. Sirohi B, Powles R. Multiple myeloma. *Lancet*. 2004;363(9412):875-87.
33. Rajkumar SV. Treatment of multiple myeloma. *Nature reviews Clinical oncology*. 2011;8(8):479-91.
34. Rajkumar SV. Multiple myeloma: 2016 update on diagnosis, risk-stratification, and management. *American journal of hematology*. 2016;91(7):719-34.
35. Hideshima T, Mitsiades C, Tonon G, Richardson PG, Anderson KC. Understanding multiple myeloma pathogenesis in the bone marrow to identify new therapeutic targets. *Nature reviews Cancer*. 2007;7(8):585-98.
36. Manier S, Sacco A, Leleu X, Ghobrial IM, Roccaro AM. Bone marrow microenvironment in multiple myeloma progression. *Journal of biomedicine & biotechnology*. 2012;2012:157496.
37. Katz BZ. Adhesion molecules--The lifelines of multiple myeloma cells. *Seminars in cancer biology*. 2010;20(3):186-95.
38. Hideshima T, Akiyama M, Hayashi T, Richardson P, Schlossman R, Chauhan D, et al. Targeting p38 MAPK inhibits multiple myeloma cell growth in the bone marrow milieu. *Blood*. 2003;101(2):703-5.
39. Annunziata CM, Davis RE, Demchenko Y, Bellamy W, Gabrea A, Zhan F, et al. Frequent engagement of the classical and alternative NF-kappaB pathways by diverse genetic abnormalities in multiple myeloma. *Cancer cell*. 2007;12(2):115-30.
40. Wu D, Guo X, Su J, Chen R, Berenson D, Guthold M, et al. CD138-negative myeloma cells regulate mechanical properties of bone marrow stromal cells through SDF-1/CXCR4/AKT signaling pathway. *Biochimica et biophysica acta*. 2015;1853(2):338-47.
41. Ponomaryov T, Peled A, Petit I, Taichman RS, Habler L, Sandbank J, et al. Induction of the chemokine stromal-derived factor-1 following DNA damage improves human stem cell function. *The Journal of clinical investigation*. 2000;106(11):1331-9.

42. Alsayed Y, Ngo H, Runnels J, Leleu X, Singha UK, Pitsillides CM, et al. Mechanisms of regulation of CXCR4/SDF-1 (CXCL12)-dependent migration and homing in multiple myeloma. *Blood*. 2007;109(7):2708-17.
43. Ullah TR. The role of CXCR4 in multiple myeloma: Cells' journey from bone marrow to beyond. *Journal of bone oncology*. 2019;17:100253.
44. Marino S, Roodman GD. Multiple Myeloma and Bone: The Fatal Interaction. *Cold Spring Harbor perspectives in medicine*. 2018;8(8).
45. Kawano Y, Moschetta M, Manier S, Glavey S, Gorgun GT, Roccaro AM, et al. Targeting the bone marrow microenvironment in multiple myeloma. *Immunological reviews*. 2015;263(1):160-72.
46. Artavanis-Tsakonas S, Rand MD, Lake RJ. Notch signaling: cell fate control and signal integration in development. *Science*. 1999;284(5415):770-6.
47. Platonova N, Lesma E, Basile A, Bignotto M, Garavelli S, Palano MT, et al. Targeting Notch as a Therapeutic Approach for Human Malignancies. *Current pharmaceutical design*. 2017;23(1):108-34.
48. Colombo M, Mirandola L, Platonova N, Apicella L, Basile A, Figueroa AJ, et al. Notch-directed microenvironment reprogramming in myeloma: a single path to multiple outcomes. *Leukemia*. 2013;27(5):1009-18.
49. Ilagan MX, Kopan R. SnapShot: notch signaling pathway. *Cell*. 2007;128(6):1246.
50. de Celis JF, Bray SJ. The Abruption domain of Notch regulates negative interactions between Notch, its ligands and Fringe. *Development*. 2000;127(6):1291-302.
51. Kopan R, Ilagan MX. The canonical Notch signaling pathway: unfolding the activation mechanism. *Cell*. 2009;137(2):216-33.
52. Arruga F, Vaisitti T, Deaglio S. The NOTCH Pathway and Its Mutations in Mature B Cell Malignancies. *Frontiers in oncology*. 2018;8:550.
53. Wolfe MS, Kopan R. Intramembrane proteolysis: theme and variations. *Science*. 2004;305(5687):1119-23.
54. Lubman OY, Korolev SV, Kopan R. Anchoring notch genetics and biochemistry; structural analysis of the ankyrin domain sheds light on existing data. *Molecular cell*. 2004;13(5):619-26.
55. Friedmann DR, Wilson JJ, Kovall RA. RAM-induced allostery facilitates assembly of a notch pathway active transcription complex. *The Journal of biological chemistry*. 2008;283(21):14781-91.
56. Iso T, Kedes L, Hamamori Y. HES and HRP families: multiple effectors of the Notch signaling pathway. *Journal of cellular physiology*. 2003;194(3):237-55.
57. Palomero T, Lim WK, Odom DT, Sulis ML, Real PJ, Margolin A, et al. NOTCH1 directly regulates c-MYC and activates a feed-forward-loop transcriptional network promoting leukemic cell growth. *Proceedings of the National Academy of Sciences of the United States of America*. 2006;103(48):18261-6.
58. Ronchini C, Capobianco AJ. Induction of cyclin D1 transcription and CDK2 activity by Notch(ic): implication for cell cycle disruption in transformation by Notch(ic). *Molecular and cellular biology*. 2001;21(17):5925-34.
59. Joshi I, Minter LM, Telfer J, Demarest RM, Capobianco AJ, Aster JC, et al. Notch signaling mediates G1/S cell-cycle progression in T cells via cyclin D3 and its dependent kinases. *Blood*. 2009;113(8):1689-98.
60. Rangarajan A, Talora C, Okuyama R, Nicolas M, Mammucari C, Oh H, et al. Notch signaling is a direct determinant of keratinocyte growth arrest and entry into differentiation. *The EMBO journal*. 2001;20(13):3427-36.
61. Oswald F, Liptay S, Adler G, Schmid RM. NF-kappaB2 is a putative target gene of activated Notch-1 via RBP-Jkappa. *Molecular and cellular biology*. 1998;18(4):2077-88.
62. Jin S, Hansson EM, Tikka S, Lanner F, Sahlgren C, Farnebo F, et al. Notch signaling regulates platelet-derived growth factor receptor-beta expression in vascular smooth muscle cells. *Circulation research*. 2008;102(12):1483-91.
63. Siebel C, Lendahl U. Notch Signaling in Development, Tissue Homeostasis, and Disease. *Physiological reviews*. 2017;97(4):1235-94.
64. Takebe N, Nguyen D, Yang SX. Targeting notch signaling pathway in cancer: clinical development advances and challenges. *Pharmacology & therapeutics*. 2014;141(2):140-9.

65. Skrtic A, Korac P, Kristo DR, Ajdukovic Stojisavljevic R, Ivankovic D, Dominis M. Immunohistochemical analysis of NOTCH1 and JAGGED1 expression in multiple myeloma and monoclonal gammopathy of undetermined significance. *Human pathology*. 2010;41(12):1702-10.
66. van Stralen E, van de Wetering M, Agnelli L, Neri A, Clevers HC, Bast BJ. Identification of primary MAFB target genes in multiple myeloma. *Experimental hematology*. 2009;37(1):78-86.
67. Korde N, Kristinsson SY, Landgren O. Monoclonal gammopathy of undetermined significance (MGUS) and smoldering multiple myeloma (SMM): novel biological insights and development of early treatment strategies. *Blood*. 2011;117(21):5573-81.
68. Houde C, Li Y, Song L, Barton K, Zhang Q, Godwin J, et al. Overexpression of the NOTCH ligand JAG2 in malignant plasma cells from multiple myeloma patients and cell lines. *Blood*. 2004;104(12):3697-704.
69. Nefedova Y, Cheng P, Alsina M, Dalton WS, Gabrilovich DI. Involvement of Notch-1 signaling in bone marrow stroma-mediated de novo drug resistance of myeloma and other malignant lymphoid cell lines. *Blood*. 2004;103(9):3503-10.
70. Mirandola L, Apicella L, Colombo M, Yu Y, Berta DG, Platonova N, et al. Anti-Notch treatment prevents multiple myeloma cells localization to the bone marrow via the chemokine system CXCR4/SDF-1. *Leukemia*. 2013;27(7):1558-66.
71. Colombo M, Galletti S, Bulfamante G, Falleni M, Tosi D, Todoerti K, et al. Multiple myeloma-derived Jagged ligands increases autocrine and paracrine interleukin-6 expression in bone marrow niche. *Oncotarget*. 2016;7(35):56013-29.
72. Chiron D, Maiga S, Descamps G, Moreau P, Le Gouill S, Marionneau S, et al. Critical role of the NOTCH ligand JAG2 in self-renewal of myeloma cells. *Blood cells, molecules & diseases*. 2012;48(4):247-53.
73. Kumar S, Witzig TE, Timm M, Haug J, Wellik L, Fonseca R, et al. Expression of VEGF and its receptors by myeloma cells. *Leukemia*. 2003;17(10):2025-31.
74. Kuhn DJ, Berkova Z, Jones RJ, Woessner R, Bjorklund CC, Ma W, et al. Targeting the insulin-like growth factor-1 receptor to overcome bortezomib resistance in preclinical models of multiple myeloma. *Blood*. 2012;120(16):3260-70.
75. Gado K, Domjan G, Hegyesi H, Falus A. Role of INTERLEUKIN-6 in the pathogenesis of multiple myeloma. *Cell biology international*. 2000;24(4):195-209.
76. Colombo M, Garavelli S, Mazzola M, Platonova N, Giannandrea D, Colella R, et al. Multiple myeloma exploits Jagged1 and Jagged2 to promote intrinsic and bone marrow-dependent drug resistance. *Haematologica*. 2020;105(7):1925-36.
77. Colombo M, Thummler K, Mirandola L, Garavelli S, Todoerti K, Apicella L, et al. Notch signaling drives multiple myeloma induced osteoclastogenesis. *Oncotarget*. 2014;5(21):10393-406.
78. Palano MT, Giannandrea D, Platonova N, Gaudenzi G, Falleni M, Tosi D, et al. Jagged Ligands Enhance the Pro-Angiogenic Activity of Multiple Myeloma Cells. *Cancers*. 2020;12(9).
79. Thery C, Witwer KW, Aikawa E, Alcaraz MJ, Anderson JD, Andriantsitohaina R, et al. Minimal information for studies of extracellular vesicles 2018 (MISEV2018): a position statement of the International Society for Extracellular Vesicles and update of the MISEV2014 guidelines. *Journal of extracellular vesicles*. 2018;7(1):1535750.
80. Russell AE, Sneider A, Witwer KW, Bergese P, Bhattacharyya SN, Cocks A, et al. Biological membranes in EV biogenesis, stability, uptake, and cargo transfer: an ISEV position paper arising from the ISEV membranes and EVs workshop. *Journal of extracellular vesicles*. 2019;8(1):1684862.
81. Huotari J, Helenius A. Endosome maturation. *The EMBO journal*. 2011;30(17):3481-500.
82. Henne WM, Stenmark H, Emr SD. Molecular mechanisms of the membrane sculpting ESCRT pathway. *Cold Spring Harbor perspectives in biology*. 2013;5(9).
83. Stuffers S, Sem Wegner C, Stenmark H, Brech A. Multivesicular endosome biogenesis in the absence of ESCRTs. *Traffic*. 2009;10(7):925-37.
84. Hessvik NP, Llorente A. Current knowledge on exosome biogenesis and release. *Cellular and molecular life sciences : CMLS*. 2018;75(2):193-208.
85. van Niel G, D'Angelo G, Raposo G. Shedding light on the cell biology of extracellular vesicles. *Nature reviews Molecular cell biology*. 2018;19(4):213-28.

86. Dang XTT, Kavishka JM, Zhang DX, Pirisinu M, Le MTN. Extracellular Vesicles as an Efficient and Versatile System for Drug Delivery. *Cells*. 2020;9(10).
87. Mathieu M, Martin-Jaular L, Lavieu G, Thery C. Specificities of secretion and uptake of exosomes and other extracellular vesicles for cell-to-cell communication. *Nature cell biology*. 2019;21(1):9-17.
88. Becker A, Thakur BK, Weiss JM, Kim HS, Peinado H, Lyden D. Extracellular Vesicles in Cancer: Cell-to-Cell Mediators of Metastasis. *Cancer cell*. 2016;30(6):836-48.
89. Al-Nedawi K, Meehan B, Micallef J, Lhotak V, May L, Guha A, et al. Intercellular transfer of the oncogenic receptor EGFRvIII by microvesicles derived from tumour cells. *Nature cell biology*. 2008;10(5):619-24.
90. Kim H, Lee S, Shin E, Seong KM, Jin YW, Youn H, et al. The Emerging Roles of Exosomes as EMT Regulators in Cancer. *Cells*. 2020;9(4).
91. Wieckowski EU, Visus C, Szajnik M, Szczepanski MJ, Storkus WJ, Whiteside TL. Tumor-derived microvesicles promote regulatory T cell expansion and induce apoptosis in tumor-reactive activated CD8+ T lymphocytes. *Journal of immunology*. 2009;183(6):3720-30.
92. Ashiru O, Boutet P, Fernandez-Messina L, Aguera-Gonzalez S, Skepper JN, Vales-Gomez M, et al. Natural killer cell cytotoxicity is suppressed by exposure to the human NKG2D ligand MICA\*008 that is shed by tumor cells in exosomes. *Cancer research*. 2010;70(2):481-9.
93. Valenti R, Huber V, Filipazzi P, Pilla L, Sovena G, Villa A, et al. Human tumor-released microvesicles promote the differentiation of myeloid cells with transforming growth factor-beta-mediated suppressive activity on T lymphocytes. *Cancer research*. 2006;66(18):9290-8.
94. Peinado H, Aleckovic M, Lavotshkin S, Matei I, Costa-Silva B, Moreno-Bueno G, et al. Melanoma exosomes educate bone marrow progenitor cells toward a pro-metastatic phenotype through MET. *Nature medicine*. 2012;18(6):883-91.
95. Zeng Z, Li Y, Pan Y, Lan X, Song F, Sun J, et al. Cancer-derived exosomal miR-25-3p promotes pre-metastatic niche formation by inducing vascular permeability and angiogenesis. *Nature communications*. 2018;9(1):5395.
96. Zhou W, Fong MY, Min Y, Somlo G, Liu L, Palomares MR, et al. Cancer-secreted miR-105 destroys vascular endothelial barriers to promote metastasis. *Cancer cell*. 2014;25(4):501-15.
97. Rana S, Malinowska K, Zoller M. Exosomal tumor microRNA modulates premetastatic organ cells. *Neoplasia*. 2013;15(3):281-95.
98. Fong MY, Zhou W, Liu L, Alontaga AY, Chandra M, Ashby J, et al. Breast-cancer-secreted miR-122 reprograms glucose metabolism in premetastatic niche to promote metastasis. *Nature cell biology*. 2015;17(2):183-94.
99. Urabe F, Kosaka N, Ito K, Kimura T, Egawa S, Ochiya T. Extracellular vesicles as biomarkers and therapeutic targets for cancer. *American journal of physiology Cell physiology*. 2020;318(1):C29-C39.
100. Taylor DD, Gercel-Taylor C. MicroRNA signatures of tumor-derived exosomes as diagnostic biomarkers of ovarian cancer. *Gynecologic oncology*. 2008;110(1):13-21.
101. Hoshino A, Costa-Silva B, Shen TL, Rodrigues G, Hashimoto A, Tesic Mark M, et al. Tumour exosome integrins determine organotropic metastasis. *Nature*. 2015;527(7578):329-35.
102. Matsumura T, Sugimachi K, Iinuma H, Takahashi Y, Kurashige J, Sawada G, et al. Exosomal microRNA in serum is a novel biomarker of recurrence in human colorectal cancer. *British journal of cancer*. 2015;113(2):275-81.
103. Li Z, Ma YY, Wang J, Zeng XF, Li R, Kang W, et al. Exosomal microRNA-141 is upregulated in the serum of prostate cancer patients. *OncoTargets and therapy*. 2016;9:139-48.
104. Bryant RJ, Pawlowski T, Catto JW, Marsden G, Vessella RL, Rhee B, et al. Changes in circulating microRNA levels associated with prostate cancer. *British journal of cancer*. 2012;106(4):768-74.
105. Alegre E, Sanmamed MF, Rodriguez C, Carranza O, Martin-Algarra S, Gonzalez A. Study of circulating microRNA-125b levels in serum exosomes in advanced melanoma. *Archives of pathology & laboratory medicine*. 2014;138(6):828-32.
106. Liao J, Liu R, Shi YJ, Yin LH, Pu YP. Exosome-shuttling microRNA-21 promotes cell migration and invasion-targeting PDCD4 in esophageal cancer. *International journal of oncology*. 2016;48(6):2567-79.

107. Di Noto G, Paolini L, Zandrini A, Radeghieri A, Caimi L, Ricotta D. C-src enriched serum microvesicles are generated in malignant plasma cell dyscrasia. *PloS one*. 2013;8(8):e70811.
108. Caivano A, Laurenzana I, De Luca L, La Rocca F, Simeon V, Trino S, et al. High serum levels of extracellular vesicles expressing malignancy-related markers are released in patients with various types of hematological neoplastic disorders. *Tumour biology : the journal of the International Society for Oncodevelopmental Biology and Medicine*. 2015;36(12):9739-52.
109. Harshman SW, Canella A, Ciarlariello PD, Agarwal K, Branson OE, Rocci A, et al. Proteomic characterization of circulating extracellular vesicles identifies novel serum myeloma associated markers. *Journal of proteomics*. 2016;136:89-98.
110. Hertweck MK, Erdfelder F, Kreuzer KA. CD44 in hematological neoplasias. *Annals of hematology*. 2011;90(5):493-508.
111. Manier S, Liu CJ, Avet-Loiseau H, Park J, Shi J, Campigotto F, et al. Prognostic role of circulating exosomal miRNAs in multiple myeloma. *Blood*. 2017;129(17):2429-36.
112. Jung SH, Lee SE, Lee M, Kim SH, Yim SH, Kim TW, et al. Circulating microRNA expressions can predict the outcome of lenalidomide plus low-dose dexamethasone treatment in patients with refractory/relapsed multiple myeloma. *Haematologica*. 2017;102(11):e456-e9.
113. Zhang L, Pan L, Xiang B, Zhu H, Wu Y, Chen M, et al. Potential role of exosome-associated microRNA panels and in vivo environment to predict drug resistance for patients with multiple myeloma. *Oncotarget*. 2016;7(21):30876-91.
114. Wang J, Faict S, Maes K, De Bruyne E, Van Valckenborgh E, Schots R, et al. Extracellular vesicle cross-talk in the bone marrow microenvironment: implications in multiple myeloma. *Oncotarget*. 2016;7(25):38927-45.
115. Arendt BK, Walters DK, Wu X, Tschumper RC, Jelinek DF. Multiple myeloma cell-derived microvesicles are enriched in CD147 expression and enhance tumor cell proliferation. *Oncotarget*. 2014;5(14):5686-99.
116. Arendt BK, Walters DK, Wu X, Tschumper RC, Huddleston PM, Henderson KJ, et al. Increased expression of extracellular matrix metalloproteinase inducer (CD147) in multiple myeloma: role in regulation of myeloma cell proliferation. *Leukemia*. 2012;26(10):2286-96.
117. Faict S, Oudaert I, D'Auria L, Dehairs J, Maes K, Vlummens P, et al. The Transfer of Sphingomyelinase Contributes to Drug Resistance in Multiple Myeloma. *Cancers*. 2019;11(12).
118. Cheng Q, Li X, Wang Y, Dong M, Zhan FH, Liu J. The ceramide pathway is involved in the survival, apoptosis and exosome functions of human multiple myeloma cells in vitro. *Acta pharmacologica Sinica*. 2018;39(4):561-8.
119. Liu Z, Liu H, Li Y, Shao Q, Chen J, Song J, et al. Multiple myeloma-derived exosomes inhibit osteoblastic differentiation and improve IL-6 secretion of BMSCs from multiple myeloma. *Journal of investigative medicine : the official publication of the American Federation for Clinical Research*. 2020;68(1):45-51.
120. Cheng Q, Li X, Liu J, Ye Q, Chen Y, Tan S, et al. Multiple Myeloma-Derived Exosomes Regulate the Functions of Mesenchymal Stem Cells Partially via Modulating miR-21 and miR-146a. *Stem cells international*. 2017;2017:9012152.
121. Khalife J, Ghose J, Martella M, Viola D, Rocci A, Troadec E, et al. MiR-16 regulates crosstalk in NF-kappaB tolerogenic inflammatory signaling between myeloma cells and bone marrow macrophages. *JCI insight*. 2019;4(21).
122. Wang J, De Veirman K, Faict S, Frassanito MA, Ribatti D, Vacca A, et al. Multiple myeloma exosomes establish a favourable bone marrow microenvironment with enhanced angiogenesis and immunosuppression. *The Journal of pathology*. 2016;239(2):162-73.
123. Xiong WJ, Liu HX, Shi DY, Lou J, Zhang QL. [Effect of Myeloma-Derived Exosomes on Surface Activating Receptors of NK Cells]. *Zhongguo shi yan xue ye xue za zhi*. 2017;25(6):1713-7.
124. Chen X, Wang Z, Duan N, Zhu G, Schwarz EM, Xie C. Osteoblast-osteoclast interactions. *Connective tissue research*. 2018;59(2):99-107.



125. Giuliani N, Colla S, Morandi F, Lazzaretti M, Sala R, Bonomini S, et al. Myeloma cells block RUNX2/CBFA1 activity in human bone marrow osteoblast progenitors and inhibit osteoblast formation and differentiation. *Blood*. 2005;106(7):2472-83.
126. Mahtouk K, Moreaux J, Hose D, Reme T, Meissner T, Jourdan M, et al. Growth factors in multiple myeloma: a comprehensive analysis of their expression in tumor cells and bone marrow environment using Affymetrix microarrays. *BMC cancer*. 2010;10:198.
127. Pozzi S, Raje N. The role of bisphosphonates in multiple myeloma: mechanisms, side effects, and the future. *The oncologist*. 2011;16(5):651-62.
128. Henry DH, Costa L, Goldwasser F, Hirsh V, Hungria V, Prausova J, et al. Randomized, double-blind study of denosumab versus zoledronic acid in the treatment of bone metastases in patients with advanced cancer (excluding breast and prostate cancer) or multiple myeloma. *Journal of clinical oncology : official journal of the American Society of Clinical Oncology*. 2011;29(9):1125-32.
129. Giuliani N, Morandi F, Tagliaferri S, Lazzaretti M, Bonomini S, Crugnola M, et al. The proteasome inhibitor bortezomib affects osteoblast differentiation in vitro and in vivo in multiple myeloma patients. *Blood*. 2007;110(1):334-8.
130. Accardi F, Toscani D, Bolzoni M, Dalla Palma B, Aversa F, Giuliani N. Mechanism of Action of Bortezomib and the New Proteasome Inhibitors on Myeloma Cells and the Bone Microenvironment: Impact on Myeloma-Induced Alterations of Bone Remodeling. *BioMed research international*. 2015;2015:172458.
131. Yu J, Canalis E. Notch and the regulation of osteoclast differentiation and function. *Bone*. 2020;138:115474.
132. Goel PN, Moharrer Y, Hebb JH, Egol AJ, Kaur G, Hankenson KD, et al. Suppression of Notch Signaling in Osteoclasts Improves Bone Regeneration and Healing. *Journal of orthopaedic research : official publication of the Orthopaedic Research Society*. 2019;37(10):2089-103.
133. Fukushima H, Nakao A, Okamoto F, Shin M, Kajiya H, Sakano S, et al. The association of Notch2 and NF-kappaB accelerates RANKL-induced osteoclastogenesis. *Molecular and cellular biology*. 2008;28(20):6402-12.
134. Ganguly SS, Hostetter G, Tang L, Frank SB, Saboda K, Mehra R, et al. Notch3 promotes prostate cancer-induced bone lesion development via MMP-3. *Oncogene*. 2020;39(1):204-18.
135. Ping Y, Lou F, Yang X, Zhang P. [Up-regulation of Notch1 inhibits proliferation and differentiation of osteoclast in vitro]. *Hua xi kou qiang yi xue za zhi = Huaxi kouqiang yixue zazhi = West China journal of stomatology*. 2016;34(2):121-4.
136. Sekine C, Koyanagi A, Koyama N, Hozumi K, Chiba S, Yagita H. Differential regulation of osteoclastogenesis by Notch2/Delta-like 1 and Notch1/Jagged1 axes. *Arthritis research & therapy*. 2012;14(2):R45.
137. Guo J, Fei C, Zhao Y, Zhao S, Zheng Q, Su J, et al. Lenalidomide restores the osteogenic differentiation of bone marrow mesenchymal stem cells from multiple myeloma patients via deactivating Notch signaling pathway. *Oncotarget*. 2017;8(33):55405-21.
138. Xu S, Evans H, Buckle C, De Veirman K, Hu J, Xu D, et al. Impaired osteogenic differentiation of mesenchymal stem cells derived from multiple myeloma patients is associated with a blockade in the deactivation of the Notch signaling pathway. *Leukemia*. 2012;26(12):2546-9.
139. Colombo M, Galletti S, Garavelli S, Platonova N, Paoli A, Basile A, et al. Notch signaling deregulation in multiple myeloma: A rational molecular target. *Oncotarget*. 2015;6(29):26826-40.
140. Raimondi L, De Luca A, Amodio N, Manno M, Raccosta S, Taverna S, et al. Involvement of multiple myeloma cell-derived exosomes in osteoclast differentiation. *Oncotarget*. 2015;6(15):13772-89.
141. Faict S, Muller J, De Veirman K, De Bruyne E, Maes K, Vrancken L, et al. Exosomes play a role in multiple myeloma bone disease and tumor development by targeting osteoclasts and osteoblasts. *Blood cancer journal*. 2018;8(11):105.
142. Raimondi L, De Luca A, Fontana S, Amodio N, Costa V, Carina V, et al. Multiple Myeloma-Derived Extracellular Vesicles Induce Osteoclastogenesis through the Activation of the XBP1/IRE1alpha Axis. *Cancers*. 2020;12(8).

143. Raimondo S, Saieva L, Vicario E, Pucci M, Toscani D, Manno M, et al. Multiple myeloma-derived exosomes are enriched of amphiregulin (AREG) and activate the epidermal growth factor pathway in the bone microenvironment leading to osteoclastogenesis. *Journal of hematology & oncology*. 2019;12(1):2.
144. Zhang L, Lei Q, Wang H, Xu C, Liu T, Kong F, et al. Tumor-derived extracellular vesicles inhibit osteogenesis and exacerbate myeloma bone disease. *Theranostics*. 2019;9(1):196-209.
145. Li B, Xu H, Han H, Song S, Zhang X, Ouyang L, et al. Exosome-mediated transfer of IncRUNX2-AS1 from multiple myeloma cells to MSCs contributes to osteogenesis. *Oncogene*. 2018;37(41):5508-19.
146. Gerhardt H, Golding M, Fruttiger M, Ruhrberg C, Lundkvist A, Abramsson A, et al. VEGF guides angiogenic sprouting utilizing endothelial tip cell filopodia. *The Journal of cell biology*. 2003;161(6):1163-77.
147. Phng LK, Gerhardt H. Angiogenesis: a team effort coordinated by notch. *Developmental cell*. 2009;16(2):196-208.
148. Ribatti D, Vacca A. New Insights in Anti-Angiogenesis in Multiple Myeloma. *International journal of molecular sciences*. 2018;19(7).
149. Ria R, Melaccio A, Racanelli V, Vacca A. Anti-VEGF Drugs in the Treatment of Multiple Myeloma Patients. *Journal of clinical medicine*. 2020;9(6).
150. Dankbar B, Padro T, Leo R, Feldmann B, Kropff M, Mesters RM, et al. Vascular endothelial growth factor and interleukin-6 in paracrine tumor-stromal cell interactions in multiple myeloma. *Blood*. 2000;95(8):2630-6.
151. Pellegrino A, Ria R, Di Pietro G, Cirulli T, Surico G, Pennisi A, et al. Bone marrow endothelial cells in multiple myeloma secrete CXC-chemokines that mediate interactions with plasma cells. *British journal of haematology*. 2005;129(2):248-56.
152. Lobov IB, Renard RA, Papadopoulos N, Gale NW, Thurston G, Yancopoulos GD, et al. Delta-like ligand 4 (Dll4) is induced by VEGF as a negative regulator of angiogenic sprouting. *Proceedings of the National Academy of Sciences of the United States of America*. 2007;104(9):3219-24.
153. Hainaud P, Contreres JO, Villemain A, Liu LX, Plouet J, Tobelem G, et al. The role of the vascular endothelial growth factor-Delta-like 4 ligand/Notch4-ephrin B2 cascade in tumor vessel remodeling and endothelial cell functions. *Cancer research*. 2006;66(17):8501-10.
154. Thurston G, Kitajewski J. VEGF and Delta-Notch: interacting signalling pathways in tumour angiogenesis. *British journal of cancer*. 2008;99(8):1204-9.
155. Benedito R, Roca C, Sorensen I, Adams S, Gossler A, Fruttiger M, et al. The notch ligands Dll4 and Jagged1 have opposing effects on angiogenesis. *Cell*. 2009;137(6):1124-35.
156. Takeuchi H, Haltiwanger RS. Significance of glycosylation in Notch signaling. *Biochemical and biophysical research communications*. 2014;453(2):235-42.
157. Patenaude A, Fuller M, Chang L, Wong F, Paliouras G, Shaw R, et al. Endothelial-specific Notch blockade inhibits vascular function and tumor growth through an eNOS-dependent mechanism. *Cancer research*. 2014;74(9):2402-11.
158. Djokovic D, Trindade A, Gigante J, Pinho M, Harris AL, Duarte A. Incomplete Dll4/Notch signaling inhibition promotes functional angiogenesis supporting the growth of skin papillomas. *BMC cancer*. 2015;15:608.
159. Pisklakova A, Grigson E, Ozerova M, Chen F, Sullivan DM, Nefedova Y. Anti-myeloma effect of pharmacological inhibition of Notch/gamma-secretase with RO4929097 is mediated by modulation of tumor microenvironment. *Cancer biology & therapy*. 2016;17(5):477-85.
160. Saltarella I, Frassanito MA, Lamanuzzi A, Brevi A, Leone P, Desantis V, et al. Homotypic and Heterotypic Activation of the Notch Pathway in Multiple Myeloma-Enhanced Angiogenesis: A Novel Therapeutic Target? *Neoplasia*. 2019;21(1):93-105.
161. Kume T. Novel insights into the differential functions of Notch ligands in vascular formation. *Journal of angiogenesis research*. 2009;1:8.
162. Liu Y, Zhu XJ, Zeng C, Wu PH, Wang HX, Chen ZC, et al. Microvesicles secreted from human multiple myeloma cells promote angiogenesis. *Acta pharmacologica Sinica*. 2014;35(2):230-8.
163. Umezu T, Tadokoro H, Azuma K, Yoshizawa S, Ohyashiki K, Ohyashiki JH. Exosomal miR-135b shed from hypoxic multiple myeloma cells enhances angiogenesis by targeting factor-inhibiting HIF-1. *Blood*. 2014;124(25):3748-57.

164. Zhang L, Sun ZJ, Bian Y, Kulkarni AB. MicroRNA-135b acts as a tumor promoter by targeting the hypoxia-inducible factor pathway in genetically defined mouse model of head and neck squamous cell carcinoma. *Cancer letters*. 2013;331(2):230-8.
165. Li B, Hong J, Hong M, Wang Y, Yu T, Zang S, et al. piRNA-823 delivered by multiple myeloma-derived extracellular vesicles promoted tumorigenesis through re-educating endothelial cells in the tumor environment. *Oncogene*. 2019;38(26):5227-38.
166. Zarfati M, Avivi I, Brenner B, Katz T, Aharon A. Extracellular vesicles of multiple myeloma cells utilize the proteasome inhibitor mechanism to moderate endothelial angiogenesis. *Angiogenesis*. 2019;22(1):185-96.
167. Guo HM, Sun L, Yang L, Liu XJ, Nie ZY, Luo JM. Microvesicles shed from bortezomib-treated or lenalidomide-treated human myeloma cells inhibit angiogenesis in vitro. *Oncology reports*. 2018;39(6):2873-80.
168. Liu L, Ye Q, Liu L, Bihl JC, Chen Y, Liu J, et al. C6-ceramide treatment inhibits the proangiogenic activity of multiple myeloma exosomes via the miR-29b/Akt pathway. *Journal of translational medicine*. 2020;18(1):298.
169. Bollati V, Angelici L, Rizzo G, Pergoli L, Rota F, Hoxha M, et al. Microvesicle-associated microRNA expression is altered upon particulate matter exposure in healthy workers and in A549 cells. *Journal of applied toxicology : JAT*. 2015;35(1):59-67.
170. Faul F, Erdfelder E, Lang AG, Buchner A. G\*Power 3: a flexible statistical power analysis program for the social, behavioral, and biomedical sciences. *Behavior research methods*. 2007;39(2):175-91.
171. Motulsky HJ, Brown RE. Detecting outliers when fitting data with nonlinear regression – a new method based on robust nonlinear regression and the false discovery rate. *BMC Bioinformatics*. 2006;7(1):123.
172. Ribatti D, Moschetta M, Vacca A. Microenvironment and multiple myeloma spread. *Thrombosis research*. 2014;133 Suppl 2:S102-6.
173. Colombo M, Giannandrea D, Lesma E, Basile A, Chiamonte R. Extracellular Vesicles Enhance Multiple Myeloma Metastatic Dissemination. *International journal of molecular sciences*. 2019;20(13).
174. Vestad B, Llorente A, Neurauter A, Phuyal S, Kierulf B, Kierulf P, et al. Size and concentration analyses of extracellular vesicles by nanoparticle tracking analysis: a variation study. *Journal of extracellular vesicles*. 2017;6(1):1344087.
175. Sacco A, Roccaro AM, Ma D, Shi J, Mishima Y, Moschetta M, et al. Cancer Cell Dissemination and Homing to the Bone Marrow in a Zebrafish Model. *Cancer research*. 2016;76(2):463-71.
176. Dang TP. Notch, apoptosis and cancer. *Advances in experimental medicine and biology*. 2012;727:199-209.
177. Garcia-Ortiz A, Rodriguez-Garcia Y, Encinas J, Maroto-Martin E, Castellano E, Teixido J, et al. The Role of Tumor Microenvironment in Multiple Myeloma Development and Progression. *Cancers*. 2021;13(2).
178. Lomas OC, Tahri S, Ghobrial IM. The microenvironment in myeloma. *Current opinion in oncology*. 2020;32(2):170-5.
179. De Luca L, Laurenzana I, Trino S, Lamorte D, Caivano A, Musto P. An update on extracellular vesicles in multiple myeloma: a focus on their role in cell-to-cell cross-talk and as potential liquid biopsy biomarkers. *Expert review of molecular diagnostics*. 2019;19(3):249-58.
180. Yamamoto T, Kosaka N, Hattori Y, Ochiya T. A Challenge to Aging Society by microRNA in Extracellular Vesicles: microRNA in Extracellular Vesicles as Promising Biomarkers and Novel Therapeutic Targets in Multiple Myeloma. *Journal of clinical medicine*. 2018;7(3).
181. Ribatti D, Vacca A. Role of Endothelial Cells and Fibroblasts in Multiple Myeloma Angiogenic Switch. *Cancer treatment and research*. 2016;169:51-61.
182. Funahashi Y, Hernandez SL, Das I, Ahn A, Huang J, Vorontchikhina M, et al. A notch1 ectodomain construct inhibits endothelial notch signaling, tumor growth, and angiogenesis. *Cancer research*. 2008;68(12):4727-35.
183. Vacca A, Ribatti D. Bone marrow angiogenesis in multiple myeloma. *Leukemia*. 2006;20(2):193-9.

184. Gupta D, Treon SP, Shima Y, Hideshima T, Podar K, Tai YT, et al. Adherence of multiple myeloma cells to bone marrow stromal cells upregulates vascular endothelial growth factor secretion: therapeutic applications. *Leukemia*. 2001;15(12):1950-61.
185. Zahoor M, Westhryn M, Aass KR, Moen SH, Misund K, Psonka-Antonczyk KM, et al. Hypoxia promotes IL-32 expression in myeloma cells, and high expression is associated with poor survival and bone loss. *Blood advances*. 2017;1(27):2656-66.
186. Sheldon H, Heikamp E, Turley H, Dragovic R, Thomas P, Oon CE, et al. New mechanism for Notch signaling to endothelium at a distance by Delta-like 4 incorporation into exosomes. *Blood*. 2010;116(13):2385-94.
187. Sharghi-Namini S, Tan E, Ong LL, Ge R, Asada HH. Dll4-containing exosomes induce capillary sprout retraction in a 3D microenvironment. *Scientific reports*. 2014;4:4031.
188. Lazar I, Clement E, Ducoux-Petit M, Denat L, Soldan V, Dauvillier S, et al. Proteome characterization of melanoma exosomes reveals a specific signature for metastatic cell lines. *Pigment cell & melanoma research*. 2015;28(4):464-75.
189. Wang Q, Lu Q. Plasma membrane-derived extracellular microvesicles mediate non-canonical intercellular NOTCH signaling. *Nature communications*. 2017;8(1):709.
190. Patel B, Patel J, Cho JH, Manne S, Bonala S, Henske E, et al. Exosomes mediate the acquisition of the disease phenotypes by cells with normal genome in tuberous sclerosis complex. *Oncogene*. 2016;35(23):3027-36.
191. Suwakulsiri W, Rai A, Xu R, Chen M, Greening DW, Simpson RJ. Proteomic profiling reveals key cancer progression modulators in shed microvesicles released from isogenic human primary and metastatic colorectal cancer cell lines. *Biochimica et biophysica acta Proteins and proteomics*. 2019;1867(12):140171.
192. Zheng Y, Tu C, Zhang J, Wang J. Inhibition of multiple myeloma-derived exosomes uptake suppresses the functional response in bone marrow stromal cell. *International journal of oncology*. 2019;54(3):1061-70.
193. Ogawa K, Lin Q, Li L, Bai X, Chen X, Chen H, et al. Prometastatic secretome trafficking via exosomes initiates pancreatic cancer pulmonary metastasis. *Cancer letters*. 2020;481:63-75.
194. Roccaro AM, Sacco A, Maiso P, Azab AK, Tai YT, Reagan M, et al. BM mesenchymal stromal cell-derived exosomes facilitate multiple myeloma progression. *The Journal of clinical investigation*. 2013;123(4):1542-55.
195. Dabbah M, Jarchowsky-Dolberg O, Attar-Schneider O, Tartakover Matalon S, Pasmanik-Chor M, Drucker L, et al. Multiple myeloma BM-MSCs increase the tumorigenicity of MM cells via transfer of VLA4-enriched microvesicles. *Carcinogenesis*. 2020;41(1):100-10.
196. Wang J, Hendrix A, Hernot S, Lemaire M, De Bruyne E, Van Valckenborgh E, et al. Bone marrow stromal cell-derived exosomes as communicators in drug resistance in multiple myeloma cells. *Blood*. 2014;124(4):555-66.
197. Maetzel D, Denzel S, Mack B, Canis M, Went P, Benk M, et al. Nuclear signalling by tumour-associated antigen EpCAM. *Nature cell biology*. 2009;11(2):162-71.
198. Kopan R, IJagan MX. Gamma-secretase: proteasome of the membrane? *Nature reviews Molecular cell biology*. 2004;5(6):499-504.
199. Tolcher AW, Messersmith WA, Mikulski SM, Papadopoulos KP, Kwak EL, Gibbon DG, et al. Phase I study of RO4929097, a gamma secretase inhibitor of Notch signaling, in patients with refractory metastatic or locally advanced solid tumors. *Journal of clinical oncology : official journal of the American Society of Clinical Oncology*. 2012;30(19):2348-53.
200. Yen WC, Fischer MM, Axelrod F, Bond C, Cain J, Cancilla B, et al. Targeting Notch signaling with a Notch2/Notch3 antagonist (tarextumab) inhibits tumor growth and decreases tumor-initiating cell frequency. *Clinical cancer research : an official journal of the American Association for Cancer Research*. 2015;21(9):2084-95.
201. Platonova N, Parravicini C, Sensi C, Paoli A, Colombo M, Neri A, et al. Identification of small molecules uncoupling the Notch::Jagged interaction through an integrated high-throughput screening. *PLoS one*. 2017;12(11):e0182640.

202. Kangsamaksin T, Murtomaki A, Kofler NM, Cuervo H, Chaudhri RA, Tattersall IW, et al. NOTCH decoys that selectively block DLL/NOTCH or JAG/NOTCH disrupt angiogenesis by unique mechanisms to inhibit tumor growth. *Cancer discovery*. 2015;5(2):182-97.
203. Briot A, Iruela-Arispe ML. Blockade of specific NOTCH ligands: a new promising approach in cancer therapy. *Cancer discovery*. 2015;5(2):112-4.
204. Wang Y, Hoinka J, Liang Y, Adamus T, Swiderski P, Przytycka TM. AptaBlocks: Designing RNA complexes and accelerating RNA-based drug delivery systems. *Nucleic acids research*. 2018;46(16):8133-42.

## LIST OF FIGURES AND TABLES

Figure 1: Pathogenesis of MM (page 7)

Figure 2: Notch pathway family (page 11)

Figure 3: Notch signaling pathway activation (page 13)

Figure 4: Biogenesis of EVs (page 16)

Figure 5: Notch pathway in the osteolastogenic process in MM (page 22)

Figure 6: Notch pathway in the angiogenic process (page 26)

Figure 7: schematic protocol of the *in vitro* system of cellular communication mediated by EVs (page 42).

Figure 8: analysis of Jagged1 and 2 KD efficiency both at a gene and protein level (page 48)

Figure 9: tube formation assay on Matrigel with co-culture systems of HMCLs<sup>SCR</sup> or HCMLs<sup>J1/2KD</sup> and HPAECs (page 49)

Figure 10: tube formation stimulated by Jagged1 and Jagged2 peptides 20 µg/ml (page 50)

Figure 11: tube formation assay on HPAECs with conditioned media (CM) of HMCLs<sup>SCR</sup> or HCMLs<sup>J1/2KD</sup> (page 51)

Figure 12: VEGF variation in HMCLs<sup>SCR</sup> and HMCLs<sup>J1/2KD</sup> (page 52)

Figure 13: activation of Notch signaling and VEGF-A expression in HS5 cells or in co-cultured with HMCLs<sup>SCR</sup> or HMCLs<sup>J1/2KD</sup> (page 53)

Figure 14: tube formation assay of the HPAECs stimulated with CM secreted by co-culture systems of the HS5 cells and HMCLs<sup>SCR</sup> or HMCLs<sup>J1/2KD</sup> (page 54)

Figure 15: representative NTA analysis on MM-EVs from RPMI8226 and OPM2 cell lines (page 56)

Figure 16: representative TEM images of MM-EVs from RPMI8226 and OPM2 (page 57)

Figure 17: uptake experiments with MM-EVs from RPMI8226 (page 59)

Figure 18: Western blot analysis for Notch2 expression in MM-EVs from 7 HMCLs (page 60)

Figure 19: Western blot analysis for Notch1, Notch3 and Notch4 expressed in 7 different HMCLs and their EVs (page 61)

Figure 20: Western blot analysis for the expression of Notch2 in small and large vesicles (page 62)

Figure 21: western blot analysis of Notch2-HA transfer *via* EVs (page 63)

Figure 22: western blot on Notch2 expression on MM<sup>SCR</sup> and MM<sup>N2KD</sup> cell lysates and their derived EVs (page 65)

Figure 23: Western blot for the expression of Notch receptor 1,3 and 4 in MM<sup>SCR</sup> and MM<sup>N2KD</sup> cell and their EVs (page 67)

Figure 24: NTA on MM-EVs<sup>SCR</sup> and MM-EVs<sup>N2KD</sup> (page 68).

Figure 25: luciferase Notch reporter assay on HeLa cells treated with MM-EVs<sup>SCR</sup> and MM-EVs<sup>N2KD</sup> (page 69).

Figure 26. *In vivo* Notch reporter assay (page 70).

Figure 27: OCLs differentiation assay on the monocyte cell line Raw264.7 treated with MM-EVs<sup>SCR</sup> and MM-EVs<sup>N2KD</sup> (page 71).

Figure 28: tube formation assay on endothelial cells HPAECs treated with MM-EVs<sup>SCR</sup> and MM-EVs<sup>N2KD</sup> (page 72).

Figure 29: osteoclast differentiation of Raw267.4 cells treated with MM-EVs in the presence of DAPT (50  $\mu$ M) (page 73).

Figure 30: tube formation assay on HPAECs treated with MM-EVs in the presence or absence of DAPT (50  $\mu$ M) (page 74)

Figure 31: MTT assay on Raw264.7 and HPAECs treated with DAPT 50  $\mu$ M (page 75)

Figure 32: tube formation assay on HPAEC treated with BM-derived EVs from MM patients at different stage of disease (page 76)

Table 1: schematic protocol used for HMCLs transfection (page 31).

Table 2: schematic protocol for HMCLs infection (page 33)

Table 3: sequence of the primers used for qRT-PCR (page 35)

Table 4: list of the monoclonal antibody used for western blot analysis (page 40)

Table 5: clinical characteristics at presentation of patients (page 45)

## DISSEMINATION OF RESULTS

To successfully disseminate the results of my PhD project, I aimed to target the scientific community.

During my PhD, I divulgated my results on the role of Jagged ligands in MM-associated angiogenesis and on the emerging role of EVs in myeloma progression through open-access publications on international journals. Indeed, I am first co-author in the original paper published on Cancers entitled “Jagged Ligands Enhance the Pro-Angiogenic Activity of Multiple Myeloma Cells”; I am also first author of an original manuscript entitled “Extracellular vesicles mediate the communication between multiple myeloma and bone marrow microenvironment in a NOTCH dependent way”, concerning the role of Notch pathway in the pro-tumorigenic role of EVs, which has been accepted for the publication to the journal Haematologica.

To further stress the role of EVs in the pathological pro-tumoral mechanisms and encouraging further studies in this new promising field of cellular communication, I contributed to the review “Extracellular Vesicles Enhance Multiple Myeloma Metastatic Dissemination”, (Colombo M, **Giannandrea et al.**, Int J Mol Sci. 2019), and wrote a review with my research group entitled “Restoring Tissue Homeostasis at Metastatic Sites: A Focus on Extracellular Vesicles in Bone Metastasis” (Giannandrea et al., Front Oncol. 2021) to recapitulate the scientific data supporting the importance of EVs in myeloma and in the bone metastasis process, as new promising therapeutic targets.

To further disseminate the results, during my PhD, I discussed my results in the presence of experts of the field, participating to the following international congress:

- Giannandrea et al., “The role of NOTCH2 in the extracellular vesicles-mediated angiogenesis and osteoclastogenesis in multiple myeloma”. Oral presentation at the Young Scientist Meeting: “Molecular Pathology: from bench to bedside” organized by the “Società Italiana di Patologia e Medicina traslazionale” (SIPmet), Perugia, December 2021.
- Giannandrea et al., “The role of Notch pathway in the pro-tumorigenic activity of extracellular vesicles in multiple myeloma”. Oral presentation at the annual meeting of International Society of extracellular vesicles (ISEV), May 2021

- Giannandrea *et al.*, “Targeting extracellular vesicles in multiple myeloma: a new role for the Notch pathway”. Oral presentation at the congress of the Italian society of extracellular vesicles (EVITA), Palermo, November 2019

I also presented my scientific data to the researchers and clinicians belonging to the annual congress of the Department of Health Science (DISS) where I belonged to:

- Giannandrea *et al.*, “The role of NOTCH2 in the Extracellular vesicles mediated communication in Multiple Myeloma: a focus on angiogenesis and osteoclastogenesis”. Poster presentation at the DISS congress, Milano, November 2021
- Giannandrea *et al.*, “The key role of Jagged1 and Jagged2 in promoting the angiogenic process in multiple myeloma”. Poster presentation at the DISS congress, Milano, November 2020.
- Giannandrea *et al.*, “Extracellular vesicles-mediated communication in remodeling multiple myeloma microenvironment: a new role for the Notch pathway”. Poster presentation at the DISS congress, Milano, November 2019

Moreover, during the first year I have presented my first data participating to monthly scientific initiative (Breakfast Meetings) organized by the Dept of Health Science.

Finally, in the occasion of the final thesis defense, I am going to share of my results by taking advantages of the web site of Dept of Health Sciences <http://www.diss.unimi.it/ecm/home>, in order to keep updated the local scientific community about my research.

### *Summary*

English: Multiple myeloma is a still incurable tumor of B cells. Malignant B cells can migrate in the bone marrow where they found a supportive microenvironment. Myeloma cells can induce the healthy cells to favor tumor progression by different type of cellular communication that may include the direct contact through the Notch pathway or the packaging of molecular signals in small lipid bodies named extracellular vesicles. The extracellular vesicles, thanks to their ability to reach long distance through the blood circulation, mediate tumorigenic processes essential in myeloma progression, such as angiogenesis, osteoclastogenesis, drug resistance and immune escape. In this thesis, I elucidated the effect of Notch in the formation of new vessels, used from tumor cells to obtain oxygen and nutrients. I found out that Notch can be carried by tumor-derived vesicles



promoting not only the angiogenesis but also the creation of bone lesions, which mainly affect the quality of life of patients.

This thesis contributes to provide new information regarding the role of Notch in the bone marrow microenvironment and on the effect of extracellular vesicles in myeloma progression, representing a promising target for a new pharmacological approach.










Italian: Il mieloma multiplo è un tumore incurabile causato da mutazioni nei linfociti B in grado di migrare nel midollo osseo, dove trovano un ambiente favorevole contribuendo alla progressione del mieloma. Le cellule tumorali favoriscono il supporto alla sua crescita da parte della componente sana midollare, tramite interazione diretta mediata dalla segnalazione di Notch o il rilascio di vescicole extracellulari in grado di trasferire informazioni molecolari anche in siti distanti favorendo processi cruciali quali angiogenesi, osteoclastogenesi, resistenza farmacologica ed evasione dalla sorveglianza immunitaria. In questa tesi, ci siamo concentrati sulla capacità di Notch di indurre la formazione di nuovi vasi, quale aspetto importante nella progressione tumorale. Inoltre, abbiamo indagato se esso potesse agire anche a distanza tramite trasporto nelle vescicole, mediando non solo l'angiogenesi ma anche l'osteoclastogenesi, importante per la formazione delle lesioni ossee caratterizzanti i pazienti con mieloma. I risultati da noi ottenuti non solo incrementano le conoscenze sul ruolo chiave di Notch nel microambiente tumorale, anche come mediatore dell'effetto pro-tumorale delle vescicole, ma pongono le basi per lo sviluppo di una terapia farmacologica finalizzata a bloccare la comunicazione vescicolare mediata da Notch.

## **APPENDIX**

- Published paper entitled “ Jagged Ligands Enhance the Pro-Angiogenic Activity of Multiple Myeloma Cells”
- Manuscript accepted for the publication on Haematologica entitled “Extracellular vesicles mediate the communication between multiple myeloma and bone marrow microenvironment in a NOTCH dependent way”.

Article

# Jagged Ligands Enhance the Pro-Angiogenic Activity of Multiple Myeloma Cells

Maria Teresa Palano <sup>1,†</sup>, Domenica Giannandrea <sup>1,†</sup>, Natalia Platonova <sup>1</sup>, Germano Gaudenzi <sup>2</sup>, Monica Falleni <sup>1</sup>, Delfina Tosi <sup>1</sup>, Elena Lesma <sup>1</sup>, Valentina Citro <sup>1</sup>, Michela Colombo <sup>1</sup>, Iliaria Saltarella <sup>3</sup>, Roberto Ria <sup>3</sup>, Nicola Amodio <sup>4</sup>, Elisa Taiana <sup>5</sup>, Antonino Neri <sup>5</sup>, Giovanni Vitale <sup>2,6</sup> and Raffaella Chiaramonte <sup>1,\*</sup>

<sup>1</sup> Department of Health Sciences, Università degli Studi di Milano, 20142 Milano, Italy;

mariateresa.palano@multimedica.it (M.T.P.); domenica.giannandrea@unimi.it (D.G.);

natalia.platonova@unimi.it (N.P.); monica.falleni@unimi.it (M.F.); delfina.tosi@unimi.it (D.T.);

elena.lesma@unimi.it (E.L.); valentina.citro@unimi.it (V.C.); michela.colombo@ndcls.ox.ac.uk (M.C.)

<sup>2</sup> Istituto Auxologico Italiano, IRCCS, Laboratory of Geriatric and Oncologic Neuroendocrinology Research,

20095 Cusano Milanino, Italy; germano.gaudenzi@gmail.com (G.G.); giovanni.vitale@unimi.it (G.V.)

<sup>3</sup> Department of Biomedical Sciences and Human Oncology, Unit of Internal Medicine and Clinical Oncology, University of Bari Medical School, 70124 Bari, Italy; ilaria.saltarella@libero.it (I.S.); roberto.ria@uniba.it (R.R.)

<sup>4</sup> Department of Experimental and Clinical Medicine, Magna Graecia University of Catanzaro, 88100 Catanzaro, Italy; amodio@unicz.it

<sup>5</sup> Department of Oncology and Hemato-Oncology, University of Milano. Hematology, Fondazione Ca' Granda IRCCS Policlinico, 20122 Milano, Italy; elisa.taiana@unimi.it (E.T.); antonino.neri@unimi.it (A.N.)

<sup>6</sup> Department of Clinical Sciences and Community Health (DISCCO), University of Milan, 20122 Milan, Italy

\* Correspondence: raffaella.chiaramonte@unimi.it; Tel.: +39-02-50323249

† These authors contributed equally to this work.

Received: 7 August 2020; Accepted: 9 September 2020; Published: 11 September 2020



**Simple Summary:** The Jagged family of ligands are aberrantly expressed during multiple myeloma progression and contributes to activate Notch signaling both in myeloma cells and in the nearby bone marrow cell populations activating several pro-tumor effects. This work elucidates, *in vitro*, *in vivo* as well as in patients' bone marrow biopsies, different mechanisms by which tumor cell-derived Jagged1 and 2 contribute to myeloma-associated angiogenesis. These include the ability to induce myeloma and bone marrow stromal cell secretion of VEGF along with a direct activation of the pro-angiogenic Notch signaling pathway in endothelial cells. This research provides a rationale for a Jagged-directed therapy in multiple myeloma.

**Abstract:** Multiple myeloma (MM) is an incurable plasma cell malignancy arising primarily within the bone marrow (BM). During MM progression, different modifications occur in the tumor cells and BM microenvironment, including the angiogenic shift characterized by the increased capability of endothelial cells to organize a network, migrate and express angiogenic factors, including vascular endothelial growth factor (VEGF). Here, we studied the functional outcome of the dysregulation of Notch ligands, Jagged1 and Jagged2, occurring during disease progression, on the angiogenic potential of MM cells and BM stromal cells (BMSCs). Jagged1–2 expression was modulated by RNA interference or soluble peptide administration, and the effects on the MM cell lines' ability to induce human pulmonary artery cells (HPAECs) angiogenesis or to indirectly increase the BMSC angiogenic potential was analyzed *in vitro*; *in vivo* validation was performed on a zebrafish model and MM patients' BM biopsies. Overall, our results indicate that the MM-derived Jagged ligands (1) increase the tumor cell angiogenic potential by directly triggering Notch activation in the HPAECs or stimulating the release of angiogenic factors, *i.e.*, VEGF; and (2) stimulate the BMSCs to promote angiogenesis through VEGF secretion. The observed pro-angiogenic effect of Notch activation in

the BM during MM progression provides further evidence of the potential of a therapy targeting the Jagged ligands.

**Keywords:** multiple myeloma; angiogenesis; Notch; Jagged; VEGF; bone marrow stromal cells

---

## 1. Introduction

Multiple myeloma (MM) is a plasma cell malignancy mainly settled in the bone marrow (BM) where it establishes tight communication with the stromal cell populations, including BM stromal cells (BMSCs) and endothelial cells (ECs), and promotes a pro-tumor microenvironment (TME), inducing the angiogenic switch [1] and favoring MM growth and progression [2].

MM may rise as an asymptomatic monoclonal gammopathy of undetermined significance (MGUS), a benign avascular phase of the disease [3]. The progression from MGUS to MM is characterized by clonal expansion of tumor cells within the BM (infiltrating a cell number higher than 10%) and it is coupled with an angiogenic switch that brings forth neo-vessels formation throughout the BM [4]. Consistently, MM-associated endothelial cells (MM-ECs) differ from MGUS-ECs due to their higher intrinsic angiogenic capability [5,6].

Increasing evidence supports the role of the Notch pathway in MM progression [7]. Notch is composed of four trans-membrane receptors (Notch1 to 4) and 2 classes of ligands, named Delta-like (Dll1, 3 and 4) and Jagged (Jagged1 and 2) [8]. The interaction between the ligand and receptor induces two proteolytic cleavages that releases the intracellular portion of Notch, which in turn activates the transcription of the Notch-responsive genes [9].

The Notch pathway plays a relevant role in MM development and progression, mediating the communication between the MM cells and the surrounding cell population of the BM microenvironment, including the BMSCs [10,11] and osteoclasts [12]. This interplay is possibly due to the increased expression of the Jagged ligands on the MM cell surface. Specifically, Jagged2 is already expressed at higher levels in the benign MGUS phase [13], while Jagged1 upregulation occurs later during the progression to the symptomatic MM [14]. Jagged ligands' increase leads to the aberrant activation of the Notch signaling, not only in MM cells through homotypic interaction, but also in the surrounding BM cells via heterotypic interaction [10,11].

Notch signaling is also involved in physiologic and tumor angiogenesis [15–18] in coordination with the vascular endothelial growth factor (VEGF)–VEGFR axis [19]. The angiogenic switch in MM, characterized by an increased BM microvessel density (MVD), is associated with a poor prognosis [20] and represents a major event in tumor progression, resulting in increased availability of nutrients and oxygen, necessary for MM cell proliferation, the release of angiocrine factors from the newly formed vessels and a possible way for tumor spread [21].

We recently demonstrated that MM angiogenesis relies on the activation of the Notch pathway in MM-ECs. Notch signaling in MM-ECs is due to the increased expression of the Notch receptor and ligands, resulting in homotypic Notch activation [6]. On the other side, we also observed that MM cell-derived Jagged ligands represents an important source of Notch signaling activation in ECs [6].

In this work, we explored the impact of the aberrant expression of MM-derived Jagged1 and Jagged2 on MM angiogenesis, dissecting their contribution on the angiogenic potential of MM-ECs and BMSCs. Moreover, we investigated the mechanisms mediated by the release of angiogenic factors as well as the direct cell–cell interaction.

## 2. Results

### 2.1. Myeloma Cell-Derived Jagged Ligands Regulate Late Myeloma Cell Angiogenic Potential

To assess the involvement of MM cell-derived Jagged ligands in angiogenesis promotion, we knocked down (KD) the ligands in two human myeloma cell lines (HMCLs), namely RPMI8226 and OPM2, by using siRNAs targeting Jagged1 or Jagged2 (HMCLs<sup>KD</sup>) or the corresponding scrambled siRNA as the control (HMCLs<sup>SCR</sup>), as previously reported [6,10]. We assessed the KD efficacy on Jagged1 and 2 mRNA as well as on the Notch transcriptional targets by using quantitative qRT-PCR (Figure 1A, upper panel) and confirmed the downregulation of the corresponding protein levels by Western blotting (Figure 1A, lower panel).

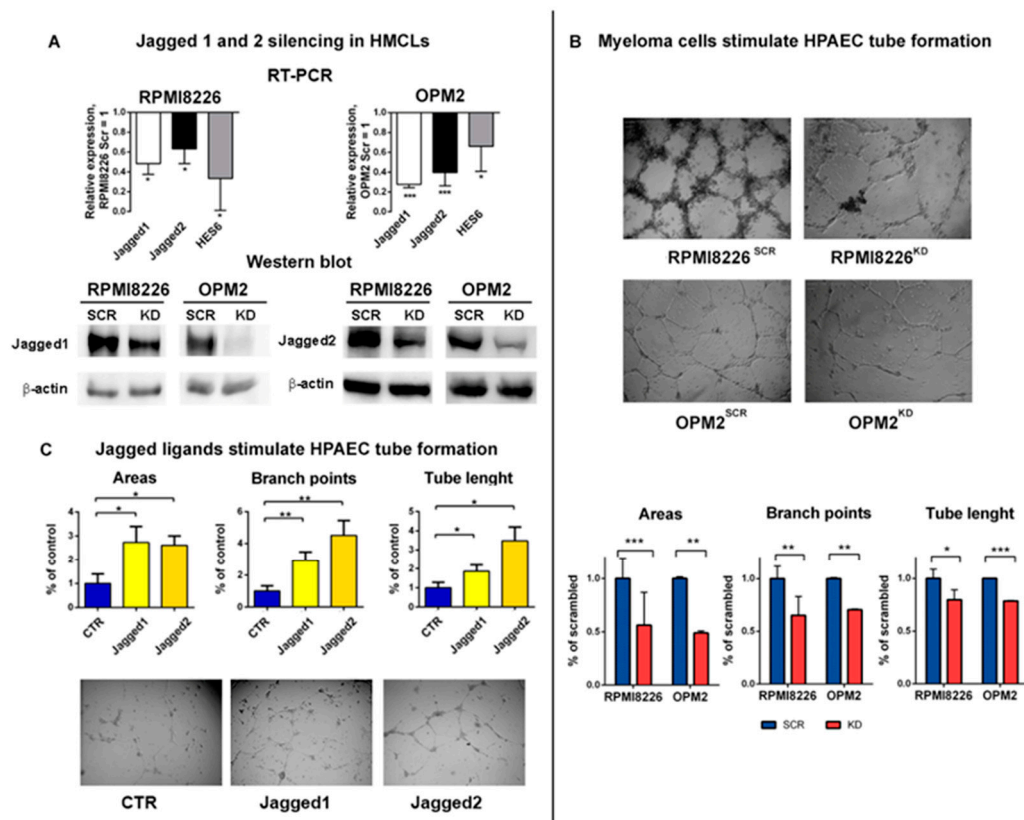


**Figure 1.** Multiple myeloma (MM) cell-derived Jagged promotes angiogenesis: (A) Up: Jagged1 and 2 knock-down (KD) efficiency in RPMI8226<sup>KD</sup> and OPM2<sup>KD</sup> cells was obtained by qRT-PCR assay of the relative gene expression variation (normalized to GAPDH) of Jagged1 and Jagged2 and the Notch target gene HES6, calculated by the  $2^{-\Delta\Delta C_t}$  formula. Data are expressed as the mean value  $\pm$  SD. Down: Western blot analysis of Jagged1 and Jagged2 in HMCLs<sup>SCR</sup> or HCMLs<sup>KD</sup>. Protein loading was normalized to -actin. The shown images are representative of three independent experiments. (B) Up: Tube formation assay on Matrigel with co-culture systems of HMCLs<sup>SCR</sup> or HCMLs<sup>KD</sup> and primary human pulmonary artery endothelial cells (HPAECs). 4X magnification images are shown. Down: Graphs show quantification of the number of areas and branch points and total tube length. (C) HPAEC tube formation stimulated by Jagged1 and Jagged2 peptides. Images are a 4X magnification. Statistical analysis was carried out by a one-tailed t test; \* is for  $p \leq 0.05$ ; \*\* is for  $p \leq 0.01$ ; \*\*\* is for  $p \leq 0.001$ .

Our recent findings indicate that the MM cell-derived Jagged1/2 triggered Notch activation in the ECs [6], prompting us to verify if this heterotypic activation could promote angiogenesis. To address this issue, we used different approaches. First, we set up a co-culture system, including HMCLs<sup>SCR</sup> or HMCLs<sup>KD</sup> cultured in direct contact with primary human pulmonary artery endothelial cells (HPAECs)

laid on a Matrigel-coated support, and explored the changes in the HPAECs' ability to organize a tube-like network. In Figure 1B, representative images show the tube formation assay (upper panel) and the graphs (lower panel) illustrate the different ability of HMCLs<sup>SCR</sup> or HMCLs<sup>KD</sup> to induce HPAECs to form a tube-like network, assessed by counting the number of areas, branch points and the total tube length. HPAECs cultured with both HMCLs<sup>SCR</sup> displayed a significantly increased complexity of the grid compared to HPAECs cultured with HMCLs<sup>KD</sup>, indicating that the angiogenic potential of the MM cell relies on the expression of Jagged ligands on the MM cells.

This result prompted us to verify if the MM cell-derived Jagged ligands could trigger the angiogenic Notch signaling in HPAECs by direct contact or, instead, if this effect could be mediated by the release of soluble angiogenic factors induced by Jagged-mediated Notch activation through homotypic interaction in the MM cells.

To distinguish between the effect of the MM cell-derived soluble angiogenic factors and the MM cell-derived Jagged-mediated activation of the angiogenic Notch signaling in the HPAECs, we set up a 24 h tube formation assay stimulating the HPAECs with soluble Jagged1 and Jagged2 peptides. The obtained results showed that the Jagged-mediated stimulation might increase the HPAECs' organizing ability (Figure 1C), and indicated that the MM cell-derived Jagged ligands can engage directly with the Notch receptor on the EC surface and induce its activation as well as the angiogenic response.

Since the Jagged ligands can activate Notch signaling also by homotypic interaction in the same MM cells, we wondered if the angiogenic potential of the HMCLs could be ascribed also to a Notch-dependent release of pro-angiogenic soluble factors. To address this issue, we performed a tube formation assay for 24 h on a Matrigel layer with or without the conditioned medium (CM) of HMCLs<sup>SCR</sup> or HMCLs<sup>KD</sup>. As shown in Figure 2A, the HMCLs<sup>SCR</sup>-derived CM ability to induce HPAECs to organize a grid-like structure is significantly reduced in the presence of HMCLs<sup>KD</sup>-derived CM. We also examined the effect of CM on EC adhesion and migration, two further biological events associated with angiogenesis.

To test EC adhesion, we treated ECs with HMCL-derived CM and assessed the adhesion by measuring the fluorescence intensity after 1 h plating on a fibronectin-coated plate. The results showed a different adhesion capability of the ECs stimulated with CM derived from HMCLs<sup>SCR</sup> or HMCLs<sup>KD</sup>, since the Jagged ligands' depletion impaired the EC adhesion, as shown in Figure 2B.

Moreover, the analysis of EC migratory ability confirmed the effects induced by the Jagged KD on the HMCLs. Images and graph in Figure 2C report EC motility after 24 h incubation with the CM derived from HMCLs<sup>SCR</sup> or HMCLs<sup>KD</sup>. The quantification of the wound area confirmed a reduced motility of the ECs treated with the CM from HMCLs<sup>KD</sup>. Indeed, the wound areas increased by 70% when the ECs were treated with RPMI8226<sup>KD</sup>-derived CM and this effect was even more evident with CM from OPM2<sup>KD</sup>, which showed a 6–7-fold increase in the wound area.

The evidence that Jagged1 and 2 KD reduced the HMCLs' ability to secrete pro-angiogenic factors in the CM prompted us to assess possible variations in VEGF-A level upon Jagged KD. qRT-PCR analysis showed that the Jagged ligands KD caused a concomitant negative modulation of VEGF-A mRNA in all HMCLs (Figure 2D). An ELISA assay (Figure 2E) confirmed that the down-modulation of VEGF-A mRNA affected also the protein secretion.

Overall, these results indicated that the HMCLs may promote angiogenesis by activating the Notch signaling in ECs via heterotypic Jagged-mediated Notch activation and, additionally, HMCL-mediated secretion of pro-angiogenic VEGF-A is influenced by homotypic activation of the Notch signaling induced by the Jagged ligands. Both these pro-angiogenic ways may be hampered by inhibiting the Jagged-mediated Notch activation.

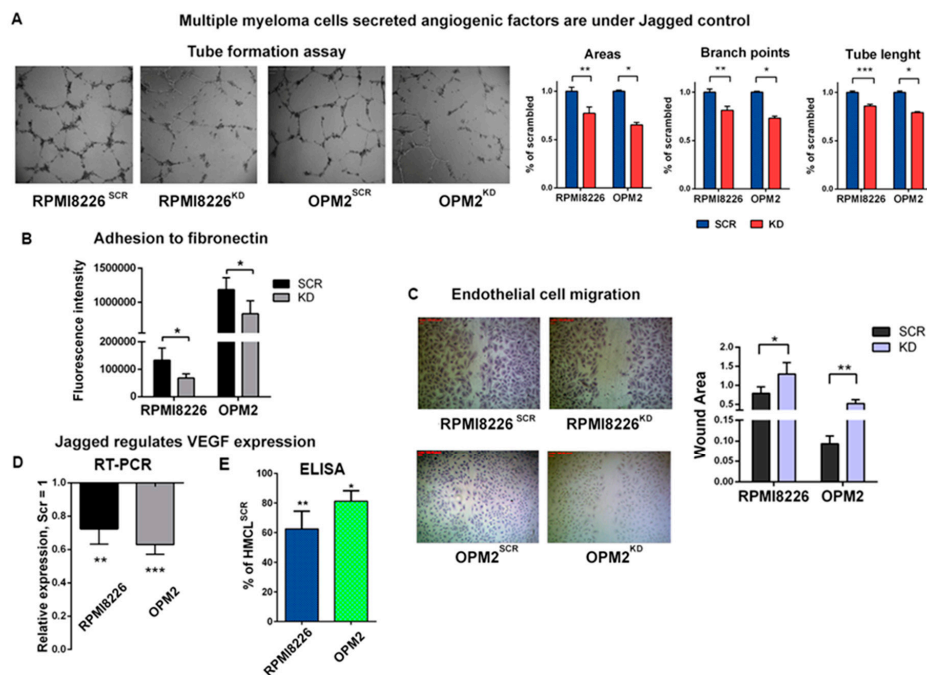


**Figure 2.** MM cell-derived Jagged promotes angiogenesis: (A) Tube formation assay on HPAECs with conditioned media (CM) of HMCLs<sup>SCR</sup> or HCMLs<sup>KD</sup>. 4X magnification images are shown on the left. Graphs (on the right) show the percentage variation of areas and branch points and total tube length +/-SEM. (B) Adhesion to fibronectin of HPAECs treated with CM from HMCLs<sup>SCR</sup> and HMCLs<sup>KD</sup> and stained with Calcein-AM. The graph reports the intensity of the adherent fluorescent cells. (C) Motility of the HPAECs treated with CM of HMCLs<sup>SCR</sup> and HMCLs<sup>KD</sup> was assessed by wound healing assays. Up: Representative pictures at 4X magnification. Down: The graph shows the average open area of the wounds expressed in pixels. (D,E) Variation of vascular endothelial growth factor (VEGF) expression in HMCLs<sup>SCR</sup> and HMCLs<sup>KD</sup> assessed at the mRNA level (D) by qRT-PCR of the relative gene expression variation (normalized to GAPDH) calculated by the 2<sup>-ΔΔCt</sup> formula (data are expressed as the mean value ± SD) and at the protein levels (E) by ELISA on 48 h CM. Data are expressed as the amount of VEGF-A released by HMCLs<sup>KD</sup> normalized on VEGF-A expressed by HMCLs<sup>SCR</sup>. For each sample, the amount of VEGF-A (pg/mL) was normalized to the cell concentration. Statistical analyses were carried out by one-tailed t-tests; \* is for  $p \leq 0.05$ ; \*\* is for  $p \leq 0.01$ ; \*\*\* is for  $p \leq 0.001$ .

## 2.2. Myeloma Cell-Derived Jagged Ligands Increase the Angiogenic Potential of Stromal Cells

It is well known that the MM-associated BMSCs play a key role in supporting tumor angiogenesis [22,23] and the interaction between the Notch ligands and receptors is relevant in the communication between MM cells and stromal cells, mediating important effects, such as BMSC-induced drug resistance [10,11]. We wondered if the MM cell-derived Jagged ligands might trigger Notch signaling to boost the pro-angiogenic potential of the BMSCs.

To address this issue, we exploited a co-culture system of the BMSCs and HMCLs<sup>SCR</sup> or HMCLs<sup>KD</sup> and analyzed if the ability of tumor cells to activate Notch signaling in stromal cells paralleled a change in the angiogenic potential.

First, we assessed if the MM-derived Jagged ligands were able to activate Notch signaling in the BMSCs. To this, we verified if co-cultivating the HMCLs<sup>SCR</sup> and HMCLs<sup>KD</sup> with the human BMSC line HS5 induced a variation in the levels of the Notch target genes expression. Results of qRT-PCR analysis in Figure 3A indicate that HMCLs<sup>SCR</sup> upregulate the transcription of the Notch target gene HES1 in HS5 cells in comparison to the lower basal expression level observed in HS5 cultured alone; on the contrary, the corresponding HMCLs<sup>KD</sup> displayed a significantly reduced ability to activate HES1 in HS5 cells, consistently with a decreased Notch activation.

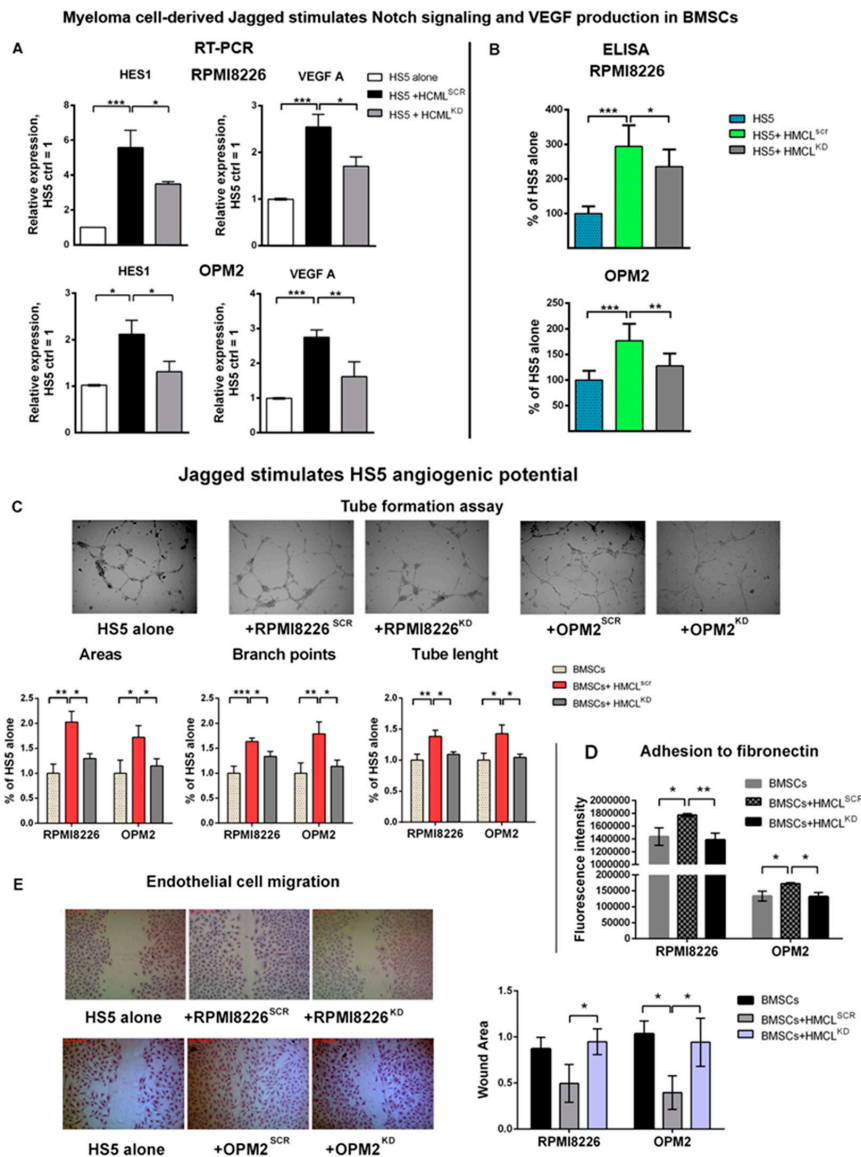


**Figure 3.** MM cell-derived Jagged stimulates bone marrow stromal cell (BMSC) angiogenic potential: (A) Activation of Notch signaling and VEGF-A expression induced in HS5 cells co-cultured with HMCLs<sup>SCR</sup> or HMCLs<sup>KD</sup> assessed by qRT-PCR of the relative gene expression variation for the Notch target gene HES1 and VEGF (normalized to HRPT) calculated by the  $2^{-\Delta\Delta Ct}$  formula (data are expressed as the mean value  $\pm$  SD). Statistical analyses were carried out by one-way ANOVA and Tukey post-hoc test; \* is for  $p \leq 0.05$ ; \*\* is for  $p \leq 0.01$ ; \*\*\* is for  $p \leq 0.001$ . (B) ELISA for VEGF-A secreted by co-culture systems of HS5 cells and HMCLs<sup>SCR</sup> or HMCLs<sup>KD</sup>. Data represent the amount of VEGF released by each culture normalized on VEGF expressed by HMCL cultured alone. In each sample, the amount of VEGF (pg/mL) was normalized to the cell concentration. (C) Tube formation assay of the HPAECs stimulated with CM secreted by co-culture systems of the HS5 cells and HMCLs<sup>SCR</sup> or HMCLs<sup>KD</sup>. 4X magnification images are shown. Graphs show the quantification of the number of areas, branch points and total tube length. (D) Adhesion to fibronectin of the HPAECs stained with Calcein-AM and treated with CM secreted by the co-culture systems of the HS5 cells and HMCLs<sup>SCR</sup> or HMCLs<sup>KD</sup>. The graph reports the intensity of the adherent fluorescent cells. (E) Migration of the HPAECs treated with CM of co-culture systems of HS5 cells and HMCLs<sup>SCR</sup> or HMCLs<sup>KD</sup> was assessed by wound healing assays. Representative pictures at 4X magnification. The graph shows the average open area of the wounds expressed in pixels. Statistical analyses were carried out by ANOVA and Tukey post-hoc tests; \* is for  $p \leq 0.05$ ; \*\* is for  $p \leq 0.01$ ; \*\*\* is for  $p \leq 0.001$ .



In the same cells, we also assessed the possible variation in VEGF-A gene expression and observed that, while HMCLs<sup>SCR</sup> increased VEGF-A gene expression in HS5 cells, HMCLs<sup>KD</sup> triggered no or significantly lower levels of VEGF transcription (Figure 3A). Additionally, we showed a consistent decrease in secreted BMSC-derived VEGF-A. At this purpose, VEGF secreted in the CM of HS5 or HS5 cultured with HMCLs<sup>SCR</sup> or HMCLs<sup>KD</sup> was assessed by ELISA. Results shown in Figure 3B confirmed that the VEGF-A protein expression in the HS5 cells was upregulated by HMCLs<sup>SCR</sup>, but not or significantly less by HMCLs<sup>KD</sup>, indicating that the MM cells' ability to induce VEGF-A secretion depends on the MM-cell-derived, Jagged-mediated Notch signaling activation in the BMSCs.

We assessed if the HMCLs' ability to induce BMSC-mediated VEGF-A through Notch signaling activation had a biological consequence on angiogenesis. For this purpose, we verified if the CM derived from the BMSCs co-cultured with the HMCLs induced a variation in EC ability to form tube-like structures, as well as in their adhesive and migratory properties.

Variations in the BMSCs' ability to stimulate EC organization was assessed by a tube formation assay after 24 h stimulation with the different CM. Results in Figure 3C show that the CM from the HS5 cells cultured alone displayed an intrinsic ability to stimulate EC organization, but all the parameters are significantly increased by CM from HS5 + HMCLs<sup>SCR</sup>. On the contrary, CM from HS5 + HMCLs<sup>KD</sup> did not increase the tube organization ability of the HPAECs in comparison to the CM from unstimulated HS5.

To assess the effect on EC adhesion, they were stimulated with the same CM. Results reported in Figure 3D show that the intrinsic stromal cell capability to induce EC adhesion was significantly increased in the presence of CM from HS5+HMCLs<sup>SCR</sup> but remained unchanged when CM was obtained from HS5+HMCLs<sup>KD</sup>.

Variation in the BMSCs' ability to induce EC migration after stimulation with HMCLs<sup>SCR</sup> or HMCLs<sup>KD</sup> was assessed by performing wound healing assays on HPAECs treated with the CM and measuring the wound open area. Figure 3E shows that motility of the ECs treated with CM from HS5 + HMCLs<sup>SCR</sup> was higher if compared to CM from HS5 cultured alone or HS5 + HMCLs<sup>KD</sup>. Indeed, CM from HS5+HMCLs<sup>SCR</sup> decreased the wound area, while the effect of the CM from HS5+HMCLs<sup>KD</sup> was comparable to that from HS5 cultured alone.

Overall, these results indicated that Notch signaling activation in the BMSCs mediated by the MM-cell-derived Jagged ligands boosted the BMSC angiogenic potential by inducing the release of soluble factors, such as VEGF-A.

### 2.3. Jagged Ligands Promote MM-Associated Angiogenesis in a Zebrafish Model

To further investigate the role of the Notch pathway in angiogenesis stimulation and to confirm our *in vitro* results, we investigated the effect of Jagged1 and Jagged2 in an *in vivo* zebrafish embryonic model. The transgenic zebrafish model *Tg (fli1a:EGFP)<sup>y1</sup>* allows the detection of ECs in blood vessels with constitutive EGFP expression. RPMI8226<sup>SCR</sup> or RPMI8226<sup>KD</sup> cells, pre-stained with the red fluorescent cell tracker CM-Dil, were grafted in 48 h post fertilization (hpf) zebrafish embryos. As negative control of the implantation, embryos were injected with PBS, the cell resuspension medium. Injection was performed in the sub-peridermal space, close to the sub-intestinal vein (SIV) plexus. The sprouting of tumor-induced endothelial structures from the SIV toward the tumor engraftment was evaluated 24 h post-injection (hpi). Injected RPMI8226 cells displayed a comparable localization at 24 hpi (Figure 4A) and length measurements of the vessels arising from SIV (Figure 4B) indicated different stimulation capabilities. Fish embryos receiving RPMI8226<sup>SCR</sup> cells displayed a significant increase in angiogenic sprouts, which were not visible in embryos receiving PBS, confirming the MM cells' ability to stimulate angiogenesis. On the contrary, RPMI8226<sup>KD</sup> cells displayed a mild stimulation of angiogenesis, approximately 35% less RPMI8226<sup>SCR</sup> cells, indicating that the decrease in Jagged expression in the MM cells impairs their ability to stimulate sprout angiogenesis.

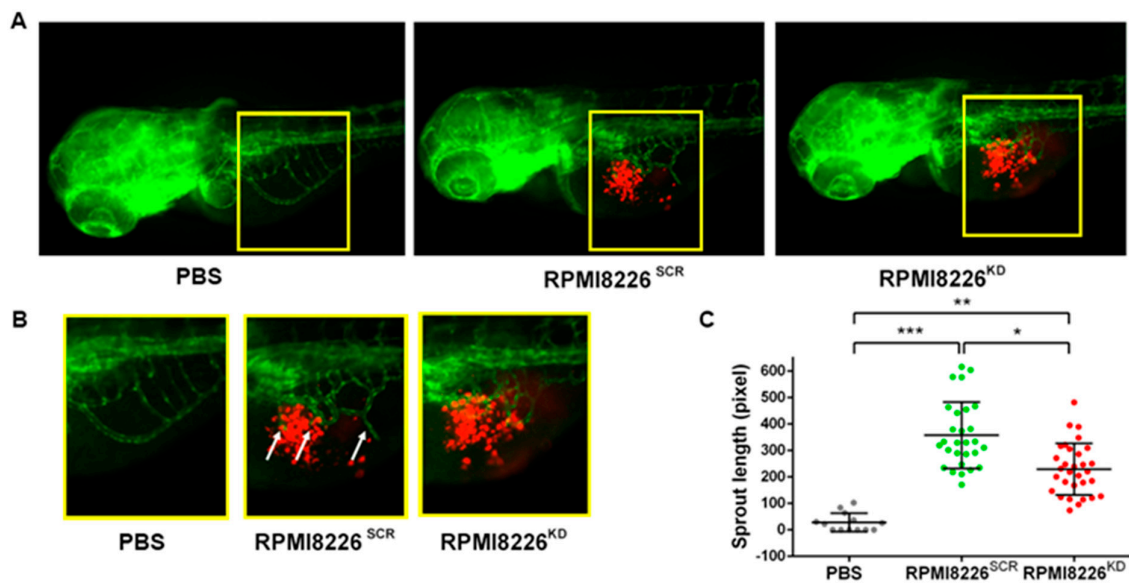


**Figure 4.** Zebrafish embryo in vivo model to evaluate tumor-induced angiogenesis in relation to Jagged expression in HMCLs. (A) Representative images of Tg(fli1a:EGFP)<sup>y1</sup> zebrafish embryos with GFP expressing vessels (green) and RPMI8226<sup>SCR</sup> or RPMI8226<sup>KD</sup> stained with CM-Dil fluorescent dye (red). Epifluorescence images were acquired with a Leica DM 5500B microscope equipped with a DC480 camera. (B) Inset of sprouting vessels from SIV in zebrafish embryos 24 hpi; white arrows indicate angiogenic sprouts. (C) Quantification of endothelial sprouts from the SIV plexus was performed in 24 h post-injection (hpi) zebrafish embryos injected with RPMI8226<sup>SCR</sup> (N = 24) and RPMI8226<sup>KD</sup> cells (N = 31) using ImageJ software (National Institutes of Health, USA). Statistical analysis was carried out by one-way ANOVA with Tukey post hoc tests of three independent experiments; \* is for  $p \leq 0.05$ ; \*\* is for  $p \leq 0.01$ ; \*\*\* is for  $p \leq 0.001$ .

#### 2.4. Identification of a Correlation between Jagged Expression in MM Cells and Angiogenesis in Patients' Bone Marrow

To validate in vitro and in vivo findings, BM biopsies (BMBs) from 34 MM patients were evaluated. Patients analyzed were at the onset of the disease and had not received any drug treatment. Clinical information concerning tumor BM infiltration by MM cells was associated with Jagged1 and Jagged2 expression, Notch activation and angiogenesis investigated by immunohistochemistry.

Antigen immunoreactivity was evaluated both in the MM cells and non-tumor cell populations. Results are tabulated in Table 1 and shown in Figure 5.

As expected, in neoplastic areas, new vessels were very small in the early stages of MM infiltration and progressively increased in number and size, showing bigger lumina and strong CD34 immunoreactivity in plump endothelium with higher levels of infiltration (Figure 5A). All the markers analyzed increased with tumor infiltration levels in BMBs, with some differences (Figure 5A and Table 1): Jagged2 was expressed with higher intensity in MM cells at a low level of tumor infiltration in comparison with Jagged1, whose expression was weaker in infiltration degree I and showed a more evident progressive increase at higher infiltration levels. Similarly, VEGF-A expression in the MM cells showed an increasing trend.

To confirm that the Jagged ligand-directed Notch activation in MM cells was associated with an increased angiogenic potential, we performed the correlation analyses reported in Figure 5B,C and Supplementary Table S1. Findings indicate that in the MM cells the expression of both Jagged1 and Jagged2 correlates with HES6 immunoreactivity, an index of Notch pathway activation [7], with  $r = 0.7046$  and  $r = 0.8048$ , respectively. In turn, the HES6 levels in the MM cells significantly correlates with VEGF-A expression and MVD. Jagged ligands immunoreactivity also directly correlated with MM cell-derived VEGF-A and MVD (Table S1).

We also validated the Jagged-mediated MM cells' ability to boost the BMSC angiogenic potential by examining the correlation of MM-derived Jagged ligands with the immunoreactivity of the other markers on stromal non-tumor cells. As reported in Figure 5D–E, Jagged1 and Jagged2 expressed in the MM cells correlated with the HES6 expression in non-tumor cells ( $r = 0.5673$  and  $r = 0.5516$ , respectively), confirming a role of MM cell-derived Jagged in activating the Notch signaling in stromal cells. In turn, HES6 immunoreactivity was associated with VEGF-A expression in non-tumor cells and MVD, suggesting that Notch activation in stromal cells contributes to induce angiogenesis.

On the whole, the immunohistochemistry results of the MM patients' BMBs appear to be consistent with in vitro and in vivo evidence.

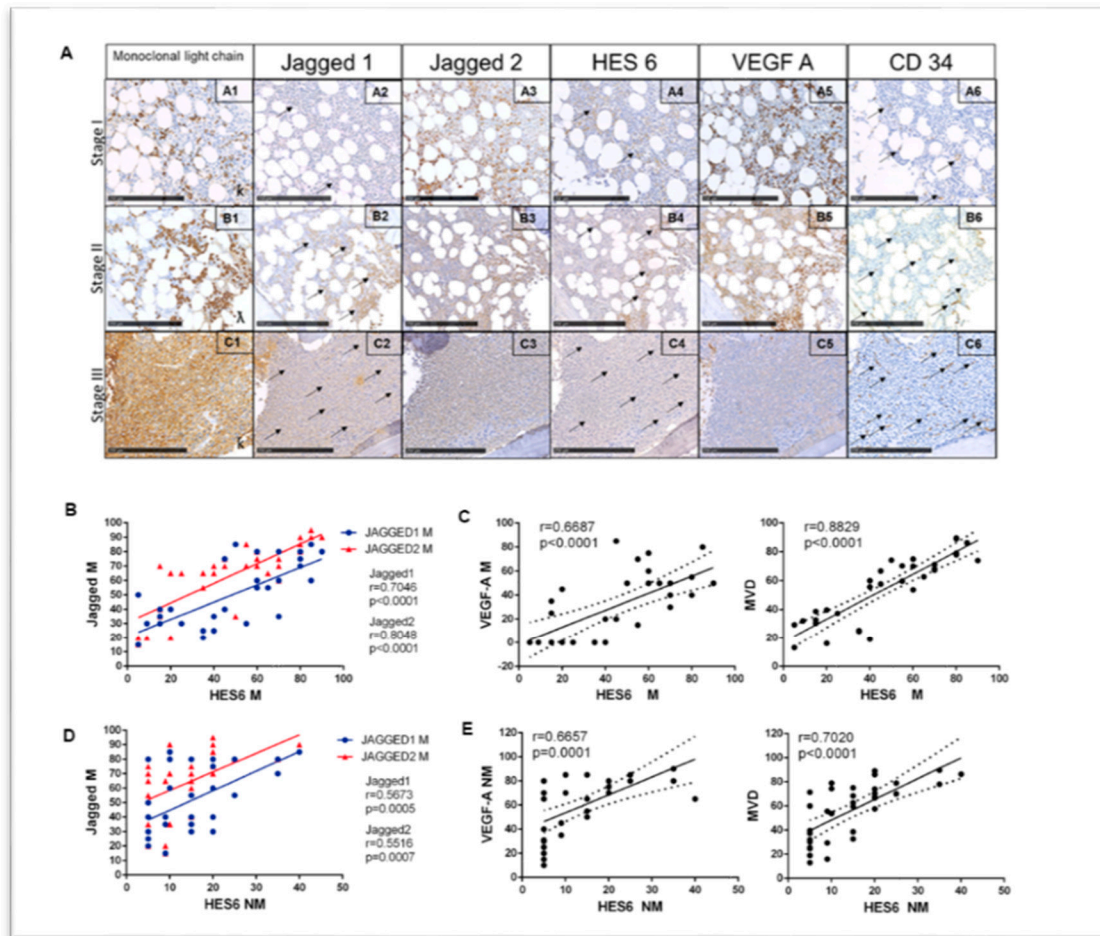


**Figure 5.** Correlation analysis of the Jagged ligands, Notch activation and angiogenesis in MM patients' BMBs. (A) representative images of the antigen immunoreactivity for the monoclonal Ig light chain, Jagged1, Jagged2, HES6, VEGF-A and CD34 in BMBs from 34 MM patients at different degrees of tumor infiltration (I: less than 20%; II: 21–50%; III: >51%). The arrows indicate specific immunoreactive signals. Photos were acquired at Nano-Zoomer 2.0 and scale bar is for 250  $\mu$ m. Pearson's correlation coefficient ( $r$ ) and the  $p$ -values are reported for the correlation analyses between (B) Jagged1 and Jagged 2 expressed in MM cells and the Notch transcriptional target HES6 in the same tumor cells; (C) HES6 and VEGF-A expressed in MM cells or MVD; (D) Jagged1 and Jagged 2 expressed in MM cells and the Notch transcriptional target HES6 in nearby non-tumor cells; and (E) HES6 in non-tumor cells and VEGF-A in non-tumor cells and MVD. M = MM cells; NM = non tumor cells. Statistical analysis was carried out using two-tailed  $t$ -tests.

**Table 1.** Immunohistochemical analysis of the Jagged ligands, Notch activation and angiogenesis in MM patients' bone marrow biopsies (BMBs). The degree of malignant plasma cell infiltration in the BM is reported along with the antigen immunoreactivity for monoclonal or Ig light chains. Additionally, the percentage of immunoreactive cells out of the total cells for Jagged1 and 2, HES6 and VEGF-A is reported both for MM (M) and non-MM (NM) cells, along with the microvessel density (MVD) evaluated as the average number of cell determinant 34+ (CD34+) vessels per field.

| PATIENT N. | INFILTRATION DEGREE | LIGHT CHAIN | JAGGED1 M | JAGGED1 NM | JAGGED2 M | JAGGED2 NM | HES6 M | HES6 NM | VEGF-A M | VEGF-A NM | MVD  |
|------------|---------------------|-------------|-----------|------------|-----------|------------|--------|---------|----------|-----------|------|
| 1          | I                   | K           | 50        | 5          | 20        | 15         | 5      | 5       | 0        | 30        | 13.0 |
| 2          | I                   | L           | 30        | 5          | 35        | 40         | 15     | 5       | 0        | 40        | 30.3 |
| 3          | I                   | L           | 30        | 9          | 20        | 25         | 9      | 5       | 0        | 15        | 32.0 |
| 4          | I                   | L           | 40        | 9          | 20        | 20         | 20     | 9       | 0        | 35        | 16.0 |
| 5          | I                   | L           | 15        | 9          | 15        | 20         | 5      | 9       | 0        | 35        | 29.3 |
| 6          | I                   | L           | 20        | 5          | 65        | 35         | 35     | 5       | 0        | 31        | 24.7 |
| 7          | I                   | K           | 25        | 5          | 70        | 40         | 40     | 5       | 0        | 10        | 19.0 |
| 8          | I                   | K           | 35        | 9          | 65        | 80         | 40     | 9       | 0        | 45        | 55.7 |
| 9          | I                   | L           | 30        | 9          | 65        | 60         | 25     | 5       | 0        | 20        | 37.3 |
| 10         | I                   | L           | 25        | 9          | 55        | 30         | 35     | 5       | 0        | 25        | 25.3 |
| 11         | II                  | L           | 25        | 15         | 65        | 40         | 40     | 5       | 20       | 70        | 60.0 |
| 12         | II                  | K           | 30        | 15         | 70        | 45         | 55     | 15      | 15       | 50        | 59.7 |
| 13         | II                  | L           | 35        | 20         | 70        | 70         | 15     | 15      | 35       | 65        | 38.7 |
| 14         | II                  | K           | 40        | 35         | 65        | 75         | 20     | 5       | 45       | 80        | 39.7 |
| 15         | II                  | K           | 40        | 25         | 70        | 50         | 45     | 20      | 20       | 75        | 57.7 |
| 16         | II                  | K           | 40        | 25         | 40        | 55         | 15     | 15      | 25       | 55        | 32.7 |
| 17         | II                  | K           | 85        | 15         | 35        | 80         | 50     | 10      | 50       | 70        | 74.3 |
| 18         | II                  | K           | 60        | 40         | 70        | 75         | 60     | 10      | 60       | 70        | 53.7 |
| 19         | II                  | K           | 80        | 30         | 75        | 55         | 70     | 5       | 30       | 65        | 71.3 |
| 20         | II                  | L           | 55        | 25         | 65        | 80         | 65     | 15      | 50       | 65        | 62.7 |
| 21         | II                  | K           | 60        | 50         | 70        | 85         | 70     | 20      | 40       | 70        | 67.3 |
| 22         | III                 | K           | 30        | 25         | 85        | 85         | 55     | 20      | 70       | 80        | 70.3 |
| 23         | III                 | K           | 80        | 55         | 75        | 90         | 60     | 15      | 75       | 85        | 75.0 |
| 24         | III                 | L           | 65        | 25         | 60        | 80         | 70     | 15      | 50       | 85        | 68.3 |
| 25         | III                 | L           | 80        | 30         | 90        | 85         | 80     | 10      | 55       | 85        | 79.0 |
| 26         | III                 | K           | 70        | 30         | 95        | 90         | 85     | 20      | 80       | 80        | 86.0 |
| 27         | III                 | K           | 75        | 25         | 75        | 80         | 45     | 20      | 85       | 70        | 66.7 |
| 28         | III                 | K           | 55        | 30         | 80        | 80         | 60     | 25      | 50       | 85        | 70.0 |
| 29         | III                 | K           | 80        | 50         | 80        | 90         | 80     | 35      | 40       | 90        | 78.0 |
| 30         | III                 | K           | 80        | 30         | 80        | 95         | N.A.   | 25      | 45       | 80        | 79.0 |
| 31         | III                 | K           | 75        | 25         | 85        | 95         | 80     | 20      | 40       | 80        | 89.0 |
| 32         | III                 | L           | 85        | 55         | 90        | 90         | 85     | 40      | 80       | 65        | 86.3 |
| 33         | III                 | K           | 70        | 45         | 80        | 85         | 80     | 35      | 40       | 80        | 89.7 |
| 34         | III                 | K           | 80        | 30         | 90        | 85         | 90     | 20      | 50       | 70        | 74.0 |

### 3. Discussion

The interplay between malignant plasma cells and the BM cell populations has been extensively studied in the past years since it is a key step in MM progression and an important target for new anti-tumor therapeutic approaches [24].

Notch signaling plays a pleiotropic role in different cellular contexts; it mediates cell–cell communication in cell fate decision, stem cell maintenance, cell proliferation and survival [25]. Mutations or aberrant expression of the Notch pathway members lead to increased signaling and are frequently present in solid and hematologic cancers [8]. In MM, the widespread Notch signaling activation characterizes the whole TME with important consequences ranging from drug resistance [10,26–28] to proliferation [7,29] and bone disease [12,30].

MM cell-derived Jagged ligands play a key role in the activation of Notch signaling in the BM cell populations. Accordingly, Jagged1 expression significantly correlates with disease progression, as we and others previously reported [7,14], while Jagged2 deregulation is an early event occurring at the benign MGUS phase [13], which results from both changes in the transcription level [13,31] or aberrant expression of Skeletraphin, an ubiquitin ligase that regulates Jagged2 activity [32].

Given the relevance of Jagged ligands in this disease, here we have analyzed the role of the Notch pathway in MM-induced angiogenesis, a key feature of MM progression that involves the communication with BM resident cell populations.

The angiogenic switch represents an important change in the BM of MM patients and fosters tumor growth and dissemination. The BM circulation is maintained by different stimuli provided by BM resident cells [33]. It is now well established that the accumulation of malignant plasma cells in the BM destabilizes this balance, leading to neovascularization, which in turn contributes to tumor progression [33].

We recently showed that Notch signaling in the ECs is necessary for angiogenesis activation since the inhibition of Notch1 and 2 activity in the ECs hampered their angiogenic potential [6]. Notch activation in the ECs may be triggered by homotypic activation due to the increased expression of Notch receptors and ligands in MM-ECs during the progression from MGUS to MM [6]. Additionally, we showed that the hyperexpression of Jagged1 and 2 ligands, which can be observed during MM cell progression [7,13,14], may trigger Notch activation in ECs by heterotypic interaction [6].

The importance of Jagged1 and 2 dysregulated expression in MM prompted us to investigate their role in MM angiogenesis exploring their effect on Notch signaling activation in ECs as well as their ability to stimulate the angiogenic potential of the BMSCs.

To study the direct effect of MM-derived Jagged on tumor angiogenesis, we interfered with the Jagged1 and Jagged2 expression in two MM cell lines, RPMI8226 and OPM2, and demonstrated that their silencing was associated with a reduced ability of MM cells to induce HPAEC organization in tube-like structures. The angiogenic stimulus provided by the MM cells was dual: it could be mediated by a direct cell-to-cell contact or by soluble tumor-derived factors. Indeed, we demonstrated that the administration of Jagged1 and 2 peptides triggered the activation of Notch signaling in ECs stimulating angiogenesis. This indicated that the Jagged ligands on the surface of the MM cells were able to activate the angiogenic signals in nearby ECs. On the other side, Jagged-mediated Notch signaling activation in MM cells could promote the secretion of soluble factors, activating the EC angiogenic potential. In fact, the CM from MM cells increased the ECs' ability to form tube-like structures, promoting their adhesion and migration. The observed effect relied on Jagged-induced Notch activity in MM cells, since the CM from HMCLs<sup>KD</sup> displayed a significantly reduced angiogenic potential, indicating that the release of MM-derived angiogenic factors depends on Notch signaling activation. VEGF-A was identified as a Notch-dependent angiogenic soluble factor released from MM cells upon Jagged-mediated Notch signaling activation, since its mRNA and protein level were inhibited by Jagged1 and 2 KD.

Additionally, since tumor-angiogenesis is a team effort of BM resident cells characterizing the TME, we also investigated the contribution of BMSCs, which display important angiogenic properties. We verified if the BMSC angiogenic properties could be increased by MM-cell-derived Jagged ligands by

using a co-culture system, including HMCLs and the human BM stromal cell line, HS5. We found that the BMSCs pre-stimulated with HMCLs increased their ability to release soluble factors, which could activate the angiogenic potential of the HPAECs, assessed as tube organization ability, motility and adhesion to fibronectin.

We showed that this effect was dependent on the MM-cell-derived Jagged ligands' ability to trigger Notch signaling in the BMSCs. As a matter of fact, when the HMCLs were depleted of Jagged1 and 2, the ability to trigger Notch signaling in the BMSCs and to stimulate their pro-angiogenic activity was significantly reduced. Additionally, since the BMSCs represent the major source of VEGF-A in the BM, we verified if the Notch signaling, activated by the MM-cell-derived Jagged ligands, was associated with an increase in VEGF-A secretion by the BMSCs. Our results confirmed that the control HMCLs<sup>SCR</sup> were able to induce VEGF-A secretion by the BMSCs, while HMCL<sup>KD</sup> did not.

The obtained results clearly show that the MM-derived Jagged ligands may unbalance the levels in Notch activation in the different cell populations, including the MM cells, ECs and BMSCs, thus spreading widely the angiogenic potential in the TME.

To validate in vivo the role played by Notch signaling in MM-associated angiogenesis, we used the zebrafish embryo model *Tg(fli1a:EGFP)<sup>y1</sup>*, which allows to detect the formation of new vessels sprouting from the sub-intestinal plexus 24 h following the injection of HMCLs<sup>SCR</sup> or HMCL<sup>KD</sup>. The evidence that the angiogenic sprout induced by control HMCLs<sup>SCR</sup> was significantly decreased upon Jagged1 and 2 KD prompted us to hypothesize that also in vivo MM-cell-directed angiogenesis relies on the expression of Jagged1 and 2 in MM cells.

Finally, by analyzing the MM patients' BMBs, we confirmed that the Jagged ligands expressed by the tumor cells are associated with the diffusion of Notch activation in the whole TME, including tumor and non-tumor cells. We found a strong positive correlation among the Jagged ligand levels in MM cells and Notch signaling activation (HES6 expression) in MM cells, as well as in nearby non-tumor stromal cells. Moreover, Notch activation significantly correlated with the expression of VEGF-A in the same cells, and also with MVD. These results show that such an association occurs in MM patient's BM between the activation of Notch in tumor cells, TME and the angiogenic switch.

The result is even more interesting considering the significant correlation between the level of MM cells BM infiltration, the expression of Jagged ligands in MM cells and the increase in MVD, which associate the aberrant expression of Jagged1 and 2 with the angiogenic switch occurring during MM progression. Indeed, our evidence indicates that the Jagged ligands' levels increase with BMB infiltration; in particular, while Jagged1 expression rises slowly and progressively increases, Jagged2 is already expressed at higher levels in the BMBs with the lower levels of infiltration (Table 1). This is consistent with other pieces of evidence, including (1) our recent analysis of tumor cells from MM patients' gene expression profiling, which indicated that Jagged1 and the Notch transcriptional target HES5 are overexpressed in tumor cells compared to healthy controls, and reach a higher expression level in the more aggressive primary plasma cell leukemia [7]; (2) a refined immunohistochemical analysis revealed that Jagged1 dysregulation occurs during the progression from monoclonal gammopathy of uncertain significance (MGUS) to MM [14]; and (3) Jagged2 overexpression is an earlier event that precedes MGUS and correlates with disease progression [13].

The obtained results contribute to provide a more comprehensive picture of the major drivers of the angiogenic switch during MM progression and of the role played by the Notch pathway: MM cells increase the expression levels of Jagged1, 2 and Notch1 and 2 receptors, promoting (1) homotypic activation of Notch signaling in MM cells that, in turn, results in the secretion of VEGF; (2) heterotypic activation of the angiogenic Notch signaling in ECs; and (3) heterotypic activation of Notch signaling in BMSCs that, in turn, boosts the secretion of VEGF, inducing a potent angiogenic signal. It should be noted that BMSCs may release a higher amount of VEGF in comparison with MM cells (our ELISA results indicate that they may release  $2035 \pm 96$  pg/mL of VEGF compared to  $938 \pm 72$  pg/mL for RPMI8226 and  $797 \pm 85$  pg/mL for OPM2 cells, even if in our experimental conditions the HCMLs were maintained four times more concentrated than the HS5 cell line. Additionally,

we demonstrated that the BMSC-mediated VEGF secretion may be further increased by MM cell stimulation. Therefore, we believe that the more effective angiogenic effect of the Notch signaling widespread in the TME is probably mediated by MM-stimulated BMSCs. This effect may be further enhanced by the previously reported increase in Notch receptors and ligands expression occurring in the ECs during MM progression [6]. This may intensify the homotypic interactions between the ECs and provide a greater availability of Notch1 and 2 receptors for the interaction with MM-cell-derived Jagged1 and 2.

In conclusion, the tight spatial and temporal regulation of Notch ligands necessary for the balanced differentiation of new vessels seems to be deranged by the accumulation of MM cells and MM-derived Jagged ligands.

## 4. Materials and Methods

### 4.1. Cell Lines

The HMCLs used in this study, RPMI8226 (ATCC<sup>®</sup> CCL-155TM) and OPM2 (ACC-50), were cultured in RPMI1640 medium (Lonza, Swiss) supplemented with 10% fetal bovine serum (FBS) (Euroclone S.p.A., Italy), 100 U/mL P/S (penicillin/streptomycin) (Microgem, IT, USA) and 2 mM L-glutamine (Microgem, Italy). Cell lines were seeded at  $3 \times 10^5$  cells/mL and split every 48 h. HPAECs (Human Pulmonary Artery endothelial cells—ATCC<sup>®</sup> PCS-100-022TM) were cultured in Vascular Basal medium (ATCC<sup>®</sup> PCS-100-030TM) supplemented with the Endothelial Cells Growth Kit-VEGF (ATCC<sup>®</sup> PCS-100-041TM), following the manufacturer's instruction (complete vascular medium). The HPAECs were seeded at a final concentration of  $3 \times 10^3$  cells/cm<sup>2</sup>. The human BMSC line HS5 (ATCC<sup>®</sup> CRL-11882<sup>TM</sup>) was cultured in DMEM (Lonza, Swiss) supplemented with 10% FBS, 100 U/mL P/S and 2 mM L-glutamine.

### 4.2. HMCL Knockdown and Co-Culture Experiments

HMCLs were transfected using specific siRNAs directed against Jagged1 and Jagged2 at a final concentration of 25 nM each and a Lipofectamine RNAiMAX Transfection Reagent [10]. For the co-culture system of the HS5 cell line with transfected HMCLs, HS5 cells were seeded in 24-well plates at a density of  $1.5 \times 10^5$  cells/mL, and transfected HMCLs were added at the concentration  $6 \times 10^5$  cells/mL (ratio 1:4). Cells were co-cultured for 40 h and the CM of the last 24 h was analyzed by ELISA or used for tube formation assay. HS5 cells were collected and extracted RNA was analyzed by qRT-PCR. For the in vivo experiments, the HEK293 cell line was transfected using CaCl<sub>2</sub> with the pTRIPZ vector carrying a doxycycline-inducible system expressing shRNA against Jagged1 and Jagged2 or the corresponding scramble shRNA (ThermoFisher, MA, USA). RPMI8226 infection with lentiviral particles were carried out in the presence of 10 µg/mL polybrene (Sigma Aldrich), 20 ng/mL IL6 (Peprotech Inc., USA) and 20 ng/mL IGF1 (Peprotech Inc., USA). After 48 h, the infected cells were selected with puromycin 1 µg/mL. Before injection, the cells were stimulated with doxycycline, 1 µg/mL for 72 h.

### 4.3. Tube Formation Assay

Reduced Matrigel (Corning, NY, USA) was dispensed in a 96-well plate, 50 µL/well, and incubated for 1 h at 37 °C. The HPAECs were seeded on Matrigel-coated wells at  $2 \times 10^4$  cells/well. The assay was carried out using different stimuli as follows: (i) HMCLs<sup>SCR</sup> or HMCLs<sup>KD</sup> were seeded on a layer of HPAECs at a ratio 1:2 (HPAECs:HMCLs); (ii) 100 µL CM from HMCLs<sup>SCR</sup> and HMCLs<sup>KD</sup> or CM from co-cultures systems of HS5 cells and HMCLs<sup>SCR</sup> or HMCLs<sup>KD</sup> were dispensed in each well; (iii) human recombinant Jagged1 (#188-204—AnaSpec) or Jagged2 (R&D Systems Inc., Minneapolis, MN, USA) were added to RPMI1640 medium at the concentration of 20 µg/mL according to manufacturer's instruction. Photos of the tube-like structures were acquired after overnight incubation with the EVOS-inverted microscope (Euroclone S.p.A., Italy) or PrimoVert Microscope (Zeiss, Germany) at  $\times 4$

magnification. Numbers of area, numbers of branch points and total tube length were analyzed using the ImageJ program.

#### 4.4. Adhesion Assay

HPAECs were seeded in a 6-well plate at  $3 \times 10^3$  cells/cm<sup>2</sup> density. After 24 h, the medium was changed with CM from HMCLs<sup>SCR</sup> and HMCLs<sup>KD</sup> cultured alone or co-cultured with the HS5 cell line for 72 h and diluted 1:1 with fresh RPMI1640 medium supplemented with 2% FBS, 100 U/mL P/S and 2 mM L-glutamine. The HPAECs were incubated for 24 h and a black 96-well plate was coated overnight at 37 °C with 100 µg/mL fibronectin diluted in 0.005M Tris-HCl, pH 7.4. The day after the HPAECs were stained with 5 µM Calcein AM 1 h at 37 °C and were seeded on fibronectin at  $2.5 \times 10^4$  cells/well in fresh-RPMI1640 for 1 h in an incubator at 37 °C with 5% CO<sub>2</sub>. The fluorescence intensity was read with an EnSight Multimode Plate Reader (Perkin Elmer, Inc. MA, USA).

#### 4.5. Wound Healing Assay

The HPAECs were seeded in a 48-well plate in complete vascular medium in order to have a confluent well after 48 h. When cells reached confluence, the medium was substituted with CM from HMCLs<sup>SCR</sup> and HMCLs<sup>KD</sup> cultured alone or co-cultured with the HS5 cell line for 72 h and diluted 1:1 with fresh RPMI1640 medium supplemented with 2% FBS, 100 U/mL P/S, 2mM L-glutamine and the wound was done using a p200 tip. After 24 h incubation, the HPAECs were washed once with 1× PBS, stained with Comassie Blue and the photos were acquired with a PrimoVert Microscope (Zeiss, Germany) at ×4 magnification. Migration was determined using the ImageJ program as an average open area of the wound.

#### 4.6. RNA Extraction and qRT-PCR

Total RNA samples from the HS5 cells cultured alone or with HMCLs<sup>SCR</sup> or HMCLs<sup>KD</sup> were extracted by TRI Reagent (Merck, Italy), following the manufacturer's instructions. Total RNA (1 µg) was retrotranscribed using RevertAid M-MuLV Reverse Transcriptase (ThermoFisher). Quantitative PCR (qRT-PCR) reactions were carried out on a Step-One Plus PCR system (Applied Biosystems, Life Technologies Italia, Italy) using GoTaq<sup>®</sup> qPCR (Promega, Italy). The primer sequences are reported in Table 2.

**Table 2.** Sequences of the primers used for the qRT-PCR.

| hGAPDH   | 5'-ACAGTCAGCCG ATC TTC TT-3' | 5'-AATGGAGGGGTCATTGATGG-3'   |
|----------|------------------------------|------------------------------|
| h18S     | 5'-GTAACCCGTTGAACCCATT-3'    | 5'-CCATCCAATCGGTAGTAGCG-3'   |
| hJagged1 | 5'-GCAACACCTTCAACCTCAAG-3'   | 5'-GTTGAACGGTGTTCATTACTGG-3' |
| hJagged2 | 5'-TCATCCCCTTCCAGTTCG-3'     | 5'-TGGTATCGTTGTCCAGTC-3'     |
| hHES1    | 5'-AGGCGGACATTCTGGAAATG-3'   | 5'-CGGTACTTCCCCAGCACACTT-3'  |
| hHES6    | 5'-CGTGAGGATGAGGACGG-3'      | 5'-AGGCTCTCGTTGATCCG-3'      |
| hVEGF-A  | 5'-GGGCAGAATCATCACGAAGT-3'   | 5'-TGGTGATGTTGGACTCCTCA-3'   |
| hHPRT    | 5'-TTTATGTCCCCTGTTGACTGGT-3' | 5'-GTAGCCCTCTGTGTGCTCAA-3'   |

#### 4.7. ELISA for VEGF-A

VEGF-A ELISA kit (Thermo Scientific) was used to detect human VEGF-A in supernatants of single cultures or co-cultures diluted 10 times, following manufacturer instructions. All analyses were performed in duplicate. Secreted VEGF protein concentration was normalized to the numbers of cells. For co-cultures, the total VEGF protein content was subtracted from the VEGF protein content of the HMCLs and normalized to the number of HS5 cells.



#### 4.8. Zebrafish Injection

Adult zebrafish (*Danio rerio*) were maintained according to European laws (2010/63/EU and 86/609/EEC). The 48-hpf *Tg(fli1a:EGFP)<sup>y1</sup>* transgenic embryos [34] were implanted with 72 h-induced HMCLs<sup>SCR</sup> or HMCLs<sup>I1/2KD</sup> cells, using a previously described procedure for neuroendocrine tumors [35]. In brief, cells were labeled with a red fluorescent viable dye (CM-Dil, Molecular Probes-Invitrogen, MA, USA) and resuspended with PBS. The 48 hpf zebrafish embryos were anesthetized with 0.02 mg/mL tricaine and injected with stained tumor cells (about 600 cells in each embryo) into the sub-peridermal space, close to the developing SIV plexus. At 24 h hpi, epifluorescence images were acquired with a Leica DM 5500B microscope equipped with a DC480 camera. The cumulative length of the tumor-induced endothelial structures, sprouting from the SIV plexus, were measured in each implanted embryo using ImageJ software.

#### 4.9. Immunohistochemical Analysis of Human Bone Marrow Biopsies

Archival BMBs from 34 MM patients diagnosed at the Unit of Pathology, A.O. San Paolo, Department of Health Sciences, University of Milan, Italy were evaluated in the present study approved by the Ethical Committee of Milano University (No. 8/15—4 March 2015).

Histopathological diagnosis of MM was carried out according to the WHO classification criteria; BMPs were subdivided according to the extent of the BM infiltration by the myeloma cells as follows: degree of infiltration I = less than 20% (10 cases); II = 21–50% (11 cases), III > 51% (13 cases). Notch activation and angiogenesis were investigated by immunohistochemistry (IHC) with an automatic immunostainer (DAKO OMNIS) using diaminobenzidine as the chromogen. Used antibodies were reported in Table 3. Digital images were obtained by the NanoZoomer 2.0 scanner (Hamamatsu Photonics, Japan).

**Table 3.** Antibodies and experimental conditions used for the IHC.

| Antigen            | Clone                     | Source     | Dilution/Time | Unmasking       |
|--------------------|---------------------------|------------|---------------|-----------------|
| Kappa light chain  | -                         | Agilent    | 1:10; 1 h     | FLEX TRS Low pH |
| Lambda light chain | -                         | Agilent    | 1:10; 1 h     | FLEX TRS Low pH |
| Jagged 1           | AF1277 Goat               | R&D syst.  | 1:100; 1 h    | EDTA            |
| Jagged 2           | 4F10 Mouse                | Santa Cruz | 1:200; o.n.   | Citrate         |
| HES6               | Polyclonal Rabbit         | Abcam      | 1:300; o.n.   | Citrate         |
| VEGF-A             | A-20 Polyclonal Rabbit    | Santa Cruz | 1:800; 1 h    | Citrate         |
| CD34               | QBEnd 10 Monoclonal Mouse | Agilent    | Ready-to-Use  | FLEX TRS Low pH |

Statistical analysis and percentage variation among the HMCL experimental conditions.

Statistical analyses were performed using GraphPad Prism 6 software (GraphPad software, San Diego, CA, USA). For the in vitro assays including two groups, we carried out one-tailed Student's *t*-tests; when including 3 or more groups, we performed a one-way ANOVA with Tukey's post-hoc tests. For in vivo experiments, the minimum size of each group was determined using an a priori power analysis for a one-way ANOVA with an alpha = 0.05 with G-power 3.2 software.

## 5. Conclusions

Jagged ligands dysregulation is frequent in different types of tumors and is often reported to influence angiogenesis in different neoplasms besides MM, i.e., breast cancer [36–38] and head and neck squamous cell carcinoma [39]. Boareto and colleagues reported that Jagged ligand expression mediates the differences between physiologic and tumor angiogenesis by affecting the tip-stalk cell fate decisions during vessel formation. Indeed, normal angiogenesis is characterized by a balanced expression of Notch ligands where Dll ligands, expressed in the tip cells, drive new vessels sprouting, and Jagged1

and 2 in the stalk cells drive vessel elongation. In contrast, Jagged overexpression observed in MM and in other types of tumors results in a hybrid tip/stalk phenotype characterized by compromised migration traits compared to tip cells and therefore leading to smaller and poorly perfused vessels compared to those led by the tip cells [40].

Overall, the Jagged ligands' overexpression has a pleiotropic effect, influencing tumor biology and the pathological communication with the TME. This also includes the promotion of a key step in tumor progression, such as MM-associated angiogenesis, and further strengthen the indication for a therapeutic approach directed to inhibit Jagged-mediated Notch activation by specific monoclonal antibodies [41] or small molecules [42].

**Supplementary Materials:** The following are available online at <http://www.mdpi.com/2072-6694/12/9/2600/s1>, Table S1: Correlation matrix of markers for ligand and target gene of Notch pathway and angiogenesis quantified in MM patients' BM biopsies.

**Author Contributions:** Conceptualization, R.C., A.N. and R.R.; methodology, M.T.P., D.G., N.P., D.T., M.F., G.G., M.C., V.C., E.T. and E.L.; validation R.C., D.G. and N.P., formal analysis M.T.P., D.G., N.P., D.T., M.F. and G.G.; investigation, R.C., M.T.P., D.G., N.P. and G.V.; resources, R.C., R.R. and A.N.; data curation, E.L., E.T., R.C., N.A. and I.S.; writing—original draft preparation, R.C., M.T.P., D.G., N.P., M.F. and D.T.; writing—review and editing, R.C., N.A., G.V., G.G., D.G., N.P., E.L., V.C., M.C., I.S., R.R., E.T., A.N. and M.T.P.; funding acquisition, R.C. and A.N. All authors have read and agreed to the published version of the manuscript.

**Funding:** This research was funded by Associazione Italiana Ricerca sul Cancro, AIRC Investigator Grant to RC grant number 20614 and AN grant number 16722 and by University of Milano grant number Linea 2B-2017 - Dept. Health Sciences to RC; AIRC post-doctoral fellowship to MC grant number 18013 and to V.C. (financed with Investigator Grant 20614 to RC). Università degli Studi di Milano awarded MTP with a PhD fellowship in Molecular and Translational Medicine, DG with a PhD fellowship in Experimental Medicine and NP with a post-doctoral fellowship type A.

**Conflicts of Interest:** The authors declare no conflict of interest.

## References

- Ribatti, D.; Vacca, A. Role of Endothelial Cells and Fibroblasts in Multiple Myeloma Angiogenic Switch. *Cancer Treat. Res.* **2016**, *169*, 51–61.
- Hideshima, T.; Mitsiades, C.; Tonon, G.; Richardson, P.G.; Anderson, K.C. Understanding multiple myeloma pathogenesis in the bone marrow to identify new therapeutic targets. *Nat. Rev. Cancer* **2007**, *7*, 585–598. [[CrossRef](#)] [[PubMed](#)]
- Ribatti, D.; Vacca, A. The role of microenvironment in tumor angiogenesis. *Genes Nutr.* **2008**, *3*, 29–34. [[CrossRef](#)] [[PubMed](#)]
- Ria, R.; Reale, A.; De Luisi, A.; Ferrucci, A.; Moschetta, M.; Vacca, A. Bone marrow angiogenesis and progression in multiple myeloma. *Am. J. Blood Res.* **2011**, *1*, 76–89. [[PubMed](#)]
- Vacca, A.; Ria, R.; Semeraro, F.; Merchionne, F.; Coluccia, M.; Boccarelli, A.; Scavelli, C.; Nico, B.; Gernone, A.; Battelli, F.; et al. Endothelial cells in the bone marrow of patients with multiple myeloma. *Blood* **2003**, *102*, 3340–3348. [[CrossRef](#)]
- Saltarella, I.; Frassanito, M.A.; Lamanuzzi, A.; Brevi, A.; Leone, P.; Desantis, V.; Di Marzo, L.; Bellone, M.; Derudas, D.; Ribatti, D.; et al. Homotypic and Heterotypic Activation of the Notch Pathway in Multiple Myeloma-Enhanced Angiogenesis: A Novel Therapeutic Target? *Neoplasia* **2019**, *21*, 93–105. [[CrossRef](#)] [[PubMed](#)]
- Colombo, M.; Galletti, S.; Bulfamante, G.; Falleni, M.; Tosi, D.; Todoerti, K.; Lazzari, E.; Crews, L.A.; Jamieson, C.H.; Ravaioli, S.; et al. Multiple myeloma-derived Jagged ligands increases autocrine and paracrine interleukin-6 expression in bone marrow niche. *Oncotarget* **2016**, *7*, 56013–56029. [[CrossRef](#)]
- Platonova, N.; Lesma, E.; Basile, A.; Bignotto, M.; Garavelli, S.; Palano, M.T.; Moschini, A.; Neri, A.; Colombo, M.; Chiaramonte, R. Targeting Notch as a Therapeutic Approach for Human Malignancies. *Curr. Pharm. Des.* **2017**, *23*, 108–134.
- Kopan, R.; Ilagan, M.X. The canonical Notch signaling pathway: Unfolding the activation mechanism. *Cell* **2009**, *137*, 216–233. [[CrossRef](#)]

10. Colombo, M.; Garavelli, S.; Mazzola, M.; Platonova, N.; Giannandrea, D.; Colella, R.; Apicella, L.; Lancellotti, M.; Lesma, E.; Ancona, S.; et al. Multiple myeloma exploits Jagged1 and Jagged2 to promote intrinsic and bone marrow-dependent drug resistance. *Haematologica* **2019**, *105*, e1925. [[CrossRef](#)] [[PubMed](#)]
11. Nefedova, Y.; Cheng, P.; Alsina, M.; Dalton, W.S.; Gabilovich, D.I. Involvement of Notch-1 signaling in bone marrow stroma-mediated de novo drug resistance of myeloma and other malignant lymphoid cell lines. *Blood* **2004**, *103*, 3503–3510. [[CrossRef](#)] [[PubMed](#)]
12. Colombo, M.; Thummler, K.; Mirandola, L.; Garavelli, S.; Todoerti, K.; Apicella, L.; Lazzari, E.; Lancellotti, M.; Platonova, N.; Akbar, M.; et al. Notch signaling drives multiple myeloma induced osteoclastogenesis. *Oncotarget* **2014**, *5*, 10393–10406. [[CrossRef](#)] [[PubMed](#)]
13. Houde, C.; Li, Y.; Song, L.; Barton, K.; Zhang, Q.; Godwin, J.; Nand, S.; Toor, A.; Alkan, S.; Smadja, N.V.; et al. Overexpression of the NOTCH ligand JAG2 in malignant plasma cells from multiple myeloma patients and cell lines. *Blood* **2004**, *104*, 3697–3704. [[CrossRef](#)]
14. Skrtic, A.; Korac, P.; Kristo, D.R.; Ajdukovic Stojisavljevic, R.; Ivankovic, D.; Dominis, M. Immunohistochemical analysis of NOTCH1 and JAGGED1 expression in multiple myeloma and monoclonal gammopathy of undetermined significance. *Hum. Pathol.* **2010**, *41*, 1702–1710. [[CrossRef](#)] [[PubMed](#)]
15. Pedrosa, A.R.; Trindade, A.; Fernandes, A.C.; Carvalho, C.; Gigante, J.; Tavares, A.T.; Dieguez-Hurtado, R.; Yagita, H.; Adams, R.H.; Duarte, A. Endothelial Jagged1 antagonizes Dll4 regulation of endothelial branching and promotes vascular maturation downstream of Dll4/Notch1. *Arterioscler. Thromb. Vasc. Biol.* **2015**, *35*, 1134–1146. [[CrossRef](#)] [[PubMed](#)]
16. Kangsamaksin, T.; Tattersall, I.W.; Kitajewski, J. Notch functions in developmental and tumour angiogenesis by diverse mechanisms. *Biochem. Soc. Trans.* **2014**, *42*, 1563–1568. [[CrossRef](#)]
17. Bridges, E.; Oon, C.E.; Harris, A. Notch regulation of tumor angiogenesis. *Future Oncol. (Lond. Engl.)* **2011**, *7*, 569–588. [[CrossRef](#)]
18. Ghiabi, P.; Jiang, J.; Pasquier, J.; Maleki, M.; Abu-Kaoud, N.; Rafii, S.; Rafii, A. Endothelial cells provide a notch-dependent pro-tumoral niche for enhancing breast cancer survival, stemness and pro-metastatic properties. *PLoS ONE* **2014**, *9*, e112424. [[CrossRef](#)]
19. Phng, L.K.; Gerhardt, H. Angiogenesis: A team effort coordinated by notch. *Dev. Cell* **2009**, *16*, 196–208. [[CrossRef](#)]
20. Rajkumar, S.V.; Leong, T.; Roche, P.C.; Fonseca, R.; Dispenzieri, A.; Lacy, M.Q.; Lust, J.A.; Witzig, T.E.; Kyle, R.A.; Gertz, M.A.; et al. Prognostic value of bone marrow angiogenesis in multiple myeloma. *Clin. Cancer Res. Off. J. Am. Assoc. Cancer Res.* **2000**, *6*, 3111–3116.
21. Vande Broek, I.; Vanderkerken, K.; Van Camp, B.; Van Riet, I. Extravasation and homing mechanisms in multiple myeloma. *Clin. Exp. Metastasis* **2008**, *25*, 325–334. [[CrossRef](#)] [[PubMed](#)]
22. Pellegrino, A.; Ria, R.; Di Pietro, G.; Cirulli, T.; Surico, G.; Pennisi, A.; Morabito, F.; Ribatti, D.; Vacca, A. Bone marrow endothelial cells in multiple myeloma secrete CXC-chemokines that mediate interactions with plasma cells. *Br. J. Haematol.* **2005**, *129*, 248–256. [[CrossRef](#)] [[PubMed](#)]
23. Ribatti, D.; Moschetta, M.; Vacca, A. Microenvironment and multiple myeloma spread. *Thromb. Res.* **2014**, *133*, S102–S106. [[CrossRef](#)]
24. Kawano, Y.; Moschetta, M.; Manier, S.; Glavey, S.; Gorgun, G.T.; Roccaro, A.M.; Anderson, K.C.; Ghobrial, I.M. Targeting the bone marrow microenvironment in multiple myeloma. *Immunol. Rev.* **2015**, *263*, 160–172. [[CrossRef](#)]
25. Hori, K.; Sen, A.; Artavanis-Tsakonas, S. Notch signaling at a glance. *J. Cell Sci.* **2013**, *126*, 2135–2140. [[CrossRef](#)] [[PubMed](#)]
26. Muguruma, Y.; Yahata, T.; Warita, T.; Hozumi, K.; Nakamura, Y.; Suzuki, R.; Ito, M.; Ando, K. Jagged1-induced Notch activation contributes to the acquisition of bortezomib resistance in myeloma cells. *Blood Cancer J.* **2017**, *7*, e650. [[CrossRef](#)]
27. Xu, D.; Hu, J.; De Bruyne, E.; Menu, E.; Schots, R.; Vanderkerken, K.; Van Valckenborgh, E. Dll1/Notch activation contributes to bortezomib resistance by upregulating CYP1A1 in multiple myeloma. *Biochem. Biophys. Res. Commun.* **2012**, *428*, 518–524. [[CrossRef](#)]
28. Nefedova, Y.; Sullivan, D.M.; Bolick, S.C.; Dalton, W.S.; Gabilovich, D.I. Inhibition of Notch signaling induces apoptosis of myeloma cells and enhances sensitivity to chemotherapy. *Blood* **2008**, *111*, 2220–2229. [[CrossRef](#)]

29. Mirandola, L.; Apicella, L.; Colombo, M.; Yu, Y.; Berta, D.G.; Platonova, N.; Lazzari, E.; Lancellotti, M.; Bulfamante, G.; Cobos, E.; et al. Anti-Notch treatment prevents multiple myeloma cells localization to the bone marrow via the chemokine system CXCR4/SDF-1. *Leukemia* **2013**, *27*, 1558–1566. [[CrossRef](#)]
30. Delgado-Calle, J.; Anderson, J.; Cregor, M.D.; Hiasa, M.; Chirgwin, J.M.; Carlesso, N.; Yoneda, T.; Mohammad, K.S.; Plotkin, L.I.; Roodman, G.D.; et al. Bidirectional Notch Signaling and Osteocyte-Derived Factors in the Bone Marrow Microenvironment Promote Tumor Cell Proliferation and Bone Destruction in Multiple Myeloma. *Cancer Res.* **2016**, *76*, 1089–1100. [[CrossRef](#)]
31. Ghoshal, P.; Nganga, A.J.; Moran-Giupati, J.; Szafranek, A.; Johnson, T.R.; Bigelow, A.J.; Houde, C.M.; Avet-Loiseau, H.; Smiraglia, D.J.; Ersing, N.; et al. Loss of the SMRT/NCoR2 corepressor correlates with JAG2 overexpression in multiple myeloma. *Cancer Res.* **2009**, *69*, 4380–4387. [[CrossRef](#)] [[PubMed](#)]
32. Takeuchi, T.; Adachi, Y.; Ohtsuki, Y. Skeletrophin, a novel ubiquitin ligase to the intracellular region of Jagged-2, is aberrantly expressed in multiple myeloma. *Am. J. Pathol.* **2005**, *166*, 1817–1826. [[CrossRef](#)]
33. Vacca, A.; Ria, R.; Reale, A.; Ribatti, D. Angiogenesis in multiple myeloma. *Chem. Immunol. Allergy* **2014**, *99*, 180–196. [[PubMed](#)]
34. Lawson, N.D.; Weinstein, B.M. In vivo imaging of embryonic vascular development using transgenic zebrafish. *Dev. Biol.* **2002**, *248*, 307–318. [[CrossRef](#)] [[PubMed](#)]
35. Vitale, G.; Gaudenzi, G.; Dicitore, A.; Cotelli, F.; Ferone, D.; Persani, L. Zebrafish as an innovative model for neuroendocrine tumors. *Endocr. Related. Cancer* **2014**, *21*, R67–R83. [[CrossRef](#)]
36. Chen, J.Y.; Li, C.F.; Chu, P.Y.; Lai, Y.S.; Chen, C.H.; Jiang, S.S.; Hou, M.F.; Hung, W.C. Lysine demethylase 2A promotes stemness and angiogenesis of breast cancer by upregulating Jagged1. *Oncotarget* **2016**, *7*, 27689–27710. [[CrossRef](#)]
37. Pietras, A.; von Stedingk, K.; Lindgren, D.; Pahlman, S.; Axelson, H. JAG2 induction in hypoxic tumor cells alters Notch signaling and enhances endothelial cell tube formation. *Mol. Cancer Res.* **2011**, *9*, 626–636. [[CrossRef](#)]
38. Soares, R.; Balogh, G.; Guo, S.; Gartner, F.; Russo, J.; Schmitt, F. Evidence for the notch signaling pathway on the role of estrogen in angiogenesis. *Mol. Endocrinol. (Baltim. Md.)* **2004**, *18*, 2333–2343. [[CrossRef](#)]
39. Zeng, Q.; Li, S.; Chepeha, D.B.; Giordano, T.J.; Li, J.; Zhang, H.; Polverini, P.J.; Nor, J.; Kitajewski, J.; Wang, C.Y. Crosstalk between tumor and endothelial cells promotes tumor angiogenesis by MAPK activation of Notch signaling. *Cancer Cell* **2005**, *8*, 13–23. [[CrossRef](#)]
40. Boareto, M.; Jolly, M.K.; Ben-Jacob, E.; Onuchic, J.N. Jagged mediates differences in normal and tumor angiogenesis by affecting tip-stalk fate decision. *Proc. Natl. Acad. Sci. USA* **2015**, *112*, E3836–E3844. [[CrossRef](#)]
41. Masiero, M.; Li, D.; Whiteman, P.; Bentley, C.; Greig, J.; Hassanali, T.; Watts, S.; Stribbling, S.; Yates, J.; Bealing, E.; et al. Development of Therapeutic Anti-JAGGED1 Antibodies for Cancer Therapy. *Mol. Cancer Ther.* **2019**, *18*, 2030–2042. [[CrossRef](#)] [[PubMed](#)]
42. Platonova, N.; Parravicini, C.; Sensi, C.; Paoli, A.; Colombo, M.; Neri, A.; Eberini, I.; Chiaramonte, R. Identification of small molecules uncoupling the Notch:Jagged interaction through an integrated high-throughput screening. *PLoS ONE* **2017**, *12*, e0182640. [[CrossRef](#)] [[PubMed](#)]



Haematologica  
HAEMATOL/2021/279716  
Version 4

Extracellular vesicles mediate the communication between multiple myeloma and bone marrow microenvironment in a NOTCH dependent way

Domenica Giannandrea, Natalia Platonova, Michela Colombo, Mara Mazzola, Valentina Citro, Raffaella Adami, Filippo Maltoni, Silvia Ancona, Vincenza Dolo, Ilaria Giusti, Andrea Basile, Anna Pistocchi, Laura Cantone, Valentina Bollati, Lavinia Casati, Elisabetta Calzavara, Mauro Turrini, Elena Lesma, and Raffaella Chiaramonte

Disclosures: This study was supported by grants from Associazione Italiana Ricerca sul Cancro, Investigator grant to RC (20614), My First Grant to AP (18714); Fondazione Italiana per la Ricerca sul Cancro to MC (post-doctoral fellowship 18013); Università degli Studi di Milano to RC (Linea 2B-2017 - Dept. Health Sciences), to NP (post-doctoral fellowship type A) and DG (PhD fellowship in Experimental Medicine).

Contributions: DG, NP, MC: Experiment design and performance, acquisition of data, drafting the manuscript; MM, VC, RA, FM, SA, EL: experiment performance, acquisition of data; VD and IG: TEM morphologic analysis; MC, MM, AP: performance of in vivo zebrafish experiment; DG, LCan and VB: NTA analysis; MT, EC: patients' sample and clinical information collection and patients' sample first processing; DG, MT, AB, LCas: Statistical analysis; DG, MT, AB, AP, EL, VB, LCas: manuscript revision; LCas: acquisition of data; RC, DG, AB, MT: interpretation of data; RC: Experiment design and supervision, interpretation of data and statistical analysis, drafting, writing and critical revision of the manuscript.

*NOTCH2 in myeloma-derived extracellular vesicles*

**Extracellular vesicles mediate the communication between multiple myeloma and bone marrow microenvironment in a NOTCH dependent way**

Domenica Giannandrea<sup>1</sup>, Natalia Platonova<sup>1</sup>, Michela Colombo<sup>1</sup>, Mara Mazzola<sup>2</sup>, Valentina Citro<sup>1</sup>, Raffaella Adami<sup>1</sup>, Filippo Maltoni<sup>1</sup>, Silvia Ancona<sup>1</sup>, Vincenza Dolo<sup>3</sup>, Ilaria Giusti<sup>3</sup>, Andrea Basile<sup>4</sup>, Anna Pistocchi<sup>2</sup>, Laura Cantone<sup>5</sup>, Valentina Bollati<sup>5</sup>, Lavinia Casati<sup>1</sup>, Elisabetta Calzavara<sup>6</sup>, Mauro Turrini<sup>6</sup>, Elena Lesma<sup>1</sup>, Raffaella Chiaramonte<sup>1</sup>

1 Department of Health Sciences, Università degli Studi di Milano

2 Department of Medical Biotechnology and Translational Medicine, Università degli Studi di Milano

3 Department of Life, Health and Environment Sciences, Università degli Studi dell'Aquila

4 Department of Oncology and Hemato-oncology, Università degli Studi di Milano

5 Department of Clinical Sciences and Community Health, Università degli Studi di Milano

6 Division of Hematology, Valduce Hospital, Como, Italy

**Correspondence:**

Raffaella Chiaramonte,  
Department of Health Sciences  
Università degli Studi di Milano  
via A. Di Rudinì, 8, Milan I-20142, Italy  
e-mail: [raffaella.chiaramonte@unimi.it](mailto:raffaella.chiaramonte@unimi.it)

**Acknowledgments**

This study was supported by grants from Associazione Italiana Ricerca sul Cancro, Investigator grant to RC (20614), My First Grant to AP (18714); Fondazione Italiana per la Ricerca sul Cancro to MC (post-doctoral fellowship 18013); Università degli Studi di Milano to RC (Linea 2B-2017 - Dept. Health Sciences), to NP (post-doctoral fellowship type A) and DG (PhD fellowship in Experimental Medicine).

**Conflict of interest statement**

The authors declare no conflicts of interest.

**Contributions**

*NOTCH2 in myeloma-derived extracellular vesicles*

DG, NP, MC: Experiment design and performance, acquisition of data, drafting the manuscript; MM, VC, RA, FM, SA, EL: experiment performance, acquisition of data; VD and IG: TEM morphologic analysis; MC, MM, AP: performance of in vivo zebrafish experiment; DG, LCan and VB: NTA analysis; MT, EC: collection of patients' sample and clinical information and patients' sample first processing; DG, MT, AB, LCas: Statistical analysis; DG, MT, AB, AP, EL, VB, LCas: manuscript revision; LCas: acquisition of data; RC, DG, AB, MT: interpretation of data; RC: Experiment design and supervision, interpretation of data and statistical analysis, drafting, writing and critical revision of the manuscript.

**Data sharing statement:** for any question, please contact the corresponding author.

**Keywords:** multiple myeloma, NOTCH, extracellular vesicles, osteoclastogenesis, angiogenesis.

**Word count**

Abstract: 248

Main text: 4109 words

*NOTCH2 in myeloma-derived extracellular vesicles***Abstract**

Multiple myeloma (MM) is an incurable hematologic neoplasm, whose poor prognosis is deeply affected by the propensity of tumor cells to localize in the bone marrow (BM) and induce the pro-tumorigenic activity of normal BM cells, leading to events associated with tumor progression, including tumor angiogenesis, osteoclastogenesis, and the spread of osteolytic bone lesions.

The interplay between MM cells and the BM niche does not rely only on direct cell-cell interaction, but a crucial role is also played by MM-derived extracellular vesicles (MM-EV). Here, we demonstrated that the oncogenic NOTCH receptors are part of MM-EV cargo and play a key role in EV pro-tumorigenic ability. We used *in vitro* and *in vivo* models to investigate the role of EV-derived NOTCH2 in stimulating the pro-tumorigenic behaviour of endothelial cells and osteoclast progenitors. Importantly, MM-EV can transfer NOTCH2 between distant cells and increase NOTCH signaling in target cells. MM-EV stimulation increases endothelial cell angiogenic ability and osteoclast differentiation in a NOTCH2 dependent way. Indeed, interfering with NOTCH2 expression in MM cells may decrease the amount of NOTCH2 also in MM-EV and affect their angiogenic and osteoclastogenic potential. Finally, we demonstrated that the pharmacologic blockage of NOTCH activation by  $\gamma$ -Secretase inhibitors may hamper the biological effect of EV derived by MM cell lines and by the BM of MM patients.

These results provide the first evidence that targeting the NOTCH pathway may be a valid therapeutic strategy to hamper the pro-tumorigenic role of EV in MM as well as other tumors.



*NOTCH2 in myeloma-derived extracellular vesicles***Introduction**

Multiple myeloma (MM) is a clonal plasma cell neoplasm representing alone 13% of all hematological malignancies [1]. Despite the development of new therapies, MM still remains incurable [2], mainly due to MM cell ability to shape the bone marrow (BM) niche sustaining tumor progression. Upon the localization in the BM, MM cells establish anomalous signaling loops with the neighboring cells and "educate" BM-residing non-tumor cells to support different steps of MM progression, including tumor cell growth, survival, angiogenesis, and bone osteolysis [3].

In this complex picture, extracellular vesicles (EV) are new key players recently come to light. EV include a heterogeneous group of cell-derived membranous structures classified into two main subtypes according to their origin. Exosomes, the smaller ones, originate from the endosomal system, while the larger vesicles are shed from the plasma cell membrane. Due to the difficulty to distinguish these subtypes based on their origin, a recent position statement of the International Society for Extracellular Vesicles has suggested a distinction based on their size: i.e. small EV < 200nm and large EV > 200nm [4].

EV are key mediators in the communication between tumor and stroma due to their ability to transport proteins and RNAs [5]. Circulating EV from MM patients display characteristic size distribution and concentration [6, 7], and their miRNA cargo is prognostic in MM [8-10]. Recent evidence indicates that MM cell-derived EV (MM-EV) modulate the BM niche, promoting angiogenesis, immunosuppression [11], and bone disease [12]. Additionally, several features of MM-EV may contribute to MM dissemination at distant sites, thereby favoring skeletal metastasis formation, progression and bone disease [13].

This work elucidates how MM cells exploit the aberrantly expressed NOTCH2 oncogene to shape the BM niche *via* MM-EV, specifically focusing on tumor angiogenesis and osteoclastogenesis.

NOTCH is a family of transmembrane receptors (NOTCH1-4) activated by the interaction with five different membrane-bound ligands (JAGGED1-2 and DLL1-3-4) present on the adjacent cells. The consequence of this interaction is the cleavage by  $\gamma$ -Secretase, which releases the active form of NOTCH (NOTCH-IC) from the cell membrane and allows its translocation to the nucleus and the activation of the CSL transcription factors [14].

NOTCH deregulation in MM cells is due to the aberrant expression of NOTCH receptors and/or ligands [15]. High levels of NOTCH pathway activity are associated with increased myeloma cell infiltration in BM biopsies of MM patients [16]. Other studies suggest that MM cell skeletal infiltration may be due to events promoted by NOTCH, including MM cell recruitment at the BM [17], mitogenic or anti-apoptotic effect [17-19], or MM stem cell self-renewal [20]. Additionally, MM infiltration of BM niche is also associated with the activation of NOTCH signaling in the tumor niche, which promotes angiogenesis [16, 21], osteoclastogenesis [22-24], and bone marrow stromal cell (BMSC) release of cytokines involved in these events (IL-6, VEGF, IGF-1, SDF-1, RANKL, etc.) [16, 18, 19, 25].

*NOTCH2 in myeloma-derived extracellular vesicles*

Up to now, the increased activation of NOTCH signaling in the tumor microenvironment has been attributed to the presence of high levels of MM cell-derived-JAGGED ligands. Here, we demonstrate that MM cells may trigger tumor angiogenesis and osteoclastogenesis by transferring NOTCH2 receptor *via* EV. Moreover, we provide evidence that targeting the NOTCH pathway may represent a suitable strategy to hamper the MM-EV mediated pathological communication with the BM niche.

**Methods****Extracellular vesicles isolation from HMCL and MM patients' BM aspirates**

EV were obtained from supernatants of RPMI8226 and OPM2 cells cultured for 48 h in RPMI1640 medium depleted of FBS-derived bovine EV or from the plasma obtained by BM aspirates of monoclonal gammopathy of undetermined significance (MGUS) (MGUS-BM-EV) and MM patients (MM-BM-EV). The Institutional Review Board of Insubria Italy approved the design of this study (approval n. 1 on 27<sup>th</sup> February 2018). Written informed consent was obtained in accordance with the Declaration of Helsinki. Clinical information of patients is reported in table S1.

EV pellets were resuspended in the appropriate buffer/medium for subsequent studies. Further details are reported in Supplemental experimental procedures.

**Production of viral supernatants and NOTCH2 knockdown**

Viral supernatants were generated by calcium phosphate-DNA transfection of HEK293T cells with the Dharmacon Trans-lentiviral packaging kit containing pTRIPZ vector carrying a doxycycline-inducible system (Tet-on) expressing shRNAs against NOTCH2, or the corresponding scrambled shRNA (Horizon Discovery, United Kingdom). A pilot experiment on HEK293T cells was carried out by transient transfection of 4 shRNAs for NOTCH2 to select the more effective NOTCH2 shRNA (Cat.ID RHS5087-EG4853 - mature antisense sequence: ATGTCACAAGAGACATTGG). Lentiviral supernatants were used to infect and generate stable clones of RPMI8226 and OPM2 cells. shRNA expression was induced by treatment with 1µg/ml Doxycycline (Sigma Aldrich, Italy).

***In vivo* experiments**

*In vivo* experiments were carried out on transgenic zebrafish (*Danio rerio*) embryos obtained by crossing *Tg(T2KTp1bglob:hmgb1-mCherry)* with *Tg(fli1a:EGFP)* obtained from the Wilson lab, University College London, United Kingdom. Zebrafish embryos were raised and maintained under standard conditions and national guidelines (Italian decree 4th March 2014, n.26). All experiments have been conducted within 5 days post fertilization (dpf). EV were injected into the duct of Cuvier of embryos at 48 h post fertilization (hpf) with a manual microinjector (Eppendorf, Germany) using glass microinjection needles.

*NOTCH2 in myeloma-derived extracellular vesicles*

Further details on the above procedures and information concerning cell cultures, transmission electron microscopy, *in vitro* uptake, western blot, EV-derived NOTCH2 tracking system, viral particle production, luciferase reporter assay, *in vivo* experiments, osteoclastogenesis and angiogenesis assays, *ex vivo* experiments and statistical analyses are reported in Supplemental experimental procedures.

## Results

### Multiple myeloma-derived extracellular vesicles are uptaken by bone marrow cell populations

EV produced by two different human MM cell lines (HMCL), RPMI8226 and OPM2, were isolated by ultracentrifugation and fully characterized. Particle size distribution assessed by nanoparticle tracking analysis (NTA) revealed that the EV populations produced by the two HMCL were characterized by the presence of both small (30-200 nm) and large (200-1000 nm) vesicles (Fig. 1A). The shape and integrity of MM-EV have been assessed by transmission electronic microscopy (TEM), showing the presence of whole, undamaged small and large EV (Fig. 1B).

We assessed the ability of MM-EV to transfer their content to two key BM cell populations crucial in supporting MM progression, osteoclasts (OCL) and endothelial cells (EC). The uptake was assessed in a quantitative (Fig. 2A and 2B) and qualitative way (Fig. 2C). EV isolated by a 48 h culture of RPMI8226 cells were stained with the fluorescent lipophilic dye CM-DIL and put in contact with a monolayer of OCL progenitors (Raw264.7 cells) and EC (primary human pulmonary arterial cells – HPAEC) for 4 h at 37°C. The negative control was maintained at 4°C to inhibit the uptake. In Fig.2A-B, MM-EV uptake was quantified through flow cytometry by measuring the CM-DIL fluorescent signal in receiving cells. The dot plot analysis clearly shows that the two different cell types uptake MM-EV with a similar efficiency. The graph in Fig.S1 summarizes the mean values and statistical analysis of flow cytometry detection. These results were confirmed by fluorescence microscopy analysis. Stack projection images (Fig. 2C) and z-stack videos (supplementary videos) show the presence of high levels of fluorescent signal in Raw264.7 (supplemental video 1) and HPAEC cells (supplemental video 2) treated with MM-EV at 37°C, indicating that MM-EV may be internalized by these cells. As expected, internalization is blocked when cells are kept at 4°C, suggesting that an active process is involved.

### Multiple myeloma-derived extracellular vesicles carry NOTCH2

Due to the important role of NOTCH in the interplay between MM and the BM microenvironment, we wondered if MM-EV contribute to NOTCH activation in BM cells by carrying NOTCH receptors and, in particular the overexpressed receptor NOTCH2 [26], as part of their cargo. By western blot analysis, we compared NOTCH2 expression in protein extracts from 7 HMCL, namely AMO1, JJN3, H929, RPMI8226, LP1, KMS12, OPM2, and EV isolated from conditioned media (CM). Fig. 3A shows that MM-EV are able to carry NOTCH2, those relative amount reflects that expressed in the different protein extracts of the HMCL.

*NOTCH2 in myeloma-derived extracellular vesicles*

The analysis of the different forms of NOTCH2 indicated that MM-EV could carry not only the transmembrane NOTCH2 (NOTCH2-TM) but also the full-length uncleaved NOTCH2 (NOTCH2-FL). Since the cleavage operated by  $\gamma$ -Secretase on the intracellular portion of NOTCH takes place inside the endocytic bodies [27] and exosomes arise from late endosomes [28], we investigated whether the active cleaved intracellular NOTCH2-IC may be included in MM-EV cargo by using a specific antibody. Results in Fig. 3A indicate that MM-EV cargo also carries NOTCH2-IC. Fig. S2 shows that also NOTCH1 is widely represented in MM-EV, while the presence of other two isoforms in MM-EV is less noticeable.

To assess which EV fraction expresses NOTCH2, we performed a western blot analysis on large and small vesicles collected from the HMCL CM by sequential ultracentrifugation at 20,000 g and 110,000 g (110 K). We found that NOTCH2-TM and NOTCH2-IC were present both in large and small vesicles (Fig.3B). Interestingly, NOTCH2-IC level was increased in 110K MM-EV fraction.

EV allow distant cells to communicate between each other, thus modifying their behaviour. To demonstrate that NOTCH2 may be involved in these processes and can be transferred to distant cells *via* EV, we developed a model system of HEK293 donor and receiving cells (Fig.3C). The first were forced to constitutively express NOTCH2 tagged with HA at the C-terminus (NOTCH2-HA) [29] to distinguish it from the endogenous NOTCH2. In addition, the position of the HA tag at the C-terminus of NOTCH2 enabled us to detect NOTCH2-FL, the NOTCH2-TM portion of the heterodimeric NOTCH2 form, matured in the trans-Golgi network upon the cleavage by a furin-like convertase [30], and the mature NOTCH2-IC, due to homotypic activation mediated by ADAM10 and the  $\gamma$ -secretase [29]. EV-donor cells were added to the culture medium of receiving HEK293 cells. Fig.3C shows a western blot analysis performed with an anti-HA antibody, confirming the presence of the HA-signal in donor cells carrying NOTCH2-HA, isolated EV, and receiving cells. This demonstrate that EV can transfer NOTCH2 between distant cells. In this model system, the EV cargo include NOTCH2-TM and NOTCH2-FL, while both donor and receiving cells show also the presence of NOTCH2-IC. The absence of NOTCH2-IC in HEK293-derived EV might be due to a lower level of NOTCH activation in HEK293 cells in comparison to HMCL.

**Multiple myeloma-derived extracellular vesicles activate NOTCH signaling in receiving cells**

To address if the variation of NOTCH2 levels in MM cells may affect MM-EV mediated communication, we studied the effect of NOTCH2 silencing in RPMI8226 and OPM2 cells. These cells were transduced with the pTRIPZ lentiviral vector conditionally expressing shRNAs for NOTCH2 (HMCL<sup>N2KD</sup>) or the scrambled sequence (HMCL<sup>SCR</sup>) and single cell clones were isolated. Fig. 4A confirms that RPMI8226 and OPM2 cells are knocked down (KD) for NOTCH2 and clearly shows that also the produced MM-EV displayed a reduced level of NOTCH2. Also NOTCH2-IC decreased in OPM2 cells with a corresponding decrease in the shed EV, while NOTCH2-IC decrease in EV release from RPMI8226 was less evident (Fig.S4). Through alignment search tool BlastN (USA National Center for Biotechnology Information) we excluded regions of local similarities between the used shRNA and the sequences of other NOTCH receptors and ligands (E

*NOTCH2 in myeloma-derived extracellular vesicles*

values range between 1 and 15). The high sequence homology between the four NOTCH receptors prompted us to analyze by western blot the expression of the other NOTCH receptor isoforms. Fig. 5S shows that NOTCH2 KD did not affect the expression of NOTCH1, 3 and 4 in protein extracts from cells and MM-EV. The outcome of NOTCH2 KD on EV size and concentration evaluated by NTA showed no significant effect on MM-EV size and concentration (Fig. 4B).

To assess if the NOTCH2 protein carried by MM-EV is functionally active and is able to trigger NOTCH signaling in receiving cells, we tested the effect of EV isolated from HMCL<sup>N2KD</sup> (MM-EV<sup>N2KD</sup>) or HMCL<sup>SCR</sup> (MM-EV<sup>SCR</sup>) through a NOTCH responsive luciferase reporter assay. This assay was carried out in the HeLa cell line, which is highly transfectable and characterized by a low level of NOTCH signaling activation (not shown). Fig. 4C shows that MM-EV<sup>SCR</sup> can activate the NOTCH signaling pathway in the receiving HeLa cells, while this ability is significantly reduced for MM-EV<sup>N2KD</sup>.

The ability of MM-EV to activate NOTCH signaling was also validated in an *in vivo* NOTCH reporter zebrafish embryo obtained by crossing *Tg(T2KTp1bglob:hmgbl-mCherry)* with *Tg(fli1a:EGFP)* that carry EGFP+ endothelial cells (green) and express the mCherry protein (red) under the control of a NOTCH-responsive element. EV isolated from RPMI8226 cells were injected in the duct of Cuvier of 48 hpf transgenic zebrafish embryos. Images were acquired 4 h post-injection. Fig. 4D shows MM-EV<sup>SCR</sup> mediated NOTCH activation in the intersegmental vessels (Se), caudal artery (CA), and in the area of the caudal hematopoietic tissue (CHT), while MM-EV<sup>N2KD</sup> induces a barely visible stimulation.

### **NOTCH2 carried by multiple myeloma-derived extracellular vesicles contributes to the education of bone marrow cell populations**

We and other groups previously reported that MM cells affect the surrounding BM microenvironment inducing osteoclastogenesis [22-24] and tumor angiogenesis [16, 21] in a NOTCH-dependent way. Moreover, recent evidence indicates that MM-EV stimulate osteoclastogenesis [13, 31-33], angiogenesis and carry pro-angiogenic proteins [11, 34]. Therefore, we verified the osteoclastogenic potential of MM-EV<sup>SCR</sup> and MM-EV<sup>N2KD</sup> by treating the monocyte cell line Raw264.7 in the presence of the osteoclastogenic chemokine RANKL (30 ng/ml). We used MM-EV released by the RPMI8226 cell line due to the ability of these cells to induce osteoclastogenesis, differently from OPM2 cells [22]. After 7 days of treatment with MM-EV, OCL count showed that MM-EV<sup>SCR</sup> induced Raw264.7 cell differentiation, while MM-EV<sup>N2KD</sup> lost this ability (Fig. 5A).

We assessed MM-EV<sup>N2KD</sup> angiogenic potential using a tube formation assay with HPAEC seeded on a Matrigel layer. Results in Fig.5B show that MM-EV<sup>SCR</sup> promotes tube organization of HPAEC, while treatment with MM-EV<sup>N2KD</sup> reduces this effect. In conclusion, this specific RNA interference approach unequivocally demonstrated that NOTCH2 KD affects the MM-EV mediated osteoclastogenesis and angiogenesis.

*NOTCH2 in myeloma-derived extracellular vesicles***Targeting NOTCH signaling blocks the pathological communication mediated by multiple myeloma-derived extracellular vesicles**

To provide a higher translational potential to our findings we exploited the strategy illustrated in Fig.6A. We used  $\gamma$ -secretase inhibitors (50  $\mu\text{g/ml}$  DAPT), used in research works and clinics to inhibit pan-Notch signaling [15] to block NOTCH activation in EC and OCL induced by MM-EV. Fig.6B and C clearly show that MM-EV induce angiogenesis and osteoclastogenesis in a NOTCH-dependent way. In consideration of the well known osteoclastogenic and angiogenic roles of NOTCH signaling [16, 21-24], we planned our experiments to distinguish the effect of the endogenous and vesicular NOTCH. Indeed, if we compare the effect of DAPT on osteoclastogenesis (fig.6B) in the absence of EV and suboptimal concentration of RANKL, we can see that it abrogates OCL differentiation with a non-statistically significant decrease, while DAPT abrogates much higher levels of osteoclastogenesis induced by MM-EV (+250%) in a statistically significant way, indicating that the greater effect of MM-EV is NOTCH dependent.

The effect of DAPT on MM-EV induced angiogenesis was analogous. The high increase of HPAEC tube organization upon the administration of MM-EV from RPMI8226 and OPM2 cells was completely abrogated by DAPT, showing a statistically significant reduction in areas and nodes (ranging from 29,5% to 51,3%). This effect was clearly higher than the slight inhibitory trend observed on basal angiogenesis upon DAPT administration (Fig. 6C). We also ruled out that the obtained results could be due to the toxic effect of DAPT on OCL and EC (Fig. S6).

Overall, these results confirm that the studied biological effects of EV are NOTCH mediated and can be blocked by treatment with  $\gamma$ -Secretase inhibitors.

Finally, to strengthen the translational potential of our *in vitro* findings, we reasoned that the BM of MM patients does not contain only MM-derived EV, but EV derived from the whole MM-educated BM cell populations. Therefore to confirm the NOTCH-dependent role of EV in the pathological communication occurring in the BM of MM patients, we have got advantage of EV from BM aspirates of patients with the benign MGUS (MGUS-BM-EV) or MM (MM-BM-EV) (Table S1), which may recapitulate the complexity of the BM microenvironment. We compared the angiogenic potential of HPAEC untreated or treated with MGUS-BM-EV or MM-BM-EV. Fig. 6D shows that MM-BM-EV boost the angiogenic potential of HPAEC while MGUS-BM-EV showed a non-statistically significant increasing trend. Importantly, the inhibitory effect of DAPT is statistically significant when added to HPAEC treated with MM-BM-EV. These results confirm the increasing angiogenic potential of EV released in the BM during MM progression, the role played by NOTCH delivered via MM-BM-EV and strengthen the potential of a NOTCH-directed therapeutic approach to block the support of MM microenvironment to the disease progression.

**Discussion**

*NOTCH2 in myeloma-derived extracellular vesicles*

The pathological interplay between malignant cells and the surrounding non-tumoral BM cells promotes neoplastic cell growth and survival as well as key events of tumor progression including bone disease and angiogenesis. These lines of evidence suggest that an effective therapeutic approach should not be focused merely on the MM cells, but it should target their interaction with the surrounding BM niche.

Recently, EV have been reported as critical players in the communication between MM cells and the nearby BM cells and leading to MM progression. Indeed, MM-EV promote different events associated with MM progression, including angiogenesis [11, 13, 34, 35] and osteoclastogenesis [13, 31-33].

Here, we contribute to elucidate the molecular mechanisms involved in MM-EV pathological communication with the BM microenvironment, strengthening the role of the EV pathological communication as a promising therapeutic target in MM.

The evidence that NOTCH signaling activation, mediated by MM cell heterotypic interaction with the surrounding BM cells, plays a key role in tumor angiogenesis [16, 21] and osteoclastogenesis [22-24] prompted us to investigate whether NOTCH signaling contributes to determine the impact of MM-EV on these processes.

Our analysis on a panel of HMCL and the respective shed EV indicate that NOTCH receptors were present in MM-EV cargo with high levels of NOTCH2 and slightly lower levels of NOTCH1, consistently with evidence from other cell types [36]. We focused on NOTCH2 receptor, widely expressed in MM cell lines and in primary MM cells, particularly from high-risk patients [18, 26]. In details, we found that MM-EV carried the mature heterodimeric form of NOTCH2 (since we detected the NOTCH2-TM portion), the immature NOTCH2-FL and the activated NOTCH2-IC, that upon delivering to target cells might directly activate the transcription of the NOTCH target genes without requiring the interaction with ligands and the activation by ADAM protease and  $\gamma$ -Secretase.

The expression of NOTCH receptors has been reported in exosomes [37] but also in microvesicles [38]. Thereby, we wondered which of the two subpopulations of EV hosted NOTCH2. We separated large and small vesicles and found the presence of NOTCH2-TM both in large and small particles, while NOTCH2-IC level was higher in 110K small EV fraction. Although it is not possible to distinguish exosome and microvesicles only on the basis of their dimension, we presume that small vesicles are enriched with exosomes respect to large vesicles. Therefore our results suggest the presence of NOTCH2-IC within exosomes consistently with its presence in the endosomal compartment from which exosomes take origin.

Before validating the hypothesis that vesicular NOTCH2 contributes to molecular and biological effects on relevant BM cell population as OCL and EC, we monitored if these cells uptake MM-EV, using respectively Raw264.7 and HPAEC cells. Flow cytometry detection showed a quick (4 h) uptake of MM-EV by the majority of cells in both models, confirmed by a Z-stack analysis in confocal microscopy.

Additionally, we unequivocally assessed that NOTCH signaling members could be transferred via EV from one cell to another using an experimental system model based on HEK293 cells forced to express NOTCH2 tagged with HA. This model system allowed us to assess that NOTCH2-HA could be released

*NOTCH2 in myeloma-derived extracellular vesicles*

within EV and be transferred to distant cells. In this system, we have confirmed that EV carried high levels of NOTCH2-TM form and NOTCH2-FL, even if at much lower level. On the contrary, although the NOTCH2-IC form was present in MM-EV shed by HMCL, we could not detect it in HEK293-derived EV, possibly due to a lower level of NOTCH2 activation in HEK293 cells in comparison to HMCL. Receiving cells clearly uptook the transmembrane form of NOTCH2-HA, but also showed a very faint band corresponding to NOTCH2-IC, consistently with a slight NOTCH2 activation after EV uptake. This result provided a first indication that EV carrying NOTCH2 may activate NOTCH signaling in receiving cells.

Using a selective RNA interference of NOTCH2 in RPMI8226 and OPM2 cells, we confirmed that NOTCH2 KD in HMCL impacted the levels of vesicular NOTCH2-TM, NOTCH2-FL and NOTCH2-IC, although the decrease of the activated form was evident only in OPM2 cells. On the contrary, NOTCH2 KD did not significantly affect MM-EV size and concentration.

To confirm that MM-EV might activate the oncogenic NOTCH signaling in receiving cells, we tested MM-EV<sup>SCR</sup> or MM-EV<sup>N2KD</sup> in *in vitro* and *in vivo* NOTCH reporter systems. The first *in vitro* cellular model transfected with a Nanoluc-based NOTCH reporter vector, indicated that MM-EV<sup>SCR</sup> might activate a NOTCH-dependent gene reporter, while MM-EV<sup>N2KD</sup> induced a significantly lower activation. This result was confirmed by a second reporter *in vivo* system recapitulating the complexity of a whole organism. The injection of MM-EV<sup>SCR</sup> or MM-EV<sup>N2KD</sup> in transgenic zebrafish embryo reporter for NOTCH not only confirmed the observed MM-EV mediated NOTCH signaling activation but also provided evidence of MM-EV ability to induce NOTCH signaling activation at distant sites through the circulation. Indeed, MM-EV injected in the duct of Cuvier may be transported through the circulation and activate NOTCH signaling in the caudal hematopoietic tissue which represents the main hematopoietic organ in zebrafish embryo, analogously to the human BM [39]. In contrast, NOTCH signaling activation mediated by MM-EV<sup>N2KD</sup> was significantly lower. MM-EV effectiveness in inducing NOTCH signaling activation at distant sites in zebrafish embryos carried by the blood stream suggests that MM-EV could also play an important role in the metastatic process, as reported for pancreatic cancer [40]. For instance they may help preparing the pre-metastatic niche through the formation of new permeable vessels for the extravasation of tumor cells, and destructing of the bone matrix to make space for metastatic cells.

Taken as a whole, the *in vitro* and *in vivo* NOTCH reporter assays confirmed that NOTCH activity in target cells was due to NOTCH2 delivered by the injected MM-EV.

This evidence and the acknowledged effect of NOTCH signaling on OCL and EC, prompted us to verify if NOTCH2 delivery by MM-EV could affect the biology of these cells. Through the same specific RNA interference approach on two different HMCL, we provided an unequivocal demonstration that vesicular NOTCH2 participates in MM-induced OCL differentiation and angiogenesis, assessed by a tube-formation assay. The dependency of these processes on NOTCH signaling was clearly demonstrated by the fact that MM-EV<sup>N2KD</sup> impact was significantly lower. The presence of other NOTCH receptors in MM-EV cargo, even if at a lower level, (i.e. NOTCH1) suggests that they may also provide a contribution.



*NOTCH2 in myeloma-derived extracellular vesicles*

In order to strengthen the translational potential of our results we used a dual approach: 1) the outcome of an anti-NOTCH therapeutic approach already tested in clinics was assessed *in vitro* and *ex vivo*; 2) *ex vivo* experiments were carried out with EV released in the BM of MM patients, taking into account that a systemic treatment is expected to affect the communication of MM-EV, as well as that of EV from all the BM cell populations. In the first case, we showed that  $\gamma$ -Secretase inhibitors (GSI), already used in clinics [15], greatly affected MM-EV ability to inhibit angiogenesis and osteoclastogenesis *in vitro*. Concerning the second point, EV collected from the BM of MM patients, but not MGUS patients, displayed a clear pro-angiogenic effect that could be hampered by GSI.

In conclusion, the RNA interfering approach specific for NOTCH2 on HMCL, complemented by a pan-NOTCH chemical inhibition on HMCL- and MM patients' BM-derived EV, provides a new important evidence of the effect of NOTCH signaling pathway on EV mediated pathological communication in myelomatous BM. The important inhibitory effect of GSI suggests that the form of the NOTCH2 oncogene which mostly contributes to MM-EV mediated education is NOTCH2-TM and not NOTCH-IC whose activity is GSI resistant. Although, the presence of NOTCH2-IC in MM-EV cargo is much intriguing since it may deliver an active oncogenic signal, we believe that vesicular NOTCH-IC might be more relevant in tumor that expresses the constitutively active form of NOTCH, such as T-cell acute lymphoblastic leukemia.

In conclusion, our results strengthen the rationale for therapeutic approaches directed to inhibit NOTCH activation mediated by MM-EV, suggesting that they have the potential of interfering with the pathological communication of the MM cells mediated by EV in the short and potentially in the long range and, thereby, they may influence the cross-talk with the surrounding microenvironment and the dissemination of the disease at distant skeletal sites.

***Supplementary Information is available at Haematologica website.***

*NOTCH2 in myeloma-derived extracellular vesicles***References**

1. Kyle RA, Rajkumar SV. Multiple myeloma. *Blood*. 2008;111(6):2962-72.
2. Cowan AJ, Allen C, Barac A, et al. Global Burden of Multiple Myeloma: A Systematic Analysis for the Global Burden of Disease Study 2016. *JAMA Oncol*. 2018;4(9):1221-1227.
3. Manier S, Sacco A, Leleu X, Ghobrial IM, Roccaro AM. Bone marrow microenvironment in multiple myeloma progression. *J Biomed Biotechnol*. 2012;2012:157496.
4. Thery C, Witwer KW, Aikawa E, et al. Minimal information for studies of extracellular vesicles 2018 (MISEV2018): a position statement of the International Society for Extracellular Vesicles and update of the MISEV2014 guidelines. *J Extracell Vesicles*. 2018;7(1):1535750.
5. Webber J, Yeung V, Clayton A. Extracellular vesicles as modulators of the cancer microenvironment. *Semin Cell Dev Biol*. 2015;40:27-34.
6. Caivano A, Laurenzana I, De Luca L, et al. High serum levels of extracellular vesicles expressing malignancy-related markers are released in patients with various types of hematological neoplastic disorders. *Tumour Biol*. 2015;36(12):9739-52.
7. Krishnan SR, Luk F, Brown RD, et al. Isolation of Human CD138(+) Microparticles from the Plasma of Patients with Multiple Myeloma. *Neoplasia*. 2016;18(1):25-32.
8. Manier S, Liu CJ, Avet-Loiseau H, et al. Prognostic role of circulating exosomal miRNAs in multiple myeloma. *Blood*. 2017;129(17):2429-2436.
9. Caivano A, La Rocca F, Simeon V, et al. MicroRNA-155 in serum-derived extracellular vesicles as a potential biomarker for hematologic malignancies - a short report. *Cell Oncol (Dordr)*. 2017;40(1):97-103.
10. Rajeev Krishnan S, De Rubis G, Suen H, et al. A liquid biopsy to detect multidrug resistance and disease burden in multiple myeloma. *Blood Cancer J*. 2020;10(3):37.
11. Wang J, De Veirman K, Faict S, et al. Multiple myeloma exosomes establish a favourable bone marrow microenvironment with enhanced angiogenesis and immunosuppression. *J Pathol*. 2016;239(2):162-73.
12. Zhang L, Lei Q, Wang H, et al. Tumor-derived extracellular vesicles inhibit osteogenesis and exacerbate myeloma bone disease. *Theranostics*. 2019;9(1):196-209.
13. Colombo M, Giannandrea D, Lesma E, Basile A, Chiaramonte R. Extracellular Vesicles Enhance Multiple Myeloma Metastatic Dissemination. *Int J Mol Sci*. 2019;20(13).
14. Colombo M, Mirandola L, Platonova N, et al. Notch-directed microenvironment reprogramming in myeloma: a single path to multiple outcomes. *Leukemia*. 2013;27(5):1009-18.
15. Colombo M, Galletti S, Garavelli S, et al. Notch signaling deregulation in multiple myeloma: A rational molecular target. *Oncotarget*. 2015;6(29):26826-40.

*NOTCH2 in myeloma-derived extracellular vesicles*

16. Palano MT, Giannandrea D, Platonova N, et al. Jagged Ligands Enhance the Pro-Angiogenic Activity of Multiple Myeloma Cells. *Cancers (Basel)*. 2020;12(9).
17. Mirandola L, Apicella L, Colombo M, et al. Anti-Notch treatment prevents multiple myeloma cells localization to the bone marrow via the chemokine system CXCR4/SDF-1. *Leukemia*. 2013;27(7):1558-66.
18. Colombo M, Galletti S, Bulfamante G, et al. Multiple myeloma-derived Jagged ligands increases autocrine and paracrine interleukin-6 expression in bone marrow niche. *Oncotarget*. 2016;7(35):56013-56029.
19. Colombo M, Garavelli S, Mazzola M, et al. Multiple myeloma exploits Jagged1 and Jagged2 to promote intrinsic and bone marrow-dependent drug resistance. *Haematologica*. 2020;105(7):1925-1936.
20. Chiron D, Maiga S, Descamps G, et al. Critical role of the NOTCH ligand JAG2 in self-renewal of myeloma cells. *Blood Cells Mol Dis*. 2012;48(4):247-53.
21. Saltarella I, Frassanito MA, Lamanuzzi A, et al. Homotypic and Heterotypic Activation of the Notch Pathway in Multiple Myeloma-Enhanced Angiogenesis: A Novel Therapeutic Target? *Neoplasia*. 2019;21(1):93-105.
22. Colombo M, Thummler K, Mirandola L, et al. Notch signaling drives multiple myeloma induced osteoclastogenesis. *Oncotarget*. 2014;5(21):10393-406.
23. Schwarzer R, Kaiser M, Acikgoez O, et al. Notch inhibition blocks multiple myeloma cell-induced osteoclast activation. *Leukemia*. 2008;22(12):2273-7.
24. Schwarzer R, Nickel N, Godau J, et al. Notch pathway inhibition controls myeloma bone disease in the murine MOPC315.BM model. *Blood Cancer J*. 2014;4:e217.
25. Houde C, Li Y, Song L, et al. Overexpression of the NOTCH ligand JAG2 in malignant plasma cells from multiple myeloma patients and cell lines. *Blood*. 2004;104(12):3697-704.
26. van Stralen E, van de Wetering M, Agnelli L, et al. Identification of primary MAFB target genes in multiple myeloma. *Exp Hematol*. 2009;37(1):78-86.
27. Chastagner P, Brou C. Tracking trafficking of Notch and its ligands in mammalian cells. *Methods Mol Biol*. 2014;1187:87-100.
28. Rajagopal C, Harikumar KB. The Origin and Functions of Exosomes in Cancer. *Front Oncol*. 2018;8:66.
29. Groot AJ, Habets R, Yahyanejad S, et al. Regulated proteolysis of NOTCH2 and NOTCH3 receptors by ADAM10 and presenilins. *Molecular and cellular biology*. 2014;34(15):2822-2832.
30. Blaumueller CM, Qi H, Zagouras P, Artavanis-Tsakonas S. Intracellular cleavage of Notch leads to a heterodimeric receptor on the plasma membrane. *Cell*. 1997;90(2):281-91.
31. Raimondi L, De Luca A. Multiple Myeloma-Derived Extracellular Vesicles Induce Osteoclastogenesis through the Activation of the XBP1/IRE1 $\alpha$  Axis. 2020;12(8).

*NOTCH2 in myeloma-derived extracellular vesicles*

32. Raimondo S, Saieva L, Vicario E, et al. Multiple myeloma-derived exosomes are enriched of amphiregulin (AREG) and activate the epidermal growth factor pathway in the bone microenvironment leading to osteoclastogenesis. *J Hematol Oncol*. 2019;12(1):2.
33. Faict S, Muller J, De Veirman K, et al. Exosomes play a role in multiple myeloma bone disease and tumor development by targeting osteoclasts and osteoblasts. *Blood Cancer J*. 2018;8(11):105.
34. Umezu T, Tadokoro H, Azuma K, et al. Exosomal miR-135b shed from hypoxic multiple myeloma cells enhances angiogenesis by targeting factor-inhibiting HIF-1. *Blood*. 2014;124(25):3748-57.
35. Liu Y, Zhu XJ, Zeng C, et al. Microvesicles secreted from human multiple myeloma cells promote angiogenesis. *Acta Pharmacol Sin*. 2014;35(2):230-8.
36. Wang Q, Lu Q. Plasma membrane-derived extracellular microvesicles mediate non-canonical intercellular NOTCH signaling. *Nat Commun*. 2017;8(1):709.
37. Patel B, Patel J, Cho JH, et al. Exosomes mediate the acquisition of the disease phenotypes by cells with normal genome in tuberous sclerosis complex. *Oncogene*. 2016;35(23):3027-36.
38. Suwakulsiri W, Rai A, Xu R, et al. Proteomic profiling reveals key cancer progression modulators in shed microvesicles released from isogenic human primary and metastatic colorectal cancer cell lines. *Biochim Biophys Acta Proteins Proteom*. 2019;1867(12):140171.
39. Sacco A, Roccaro AM, Ma D, et al. Cancer Cell Dissemination and Homing to the Bone Marrow in a Zebrafish Model. *Cancer Res*. 2016;76(2):463-71.
40. Ogawa K, Lin Q, Li L, et al. Prometastatic secretome trafficking via exosomes initiates pancreatic cancer pulmonary metastasis. *Cancer Lett*. 2020;481:63-75.

**Figure legends**

**Fig. 1: Characterization of MM cell-released EV.** Extracellular vesicles (EV) from multiple myeloma cell lines (HMCL) RPMI8226 and OPM2 cells (MM-EV), were isolated by ultracentrifugation and analyzed by **A)** nanotracking particle analysis (NTA) and **B)** electron transmission microscopy (TEM). **A)** NTA analysis reveals the presence of small (30-200 nm) and large (200-1000 nm) vesicles. Size and concentration of EV were determined by NanoSight NS300 system (Malvern Panalytical Ltd, Malvern, UK). A camera level of 12 and five 30-s recordings were used for acquisition of each sample of 3 independent EV isolations and one representative image is shown. **B)** TEM analysis confirms the isolation of intact small and large vesicles.

**Fig.2: MM-EV can be uptaken by osteoclasts and endothelial cells. A-C)** Osteoclast (OCL) progenitors and endothelial cell (EC) uptake MM-EV from RPMI8226 cells. Raw264.7 cells and HPAEC have been treated with CM-DIL stained MM-EV or the negative control for 4 h at 37°C or 4°C. **A-B)** Representative flow cytometry dot-plots show the CM-DIL labeled RPMI8226-EV uptake by Raw264.7 cells (A) and

*NOTCH2 in myeloma-derived extracellular vesicles*

HPAEC (B) by measuring CM-DIL positive cells in the PE channel. OPM2-EV provided similar results (not shown). Data are presented as mean values of three independent experiments **C**) Maximum intensity projection of CM-DIL positive RPMI8226-EV internalization in Raw264.7 cells and HPAEC after 4 h of incubation at 37°C and 4°C. Red fluorescence: RPMI8226-EV labeled with CM-DIL dye; green fluorescence: CFSE-labeled cells; blue fluorescence: nuclei with DAPI (63x magnification).

**Fig.3: NOTCH receptors and ligands in EV.** **A)** Western blot analysis for NOTCH2-FL (full length), NOTCH2-TM (transmembrane form), and NOTCH2-IC (active intracellular NOTCH2) expressed in 7 different HMCL and the respective produced EV.  $\beta$ -Actin and TSG101 have been used as loading controls for cells and vesicle protein extracts, respectively. To perform all the hybridizations, two western blots have been performed with cell and EV extracts loaded with the identical amount of proteins. **B)** A western blot analysis show the expression of NOTCH2-TM and NOTCH2-IC in EV populations of different sizes. Large and small EV have been isolated from RPMI8226 and OPM2 cells by sequential ultracentrifugation at 20,000 g (20K) and 110,000 g (110K), and the expression of the two NOTCH2 forms was separately assessed by western blot analyses using specific antibodies for NOTCH2 and NOTCH2-IC; TSG101 was used as controls for vesicle protein extracts. **C)** EV-mediated cell-to-cell transfer of NOTCH2: the donor HEK293 cell line was forced to express HA-tagged NOTCH2 carried by pCDNA3.1 or the corresponding empty vector (negative control); EV secreted by donor cells were collected by ultracentrifugation and used to treat receiving HEK293 cells for 24 h. Cell and EV protein extracts were analyzed by western blot using a specific primary antibody anti-HA.  $\alpha$ -Tubulin and TSG101 were used to normalize cellular and vesicular protein extract loading, respectively. NOTCH2-IC identified by re-hybridization of the same membrane with anti-NOTCH-IC (see Fig.S3) is indicated by an asterisk.

**Fig.4: Molecular effects of NOTCH2 modulation on MM-EV.** **A)** Western blot analysis confirms the KD efficacy on NOTCH2-TM levels in HMCL and the produced MM-EV.  $\alpha$ -Tubulin and TSG101 have been used as loading controls for cell and vesicle protein extracts, respectively. **B)** NTA on MM-EV<sup>SCR</sup> and MM-EV<sup>N2KD</sup> from HMCL does not show significant changes in concentration and size; D50=size point below which 50% of the EV are contained. Data are expressed as mean value  $\pm$  SEM of at least four experiments (RPMI8226 n=4; OPM2 n=6). Statistics by two-tail T-test did not show any significant difference. **C)** MM-derived EV activate NOTCH signaling in receiving cells: a NOTCH reporter assay was carried out on HeLa cells stimulated with MM-EV<sup>SCR</sup> and MM-EV<sup>N2KD</sup> from HMCL (EV derived from OPM2 cells), or control fresh medium (w/o EV). Luciferase activity is expressed as the ratio between Nano/Firefly luciferase luminescence units. Data are expressed as mean value  $\pm$  SE of at 4 experiments. Statistics by ANOVA and Tukey post-test: \* $p$ <0.05. **D)** Activation of NOTCH signaling in the trunk of *Tg(T2KTp1bglob:hmgb1-mCherry)* zebrafish embryos (zf) 4 h after the injection of MM-EV<sup>SCR</sup> and MM-EV<sup>N2KD</sup> (EV derived from RPMI8226 cells), or control fresh medium (w/o EV). Representative pictures of each condition are reported

*NOTCH2 in myeloma-derived extracellular vesicles*

on the left (20x and 60x magnification, the upper and the lower respectively); a graph on the right represents the mean value  $\pm$  SEM of the corrected total fluorescence (CTF) measured in caudal hematopoietic tissue (CHT). In particular four *in vivo* experiments involved zf embryos injected with negative control (n=20) or MM-EV<sup>SCR</sup> (n=27) and MM-EV<sup>N2KD</sup> (n=27). Statistics by ANOVA and Tukey post-test excluding outliers identified through the ROUT method (Q=1%): \* $p$ <0.05; \*\*\*\*= $p$ <0.0001.

**Fig.5: NOTCH2 contributes to the protumorigenic communication of MM-EV toward osteoclasts and endothelial cells. A)** The effect of MM-EV<sup>SCR</sup> and MM-EV<sup>N2KD</sup> collected from the osteoclastogenic cell line RPMI8226. The Raw264.7 cell line was treated with or without the osteoclastogenic RANKL (30 ng/ml), MM-EV or control fresh medium (w/o EV). After 7 days TRAP positive multinucleated cells ( $\geq 3$  nuclei) were enumerated (TRAP positive multinucleated cells were indicated by an arrow). Representative images are shown for each condition on the left (4x magnification); a graph on the right represents the mean value of the absolute number of TRAP+ multinucleated cells  $\pm$  SEM. Statistical analysis by a one-way ANOVA with Tukey post-test; \* $p$  < 0.05. **B)** Tumor angiogenesis induced by MM-EV<sup>SCR</sup> and MM-EV<sup>N2KD</sup>. Tube formation assay performed for 13h with HPAEC laid on a matrigel-coated support stimulated with MM-EV<sup>SCR</sup> and MM-EV<sup>N2KD</sup> collected from RPMI8226 and OPM2 cells or control fresh medium (w/o EV). The graphs show the mean values of areas and nodes (branch points) enumerated in four quadrant of the well  $\pm$  SEM. Statistical analysis was performed by ANOVA and Tukey post-test; \* $p$  <0.05, \*\*= $p$  <0.01. Representative images are shown below for each condition (4x magnification).

**Fig.6:  $\gamma$ -Secretase blockage of NOTCH2 activation inhibits the effect of MM-EV on osteoclastogenesis and angiogenesis. A)** Experimental rationale. MM-EV derived NOTCH2 may increase NOTCH signaling activation on target cells (OCL progenitors and EC) that may be blocked by DAPT administration. **B)** Raw267.4 cells induced to differentiate into OCLs in the presence of 30 ng/ml RANKL were treated with MM-EV collected from the osteoclastogenic cell line RPMI8226 or the control fresh medium (w/o EV) and in the presence or absence of DAPT to inhibit NOTCH signaling activation. For each condition a negative control cultured in the absence of RANKL has been carried out. After 7 days TRAP+ multinucleated cells ( $\geq 3$  nuclei) were enumerated. The graph shows the mean values of TRAP+ multinucleated cells obtained in the different conditions for RANKL treated cells. Given the large number of conditions, to make the graph simpler and easier to understand, each value has been subtracted of the respective control without RANKL ( $\pm$  SEM). Statistical analysis was performed by a one-way ANOVA with Tukey post-test; \* $p$  < 0.05; \*\*\*= $p$  < 0.001. **C)** Tube formation assay on HPAEC was performed for 13 h with MM-EV collected from RPMI8226 and OPM2 cells or control fresh medium (w/o EV) in the presence or the absence of DAPT. The graphs show the mean values of areas and nodes enumerated in four quadrant of the well  $\pm$  SEM. Statistical analysis was performed by ANOVA and Tukey post-test; \* $p$  <0.05, \*\*= $p$  <0.01. **D)** Tube formation assay on HPAEC treated for 13 h with EV collected from the BM of MGUS patients or MM patients in the presence or the absence of DAPT. The graphs show the mean values of

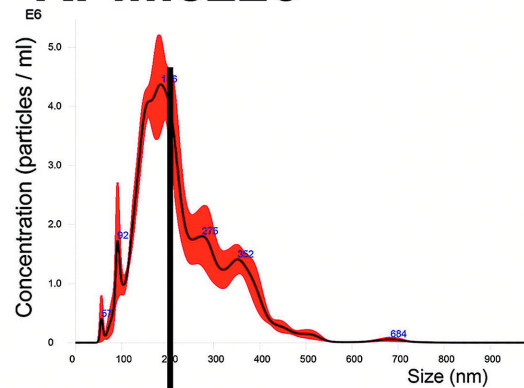
*NOTCH2 in myeloma-derived extracellular vesicles*

areas and nodes enumerated in four quadrant of the well (+/- SEM). Statistical analysis was performed by ANOVA and Tukey post-test; \*\*=  $p < 0.01$ , \*\*\*\*=  $p < 0.001$ . The characteristics and number of MM patients are reported in table S1.

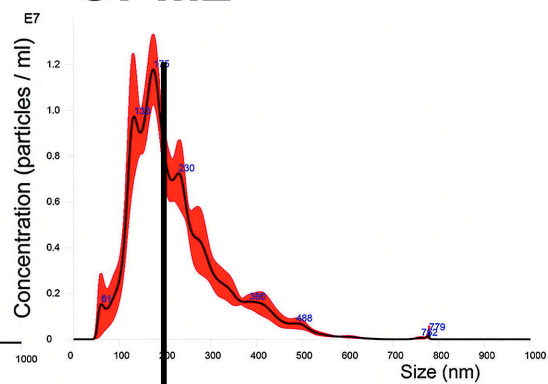
Fig.1

**A**

**RPMI8226**

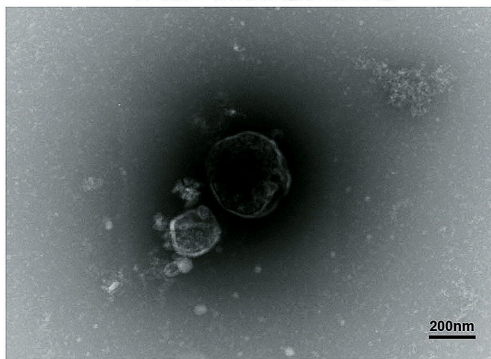


**OPM2**



**B**

**RPMI8226**



**OPM2**

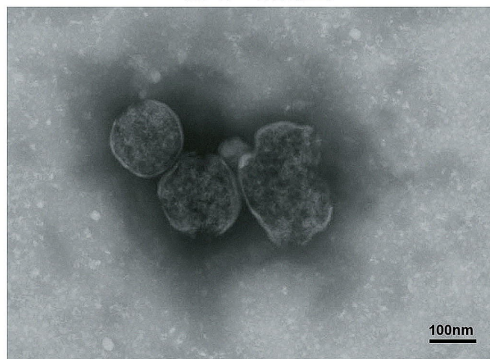
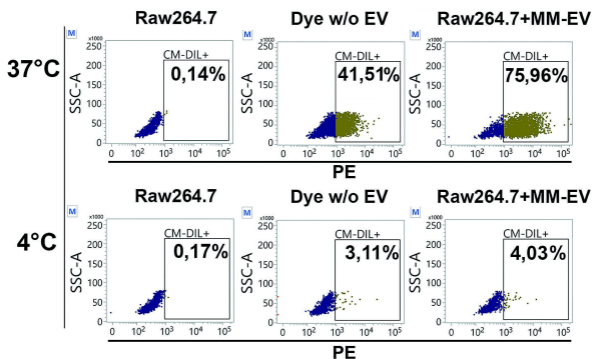




Fig.2

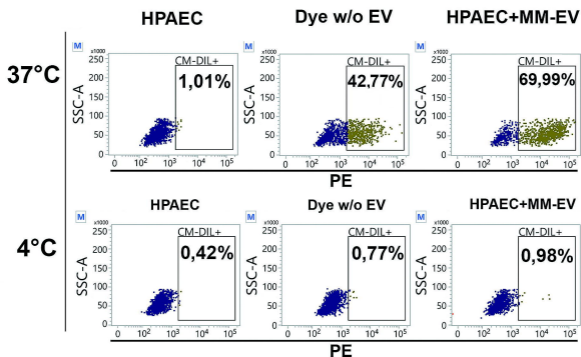
**A**

**Raw264.7**



**B**

**HPAEC**



**C**

**Raw264.7**

**HPAEC**

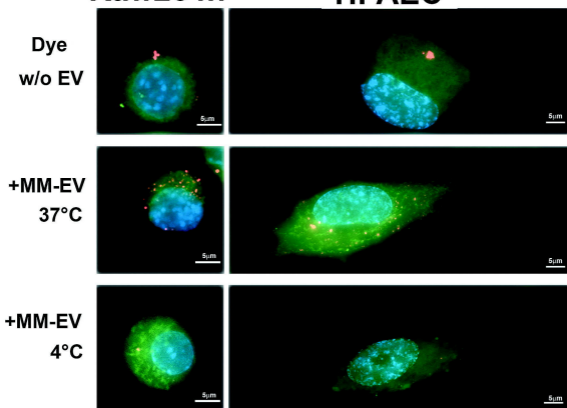
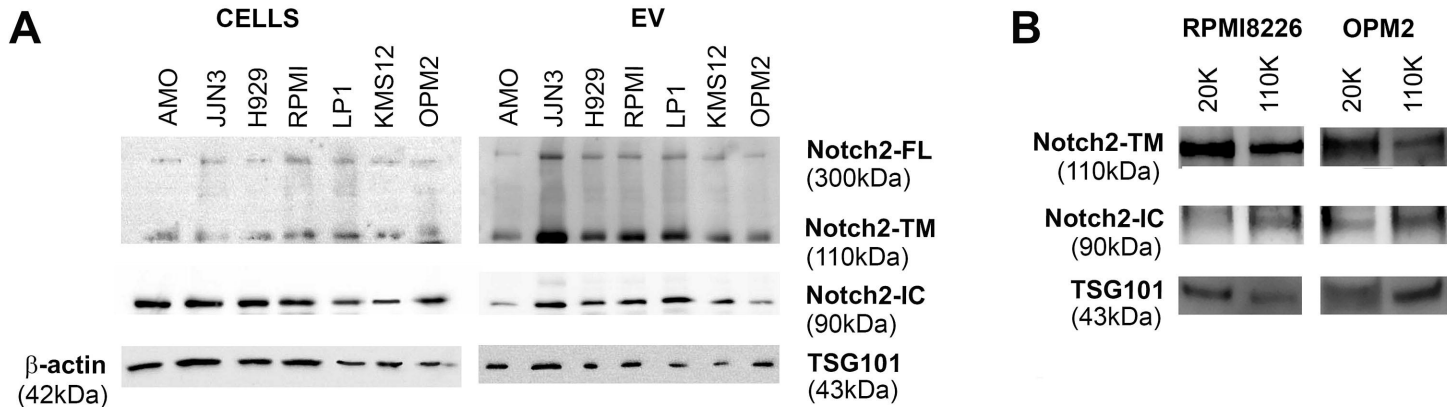


Fig.3



**C**

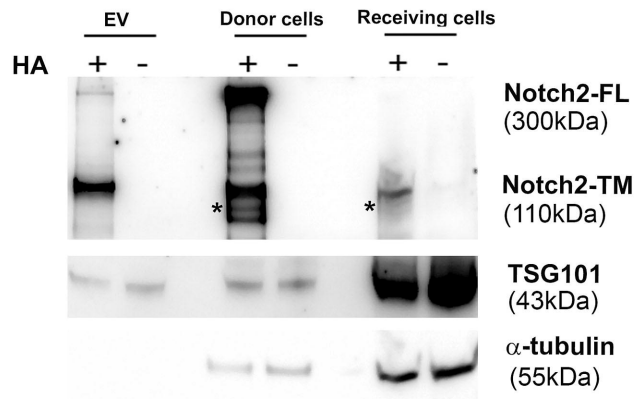
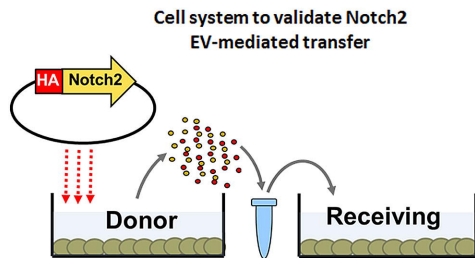


Fig.4

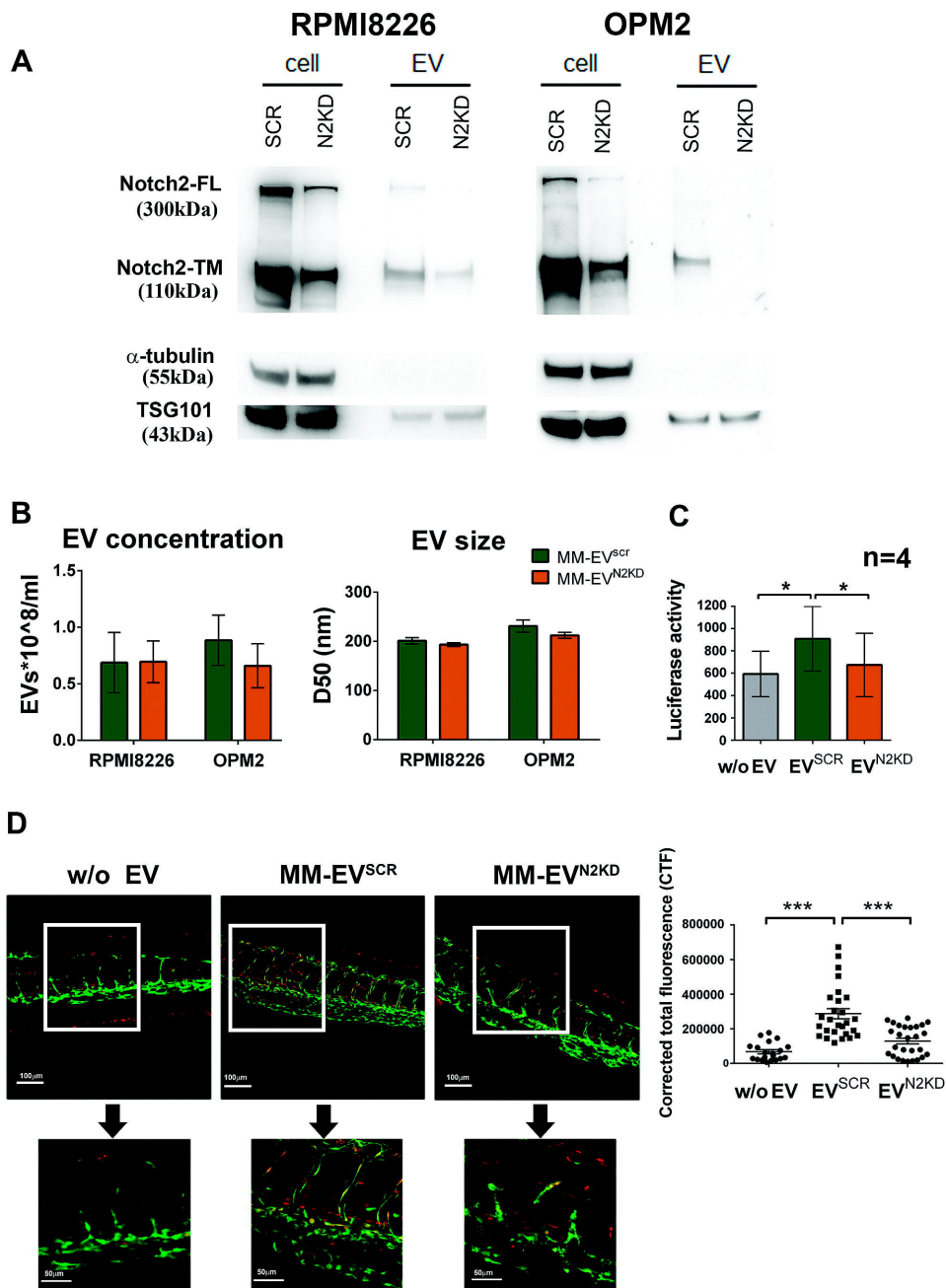
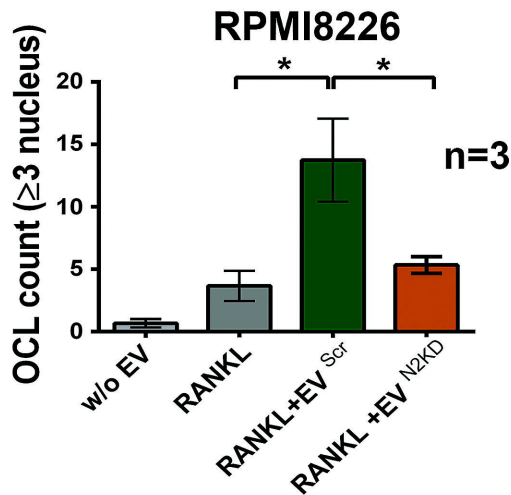
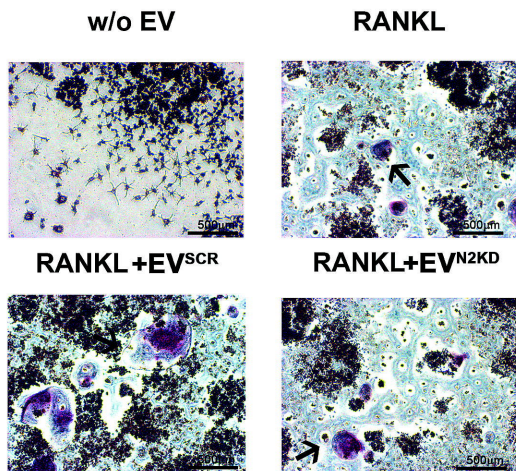


Fig.5

**A**



**B**

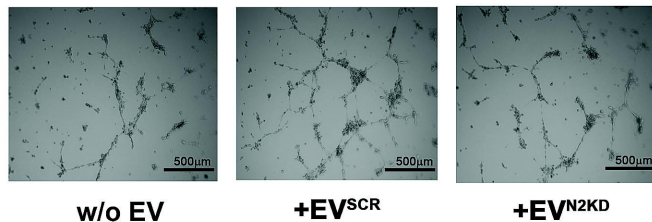
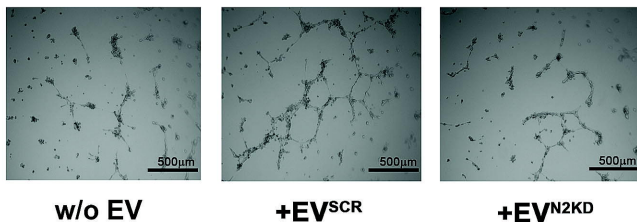
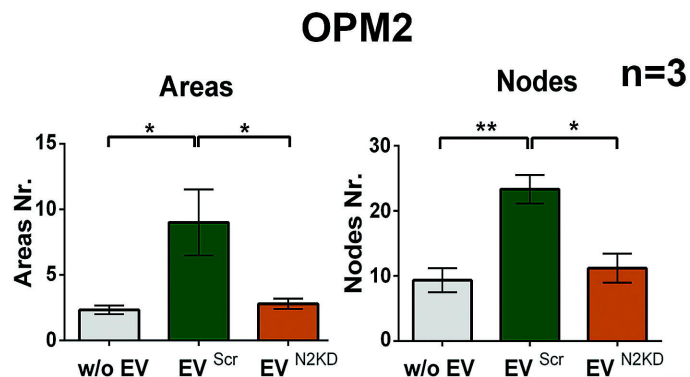
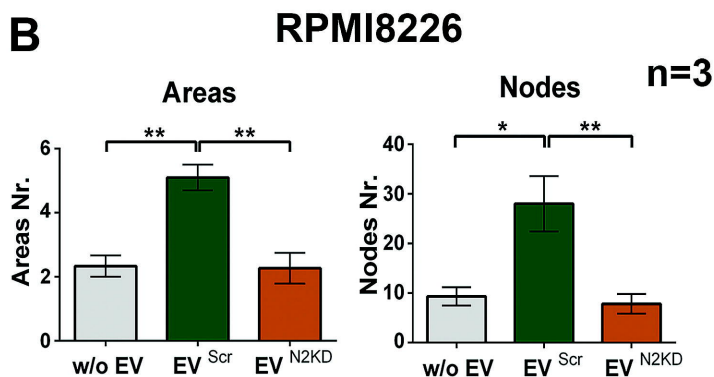


Fig.6

